ROMA TRE
UNIVERSITÀ DEGLI STUDI

SCUOLA DOTTORALE IN SCIENZE MATEMATICHE E FISCHE

CORSO DI DOTTORATO XXIII CICLO

Study of Kaon semileptonic decays on the lattice using twisted-mass fermions and stochastic techniques for light-meson propagators

Lorenzo Orifici

A.A. 2010/2011

Docente Guida/Tutor:
Dott. S. Simula & Prof. V. Lubicz
Coordinatore:
Prof. G. Altarelli

Acknowledgements

I would like to thank the Roma Tre lattice group which I joined for this *PhD* thesis work and without whom all this work would have not been possible. A special mention for Silvano Simula is in order: his help, his constant support and his patience during our discussions have been of fundamental importance for obtaining the results of this work. I wish to thank him very much for all his teachings. I am also very grateful to Roberto Frezzotti for his very precise and insightful corrections to the present thesis. Finally I would like to thank also my *colleagues* Stefano Di Vita and Francesco Sanfilippo for useful discussions as well as for their important suggestions during the writing period of this thesis. Last, but not least, I would like to thank the INFN ApeNext supercomputing center and the Ape group for keeping the ApeNext machines always at work.

Contents

List of Figures

List of Tables

Introduction

Weak hadron decays are very interesting processes because measuring the decay widths for such processes allow to extract some of the fundamental parameters of the Standard Model of electroweak interaction [1]. In particular it is possible to extract the modulus of the elements of the Cabibbo–Kobayashi–Maskawa (CKM) flavour mixing matrix [2; 3], which describe the *flavour* sector of the Standard Model.

The needed theoretical quantity, thanks to which one can obtain from the experimental measure of a given decay the related CKM matrix elements, are standard perturbative computing and the form factors which parametrize the hadron matrix element relevant for the decay.

The strong interaction physics is described by means of the Quantum Chromodynamics (QCD) [4; 5; 6]. It is known that QCD is a gauge theory characterized by the presence of the asymptotic freedom: the interaction's coupling goes to zero as the energy which describe the process become much greater than a characteristic scale of the theory, known as Λ_{QCD} ($\simeq 1\,GeV$). Conversely, in the low energy limit ($E \lesssim \Lambda_{QCD}$), it is no more possible to treat the interaction by means of perturbative methods because the coupling constant is $\mathcal{O}(1)$.

Lattice QCD (LQCD) [7] is a non-perturbative formulation of QCD based on first principles. In particular, it provides a peculiar regularization scheme in which the ultraviolet cut–off for momenta is given by the inverse of the lattice spacing; however, the specific importance of the lattice approach to QCD lies in the fact that it provides a systematic methodology via Monte Carlo simulations for carrying out *quantitative calculations* in the energy range in which it is not possible to perform perturbative estimates of the physical observables. This energy range overlaps with the energy scale characteristic of the weak hadron decays.

The processes which we are interested in are the ones in which a single hadron is present in both the initial and/or final state. These processes include leptonic decays, semileptonic decays and neutral meson oscillations. The study of processes with more than one hadron in the final state (for instance $K \to \pi\pi$ decays) present greater difficulties within LQCD standards methods.

LQCD calculation exploit the deep analogy between the lattice formulation of quantum field theories (in euclidean space–time) and the statistical mechanic description of a physical system. In particular it is possible to use Monte Carlo simulation techniques.

We would like to underline that LQCD allows a continuous improvement of the precision for the obtained results. The systematic error sources can, in fact, be kept under control using increased computational power, refined algorithms and improved techniques. Statistical errors can be reduced using bigger samples; discretization effects get less relevant reducing the lattice spacing; finite volume effects can be avoided increasing the lattice volume in which the quark and gluon's dynamics is simulated.

The present computational power strongly constraints the possible quark masses which can be simulated in LQCD, and in particular we are obliged to use light quark masses which are heavier than physical ones; thus, in order to obtain physical predictions for the quantities of interest we have to fit the dependence of our observables with respect to the quark masses. Chiral Perturbation theory can express meson masses as a function of the (bare) quark masses and so in our simulations we have chosen to study the quantities of interest as a function of meson masses (in particular the Kaon and pion mass). The light physical meson extrapolations, called *chiral* extrapolations, are another source of systematic error which must be kept under control.

For heavy mesons, another limitation is present: on a lattice with spacing a it is possible to simulate only states with mass lighter than the theory cut-off, which is given by the inverse lattice spacing (π/a). If we want to predict something about hadrons heavier than the ones which can be simulated on the lattice we will have to employ extrapolation again, this time in the heavy hadron mass.

The target is to be able to simulate energy regions in which it is possible to apply effective descriptions of QCD and perform the extrapolations using their predictions. Chiral perturbation theory (ChPT) describe the limit of vanishing light u and d (and s if one is considering $SU(3)$ ChPT) quark masses. Heavy quark effective theories (HQET, NRQCD) can instead describe the B and D meson physics. A combination of the two

theories (known as *Heavy Mesons* χPT) allow one to describe the decays of heavy to light hadrons; the subject of this work are the semileptonic kaon decays $K \to \pi l \nu_l$ and so we will limit our attention to $SU(2)$ and $SU(3)$ ChPT for extrapolating our form factors to the physical point.

In the lattice simulations performed in this work we have adopted the twisted-mass formulation of LQCD [8] and we have used the gauge configurations produced by the ETM collaboration [9] using the so-called *tree-level Symanzik improved* gauge action. The light mesons, built with two *u–* and *d–like* quarks (mass degenerate in the simulations), are heavier than the physical pion (the lightest pion used in the simulation has $M_\pi \sim 260\, MeV$) and so the chiral extrapolation to the physical point will play a fundamental role. On the other hand, the *strange* quark have masses such as the lattice K mesons are near the physical kaon and so we will only need to smoothly interpolate our results for reaching the physical kaon mass.

There is also another source of systematic error which has affected past years simulations. Because of the high computation cost of a realistic QCD simulation, usually the so–called *quenched* approximation was used which consist of neglecting the sea quark loops contribution in the generation process of gauge field configurations. This approximation, even if it has allowed to obtain results which were usually in good agreement with the experimental measures, introduce a systematic error which can be quantified only by a direct comparison with *unquenched* simulations.

Recently, the available computational power has reached a level which allow to perform unquenched QCD simulations with two, three or four flavors of dynamical quarks, in which the Dirac sea is composed by two degenerate u and d quarks ($N_f = 2$) with heavier s ($N_f = 2 + 1$) and c ($N_f = 2 + 1 + 1$) quarks.

In this thesis we have performed a lattice QCD study of semileptonic kaon decays, using the gauge configurations produced by the ETM collaboration with two dynamical light u and d quarks. We have adopted the twisted-mass formulation for the fermionic action and we have considered three different lattice spacings $a = 0.10\ fm$ ($a^{-1} = 1.94\ GeV$), $a = 0.079\ fm$ ($a^{-1} = 2.30\ GeV$) and $a = 0.063\ fm$, ($a^{-1} = 2.91\ GeV$) and two different volumes ($V \times T = 24^3 \times 48\, a^4$ and $V \times T = 32^3 \times 64\, a^4$).

In this work we provide an estimate of the form factors related to the $K \to \pi l \nu_l$ decays, for different values of the momentum transfer, using the double ratio method. We also present the calculation of the ratio of the kaon to pion decay constants, f_K/f_π,

as well as an explicit estimate of the *CKM* matrix element V_{us} using both Kl_3 and Kl_2 experimental decay rate. The comparison of our results with the *RBC/UKQCD* result obtained using $N_f = 2 + 1$ flavour of dynamical quarks shows an excellent agreement between the two theoretical calculation. We have compared also our form factor's q^2 shape with the experimental one, finding an excellent agreement as well.

In the study of the semileptonic form factors an important technical ingredient is the use of the stochastic technique for the estimate of the so–called fermionic all–to–all propagator, which will be described in detail in chapter 3. Such a technique turns out to be important for increasing significantly the signal-to-noise ratio in the correlation functions calculated in this work. At the same time it opens also the possibility to attack a different problem, namely the evaluation of a class of Feynman diagrams characterized by the presence of disconnected fermionic loops. These diagrams appear in the calculation of many important observables, like the neutron electric dipole moment (EDM), which are of utmost importance for the phenomenology of the Standard Model and its possible extensions.

The second part of this thesis deals with an exploratory study of the application of the stochastic approach to the calculation of the disconnected trace of the fermionic propagator, known as the fermionic *bubble*.

A preliminary study of stochastic techniques for disconnected diagrams

Within the standard model and its possible extensions, $\mathcal{CP}$ symmetry can be violated both in the electroweak and strong sector. In the electroweak sector by means of the complex phase present in the CKM matrix while in the strong sector because of the presence of the so–called θ*–term* [10]. This term involve the QCD field strength tensor and can induce an electric dipole moment (EDM) for the neutron. The existence of such a phenomena imply a *T–violating* effect which, assuming the validity of the *CPT* theorem, means a *CP* violating effect in the strong sector. It is known [11] that the calculation of the relevant matrix element of the neutron electric dipole moment, on the lattice, is a difficult task because it involves the topological charge operator and so the authors of [12] have proposed an alternative method which is based on the substitution

of the topological charge with the disconnected insertion of the flavour singlet pseudoscalar density. Using this method the problem of estimating the topological charge is traded with that of estimating the *disconnected insertion* of a fermion loop which involves the so–called *all-to-all* propagator.

Calculating the fermionic propagator for each degree of freedom and from every space–time point to any other space–time point of the lattice is an enormous task, well beyond the present available computational power. To solve this problem the key observation is that what is really involved in the physical amplitudes is the correlation of the hadronic propagators with a quark-antiquark loop or the correlation between quark-antiquark loop. So the interesting object is the trace of the fermionic propagator over all its degree of freedom. This means that one can profit of stochastic techniques which, focusing their attention to the trace of the fermionic propagator instead of the propagator itself, try to evaluate it with approximate methodologies. We have used as lattice testing observables for these stochastic techniques the 2–point functions of the η' and of the π^0, which involve such a trace.

The present techniques available for calculating the fermionic bubble are two: the *dilution* method of [13] and the *direct* method of [14]. After a detailed study of these techniques, we have worked out an hybrid method, which combine what we think are the best virtues of the two methods and which we have called *spin–direct* method. We will also show a third method [15], the *twisted* method, which can be employed only using twisted mass fermions and which is less general with respect to the one of [13] and [14] (and to our hybrid method too), but is particularly fast and effective in the case of η' correlation.

In the η' case, the authors of [16] have succeeded to extract a signal, using the twisted method, and were able to calculate the η' mass; although they employed some, so–called, *variance reduction* methods, these techniques are specific of the zero momentum two–points function characteristic of the η' case. It is clear that such a trick can only be used when doing spectroscopy while, on the other hand, we want to apply our methods to the neutron EDM calculation and so we can not profit of their variance reduction tricks and we will need to investigate further on a method well suited for the topology calculation characteristic of the EDM.

Analysis and physical results

All our calculations will be carried out at the ApeNext supercomputing center of INFN in Rome using a computational power of few TeraFlop.

Using the correlation functions calculated by the ETM collaboration, we have extract the semileptonic kaon decays form factors at different values of the quark masses simulated on the lattice. We have used the method of the so–called double ratios outlined in [17; 18; 19] which allows one to gain a high statistical precision in the form factors calculation.

For the $K \to \pi l \nu_l$ we have used two different strategies for the extrapolation/interpolation at the physical point: we have exploited quadratic splines to interpolate in the kaon mass, while following the works [19; 20] we have used the $SU(2)$ limit of the $SU(3)$ Gasser and Leutwyler ChPT formulae [21; 22] for reaching the physical point in the pion mass.

Our strategy will be to perform a multi–combined fit of the q^2*–shape*, M_π and a dependence of the form factors, using also the constraint given by the Callan-Treiman theorem to further reduce the number of the low–energy constants. In this way we are able give an estimate for the following physical quantities

$$f_+(0) = 0.9610(30)(28), \quad \frac{f_K}{f_\pi} = 1.189(8), \quad V_{us}^{Kl_3} = 0.2250(14), \quad V_{us}^{Kl_2} = 0.2258(16),$$

where the first error is statistical while the second, where available, is systematic. Our results are in very good agreement with the non-lattice ones obtained from the *FLAVIANET* collaboration [23] and from the lattice ones by $N_f = 2+1$ simulations of the *RBC/UKQCD* collaboration; also the compatibility of our form factor's q^2 shape with the one obtained by a dispersive fit, based on the form factor parametrization of [24], to the *experimental data* from *KLOE*, *KTeV*, *NA48* (without muons branching ratios) and *ISTRA+* performed by the authors of [23] is good as well.

As far as the use of the stochastic technique to evaluate the disconnected fermionic diagrams is concerned, our main conclusion is that the spin direct method is the most general and promising one. However, since a quite large number of stochastic sources is needed to get a statistically significant signal in the case of the fermionic bubbles, the application of such a method to the more interesting cases related to the neutron

EDM, or to other quantities of phenomenological interest, is possible only on super computers at the PetaFlop scale which will be available in the next future.

Thesis Plan

The first chapter will start introducing some basic notions about flavour physics. We will recall the basis of the Standard Model paying a particular attention to the CKM flavour mixing matrix. We will illustrate some of its related theoretical features and the (phenomenological) determination of its matrix elements. We will then move to leptonic and semileptonic kaon decays, introducing the semileptonic form factors, which are the subject of the present work, ending the chapter introducing weak and strong $\mathcal{CP}$ violation, with the latter which is responsible of the neutron electric dipole dipole moment generation.

The second chapter will be dedicated to the introduction of the calculation technique employed in this work: lattice QCD. After a general introduction we will present the Twisted Mass action used by the ETMC and we will also discuss a particular choice for the boundary conditions used in our lattice simulations, the so–called *twisted* boundary condition.

Chapter three will explain in details the methods which we will employ in our analysis of the form factors as well as the stochastic techniques which are good candidates to be used in a future calculation of the neutron EDM.

In chapter four we will present the results of this work. We will start introducing some basic information about the ETMC simulation which we have analyzed and then we will discuss statistical and systematic error analysis, present our form factor's analysis strategy and give our final physical results followed by a final discussion of the present status of our stochastic techniques.

1

Flavour Physics

1.1 The Standard Model

The standard model of electroweak and strong interaction is a Gauge theory invariant under the symmetry group $SU(3)_C \otimes SU(2)_L \otimes U(1)_Y$; more specifically, it is a quantum field theory (QFT) with the additional request of invariance under a continuous and local[1] transformation group.

$SU(3)_C$ is the group associated to the so-called *color* symmetry, on which is based the present description of the theory of the strong interaction, the quantum chromodynamics (QCD). Modern quantum field theories are described as carried by a *mediator*, mathematically represented as a gauge field, which is responsible for the force propagation and interaction and which is called *gluon* for QCD and represented as G^a, $(a = 1, \ldots, 8)$. We will describe QCD and his mathematical formalization in details in chapter 2. The group $SU(2)_L \otimes U(1)_Y$ is the correct one for describing the electromagnetic and weak coupling interactions involving gauge $(W^{\pm}, Z^0, \gamma)$ and matter fields [1]. The electroweak theory is an example of what is called a "chiral" theory, i.e. a theory in which the *left-handed* and *right-handed* components of the fermionic field undergoes different transformation properties; this is what is meant by the letter L which suggests that the interactions described by $SU(2)_L$ gauge group involve only the *left-handed* components.

Let us point out that, instead, Y labels the weak *hypercharge* group $U(1)_Y$ while with $U(1)_Q$ we will indicate the quantum electrodynamics (QED) gauge group, whose gener-

[1] A transformation whose parameter is a function of the space-time coordinate is called a *local* one.

ator, the electric charge Q, is related to Y and to the third component of weak isospin by $Q = T_3 + Y/2$. It is clear that being Y a function of the $SU(2)_L$ generator, also the hypercharge group will exibit a chiral character.
Let us now go to discuss some aspects of the model which are particularly relevant for what we will say in the rest of the work.

The gauge invariance request for the interaction is of crucial relevance in building the Standard Model because it provides precise relations between the couplings of the theory and these relations are *experimentally* confirmed with a high degree of precision; once said that, it is important to remember that for a model with unbroken gauge symmetry the vector bosons must be massless: an explicit mass term would not be gauge invariant. However the masses of the electroweak gauge bosons $W^{\pm}$ and Z^0 have been experimentally determined to be different from zero (while photons remain massless[1]). The solution to this picture was found in the *spontaneous symmetry breaking* mechanism. With the word *spontaneous* one mean that a theory, symmetric under a certain group of transformations and with a degenerate vacuum state (think about a potential with a certain number of minima), turns out to be realized selecting a particular vacuum state among the several possible ones, breaking in that way the formal invariance of the theory. In this framework one has a picture in which the symmetry group is respected by the interaction terms but it is not shared by the vacuum state.
At a somehow *practical* level, the spontaneous breaking of the electroweak symmetry group is obtained adding an appropriate scalar fields multiplet of $SU(2)_L \otimes U(1)_Y$, with vacuum expectation value (VEV) different from zero, and which makes possible the achievement of the following breaking path

$$SU(3)_C \otimes SU(2)_L \otimes U(1)_Y \rightarrow SU(3)_C \otimes U(1)_Q \,. \tag{1.1}$$

What is important to underline is that building a gauge invariant QFT including spontaneous symmetry breaking permits to generate mass terms, proportional to the scalar multiplet vacuum expectation value, for those gauge bosons associated to the broken symmetries (the so called *Higgs mechanism* [25; 26; 27; 28]). In other words, the spontaneous breaking of the symmetries associated to the $W^{\pm}, Z^0$ (*i.e.* $SU(2)_L$

[1] This, in turn, imply that because of the weak interaction has a massive mediator, its range is finite in contrast with the electromagnetic interaction which has an infinite range.

and $U(1)_Y$) allows one to keep all the gauge couplings relations but also to generate a mass term for the electroweak gauge bosons, while leaving $SU(3)_C \otimes U(1)_Q$ unbroken guaranties that the gluon and the photon remain massless.

What has been described up to here can be formalized and summarized writing down the Standard Model lagrangian

$$\mathscr{L}_{SM} = \mathscr{L}_{SU(3)_C} + \mathscr{L}_{SU(2)_L \otimes U(1)_Y} + \mathscr{L}_{Higgs}\,, \tag{1.2}$$

composed of three gauge invariant terms, the first two of them being

$$\mathscr{L}_{SU(N)} = -\frac{1}{4} F^a_{\mu\nu} F^{a\mu\nu} + i\bar{\psi}\gamma_\mu D^\mu \psi\,. \tag{1.3}$$

It is a *Yang-Mills* lagrangian [29] plus a fermionic matter field term. In (1.3) we have indicated with $F^a_{\mu\nu}$ the field strength tensor associated with the A^a_μ gauge field

$$F^a_{\mu\nu} \doteq \partial_\mu A^a_\nu - \partial_\nu A^a_\mu - g f^{abc} A^b_\mu A^c_\nu\,, \tag{1.4}$$

with ψ a fermionic field which transforms as in the fundamental gauge group representation and with D_μ the covariant derivative, defined as

$$D_\mu \doteq (\partial_\mu + i g A^a_\mu T^a)\,, \tag{1.5}$$

which, in turn, is composed of a kinetic term for the fermionic field and an interaction term between fermionic and gauge fields.
In the electroweak sector of the theory, the already mentioned fermionic fields are organized in a particular way: *left-handed* components (in the interaction *eigenstates* basis) are grouped in $SU(2)_L$ doublets

$$\begin{aligned} E^1_L &= \begin{pmatrix} \nu_e \\ e^- \end{pmatrix}_L, \quad E^2_L = \begin{pmatrix} \nu_\mu \\ \mu^- \end{pmatrix}_L, \quad E^3_L = \begin{pmatrix} \nu_\tau \\ \tau^- \end{pmatrix}_L; \\ Q^1_L &= \begin{pmatrix} u \\ d' \end{pmatrix}_L, \quad Q^2_L = \begin{pmatrix} c \\ s' \end{pmatrix}_L, \quad Q^3_L = \begin{pmatrix} t \\ b' \end{pmatrix}_L; \end{aligned} \tag{1.6}$$

while the *right-handed* components of quark fields and of the three massive leptons (neutrinos are assumed to be massless in the framework of the Standard Model) are $SU(2)_L$ singlets. The choice for the fermionic fields to transform according to this peculiar representation is motivated by the experimental observation that only the *left-handed* components of the fermion fields have a role in a weak interaction.

The "chirality feature" of the electroweak interaction forbid the presence of mass terms in the lagrangian not only for gauge bosons, but also for fermions, as can be easily seen from the behavior of a fermionic mass term under a generic gauge group transformation:

$$\mathscr{L}_m = m\left(\bar{f}_L f_R + \bar{f}_R f_L\right) \rightarrow \mathscr{L}'_m = m\left(\bar{f}_L U_L^\dagger U_R f_R + \bar{f}_R U_R^\dagger U_L f_L\right) \neq \mathscr{L}_m \ , \tag{1.7}$$

with $U_L \neq U_R$. However, it has been shown that, in a gauge invariant QFT, it is possible to obtain mass terms for fermions, once again, using the VEV of the Higgs scalar doublet.

The electroweak interaction lagrangian between matter and gauge fields emerge considering non-kinetic terms in the covariant derivatives, which can be of two kinds:

$$\mathscr{L}_{int}^{EW} = \mathscr{L}_{CC} + \mathscr{L}_{NC} \ , \tag{1.8}$$

charged currents couplings to $W^\pm$ bosons and *neutral currents* one to γ and Z^0 bosons. In particular one finds that charged currents interactions are described by

$$\mathscr{L}_{CC} = \frac{g}{2\sqrt{2}}\left(J_\mu^\dagger W^\mu + W_\mu^\dagger J^\mu\right) \ , \tag{1.9}$$

with

$$J_\mu^\dagger = \sum_{i=1,3} \bar{u}_L^i \gamma_\mu d_L^i + \bar{l}_L^i \gamma_\mu \nu_L^i \ , \tag{1.10}$$

where we have indicated with i the family index for both lepton and quark fields.

In view of the fact that we are going to deal with semileptonic meson decays, for which $|\Delta Q| = 1$, we are interested in the very (1.9) term of the Standard Model lagrangian.

We remember, for the sake of completeness, that for neutral currents interactions one has

$$\mathscr{L}_{NC} = -eJ^{\mu}_{em}A_{\mu} + \frac{g}{2\cos\theta_W}J^{\mu}_{Z}Z_{\mu}\ , \tag{1.11}$$

where

$$\begin{aligned} J^{\mu}_{em} &= \textstyle\sum_f Q_f \bar{f}\gamma^{\mu} f, \\ J^{\mu}_{Z} &= \textstyle\sum_f \bar{f}\gamma^{\mu}\left(v_f - a_f\gamma_5\right) f, \end{aligned} \tag{1.12}$$

with

$$v_f = T^f_3 - 2Q_f sin^2\theta_W\ , \quad a_f = T^f_3. \tag{1.13}$$

In these expressions Q_f and T^f_3 represents, respectively, the electric charge and the third components of weak isospin (different from zero only for *left-handed* fermions); we have also indicated with g and e the $SU(2)_L$ and $U(1)_Q$ coupling constants, respectively, and with θ_W the *weak*[1] mixing angle between the unphysical $SU(2)_L \otimes U(1)_Y$ gauge bosons W^3 and B and the physical ones Z^0 and γ. In table 1.1 we have collected all the electroweak quantum numbers for the different fermions.

	$\boldsymbol{\nu^l_L}$	$\boldsymbol{l^-_L}$	$\boldsymbol{l^-_R}$	$\boldsymbol{u_L}$	$\boldsymbol{d_L}$	$\boldsymbol{u_R}$	$\boldsymbol{d_R}$
$\boldsymbol{Q}$	0	-1	-1	2/3	-1/3	2/3	-1/3
$\boldsymbol{T_3}$	1/2	-1/2	0	1/2	-1/2	0	0
$\boldsymbol{Y}$	-1	-1	-2	1/3	1/3	4/3	-2/3

Table 1.1: Electroweak quantum numbers - for leptons and quarks. We have indicated with Q the electric charge, T_3 the third component of weak isospin and with $Q = T_3 + Y/2$ the weak hypercharge.

Finally, we can describe the so called Higgs sector of the Standard Model lagrangian

$$\mathscr{L}_{Higgs} = |D\phi|^2 - V(\phi,\phi^{\dagger}) + \mathscr{L}_Y \tag{1.14}$$

[1]The angle θ_W is sometimes wrongly called "Weinberg angle" because of the common initial letter.

whose expression is determined only by the request of being the most general gauge invariant renormalizable lagrangian for a complex scalar field, ϕ, which is an $SU(2)_L$ doublet:

$$\phi = \begin{pmatrix} \phi^+ \\ \phi^0 \end{pmatrix} . \tag{1.15}$$

The potential $V(\phi, \phi^\dagger)$ is invariant under a $SU(2)_L \otimes U(1)_Y$ transformation and, because of the renormalizabily constraint, it contains up to quartic terms in ϕ:

$$V(\phi, \phi^\dagger) = -\mu^2 \phi^\dagger \phi + \frac{1}{2}\lambda(\phi^\dagger \phi)^2 , \tag{1.16}$$

with $\lambda > 0$. In this framework, spontaneous symmetry breaking happens if the potential minimum, which represents the *classical* version of the quantum vacuum state, occurs for values of the ϕ field which are different from zero; from the shape of the potential $V(\phi, \phi^\dagger)$ it is easy to see that this will happen if $\mu^2 > 0$. Assuming that this is the case, let us choose as the VEV ϕ value

$$\langle 0 | \, \phi(x) \, | 0 \rangle = \begin{pmatrix} 0 \\ v \end{pmatrix} \neq 0 . \tag{1.17}$$

The field component with VEV different from zero is the neutral one and this imply that the vacuum has trivial transformation properties under $U(1)_Q$ and that this group will still be a symmetry of theory after the spontaneous breaking. It is possible to make more explicit the particle spectrum of the theory, taking advantage of the arbitrariness of the gauge choice. In particular one can parametrize the Higgs doublet as a VEV part plus a part which measure how much the field is different from v:

$$\phi(x) = U(x) \frac{1}{\sqrt{2}} \begin{pmatrix} 0 \\ v + h(x) \end{pmatrix} , \tag{1.18}$$

where $h(x)$ is a real field whose VEV is zero and $U(x) \in (SU(2) \otimes U(1)_Y)$; $U(x)$ can be simplified making the inverse gauge transformation $U(x)^{-1}$ which brings us in the so called *unitary* gauge. In this gauge the field ϕ becomes

$$\phi(x) = \frac{1}{\sqrt{2}} \begin{pmatrix} 0 \\ v + h(x) \end{pmatrix} , \tag{1.19}$$

and the particle content (and spectrum) of the theory is already manifest at a lagrangian level: the goldstone boson degrees of freedom appear only as the longitudinal gauge boson degrees of freedom and we are left only with physical particles[1].

Let's now describe the Standard Model lagrangian term which is responsible for the fermionic masses: $\mathscr{L}_Y$; assuming there are no right handed neutrinos, this term is the most general one describing the coupling of the Higgs doublet with fermionic fields, again constrained only by gauge invariance and renormalizability requests:

$$\mathscr{L}_Y = -\lambda_l^{ij} \bar{E}_L^i \phi e_R^j - \lambda_d^{ij} \bar{Q}_L^i \phi d_R^j - \lambda_u^{ij} \bar{Q}_L^i \bar{\phi} u_R^j + h.c. , \tag{1.20}$$

where the field $\bar{\phi}$ is defined as $\bar{\phi}^\alpha = \epsilon^{\alpha\beta} \phi_\beta^*$, with ϵ the $SU(2)_L$ antisymmetric tensor and α, β the relative (isospin) indices. The complex-valued matrices λ_l, λ_u and λ_d are not necessarily hermitian nor symmetric and $i,j = 1, 2, 3$ are generation indices; unless one don't ask for a flavour conserving symmetry, interactions with Higgs field will be flavour changing.

It is always possible to diagonalize λ_l by means of a redefinition of the leptonic fields: a generic, complex valued matrix can always be rewritten in terms of a diagonal matrix $D_l = diag(\tilde{\lambda}_e, \tilde{\lambda}_\mu \tilde{\lambda}_\tau)$ with positive eigenvalues and two unitary matrices

$$\lambda_l = U_l D_l W_l^\dagger \tag{1.21}$$

in order that, rescaling the fields

$$E_L^i \to U_l^{ij} E_L^j , \quad e_R^i \to W_l^{ij} e_R^j , \tag{1.22}$$

the leptonic part of the Yukawa term becomes

[1] We want to stress the fact that, although the unitary gauge is a good choice to analyze the particle content and mass spectrum of the theory, it is less well suited for studying quantum corrections to the classical theory and, to this end, different gauges should be chosen.

$$- \tilde{\lambda}_e \bar{E}_L^e \phi e_R - \tilde{\lambda}_\mu \bar{E}_L^\mu \phi \mu_R - \tilde{\lambda}_\tau \bar{E}_L^\tau \phi \tau_R \ . \tag{1.23}$$

Both the weak isospin doublet components undergoes the *same* U_l transformation and this imply that the matrices U_l and W_l cancels everywhere in the theory[1] and the phenomenological consequence of this cancellation is that one has exact conservation of the leptonic number for each generation and no $\mathcal{CP}$ violation, as has been precisely tested in the experiments [30]. Inserting the expression (1.19) for the ϕ field in the unitary gauge one has, for a generic lepton l^i

$$\mathscr{L}_Y^{(l)} = -m_l^i \bar{l}^i l^i \left(1 + \frac{h}{v}\right) \ , \quad m_l^i \doteq \frac{1}{\sqrt{2}} D_l^{ii} v \ . \tag{1.24}$$

The spontaneous breaking of gauge symmetry generates an interaction term with the Higgs field $h(x)$ as well as a mass term for leptons.
Next section will be dedicated to the analogous mechanism for the quark sector.

1.2 Cabibbo-Kobayashi-Maskawa matrix

In this section we will broaden the Standard Model flavour sector overview, describing the flavour mixing matrix, also known as *Cabibbo-Kobayashi-Maskawa* matrix.
What we are going to show is that weak interactions, in the quark sector, are not flavour diagonal in the mass eigenstates basis and the mixing matrix contains all the information we need to know about the relative weights for quark decays in their weak isospin partner of each generation.

1.2.1 Definition & parametrization

Let us analyze the Yukawa coupling between the Higgs doublet and the quark fields. First of all it is important to underline that the effect of the $\mathcal{CP}$ discrete symmetry is equivalent to the substitution

$$\lambda_d^{ij} \to (\lambda_d^{ij})^* \ , \quad \lambda_u^{ij} \to (\lambda_u^{ij})^* \ , \tag{1.25}$$

[1] This is a so-called *accidental* cancellation due to massless neutrinos.

and so $\mathcal{CP}$ is a symmetry only if the matrices λ^{ij} are real.
Following what has been done in the previous section for the leptonic sector we are going to perform chiral transformations of the kind

$$\lambda_u = U_u D_u W_u^\dagger \quad \text{and} \quad \lambda_d = U_d D_d W_d^\dagger \,, \tag{1.26}$$

where the matrices D are diagonal with positive eigenvalues, while U and W are unitary matrices; rescaling right-handed fields with

$$u_R^i \to W_u^{ij} u_R^j \quad \text{and} \quad d_R^i \to W_d^{ij} d_R^j \,, \tag{1.27}$$

one is able to simplify the W matrices present in the Yukawa coupling lagrangian. The same can be done in covariant derivatives leaving unchanged right-handed quarks kinetic terms. Similarly, on left-handed quark we can make the transformation

$$u_L^i \to U_u^{ij} u_L^j \,, \quad d_L^i \to U_d^{ij} d_L^j \,, \tag{1.28}$$

and we are able to simplify the U matrices from the Yukawa coupling lagrangian which become

$$\mathscr{L}_Y^{(q)} = -m_d^i \bar{d}_L^i d_R^i \left(1 + \frac{h}{v}\right) - m_u^i \bar{u}_L^i u_R^i \left(1 + \frac{h}{v}\right) \,, \tag{1.29}$$

where

$$m_{u,d} \doteq \frac{1}{\sqrt{2}} D_{u,d}^{ii} v \,. \tag{1.30}$$

What is now different is that we are analyzing left-handed field, and left-handed fields participate in the $SU(2)_L$ interaction, which is the flavour mixing one, and it makes necessary studying how does it changes, if it does, the rest of the lagrangian under the transformations (1.28).

First of all, U matrices cancel out in kinetic terms and in the interaction ones with gluonic fields because they are both flavour diagonal; the interaction terms with the

electromagnetic (A_μ) and the neutral weak mediator (Z^0) fields remain unchanged too, considered that they don't mix *up* fields with *down* fields. On the contrary, charged currents transforms as

$$J^{\mu\dagger} = \frac{1}{\sqrt{2}}\bar{u}_L^i \gamma^\mu d_L^i \rightarrow \frac{1}{\sqrt{2}}\bar{u}_L^i \gamma^\mu V_{CKM}^{ij} d_L^j \,, \tag{1.31}$$

expression in which we have defined the *Cabibbo-Kobayashi-Maskawa* (CKM) [2; 3] flavour mixing matrix as

$$V_{CKM} \doteq U_u^\dagger U_d \tag{1.32}$$

and it connects the interaction eigenstates (d', s', b') with the mass eigenstates (d, s, b):

$$\begin{pmatrix} d' \\ s' \\ b' \end{pmatrix} = \begin{pmatrix} V_{ud} & V_{us} & V_{ub} \\ V_{cd} & V_{cs} & V_{cb} \\ V_{td} & V_{ts} & V_{tb} \end{pmatrix} \begin{pmatrix} d \\ s \\ b \end{pmatrix} \,. \tag{1.33}$$

From this point of view it is clear that mass eigenstate are different from the interaction ones and that charged current interaction mix different flavours with weight V_{ij} in the mass eigenstates basis. It is worthwhile to underline that within the Standard Model the only flavour changing mechanism is represented by this matrix and that V_{CKM} unitarity guarantees that there are no flavour changing neutral currents (FCNC) to first order of perturbation theory; moreover the suppression of FCNC at higher orders, the so called GIM mechanism [31], is a consequence of V_{CKM} and well represents what has been experimentally observed in nature.

The CKM matrix, in the case of three quark generations, is a 3×3 unitary complex matrix which depends on nine real numbers[1]. Exploiting the quark fields phase redefinition freedom, it can be easily shown that V_{CKM} depends only on 4 real parameters, three angles and one phase, which, together with fermion masses, constitute the free parameters relative to the flavour sector of the Standard Model.

Once the number of the independent physical parameters of the matrix is known, one can introduce a set of different parametrization for that matrix depending on what

[1] A 3×3 unitary complex matrix has $9 \times 2 = 18$ real parameters with 9 unitarity constraint relations.

one has to study. The most natural choice is the one presented in [32] which writes the matrix as a product of three different rotations

$$V_{CKM} = \begin{pmatrix} 1 & 0 & 0 \\ 0 & c_{23} & s_{23} \\ 0 & -s_{23} & c_{23} \end{pmatrix} \begin{pmatrix} c_{13} & 0 & s_{13}e^{-i\delta} \\ 0 & 1 & 0 \\ -s_{13}e^{i\delta} & 0 & c_{13} \end{pmatrix} \begin{pmatrix} c_{12} & s_{12} & 0 \\ -s_{12} & c_{12} & 0 \\ 0 & 0 & 1 \end{pmatrix} , \quad (1.34)$$

which leads to

$$V_{CKM} = \begin{pmatrix} c_{12}c_{13} & s_{12}c_{13} & s_{13}e^{-i\delta} \\ -s_{12}c_{23} - c_{12}c_{23}s_{13}e^{i\delta} & c_{12}c_{23} - s_{12}s_{23}s_{13}e^{i\delta} & s_{23}c_{13} \\ s_{12}s_{23} - c_{12}c_{23}s_{13}e^{i\delta} & -c_{12}s_{23} - s_{12}c_{23}s_{13}e^{i\delta} & c_{13}c_{23} \end{pmatrix} , \quad (1.35)$$

where $s_{ij} = \sin\theta_{ij}$, $c_{ij} = \cos\theta_{ij}$ (and θ_{12} is the Cabibbo angle) and δ is the phase. The angles θ_{ij} can be chosen in the first quadrant in order that s_{ij} and $c_{ij} \geq 0$. What is important to underline is that if $\delta = 0$ the matrix V_{CKM} becomes real and one has no $\mathcal{CP}$ violation in the quark sector too. Another interesting feature of the matrix is that the δ phase is present in the Standard Model because the quark are organized in *three* generations. In the old Cabibbo version of the theory, which involved only two generations (u, d) and (c, s), the mixing matrix was a real rotation (in flavour space) and there was no room for $\mathcal{CP}$ violation. Moreover in order for $\mathcal{CP}$ violation to happen, it is necessary for *up - like* (as well as *down - like*) quark masses to be different because if it is not the case, by means of suitable unitary transformation, one could redefine quark fields in order to simplify the $\mathcal{CP}$ violating phase. It can be shown that the *necessary* condition for having $\mathcal{CP}$ violation is

$$(m_t^2 - m_c^2)(m_t^2 - m_u^2)(m_u^2 - m_c^2)(m_b^2 - m_s^2)(m_b^2 - m_d^2)(m_d^2 - m_s^2) \times J_{CP} \neq 0 \quad (1.36)$$

where we have introduced the Jarlskog parameter [33; 34]

$$J_{CP} \doteq |Im(V_{ij}V_{kl}V_{il}^*V_{jk}^*)| , \quad (i \neq k, j \neq l) , \quad (1.37)$$

which can be thought as a quantitative way of measuring how much $\mathcal{CP}$ symmetry is violated. J_{CP} is not dependent on quark fields phase conventions and V_{CKM} unitarity

imply that all the allowed i,j,k,l combinations will give the same quantity. Using Maiani parametrization (1.35) one has

$$J_{CP} = s_{12}s_{13}s_{23}c_{12}c_{23}c_{13}^2 \sin\delta \; ; \tag{1.38}$$

experimentally it has been measured $J_{CP} \simeq \mathcal{O}(10^{-5})$.

As one can clearly see from (1.36) the $\mathcal{CP}$ violation root can be traced back to the quark mass hierarchy problem; as already said, fermion masses are free parameters in the Standard Model. The weak interaction mixes flavors according to a specific hierarchy: the diagonal elements of the matrix (1.33) describe transition *within* the same generation and are bigger ($\sim \mathcal{O}(1)$) than off diagonal elements ($\sim \mathcal{O}(10^{-1})$ to $\sim \mathcal{O}(10^{-3})$), which, on the other hand, represent transitions *between* generations, for which experimentally one has $s_{13} \ll s_{23} \ll s_{12} \ll 1$. This has been pictorially represented in figure 1.1 where transitions within the same generation are represented with bold black lines, while transitions between different generations are represented with dashed and dotted lines of different colors.

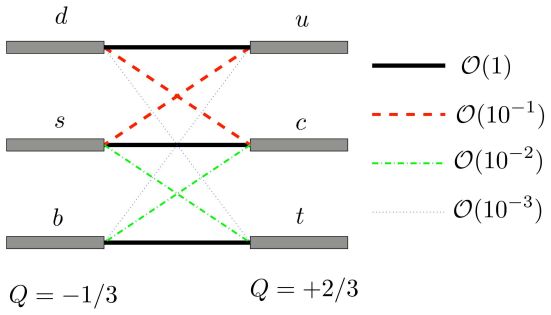

Figure 1.1: Flavour mixing hierarchy - It is shown the hierarchy of charged currents flavour mixing transition; picture taken from [35] (Fleisher's lecture).

It is convenient to exhibit this hierarchy setting

$$s_{12} \doteq \lambda \; , \quad s_{23} \doteq A\lambda^2 \; , \quad s_{13}e^{-i\delta} \doteq A\lambda^3(\rho.i\eta) \; , \tag{1.39}$$

and substituting them in (1.35) one obtains the CKM matrix parametrization in terms of (λ, A, ρ, η) proposed by Wolfenstein in [36]. Expanding the matrix elements in powers of λ, neglecting terms $\mathcal{O}(\lambda^4)$ one has

$$V_{CKM} = \begin{pmatrix} 1-\frac{\lambda^2}{2} & \lambda & A\lambda^3(\rho - i\eta) \\ -\lambda & 1-\frac{\lambda^2}{2} & A\lambda^2 \\ A\lambda^3(1-\rho-i\eta) & -A\lambda^2 & 1 \end{pmatrix} + \mathcal{O}(\lambda^4) \,. \tag{1.40}$$

With this variables the Jarlskog invariant becomes

$$J_{CP} = A\lambda^6\eta \,, \tag{1.41}$$

and the measure of $\mathcal{CP}$ violation, analogous to δ of the *standard* parametrization, is η (as can be seen from (1.40), if η is zero elements $(V_{CKM})_{13}$ and $(V_{CKM})_{31}$ become real and no $\mathcal{CP}$ violation is possible).

Other important information can be extracted from CKM matrix performing the so called *unitarity triangle* analysis. This kind of analysis is based on the unitarity of V_{CKM} which can be expressed as

$$V_{CKM}^\dagger V_{CKM} = V_{CKM} V_{CKM}^\dagger = 1 \,, \tag{1.42}$$

and, if expressed element by element, it consists of nine relations, six of orthogonality and three of normalization. The former can be represented as six triangles in a complex plane, all having the same area $A_\Delta = J_{CP}/2$; using Wolfenstein's parametrization for CKM elements it can be realized that only the triangle's sides coming from the orthogonality of first and third row and first and third column are of the same order of magnitude ($\mathcal{O}(\lambda^3)$); they are

$$V_{ud}V_{ub}^* + V_{cd}V_{cb}^* + V_{td}V_{tb}^* = 0 \tag{1.43}$$

$$V_{ud}V_{td}^* + V_{us}V_{ts}^* + V_{ub}V_{tb}^* = 0 \tag{1.44}$$

for other triangles one has a side that is smaller than the other roughly by a factor $\mathcal{O}(\lambda^2)$ o $\mathcal{O}(\lambda^4)$. Actually relations (1.43) and (1.44) are equivalent at order $\mathcal{O}(\lambda^3)$ and one can write them as

$$\left[(\rho + i\eta) + (-1) + (1 - \rho - i\eta)\right] A\lambda^3 + \mathcal{O}(\lambda^4) = 0 \tag{1.45}$$

and so at this order one has only one independent triangle and we will choose in the following the usual (1.43) also known as *unitary triangle* of CKM matrix.
It can be shown [37] that performing in (1.45) the substitution $(\rho, \eta) \to (\bar{\rho}, \bar{\eta})$, with the *barred* parameters defined by

$$\rho - i\eta = \frac{\bar{\rho} - i\bar{\eta}}{\sqrt{1-\lambda^2}} \,, \tag{1.46}$$

one can obtain a unitarity relation valid up to order $\mathcal{O}(\lambda^7)$

$$\left[(\bar{\rho} + i\bar{\eta}) + (-1) + (1 - \bar{\rho} - i\bar{\eta})\right] A\lambda^3 + \mathcal{O}(\lambda^7) = 0 \tag{1.47}$$

and the associated unitary triangle is shown in fig. 1.2

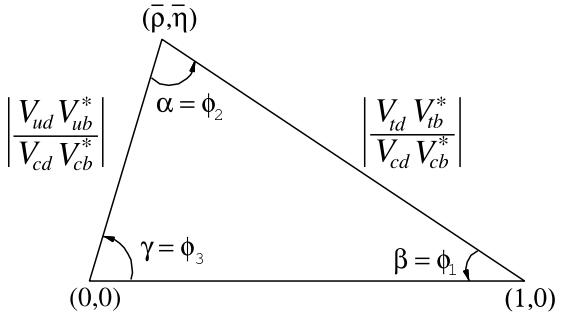

Figure 1.2: Unitary triangle - It is shown the unitary triangle related to (1.47); picture taken from [30] (PDG 2008)

where sides and angles are defined as follows

$$\alpha \doteq \phi_2 \doteq arg\left(-\frac{V_{td}V_{tb}^*}{V_{ud}V_{ub}^*}\right) \,, \tag{1.48}$$

$$\beta \doteq \phi_1 \doteq arg\left(-\frac{V_{cd}V_{cb}^*}{V_{td}V_{tb}^*}\right) \,, \tag{1.49}$$

$$\gamma \doteq \phi_3 \doteq arg\left(-\frac{V_{ud}V_{ub}^*}{V_{cd}V_{cb}^*}\right) \,, \tag{1.50}$$

$$R_b \doteq \frac{|V_{ud}V_{ub}^*|}{|V_{cd}V_{cb}^*|} \simeq \left(1 - \frac{\lambda^2}{2}\right)\frac{1}{\lambda}\left|\frac{V_{ub}}{V_{cb}}\right| \,, \tag{1.51}$$

$$R_t \doteq \frac{|V_{td}V_{tb}^*|}{|V_{cd}V_{cb}^*|} \simeq \frac{1}{\lambda}\left|\frac{V_{td}}{V_{cb}}\right| \,. \tag{1.52}$$

1.2.2 Experimental determination

Assuming the Standard Model as a *complete* model, the "experimental" measure of V_{CKM} elements should verify its unitarity. Deviation from that expected unitarity would unambiguously indicate the presence of physics beyond the Standard Model; hence it is of crucial relevance to perform as precise as possible measures to increase our knowledge of the Standard Model and of potential new physics. For instance, in view of the upcoming measures which will be performed at the LHC, it will be very important to know the flavour sector parameters as well as possible in order to better understand a possible discovery of new particles or new physics.
Within the Standard Model, all flavour violating processes, both $\mathcal{CP}$ violating and conserving ones, are ruled by CKM matrix and, as a consequence, can be described by means of four parameters (three angles and one phase or, using Wolfenstein parametrization, A,λ,ρ and η); this means that the large variety of flavour physics phenomena which are nowadays measurable (*i.e.* semileptonic decays, $\mathcal{CP}$ asymmetries, neutral mesons mixing, rare decays and so on) are all strongly connected and the unitary triangle is an optimal tool for studying these correlations. More specifically, thanks to the B-factories measures as well as to D and K decays measurements and moreover to the higher lattice QCD accuracy in providing theoretical inputs, it is possible to *overconstrain* the unitary triangle. This means that, eventually, it is possible to correctly test the CKM mechanism within the Standard Model and to set limits on the possible new physics contributes. Let us now briefly remind, according to the 2008 edition of the *Review of particle physics* [30], the physical processes from which it is possible to measure the CKM elements.

Starting from V_{ud}, the most precise determination of the module of this element comes from superallowed $J^P = 0^+ \to J^P = 0^+$ nuclear beta decays, which are pure vector transitions and are free from nuclear structure uncertainties. This yields

$$|V_{ud}| = 0.97418 \pm 0.00027 \; . \tag{1.53}$$

It is also possible to measure this matrix element using neutrino lifetimes or from the branching ratio for the process $\pi^+ \to \pi^0 e^+ \nu$ and both give results consistent with (1.53) but with a slightly bigger error.

Without going into details, as these are going to be the subject of next section, let's mention that $|V_{us}|$ can be extracted from $K_L^0 \to \pi e \nu$ decays using the form factor extracted from lattice QCD as theoretical input, and it yields [23] [1]

$$|V_{us}| = 0.2254 \pm 0.0013 \ . \tag{1.54}$$

Other possible determination of $|V_{us}|$ involve leptonic kaon decays, hyperon decays and τ decays. From the first, one can extract a value of [23]

$$|V_{us}| = 0.2312 \pm 0.0013 \ , \tag{1.55}$$

using again the lattice QCD input of the ratio of the pion and kaon decay constants togheter with the knowledge of $|V_{ud}|$.
What is important to underline is that the quoted errors in (1.54) and (1.55) are dominated by the uncertainty on the LQCD hadronic quantity used to obtain V_{us} matrix element from the experimental data (respectively, the form factor and the ratio of decay constants). It is clear that a precise determination of these quantities on the lattice is needed in order to improve more and match the experimental precision.

For extracting $|V_{cd}|$ one can use a measure based on neutrino and antineutrino interaction. The measure of the difference of the ratio of double muon to single muon production is proportional to the charm cross section off valence d-quarks and therefore to $|V_{cd}|^2$. Using a suitable average one can obtain

$$|V_{cd}| = 0.230 \pm 0.011 \ . \tag{1.56}$$

A direct determination of $|V_{cs}|$ is possible from semileptonic D or leptonic D_s decays, using again lattice QCD calculations as input for D form factors and D_s decay constants. Here the state of the art is similar to the $|V_{us}|$ one, in which the error on the CKM element is completely dominated from the theoretical one. From averaged leptonic and semileptonic determinations ref. [30] quotes

[1] The value presented here is slightly different from the one in [30] because of the updated value recently presented in [23].

$$|V_{cs}| = 1.04 \pm 0.06 \ . \tag{1.57}$$

The $|V_{cb}|$ matrix element can be determined from exclusive and inclusive semileptonic decays of B mesons to charm. The inclusive determination use the semileptonic decay rate measurement, together with the leptonic energy and the hadronic invariant mass. Exclusive determinations are based on semileptonic B decays to D and D^*. In the limit $m_{b,c} \gg \Lambda_{QCD}$ the form factors can be calculated using heavy-quark effective theory (HQET) and V_{cb} can be obtained from and extrapolation guided by this effective theory. The exclusive determination is less precise than the inclusive one, because the theoretical uncertainty in the form factors and the experimental uncertainty in the rate near the physical point are about 3%. A suitable combination of the two results yields

$$|V_{cb}| = (41.2 \pm 1.1) \times 10^{-3} \ . \tag{1.58}$$

The determination of $|V_{ub}|$ from inclusive $B \to X_u l\bar{\nu}$ decay suffers from large $B \to X_c l\bar{\nu}$ backgrounds. In most regions of phase space where the charm background is kinematically forbidden, hadronic physics enters via unknown nonperturbative functions, called *shape functions*. These functions must be measured in different processes, such as $B \to X_s\gamma$, and then applied to several spectra in $B \to X_u l\bar{\nu}$. There are also other methods in which one applies phase space methods to reduce the number of shape functions presents in the rate; another alternative approach is to extend the measurement deeper into the $B \to X_c l\bar{\nu}$ region to reduce the theoretical uncertainties. V_{ub} can also be extracted from an exclusive channel, assuming the form factors are known. Form factors can be measured or calculated using LQCD (in the kinematic region of $q^2 > 16\ GeV^2$) or light cone QCD sum rules for $q^2 < 14\ GeV^2$ and all yield similar results when used in V_{ub} calculation. The theoretical uncertainties in extracting $|V_{ub}|$ from inclusive and exclusive decays are different; a combination of the determinations is quoted as

$$|V_{ub}| = (3.93 \pm 0.36) \times 10^{-3} \ , \tag{1.59}$$

which is dominated by the inclusive measurement.

The CKM elements $|V_{td}|$ and $|V_{ts}|$ cannot be measured from tree-level decays of the top quark, so one has to rely on determinations from $B - \bar{B}$ oscillations mediated by box diagrams with top quarks, or loop-mediated rare K and B decays. Theoretical uncertainties in hadronic effects limit again the accuracy of the current determination. These can be reduced by taking ratios of processes, as an example one could quote the quantity $\Delta m_d/\Delta m_s$, that are equal in the flavour $SU(3)$ limit to determine $|V_{td}/V_{ts}|$. Without doing so and using unquenched LQCD calculation for the hadronic quantities one finds

$$|V_{td}| = (8.1 \pm 0.6) \times 10^{-3} \ , \quad |V_{ts}| = (38.7 \pm 2.3) \times 10^{-3} \ . \tag{1.60}$$

The uncertainties are dominated by LQCD calculations; however if one takes the ratio $\Delta m_d/\Delta m_s$, which in turn involve the ratio of the hadronic quantities determined on the lattice, is able to obtain the more reliable constraint for

$$\left|\frac{V_{td}}{V_{ts}}\right| = 0.209 \pm 0.001_{stat} \pm 0.006_{sys} \ . \tag{1.61}$$

A complementary determination for the ratio of these matrix elements is possible from the ratio of $B \to \rho\gamma$ and $K^*\gamma$ rates, which gives $|V_{td}/V_{ts}| = 0.21 \pm 0.04$ while for the product $|V_{td}V_{ts}^*|$ one can use the rare decay $K^+ \to \pi^+\nu\bar{\nu}$ but experimentally only three events has been observed and much more data are needed for a precision measurement.

Finally the determination of V_{tb} from top decays uses the ratio of the branching fractions $\mathcal{R} = \mathcal{B}(t \to Wb)/\mathcal{B}(t \to Wq) = |V_{tb}|^2$, with $q = b, s, d$. Experimental measures give for these quantities $|V_{tb}| > 0.78$ and $|V_{tb}| > 0.89$. Direct determination of V_{tb} without assuming unitarity is possible from single top quark production cross section. In this way it is possible to set the limit

$$|V_{tb}| > 0.74 \ . \tag{1.62}$$

Also, one can constrain $|V_{tb}|$ from electroweak data and the result, mostly driven by the top loop contribution to $\Gamma(Z \to b\bar{b})$, gives

$$|V_{tb}| = 0.77^{+0.18}_{-0.24} \, . \tag{1.63}$$

To summarize we can write, restricting our attention to the *direct* measure of the module of CKM elements

$$V_{CKM}^{exp} = \begin{pmatrix} 0.97418 \pm 0.00027 & 0.2254 \pm 0.0013 & (3.93 \pm 0.36) \times 10^{-3} \\ 0.230 \pm 0.011 & 1.04 \pm 0.06 & (41.2 \pm 1.1) \times 10^{-3} \\ (8.1 \pm 0.6) \times 10^{-3} & (38.7 \pm 2.3) \times 10^{-3} & 0.77^{+0.18}_{-0.24} \end{pmatrix} . \tag{1.64}$$

To proceed with unitary triangle angles, measurement of $\mathcal{CP}$ violation effects in neutral B mesons decays provide a determination of $\sin 2\beta$. Word average quotes

$$\sin 2\beta = 0.681 \pm 0.025 \, , \tag{1.65}$$

while the results for α, coming from time dependent $\mathcal{CP}$ asymmetries in $b \to u\bar{u}d$ dominated decays, and for γ, coming mainly from $B^{\pm} \to DK^{\pm}$ are

$$\alpha = \left(88^{+6}_{-5}\right)^{\circ} \tag{1.66}$$

$$\gamma = \left(77^{+30}_{-32}\right)^{\circ} \tag{1.67}$$

Another way for extracting values of the CKM matrix elements which are more accurate with respect to ones in (1.64), is to perform a *fit* [38; 39] of all the latest available measures imposing all the Standard Model constraints. The results obtained in that way reported in [30] are

$$V_{CKM}^{fit} = \begin{pmatrix} 0.97419 \pm 0.00022 & 0.2257 \pm 0.0010 & (3.59 \pm 0.16) \times 10^{-3} \\ 0.2256 \pm 0.0010 & 0.97344 \pm 0.00023 & \left(41.5^{+1.0}_{-1.1}\right) \times 10^{-3} \\ \left(8.74^{+0.26}_{-0.37}\right) \times 10^{-3} & (40.7 \pm 1) \times 10^{-3} & 0.999133^{+0.000044}_{-0.000043} \end{pmatrix} , \tag{1.68}$$

while Wolfenstein's parameters are

$$\lambda = 0.2257^{+9}_{-10} \, , \tag{1.69}$$

$$A = 0.814^{+21}_{-22} \, , \tag{1.70}$$

$$\bar{\rho} = 0.135^{+31}_{-16} \, , \tag{1.71}$$

$$\bar{\eta} = 0.349^{+15}_{-17} \, . \tag{1.72}$$

Let us conclude this section underlining again the importance of the lattice QCD calculation of meson decay form factors. First of all, it is important because the form factors are needed both in the theoretical as well as on the experimental side, to extract from what one experimentally measures the CKM matrix element; moreover it is important to give a precise estimate of the form factors because in most of the processes the experimental precision is so high that, at the end of the day, all the systematic error comes from the theoretical side , and in the present case, from the lattice QCD uncertainty on the hadronic quantity.
A special mention for the semileptonic K decay is in order, as the experimental precision is so high, of the order of 0.2%, that the form factor at zero momentum must be determined with a precision better that the percent level. This is feasible with a technique which will be shown in chapter 3.

1.3 Leptonic and semileptonic meson decays

Within the Standard Model, as we have already mentioned, leptonic and semileptonic meson decays can be used to obtain accurate determinations of the magnitude of the CKM elements and, in particular, semileptonic Kaon decays gives us the best determination of the magnitude of the V_{us} element. A general feature of standard analysis is that for extracting these elements from decay widths one need precise estimates about the relevant hadronic quantities involved in the process; to be more specific, it is necessary to know decay constants and semileptonic form factors, as a function of the transfer momentum, in a very precise fashion.
At the energy scale characteristic of an hadronic decay process, strong interaction cannot be treated by means of perturbative methods because $\alpha_s \gtrsim 1$. This means that the hadronic quantities involved in the decay widths must be estimated using non perturbative techniques, and in particular a lattice QCD calculation of the kaon semileptonic decay constant and form factor will be presented in chapter 4 and will be one of the main goals of this work.

Within the *quark model* mesons are represented as *quark-antiquark* bound states $\bar{q}q'$ with the two quarks, known as *valence* quarks, which can have different flavour. Writing the orbital angular momentum of the system as l, the meson parity P can be calculated as $P = (-1)^{l+1}$; total angular momentum, J, is as usual made up of orbital

angular momentum and spin angular momentum and will take values in the interval $|l-s| < J < |l+s|$, where $s = 0, 1$ if the quark's spins are antiparallel or parallel, respectively. In real word, however, mesons, and more generally hadrons, are much more complicated objects and valence quarks are responsible only for the particle's quantum numbers. An hadron is composed of an infinite number of quarks, antiquarks and *virtual* gluons, known as Dirac sea, which gives null contribution to the hadron quantum numbers. In this framework, hadron decays can be seen as their valence quarks weak decays. The matrix element spin structure is particularly simple for *pseudoscalar* mesons ($J^P = 0^-$) and their description can be done in terms of few free parameters. We will distinguish between two meson's classes: *light* mesons, composed of two light quarks $q, q' = u, d, s$ and *heavy-light* mesons, built up by one heavy quark $Q = c, b$ and one light quark $q = u, d, s$; moreover we will also restrict ourselves to that decays which are first order in the weak coupling, focusing our attention to the flavour changing processes which, as we have already seen in the previous section, at tree level come only from charged current interactions in the Standard Model because of unitarity of the CKM matrix.

Let us now introduce a new element which will be useful in the following sections: Fermi effective theory of weak interaction. Semileptonic decays are processes in which $W^\pm$ bosons (but this is true also for Z^0 boson) have masses which are large in comparison with q, the typical transfer momentum involved; in practice, this means that terms of order $\mathcal{O}(q^2/M_W^2)$ and higher, can be safely neglected from the physical amplitudes. This is usually referred to as the $W^\pm$ decouples from the theory in the low energy *regime* and they end up "integrated out". The result of this operation is an *effective* theory, valid at energies $E \ll M_{W,Z}$, in which there are no more $W^\pm$ or Z^0 and the non local interaction which were mediated by these bosons are now seen as local four fermions interactions:

$$\frac{-ig_{\mu\nu}}{q^2 - M_W^2} \xrightarrow[M_W^2 \gg q^2]{} \frac{-ig_{\mu\nu}}{M_W^2}. \tag{1.73}$$

At a lagrangian level one has

$$\mathscr{L}_{CC}^{eff} = \frac{G_F}{\sqrt{2}} J_\mu^\dagger J^\mu \left[1 + \mathcal{O}(\frac{q^2}{M_W^2})\right] , \tag{1.74}$$

where G_F is the so called *Fermi* constant defined in terms of the weak coupling constant g as

$$\frac{G_F}{\sqrt{2}} \doteq \frac{g^2}{8M_W^2} \,. \tag{1.75}$$

As charged weak currents (1.10) describe both quarks and leptons, it follows that the effective lagrangian (1.74) will in turn describe interactions between two lepton currents, which are responsible for processes such as τ or μ leptonic decays, between one lepton current and an hadronic one, which can account for leptonic and semileptonic hadron decays and, in the end, between two hadronic currents which describe non leptonic hadron decays.

1.3.1 Leptonic Kaon decays

Leptonic decays are processes in which the final state is purely leptonic. Among them one could quote

$$\begin{aligned} \pi^+ &\to \mu^+ + \nu_\mu \\ D_s^\pm &\to \mu^\pm + \nu_\mu(\bar{\nu}_\mu) \\ B^+ &\to \tau^+ + \nu_\tau \end{aligned}$$

and so the prototype, for the case of a negative meson M^-, can be represented as $M^- \to l^- \bar{\nu}_l$ which is related to the underlying quark process $q\bar{q}' \to l\nu_l$, as can be seen in figure 1.3

The decay width for such a process can be written as

$$\Gamma(M^- \to l^- \nu_l) = \frac{1}{2M} \sum_{pol} \int |A^2| d\Omega_2 \tag{1.76}$$

where M is the meson mass, the sum is over the polarization of the final state leptons, A is the Feynman amplitude for the process and $d\Omega_2$ is the two body phase space. The amplitude, at lowest order in the electroweak interaction but to all orders in the strong interaction, can be written as

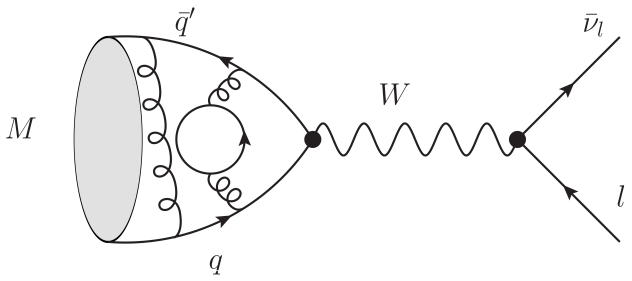

Figure 1.3: Leptonic decay prototype - Feynman diagram which contribute to a leptonic decay of a general meson M. The hadronic part (left) must be evaluated by means of non perturbative methods.

$$A(M^- \to l^- \nu_l) = -\frac{G_F}{\sqrt{2}} V^*_{q'q} \langle l^- \nu_l | \left[\bar{\nu}_l \gamma_\mu \left(1-\gamma^5\right) l\right] \left[\bar{q} \gamma^\mu \left(1-\gamma^5\right) q'\right] | M^- \rangle \ ; \quad (1.77)$$

because of the point-like interaction between the two currents, the amplitude factors out in two parts, one leptonic and one hadronic:

$$A(M^- \to l^- \nu_l) = -\frac{G_F}{\sqrt{2}} V^*_{ud} H^\mu L_\mu \quad (1.78)$$

where it has been defined

$$H^\mu \doteq \langle 0 | \, \bar{q} \gamma^\mu \gamma^5 q' \, | M^- \rangle \ , \quad (1.79)$$

$$L^\mu \doteq \langle l^- \bar{\nu}_l | \, \bar{l} \gamma^\mu \left(1-\gamma^5\right) \nu_l \, | 0 \rangle \ . \quad (1.80)$$

Two remarks are in order. First of all, the vacuum insertion is possible only because (at this order) there are no radiative corrections between the initial and the final state. The second one is that because of in (1.79) the initial and the final states have different parity, only the axial contribute to the amplitude is present. The problem is now shifted to the evaluation of H^μ. Taking into account Lorentz-invariance one knows that expression (1.79) must be parametrized as a vector times a quantity, f_M, which has the dimension of an energy and must be experimentally determined; as the only vector present in the process is the meson momentum p^μ, one can write

$$\langle 0|\,\bar{q}\gamma_\mu\gamma^5 q'\,|M^-\rangle = -if_M p_\mu\ . \tag{1.81}$$

The parameter $f_{_M}$ is called the M meson decay constant and represents the overlap of the two valence quark and antiquark wave functions.
Evaluating two body phase space and kinematics, the square module of the Feynman amplitude (1.78) and substituting them into eq. (1.76), one obtain the decay width

$$\Gamma(M^-\to l^-\nu_l) = \frac{G_F^2}{8\pi} f_M^2 |V_{q'q}|^2 M m^2 \left(1-\frac{m^2}{M^2}\right)^2\ , \tag{1.82}$$

where m is the l lepton mass, assuming antineutrinos are massless.

Formula (1.82) is the starting point for the evaluation of the CKM matrix element V_{us} using leptonic Kaon decays. In particular, what is usually employed is not expression (1.82) specified for $H^\pm = K^\pm$ alone (the so called $K^\pm_{l2}$ decay width), but the ratio of the $K^\pm\to l^\pm\nu$ to $\pi^\pm\to l^\pm\nu$ (called $\pi^\pm_{l2}$) [40; 41] decay width:

$$\frac{\Gamma_{K_{l2}}}{\Gamma_{\pi_{l2}}} = \frac{|V_{us}|^2}{|V_{ud}|^2}\frac{f_K^2}{f_\pi^2}\frac{m_K\left(1-\frac{m_l^2}{m_K^2}\right)^2}{m_\pi\left(1-\frac{m_l^2}{m_\pi^2}\right)^2}(1+\delta_{EM})\ . \tag{1.83}$$

where f_K and f_π are the kaon and the pion decay constants and δ_{EM} denotes the effect of long distance electromagnetic corrections. Short distance radiative effects are universal and cancel in the ratio. In the approximation of point-like kaons and pions, the long distance electromagnetic corrections depend only on particle masses. The dominant uncertainty on δ_{EM} comes from terms depending on the hadronic structure. Most analysis to date make use of the results quoted in ref. [42; 43], which was computed using a model with Breit - Wigner form factors for the low - lying vector resonances. These results give $\delta_{EM} = -0.0070(35)$ (see [44]). Using chiral perturbation theory (ChPT)[40; 45], it has been shown that to leading non trivial order $\mathcal{O}(e^2p^2)$, the structure dependent corrections to δ_{EM} can be expressed in terms of the electromagnetic pion mass splitting. With the relative theoretical uncertainty estimated at 25% to account for $\mathcal{O}(e^2p^4)$ effects suppressed by chiral power counting, one obtains

$$\delta_{EM} = -0.0070(18)\ . \tag{1.84}$$

With experimental measurements of the inclusive K_{l2} and π_{l2} decay rates and precise knowledge of the radiative corrections, eq. (1.83) can be used to obtain the value of the product $|V_{us}/V_{ud}|^2 \times f_K^2/f_\pi^2$, from which one can estimate V_{us} once estimated the ratio f_K/f_π on the lattice.

1.3.2 Semileptonic Kaon decays

Semileptonic decays are processes in which the final state is composed of leptons and hadrons; among them one can quote

$$N \to N' + e^{\pm} + \nu_e(\bar{\nu}_e) \tag{1.85}$$

$$\pi^+ \to \pi^0 + e^+ + \nu_e \tag{1.86}$$

$$k^+ \to \pi^0 + e^+ + \nu_e \tag{1.87}$$

$$D^+ \to \bar{K}^0 + e^+ + \bar{\nu}_e \tag{1.88}$$

where N is a generic nucleus and N' differs from N by one $u \to d$ in the valence content. In each decay the quark underlying process is $q \to q'' l \nu_l$ and the quark q' participate only as *spectator* (see fig. 1.4).

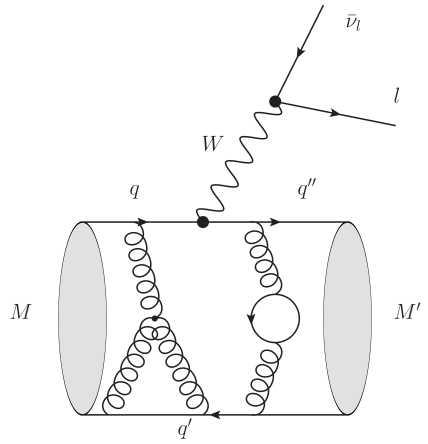

Figure 1.4: Semileptonic decay prototype - Feynman diagram which contribute to the semileptonic decay process $M \to M' l \bar{\nu}_l$. The hadronic part (bottom) must be evaluated by means of non perturbative methods.

In this case the situation is much more complicated, with respect to the leptonic case, because of the composition of the final state (leptons plus an hadron); writing

the initial state meson as M and the final state one as M', the Feynman amplitude for the process, at lowest order in the electroweak interaction but all orders in the strong interaction, can be written as

$$A(M \to M' l \nu_l) = -\frac{G_F}{\sqrt{2}} V_{q'q}^* \langle M' l^- \nu_l | \left[\bar{\nu}_l \gamma_\mu \left(1-\gamma^5\right) l\right] \left[\bar{q} \gamma^\mu \left(1-\gamma^5\right) q'\right] | M^- \rangle \ ; \quad (1.89)$$

however, the amplitude factors out in an hadronic times a leptonic part. This is again because the leptons present in the final state do not strongly interact and moreover because the hadronization process involves only the valence quark of the final state meson. This can be written as

$$A(M \to M' l^- \nu_l) = -\frac{G_F}{\sqrt{2}} V_{q'q}^* \langle l^- \nu_l | \, \bar{\nu}_l \gamma_\mu \left(1-\gamma^5\right) l \, |0\rangle \, \langle M' | \, \bar{q} \gamma^\mu \left(1-\gamma^5\right) q' \, | M \rangle \ . \quad (1.90)$$

Limiting our attention to the case in which the J^P of the initial state is the same of the final state one, that is $0^- \to 0^-$ decays which, by the way, are the subject of the present work, the hadronic matrix element receive only the vector contribution and we are left with

$$A(M \to M' l^- \nu_l) = -\frac{G_F}{\sqrt{2}} V_{q'q}^* H^\mu L_\mu \quad (1.91)$$

where

$$H^\mu \doteq \langle M'(k) | \, \bar{q} \gamma^\mu q' \, | M(p) \rangle \ , \quad (1.92)$$

$$L^\mu \doteq \langle l \bar{\nu}_l | \, \bar{l} \gamma^\mu \left(1-\gamma^5\right) \nu_l \, |0\rangle \ . \quad (1.93)$$

Eq. (1.92) tell us that the matrix element transform as a vector and so we can parametrize it using the only two vectors at our disposal in the process, *i.e.* the initial state meson momentum p and the final state meson one k, so

$$\langle M'(k) | \, \bar{q} \gamma^\mu q' \, | M(p) \rangle = (p+k)_\mu f_+(q^2) + q_\mu f_-(q^2) \quad (1.94)$$

where we have used the independent linear combinations $p+k$ and $q = p-k$ and hadronic effects, which do not follow by symmetry arguments, are described by means

of the form factors $f_{\pm}(q^2)$. $f_+(q^2)$ is called *vector* form factor and usually $f_-(q^2)$ is traded for the *scalar* form factor, defined as

$$f_0(q^2) = f_+(q^2) + \frac{q^2}{M_f^2 - M_i^2} f_-(q^2) \tag{1.95}$$

which satisfy the kinematic constraint $f_0(0) = f_+(0)$ and where $M_i(M_f)$ is the mass of the meson state $M(M')$.

Let us specialize to the case, relevant for this work, of the kaon semileptonic decays; these decays are the relevant one for extracting the CKM matrix element V_{us} and their prototype is represented by processes such as

$$K^+ \to \pi^0 + l^+ + \nu_l \tag{1.96}$$

$$K^0 \to \pi^+ + l^- + \bar{\nu}_l \tag{1.97}$$

which are usually called K_{l3} decays and in which the underlying quark transition is $s \to u + W^-$. The partial conservation of the vector current (PCVC)

$$\partial^\mu V_\mu^a = i\bar{\psi}\left[\frac{\lambda^a}{2}, m\right]\psi \ , \tag{1.98}$$

where $V_\mu^a = \bar{\psi}\gamma^\mu t^a \psi$ is the non singlet vector current, m is the quark mass matrix and $t^a = \lambda^a/2$ are the $SU(3)$ generators, can be considered for the $s \to u$ transition under exam, obtaining

$$\partial_\mu \left(\bar{u}\gamma^\mu s\right) \propto \left(m_s - m_u\right)\bar{u}s \ , \tag{1.99}$$

where $m_{s(u)}$ is the mass of the *s(u)* quark; Neglecting $SU(3)_V$ flavour breaking effects, *i.e.*

$$\delta m \to 0 \ \Rightarrow \ \partial_\mu V^\mu = 0 \tag{1.100}$$

a conserved current and a related conserved charge will exist and it is possible to show that

$$f_-(q^2) = 0\,, \tag{1.101}$$

$$f_+(0) = 1\,. \tag{1.102}$$

However for the $\delta m = m_s - m_u$ under exam, one can not neglect isospin breaking and so this means non conservation of the vector current and an $f_+(0) \neq 1$; in particular the Ademollo Gatto (AG) theorem [46], which will be explained in details in section 1.3.3, ensures that corrections to (1.102) are of second order in the breaking parameter δm. In this situation lattice QCD plays an important role as one is obliged to use a non perturbative estimate of the form factor to extract the CKM matrix elements, similarly to what happened in the leptonic channel. To be more precise, experimentally one can measure the photon inclusive $K \to \pi l \nu_l$ decay rate [23] which is described by the *master formula*

$$\Gamma_{K_{l3}} = \frac{G_F^2 m_K^5}{192\pi^3} C_K^2 S_{EW} \left(|V_{us}| f_+(0)\right)^2 I_{Kl} \times \left(1 + \delta_{EM}^{Kl} + \delta_{SU(2)}^{K\pi}\right)^2 . \tag{1.103}$$

where $S_{EW} = 1.0232(3)$ [41; 47] is the short-distance electroweak correction, C_K is a Clebsch-Gordan coefficient (1 for K^0 and $1/\sqrt{2}$ for $K^\pm$ decays), I_{Kl} is a phase space integral that is sensitive to the momentum dependence of the form factors, δ_{EM}^{Kl} is a channel dependent long distance EM correction and $\delta_{SU(2)}^{K\pi}$ a correction which takes into account isospin breaking. To extract $|V_{us}|$ from K_{l3} decays using (1.103), one must measure K_{l3} decay rate, compute the phase space integrals from the form factors measurement and make use of theoretical results for δ_{EM}^{Kl}, $\delta_{SU(2)}^{K\pi}$ and $f_+(0)$. On the theoretical side instead, one will have to calculate the $K \to \pi$ vector form factor at zero momentum, which will be one of the main results of this work, and extract the CKM matrix element V_{us} using the latest experimental result [23] for the product $(f_+(0)|V_{us}|^2) = 0.2163 \pm 0.0005$.

1.3.3 Ademollo Gatto theorem

We have said, in the previous section, that the deviation of $f_+(0)$ from unity is predicted to be second order in the $SU(3)$ symmetry breaking, *i.e.* $(m_s - m_l)^2$ where m_l is the mass of the light *u,d* quarks. We are going to prove this result, the so-called *Ademollo-Gatto* (AG) theorem, following the proof given in [48].

Let us consider the commutation of the quark vector charges,

$$\left[Q^{\bar{u}s}, Q^{\bar{s}u}\right] = Q^{\bar{u}u-\bar{s}s}\,, \tag{1.104}$$

where

$$Q^{\bar{i}j} \equiv \int d^3x \bar{q}_i(x)\gamma_0 q_j(x)\,. \tag{1.105}$$

Taking matrix elements between $K^0 - out$ and $K^0 - in$ ($|K^0\rangle = |d\bar{s}\rangle$) and inserting a complete set of intermediate states give

$$1 = \sum_n \left(|\,\langle n|\,Q^{\bar{s}u}\,|K^0\rangle\,|^2 - |\,\langle n|\,Q^{\bar{u}s}\,|K^0\rangle\,|^2\right)\,. \tag{1.106}$$

Finally we can isolate the single π^- state from the sum and note that in the $SU(3)_V$ limit the charge operator can only connect the kaon to another state within the *same* $SU(3)_V$ multiplet. This implies

$$\langle n \neq \pi^-|\,Q^{\bar{u}s}\,|K^0\rangle = \mathcal{O}(\epsilon)\,, \tag{1.107}$$

where ϵ is a measure of $SU(3)$ breaking, and thus we conclude that

$$1 - [f_+(0)]^2 = \mathcal{O}(\epsilon^2)\,, \tag{1.108}$$

which is the result we were seeking. This theorem has a number of important consequences and it will prove itself useful in section 4.7.2 when we will treat the *strange quark quenching* of our simulation setup.

1.4 CP violation

Within the standard model and its possible extensions, $\mathcal{CP}$ symmetry can be violated both in the electroweak and strong sector. In section 1.2.1 we have introduced the CKM matrix and explained that, being a 3×3 unitary matrix, it can be parametrized

by means of three angles and one phase. It is this one phase that makes some coupling of the W^+ boson to quarks complex and allows the presence of $\mathcal{CP}$ violation in the electroweak sector. However it is known from [2] that this phase can be removed in a theory with only two generations and this means that the phase of V_{CKM} can have physical consequences only in a process that involves all three generations and in practice it will manifest itself only in processes involving weak interaction loop correction or in complicated exclusive decays. Thus the $SU(3)_c \times SU(2)_L \times U(1)_Y$ theory can account for $\mathcal{CP}$ violation and it also explains why this effect is much weaker even than the weak interaction. It is interesting to note that Kobayashi and Maskawa originally proposed the existence of a third generation in order to provide a mechanism for $\mathcal{CP}$ violation [3]. At this moment there is no conclusive evidence that the origin of $\mathcal{CP}$ violation is only in the phase of CKM matrix. More general model of Higgs sector may lead to a more complicated set of quarks - Higgs couplings, and some of them may be $\mathcal{CP}$ violating as well.

There is also a still unexcluded source of $\mathcal{CP}$ violation, which finds its place in the strong sector of the theory. To simplify the Lagrangian of the gauge theory of quarks to its final form, we performed chiral rotations of the quarks fields (see e.g. (1.27), (1.28) and so on) and such a change of variable is able to introduce in the theory[1] a new T- and P- violating term. It can be shown, using the fact that these terms are total derivative, that the ones involving $SU(2)_L$ and $U(1)_Y$ field strengths have no observable effects (they can be integrated out) while the term involving QCD field strength can induce a neutron *electric dipole moment* (EDM). This is due to the fact that after the chiral rotation a term which is a total derivative involving the QCD gluon field strenghts is generated, but this term does not vanish in the integration over the whole space-time because of the presence of non trivial topological excitations, called *instantons*. Even if the present experimental upper limit on the neutron EDM is of $d_N < 6.3\dot{1}0^{-26}$, the possible existence of such a phenomenon would imply a T- violating effect which, considering the validity of the $\mathcal{CPT}$ theorem, means a $\mathcal{CP}$ violating effect in the strong sector.

The next two section will be dedicated to discuss weak and strong $\mathcal{CP}$ violation. We will start with a very brief introduction, in section 1.4.1, of the basic concepts

[1] This will became much more clear in section 1.4.2 of this chapter when the functional formalism will be introduced.

of particle-antiparticle mixing and weak $\mathcal{CP}$ violation, introducing the parameters ϵ and ϵ' relative to the standard classification of the so called *indirect* and *direct* $\mathcal{CP}$ violation[1]. In section 1.4.2 we will focus our attention to the strong $\mathcal{CP}$ violation as it is the responsible for neutron EDM, one of the most challenging observables in lattice QCD.

1.4.1 Weak CP violation

Let us start our discussion with the phenomenon of particle-antiparticle mixing, which is responsible for the *indirect* $\mathcal{CP}$ violation in the K system, discovered in 1964. Being a process known as *flavour changing neutral current* (FCNC), in the Standard Model it appears only at one loop level and involves heavy quark loops. It is consequently a sensitive measure of the top (t) quark couplings V_{ti} ($i = d, s, b$) and of the top quark mass. On the basis of the SM theory, it turns out that the main new informations obtainable from the study of this phenomenon are the values of $|V_{td}|$ and of the phase δ of the CKM matrix.
$K^0 = (\bar{s}d)$ and $\bar{K}^0 = (\bar{d}s)$ are flavour eigenstates which in the Standard Model may mix via weak interactions through the *box diagram* of fig. 1.5. We will choose the phase conventions so that

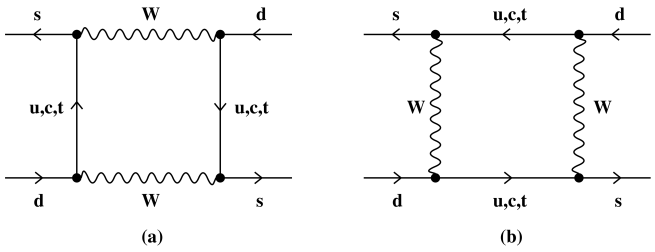

Figure 1.5: $K^0 - \bar{K}^0$ **mixing.** - Box diagram contributing to $K^0 - \bar{K}^0$ mixing in the Standard Model; picture taken from [49] (Buras 2001)

$$\mathcal{CP}\,|K^0\rangle = -\,|\bar{K}^0\rangle\,, \quad \mathcal{CP}\,|\bar{K}^0\rangle = -\,|K^0\rangle\ . \tag{1.109}$$

[1] We will use here the standard approach to the subject and split $\mathcal{CP}$ violating processes in *direct* and *indirect*, even if it exists a different and probably much more useful classification, as can be read in [49].

In the absence of mixing the time evolution of $|K^0(t)\rangle$ would be given by

$$|K^0(t)\rangle = |K^0(0)\rangle\, exp\,(-iHt)\,, \quad H = M - i\frac{\Gamma}{2}\,, \tag{1.110}$$

where M is the mass and Γ the width of K^0. A similar formula would hold for $\bar{K}^0$. On the other hand, in the presence of flavour mixing the time evolution of the $K^0 - \bar{K}^0$ system (with wave function ψ) can be described by

$$i\frac{d\psi(t)}{dt} = \hat{H}\psi(t) \quad \psi(t) = \begin{pmatrix} |K^0(t)\rangle \\ |\bar{K}^0(t)\rangle \end{pmatrix}\,, \tag{1.111}$$

where

$$\hat{H} = \hat{M} - i\frac{\hat{\Gamma}}{2} = \begin{pmatrix} M_{11} - i\frac{\Gamma_{11}}{2} & M_{12} - i\frac{\Gamma_{12}}{2} \\ M_{21} - i\frac{\Gamma_{21}}{2} & M_{22} - i\frac{\Gamma_{22}}{2} \end{pmatrix}\,, \tag{1.112}$$

with $\hat{M}$ and $\hat{\Gamma}$ being hermitian matrices having positive (real) eigenvalues. M_{ij} and Γ_{ij} are the transition matrix elements from virtual and physical intermediate states respectively. Setting

$$M_{21} = M_{12}^*\,, \quad \Gamma_{21} = \Gamma_{12}^* \quad \text{(hermiticity)}, \tag{1.113}$$

$$M_{11} = M_{22}^* \equiv M\,, \quad \Gamma_{11} = \Gamma_{22}^* \equiv \Gamma \quad \text{(CPT)}, \tag{1.114}$$

we have

$$\hat{H} == \begin{pmatrix} M - i\frac{\Gamma}{2} & M_{12} - i\frac{\Gamma_{12}}{2} \\ M_{12}^* - i\frac{\Gamma_{12}^*}{2} & M - i\frac{\Gamma}{2} \end{pmatrix}\,. \tag{1.115}$$

The next step is to diagonalize the system to obtain the mass *eigenstates*

$$K_{L,S} = \frac{(1+\bar{\epsilon})K^0 \pm (1-\bar{\epsilon}\bar{K}^0)}{\sqrt{2(1+|\bar{\epsilon}|^2)}} \tag{1.116}$$

which are a combination of the physical K^0 and $\bar{K}^0$, with $\bar{\epsilon}$ which is a small complex parameter given by

$$\frac{1-\bar{\epsilon}}{1+\bar{\epsilon}} = \sqrt{\frac{M_{12}^* - i\Gamma_{12}^*/2}{M_{12} - i\Gamma_{12}/2}}. \tag{1.117}$$

The corresponding eigenvalues are

$$M_{L,S} = M \pm Re(Q)\ , \quad \Gamma_{L,S} = \Gamma \mp 2Im(Q) \tag{1.118}$$

with

$$Q = \sqrt{(M_{12} - i\Gamma_{12}/2)\,(M_{12}^* - i\Gamma_{12}^*/2)}\ . \tag{1.119}$$

As a consequence we have

$$\Delta M = M_L - M_S = 2Re(Q), \quad \Delta\Gamma = \Gamma_L - \Gamma_S = -4Im(Q)\ . \tag{1.120}$$

Is should be noted that the mass eigenstates K_S and K_L differ from CP eigenstates

$$K_1 = \frac{1}{\sqrt{2}}\left(K^0 - \bar{K}^0\right), \quad \mathcal{CP}\,|K_1\rangle = |K_1\rangle \tag{1.121}$$

$$K_2 = \frac{1}{\sqrt{2}}\left(K^0 + \bar{K}^0\right), \quad \mathcal{CP}\,|K_2\rangle = -\,|K_2\rangle \tag{1.122}$$

by a small admixture of the *opposite* $\mathcal{CP}$ - *parity* eigenstate:

$$K_S = \frac{K_1 + \bar{\epsilon}K_2}{\sqrt{1+|\bar{\epsilon}|^2}}, \quad K_L = \frac{K_2 + \bar{\epsilon}K_1}{\sqrt{1+|\bar{\epsilon}|^2}} \tag{1.123}$$

with $\bar{\epsilon}$ defined as in (1.117). The quantity $\bar{\epsilon}$ can also be written as

$$\frac{1-\bar{\epsilon}}{1+\bar{\epsilon}} = \frac{\Delta M - i\Delta\Gamma/2}{2M_{12} - i\Gamma_{12}} \equiv r\ exp(ik). \tag{1.124}$$

It should be stressed that the small parameter $\bar{\epsilon}$ depends on the phase convention chosen for K^0 and $\bar{K}^0$. Therefore it may not be taken as a physical measure of $\mathcal{CP}$ violation. Since $\bar{\epsilon}$ is $\mathcal{O}(10^{-3})$, we find, using (1.117) that

$$Im(M_{12}) \ll Re(M_{12}), \quad Im(\Gamma_{12}) \ll Re(\Gamma_{12}). \tag{1.125}$$

Consequently, to a very good approximation

$$\Delta M_K = 2Re(M_{12}), \quad \Delta\Gamma_K = 2Re(\Gamma_{12}), \tag{1.126}$$

where the subscript K has been added to stress the fact that these formulas apply only to the $K^0 - \bar{K}^0$ system.
The $K_L - K_S$ mass difference is experimentally measured to be $\Delta M_K = (3.491 \pm 0.009)10^{-15}\ GeV$. In the Standard Model roughly 70% of the measured ΔM_K is described by the real parts of the box diagrams with charm quark and top quark exchanges and among them the contribution of the charm exchanges is by far dominant. The remaining 30% of the measured ΔM_K is imputable to long distance contributions. $\Delta\Gamma_K$ is instead fully dominated by long distance effects. Experimentally one has $\Delta\Gamma_K = -7.4 \times 10^{-15}\ GeV$ and consequently $\Delta\Gamma_K \simeq -2\Delta M_K$. A non perturbative method is needed in order to estimate these contribution.
Since two pion final state is $\mathcal{CP}$ even while three pion final state is $\mathcal{CP}$ odd, K_S and K_L mainly decay to 2π and 3π, respectively via the following $\mathcal{CP}$ conserving decay modes:

$$K_L \to 3\pi \text{ (via } K_2), \quad K_S \to 2\pi \text{ (via } K_1). \tag{1.127}$$

This difference is responsible for the large disparity in their life-times. However, K_L and K_S are not $\mathcal{CP}$ eigenstates and may decay with small branching ratios as

$$K_L \to 2\pi \text{ (via } K_1), \quad K_S \to 3\pi \text{ (via } K_2). \tag{1.128}$$

This violation of $\mathcal{CP}$ is called *indirect* as it happens not via explicit breaking of $\mathcal{CP}$ symmetry in the decay itself but via the component of the $\mathcal{CP}$ state with opposite parity with respect to the dominant one. The measure of this indirect $\mathcal{CP}$ violation is defined as

$$\epsilon = \frac{A(K_L \to (\pi\pi)_{I=0})}{A(K_S \to (\pi\pi)_{I=0})} \,, \tag{1.129}$$

where ϵ is, contrary to $\bar{\epsilon}$, independent of the phase conventions. It can be shown that [50]

$$\epsilon = \bar{\epsilon} + i\xi \qquad \text{with} \qquad \xi = \frac{Im(A_0)}{Re(A_0)} \tag{1.130}$$

where the isospin amplitude A_0 is defined below. The phase convention dependence of the term $i\xi$ cancels the convention dependence of $\bar{\epsilon}$.

While *indirect* $\mathcal{CP}$ violation reflects the fact that the mass eigenstates are not $\mathcal{CP}$ eigenstates, the so called *direct* one is realized via a direct transition of a $\mathcal{CP}$ odd to a $\mathcal{CP}$ even state or vice versa. A measure of such *direct* $\mathcal{CP}$ violation in $K_L \to \pi\pi$ is characterized by a complex parameter ϵ' defined as

$$\epsilon' = \frac{1}{\sqrt{2}} Im\left(\frac{A_2}{A_0} e^{i\Phi}\right) \,, \quad \Phi = \pi/2 + \delta_2 - \delta_0 \,, \tag{1.131}$$

where the isospin amplitudes A_I in $K \to \pi\pi$ decays are introduced through

$$A(K^+ \to \pi^+\pi^0) = \sqrt{\frac{3}{2}} A_2 e^{i\delta_2} \tag{1.132}$$

$$A(K^0 \to \pi^+\pi^-) = \sqrt{\frac{2}{3}} A_0 e^{i\delta_0} + \sqrt{\frac{1}{3}} A_2 e^{i\delta_2} \tag{1.133}$$

$$A(K^0 \to \pi^0\pi^0) = \sqrt{\frac{2}{3}} A_0 e^{i\delta_0} - 2\sqrt{\frac{1}{3}} A_2 e^{i\delta_2} \tag{1.134}$$

Here the subscript $I = 0, 2$ denotes different isospin states equivalent to $\Delta I = 1/2$ and $\Delta I = 3/2$ transitions, respectively, and $\delta_{0,2}$ are the corresponding strong phases. The weak CKM phases are contained in A_0 and A_2. By extracting the strong phases $\delta_{0,2}$ from $\pi\pi$ scattering, it turns out that $\Phi \simeq \pi/4$.

The isospin amplitudes A_I are complex quantities which depend on phase conventions. On the other hand, ϵ' measures the difference between the phases of A_2 and A_0 and is a physical quantity.

Experimentally ϵ and ϵ' can be found by measuring the ratios

$$\eta_{00} = \frac{A(K_L \to \pi^0\pi^0)}{A(K_S \to \pi^0\pi^0)} , \quad \eta_{+-} \frac{A(K_L \to \pi^+\pi^-)}{A(K_L \to \pi^0\pi^0)} . \tag{1.135}$$

Indeed, assuming ϵ and ϵ' to be small numbers one finds

$$\eta_{00} = \epsilon - \frac{2\epsilon'}{1-\sqrt{\omega}} \simeq \epsilon - 2\epsilon' , \quad \eta_{+-} = \epsilon + \frac{\epsilon'}{1+\omega/\sqrt{2}} \simeq \epsilon + \epsilon', \tag{1.136}$$

where experimentally $\omega = Re(A_2)/Re(A_0) = 0.045$ which corresponds to the $\Delta I = 1/2$ rule. In the absence of direct $\mathcal{CP}$ violation $\eta_{00} = \eta_{+-}$. The ratio ϵ'/ϵ can then be measured through

$$\left| \frac{\eta_{00}}{\eta_{+-}} \right|^2 \simeq 1 - 6Re\left(\frac{\epsilon'}{\epsilon}\right) . \tag{1.137}$$

We will conclude here our brief remind about Standard Model's weak $\mathcal{CP}$ violation and in the next section we are going to introduce the more exotic subject of strong $\mathcal{CP}$ violation.

1.4.2 Strong CP violation

Let us introduce the so called *path* integral formalisms. It is a powerful tool which is particularly suited for non perturbative treatment of a quantum field theory, as well as, in this context, it will allow us to easily show how strong $\mathcal{CP}$ violation is generated within the Standard Model.

This technique was first introduce by Feynman [51] as an alternative mean for treating non relativistic quantum mechanics, but which is also applicable to the relativistic quantum mechanic case. The fundamental element of this approach is the *generating functional* of all the green functions of the theory which can be defined starting by the so called *functional integral*

$$\mathcal{Z}[J] = \int \mathcal{D}\phi \, e^{\frac{i}{\hbar} S_J[\phi]} , \tag{1.138}$$

in which the integration measure is defined as the product of the differential of all elementary fields involved in the theory under consideration (for QCD one has the

differential of quark and gluon fields), in each space-time point, for each degree of freedom and ϕ is a generic field which stands for any field (spinorial, scalar or vectorial) from which the functional $S_J[\phi]$ may depend; $S_J[\phi]$ is the classical action for the theory's fields plus an interaction term of the kind

$$\int d^4x\ \phi_i(x) J_i(x) \tag{1.139}$$

in which fields are coupled with a generic source J_i ($i = 1, \ldots, n$ with n the number of fields of the theory) in order that, after defining the *generating functional* as $\mathcal{W} = \log \mathcal{Z}$, one is able to calculate all the relevant Green functions of the theory by simply taking the functional derivative of $\mathcal{W}$ and then setting the sources equal to zero. In the scalar case one has

$$\langle \phi(x_1) \ldots \phi(x_n) \rangle = \left. \frac{\delta \mathcal{W}}{\delta J(x_1) \ldots \delta J(x_n)} \right|_{J=0} . \tag{1.140}$$

From this is easy to prove that the expectation value of a generic operator $\mathcal{O}$, which is a function of the fields of the theory, can be written as

$$\langle \mathcal{O}(\phi) \rangle = \frac{1}{\mathcal{Z}[0]} \int \mathcal{D}\phi\ \mathcal{O}(\phi)\ e^{\frac{i}{\hbar} S_0[\phi]} , \tag{1.141}$$

where $\mathcal{Z}[0]$, as well as $S_0(\phi)$, are calculated for $J = 0$.

Expression (1.138), as it is, represents an ill-defined integral and it needs further explanations; from a mathematical point of view the *functional integral* can be regarded as an infinite field configuration sum, each weighted with an oscillating exponential factor which can not guarantee the convergence of an infinite sum. This is the reason why it is useful to consider the same theory but in a euclidean space, by means of the *Wick rotation* ($x^0_E = i x^0_M$ e $x^i_E = x^i_M$), carry out all the calculation in that space and then rotate back to the physical Minkowsky space-time. In the euclidean space, in particular, the complex exponential factor becomes a real and decreasing one. The analytic continuation to Minkowskyan space can be done only if the *Osterwalder−Schrader* positivity constraint [52] is fulfilled. Unless otherwise specified, we will always consider euclidean quantum field theories from now on. The actions, in the different geometric spaces, are connected by

$$iS = -S_E, \tag{1.142}$$

and so the functional integral, in the euclidean space, can be regarded as the partition function of a statistical system, with Boltzmann exponential factors as weights. The euclidean version of (1.138) is

$$\mathcal{Z}[J] = \int \mathcal{D}\phi \, e^{\frac{-1}{\hbar} S_J[\phi]} \, . \tag{1.143}$$

Let us now take a look at the QCD symmetry group, and to the associated conserved currents, in order to write down Ward-Takahashi Identities (WTI) for the (euclidean) theory. The symmetry group is

$$G = SU(N_f)_L \times SU(N_f)_R \times U(1)_A \times U(1)_V \; ; \tag{1.144}$$

and WTIs are a consequence of the invariance of (1.141) under (non-anomalous) local changes of fermionic integration variables (with α as local parameter):

$$\left\langle \frac{\delta \mathcal{O}(x_1, \ldots, x_n)}{\delta \alpha}\bigg|_{\alpha=0} \right\rangle - \left\langle \mathcal{O}(x_1, \ldots, x_n) \frac{\delta S}{\delta \alpha}\bigg|_{\alpha=0} \right\rangle = 0 \, . \tag{1.145}$$

in this case the action in (1.145) must be the QCD action which can be obtained from lagrangian (1.3) with gluon and quark fields as, respectively, bosonic and matter degree of freedom.

In the case of infinitesimal $SU(N_f)_L \times SU(N_f)_R \times U(1)_V$ there are no anomalies and using (1.145) one obtains

$$U(1)_V : \frac{\delta S}{\delta \alpha_V}\bigg|_{\alpha_V=0} = -\partial_\mu(\bar{\psi}\gamma_\mu\psi) \tag{1.146}$$

$$SU(N_f)_V : \frac{\delta S}{\delta \alpha_V^a}\bigg|_{\alpha_V^a=0} = -\partial_\mu(\bar{\psi}\gamma_\mu\frac{\lambda^a}{2}\psi) - \bar{\psi}\left[\frac{\lambda^a}{2}, m\right]\psi \tag{1.147}$$

$$SU(N_f)_A : \frac{\delta S}{\delta \alpha_A^a}\bigg|_{\alpha_A^a=0} = -\partial_\mu(\bar{\psi}\gamma_\mu\gamma^5\frac{\lambda^a}{2}\psi) - \bar{\psi}\left\{\frac{\lambda^a}{2}, m\right\}\gamma^5\psi \tag{1.148}$$

where the sum over flavour is understood and the λ^a matrices are the Gell-Mann matrices acting in flavour space. It is clear that all the currents are conserved in the limit of massless quarks.

The last symmetry law, $U(\mathbb{1})_A$, deserves a special treatment: at a *naïve* level, treating this symmetry as a non anomalous one, one obtains

$$U(\mathbb{1})_A : \left.\frac{\delta S}{\delta \alpha_A}\right|_{\alpha_A=0} = -\partial_\mu(\bar{\psi}\gamma_\mu\gamma^5\psi) - 2im(\bar{\psi}\gamma^5\psi) \ + \ldots \tag{1.149}$$

where the dots are there to underline that this current is the only one which is not conserved in the massless quark limit because of the presence of the so called *anomalous* term. This term is not calculable by means of (1.145) and is a typical example of a classical symmetry[1] which is spoiled at the quantum level.

The reason why (1.145) gives an incomplete answer is that it has been obtained under the assumption of performing a local change of variable which *leaves the integration measure invariant*; while under the chiral singlet rotation

$$\psi'_{L,R}(x) = \left(1 \mp i\frac{\alpha}{2}\right)\psi_{L,R}(x) \tag{1.150}$$

$$\bar{\psi}'_{L,R}(x) = \bar{\psi}_{L,R}(x)\left(1 \pm i\frac{\alpha}{2}\right) \tag{1.151}$$

the measure of the functional integral $\mathcal{D}\phi \equiv \mathcal{D}\psi\mathcal{D}\bar{\psi}$ in (1.143) changes according to [53; 54]

$$\left(\mathcal{D}\psi\mathcal{D}\bar{\psi}\right)' = \mathcal{D}\psi\mathcal{D}\bar{\psi}\ e^{iN_f\alpha\int d^4x \frac{g^2}{32\pi^2}G^a_{\mu\nu}\tilde{G}^{a,\mu\nu}} \tag{1.152}$$

where $\tilde{G}^{a,\mu\nu} = \frac{1}{2}\epsilon^{\mu\nu\rho\sigma}G^a_{\rho\sigma}$ is the dual of the gluonic field $G_{\mu\nu}$. Performing (1.150) and (1.151) transformations and applying (1.145) taking now into account (1.152) gives

$$\left.\frac{\delta S}{\delta \alpha_A}\right|_{\alpha_A=0} = -\partial_\mu(\bar{\psi}\gamma_\mu\gamma^5\psi) - 2im(\bar{\psi}\gamma^5\psi) + N_f\frac{g^2}{32\pi^2}G^a_{\mu\nu}\tilde{G}^{a,\mu\nu} \tag{1.153}$$

which is the correct anomalous WTI as found in [55; 56; 57].

We have now all the elements to understand how this affect the Standard Model lagrangian via the so called *strong* $\not{C}\not{P}$ problem. Let us see the problem from an *"inverse"*

[1] With *classical* symmetry we mean a symmetry which is an exact one at a lagrangian level.

point of view, following [10]: in the massless limit, even if QCD is formally invariant under a $U(\mathbb{1})_A$ transformation (1.150), the chiral anomaly (1.153) affects the action through

$$\Delta S = \alpha \int d^4x\, \partial_\mu J_5^\mu = \alpha \frac{g_s^2 N_f}{32\pi^2} \int d^4x\, G^{a\mu\nu} \tilde{G}^a_{\mu\nu} \tag{1.154}$$

where $J_5^\mu = \bar{\psi}\gamma_\mu\gamma^5\psi$. It is known [58] that the $G\tilde{G}$ term of (1.153) can be written as a total divergence

$$G^{a\mu\nu}\tilde{G}^a_{\mu\nu} = \partial_\mu K^\mu \tag{1.155}$$

where

$$K^\mu = \epsilon^{\mu\alpha\beta\gamma} A^a_\alpha \left(G^a_{\beta\gamma} - \frac{g_s}{3} f_{abc} A^b_\beta A^c_\gamma \right). \tag{1.156}$$

This means that the variation (1.154) is a surface integral

$$\Delta S = \alpha \frac{g_s^2 N_f}{32\pi^2} \int d^4x\, \partial_\mu K^\mu = \alpha \frac{g_s^2 N_f}{32\pi^2} \int d\sigma_\mu K^\mu \,. \tag{1.157}$$

Hence, using the *naïve* boundary condition that $A^a_\mu = 0$ at (spatial) infinity, one has $\int d\sigma_\mu K^\mu = 0$, and $U(1)_A$ appears to be a symmetry again. What was pointed out by 't Hooft [59; 60; 61], however, is that the correct boundary condition to use is that A^a_μ should be a pure gauge field at (spatial) infinity, *i.e.*, either $A^a_\mu = 0$ or a gauge transformation of 0. It turns out that, with these boundary conditions, there are gauge configurations for which $\int d\sigma_\mu K^\mu \neq 0$ and thus $U(1)_A$ is not a symmetry of QCD.
This is most easily exemplified by working in the A^a_0 gauge. Studying $SU(2)$ QCD for simplicity, in this gauge [62], one has only spatial gauge fields A^a_i and under a gauge transformation these fields transforms as

$$\frac{1}{2}\tau^a A^a_i \doteq A_i \to \Omega A_i \Omega^{-1} + \frac{i}{g_s} \nabla^i \Omega \Omega^{-1} \,, \tag{1.158}$$

where τ^a are $SU(2)$ generators. Thus, vacuum configurations either vanish or have the form $ig_s^{-1}\nabla^i\Omega\Omega^{-1}$. In the $A_0^a = 0$ gauge, one can further classify these vacuum configurations by how Ω goes to unity as $r \to \infty$:

$$\Omega \to e^{i2\pi n} \quad \text{as} \quad r \to \infty \text{ with } n = 0, \pm 1, \pm 2, \dots \ . \tag{1.159}$$

The integer n, the winding number, is related to the Jacobian of an $S_3 \to S_3$ map and is given by [63]

$$n = \frac{ig_s^3}{24\pi^2} \int d^3r \ Tr\left(\epsilon_{ijk} A^i A^j A^k\right) \ . \tag{1.160}$$

This expression is closely related to the Bardeen current K^μ. Indeed, in the $A_0^a = 0$ gauge, only $K^0 \neq 0$ and one finds for pure gauge fields

$$K^0 = -\frac{g_s}{3}\epsilon_{ijk}\epsilon_{abc}A_a^i A_b^j A_c^k = \frac{4}{3} i g_s \epsilon_{ijk} Tr\left(A^i A^j A^k\right) \ . \tag{1.161}$$

The true vacuum is a superposition of these, so called, *n-vacua* and is called $\theta-vacuum$

$$|\theta\rangle = \sum_n e^{-in\theta} |n\rangle \, . \tag{1.162}$$

It is easy to see that in the vacuum to vacuum transition amplitude there are transitions with $\int d\sigma_\mu K^\mu \neq 0$. Indeed

$$n|_{t=+\infty} - n|_{t=-\infty} = \frac{g_s^2}{24\pi^2} \int d\sigma_\mu K^\mu \Big|_{t=-\infty}^{t=+\infty} \ . \tag{1.163}$$

Using (1.163) one can write the vacuum to vacuum transition amplitude as

$$\langle \theta^+ | \, \theta^- \rangle = \sum_{m,n} e^{im\theta} e^{-in\theta} \langle m^+ | \, n^- \rangle = \sum_\nu e^{i\nu\theta} \sum_n \langle (n+\nu)^+ | \, \nu^- \rangle \ . \tag{1.164}$$

It is easy to see that the difference in winding number ν is

$$\nu = \frac{g_s^2 N_f}{32\pi^2} \int d\sigma_\mu K^\mu \Big|_{t=-\infty}^{t=+\infty} = \frac{g_s^2}{32\pi^2} \int d^4x \; G^{a\mu\nu} \tilde{G}^a_{\mu\nu} \; . \tag{1.165}$$

Using now the path integral representation for the vacuum to vacuum amplitude $\langle \theta^+ | \, \theta^- \rangle$ one finds

$$\langle \theta^+ | \, \theta^- \rangle = \sum_\nu \int \mathcal{D}A \; e^{iS_{eff}[A]} \delta \left(\nu - \frac{g_s^2}{32\pi^2} \int d^4x \; G^{a\mu\nu} \tilde{G}^a_{\mu\nu} \right) \; , \tag{1.166}$$

where

$$S_{eff}\,[A] = S_{QCD}\,[A] + \theta \frac{g_s^2}{32\pi^2} \int d^4x \; G^{a\mu\nu} \tilde{G}^a_{\mu\nu} \; . \tag{1.167}$$

The resolution of the $U(1)_A$ problem, by recognizing the complicated nature of the QCD vacuum, effectively adds an extra term to the QCD lagrangian

$$\mathscr{L}_\theta = \theta \frac{g_s^2}{32\pi^2} G^{a\mu\nu} \tilde{G}^a_{\mu\nu} \; . \tag{1.168}$$

This term violates parity and time reversal invariance but conserves charge conjugation invariance, so it violates $\mathcal{CP}$. It induces a neutron EDM d_n which, with the strong experimental bound of $|d_n| < 3 \times 10^{-26}$ *e cm* [64], implies $\theta < 10^{-9}$. Why this should be so is known as *strong* $\mathcal{CP}$ *problem*.

If besides QCD, one include also the weak interaction, as we have already seen, the quark mass matrix is complex (see (1.7)); to go to a physical basis, one must diagonalize this mass matrix and when does so, in general, one performs a chiral transformation of the kind (1.150)-(1.151) that changes θ by $\theta_{EW} = arg \; detM$. So, in the Standard Model, the coefficient of $G\tilde{G}$ is

$$\bar{\theta} = \theta + \theta_{EW} = \theta + \; \arg \det \mathrm{M} \; \; . \tag{1.169}$$

The strong $\mathcal{CP}$ problem is why this angle, which is the result of a fine tuning between strong and weak effects, results to be so small.

Whatever the order of magnitude of θ is, the interesting thing is that (1.168) is able to generate a neutron EDM, whose standard definition can be written as

$$\vec{d}_N \equiv \int d^3y \ \vec{y} \ {}_\theta\langle N|J_0(y)|N\rangle_\theta \ , \tag{1.170}$$

where J_0 is the time component of the *e.m.* current operator. If the θ-term (1.168) is neglected in the QCD Lagrangian, then the moment $\vec{d}_N$ identically vanishes. Treating $\mathscr{L}_\theta$ as a perturbation at first order, one has

$$\vec{d}_N \equiv -i\theta \frac{g^2}{32\pi^2} \int d^3y \ \vec{y} \ {}_0\langle N|J_0(y) \left[\int d^4x \ G\widetilde{G}(x) \right] |N\rangle_0 \ , \tag{1.171}$$

where $|N\rangle_0$ is a shorthand for $|N\rangle_{\theta=0}$. As well known [11], the direct calculation of (1.171) is a difficult task due to the presence of the topological charge operator. Therefore, the authors of [12] have investigated the possibility of replacing the insertion of the topological charge with the *OZI-violating* (which will be called *quark-disconnected* from now on) insertions of the flavor-singlet pseudoscalar density

$$P_S(x) = \bar{u}(x)\gamma_5 u(x) + \bar{d}(x)\gamma_5 d(x) + \bar{s}(x)\gamma_5 s(x). \tag{1.172}$$

in the presence of the charge density operator J_0. To this end, in [12], it has been shown that exploiting the axial ward identity (1.148) and the anomalous one (1.153), within the functional expectation value (1.141) in presence of the θ–term (1.168), expression (1.171) can be rewritten as

$$2N_f \frac{g_s^2}{32\pi^2} \int d^4x \ \langle \mathcal{O} G\widetilde{G}(x)\rangle = -2\overline{m} \int d^4x \ \Big\{ \ [\langle \mathcal{O} P_S(x)\rangle]_{disc.(a)} + [\langle \mathcal{O} P_S(x)\rangle]_{disc.(b)} \ \Big\} \tag{1.173}$$

with $\bar{m}^{-1} = (m_u^{-1} + m_d^{-1} + m_s^{-1})/3$ and the operator $\mathcal{O}$ of interest, looking at the definition (1.171), is given by

$$\mathcal{O} = \ N_\alpha(z) \ J_0(y) \ \bar{N}_\beta(0) \tag{1.174}$$

where $J_0(y)$ is the *e.m.* charge density

$$J_0(y) = e_u\ \bar{u}(y)\gamma_0 u(y) + e_d\ \bar{d}(y)\gamma_0 d(y) + e_s\ \bar{s}(y)\gamma_0 s(y)\ , \tag{1.175}$$

and $N_{\alpha(\beta)}$ are the interpolating fields of the neutron [65]

$$N_\alpha = \frac{1}{\sqrt{6}}\ \varepsilon^{ijk} d^i_\alpha \left(d^{Tj}\mathcal{C}\gamma_5 u^k\right) \tag{1.176}$$

i, j, k being color indexes, α and β Dirac spinor indexes, and $\mathcal{C}$ the charge conjugation operator. It is worth mentioning that the author of [12] have found that quark-connected diagrams do not contribute to the matrix element (1.173), as already found in [66]. A pictorial representation of all the explicit diagrams contributing to $[\langle \mathcal{O} P_S(x)\rangle]_{disc.(a)}$ and $[\langle \mathcal{O} P_S(x)\rangle]_{disc.(b)}$ is shown in figure 1.6. Note that: i) in the $SU(3)$ symmetric limit the diagrams of type (b) vanish, because the disconnected insertions of the charge density J_0 are zero due to the relation $e_u + e_d + e_s = 0$; ii) the r.h.s. of (1.173) is proportional to $\overline{m}$. Since $\overline{m} = 0$ when at least one of the quark masses is zero, the insertion of the topological charge has no effect in such a limit and the neutron EDM is vanishing; iii) the only insertions of the singlet pseudoscalar density, which are left in the final result (1.173), are those disconnected diagrams which are related to the operator $G\widetilde{G}$ via the anomaly.

Let us now close this section stressing out that it is now clear that the bulk of the neutron EDM calculation, as well as the main obstacle, will be the evaluation of these *disconnected insertions*, as these are known to be very difficult and time consuming quantities to be evaluated on the lattice. The details about their structure, in terms of the all-to-all fermionic propagator, as well as the present available techniques for calculating these diagrams, will be treated in section 3.3.1 in the (much more) simple case of the mesonic π^0 and 2–flavour η' correlation functions. The results and our final remarks about the different methods within this framework will be given in chapter 4.

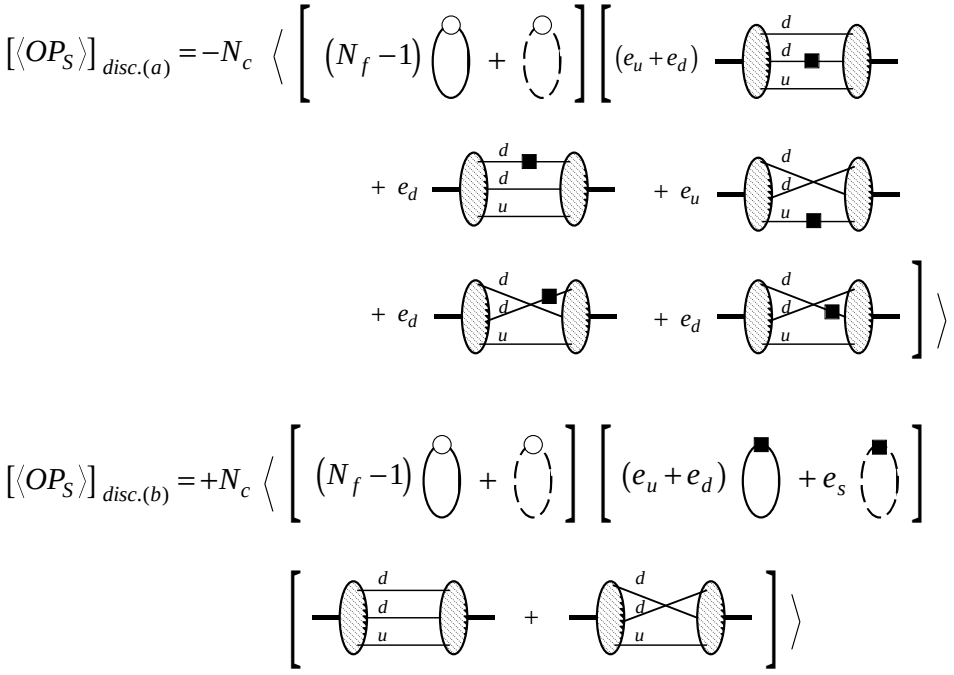

Figure 1.6: neutron EDM topology - The disconnected diagrams contributing to the r.h.s. of (1.173). Solid lines are u- and d-quark propagators, while dashed lines are s-quark propagators; the hatched ovals are the operators which create and destroy the neutron while open dots and full squares represent the insertion of γ_5 (P_S) and γ_0 (J_0), respectively. Gluon lines as well as extra quark loops are not shown; as already explained in the text quark-connected diagrams do not contribute to the relevant matrix element (1.173). Picture taken from [12] (Guadagnoli et al.).

2

Lattice Quantum Chromodynamics

This chapter will be dedicated to explain in details the technique used in this work for the non perturbative estimate of hadronic observables, which is lattice QCD (LQCD). We will start describing the fundamental theory of the strong interaction together with a particular formulation of quantum field theories, the so called Feynman's *path integral* [51] which is a well suited approach for numerical simulations. We will then show how to simulate quarks and gluons on a discrete lattice, and in particular we will discuss the *twisted mass* action which is a particular kind of fermionic action, as well as how to overcome the kinematic constraint imposed to the lattice momenta by the finite volume. We will end the chapter showing how in practice it is possible to perform Monte Carlo simulations with the introduced lattice action.

2.1 Quantum Chromodynamics

Quantum Chromodynamics (QCD) [4; 5; 6] is the model currently accepted for describing the theory of the strong interaction. This theory exhibits two different regimes depending on whether the process has an energy greater or smaller than a characteristic scale, known as $\Lambda_{QCD} \simeq 0.2 - 0.3\ GeV$. The need to distinguish between two different ranges can be traced back to the existence of the so called *asymptotic freedom* property of QCD [5; 67; 68; 69; 70], which means that the renormalized coupling goes to zero in the high energy region ($E \gg \Lambda_{QCD}$) as the first coefficient of the β *function* expansion

is[1]

$$\beta_0 = \frac{11}{3}N_c - \frac{2}{3}N_f \tag{2.1}$$

where $N_c = 3$ is the QCD color number and N_f is the number of dynamical flavors. The coefficient β_0 remains positive as long as $N_f < 16.5$ and it is known that $N_f = 6$ in nature, and this implies that the renormalized coupling at the μ^2 scale,

$$\alpha_s(\mu) = \frac{4\pi}{\beta_0 ln(\mu^2/\Lambda_{QCD})} \ , \tag{2.2}$$

gets smaller as μ^2 grows with respect to Λ_{QCD}.

This means that in a high energy process, *i.e.* a process with a characteristic energy $E \gg \Lambda_{QCD}$, quarks can be considered as free from the mutual strong interaction and a perturbative approach is able to explain processes as deep inelastic scattering, the mass spectrum of heavy quarks bound states, hadron production from e^+e^- collisions and Drell-Yan processes [71; 72]. On the other hand, in the low energy regime $E \ll \Lambda_{QCD}$, the coupling constant becomes large and one can not use perturbative methods anymore. This assumption is necessary to explain the quark *confinement* mechanism or, in other words, the phenomena for which free quarks and gluons has never been observed; LQCD works [73] support this assumption too, even if at present an analytic demonstration is still missing. As a result, for such a theory quark or hadron mass estimates, hadronic matrix elements, decay matrix elements and so on need a non perturbative approach, as they are low energy properties.

At a more formal level, QCD is a gauge theory which possess, as elementary degree of freedom, the quark and gluon fields and more specifically it is a Yang Mills theory [29] with exact (*i.e.* unbroken) *color* symmetry $SU(3)_c$; fermionic fields (spin 1/2) are described by means of Dirac spinors and each quark flavour transforms as the fundamental representation of the gauge group (a 3) while gauge fields, which represent

[1] Let us remember that the β function is defined as

$$\frac{\partial \alpha_s}{\partial ln\mu^2} = \beta(\alpha_s) = \alpha_s \left[-\beta_0 \frac{\alpha_s}{4\pi} - \beta_1 \left(\frac{\alpha_s}{4\pi}\right)^2 - \beta_2 \left(\frac{\alpha_s}{4\pi}\right)^3 - \dots \right],$$

where α_s is related to the QCD gauge coupling constant as $\alpha_s = g_s/(4\pi)$.

the massless force carrier bosons (spin 1), transforms as the adjoint representation of $SU(3)$. We will define

$$\psi_\alpha^a \qquad \text{a=1,..}N_c \tag{2.3}$$

as fermionic field, with α as Dirac index and a as color index, and with

$$A_\mu(x) = \sum_{A=1}^{N_c^2-1} A_\mu^A(x) T^A \tag{2.4}$$

we will represent gauge boson fields. $N_c = 3$ for $SU(3)_c$, $T^A = \lambda^A/2$ are the eight generators of the symmetry group proportional to the Gell-Mann matrices (λ^A) and μ is the Lorentz index ($\mu = 1, \ldots, 4$). Using the introduced fields one can write the QCD action as

$$\begin{aligned} S_{QCD} &= \int d^4x \mathcal{L}_{QCD} = \\ &= \int d^4x \left\{ \sum_{i=1}^{N_f} \bar{\psi}_{i\alpha}^a(x)(\gamma_{\alpha\beta}^\mu D_\mu^{ab} - m_i \delta^{ab}\delta_{\alpha\beta})\psi_{i\beta}^b(x) - \frac{1}{4}\sum_{A=1}^{8} G_{\mu\nu}^A G_A^{\mu\nu} \right\} , \end{aligned} \tag{2.5}$$

where i is the flavour index which labels the different (u,d,c,s,t,b) quarks, D_μ^{ab} is the covariant derivative defined as

$$D_\mu^{ab} = (\delta^{ab}\partial_\mu - i g_s (T^A)^{ab} A_\mu^A) \tag{2.6}$$

and $G_{\mu\nu}^a$ is the gauge fields strength tensor

$$G_A^{\mu\nu} = \partial_\mu A_\nu^A - \partial_\nu A_\mu^A - g_s f^{ABC} A_\mu^B A_\nu^C \, . \tag{2.7}$$

From (2.5) is clear that the interaction between gluons and quarks is a vectorial one and that means that a mass term for each flavour is not forbidden, while on the contrary being the $SU(3)_c$ symmetry unbroken, gluons remain massless.

At present, the only known technique to perform non perturbative calculations without making specifying assumptions is to simulate the theory on a space-time lattice, following the Wilson's approach [7], as we will show in the following.

2.2 Lattice gauge theories

As we have already mention in section 1.4.2, the functional formalism is more convenient with respect to a canonical approach for the formulation of a field theory because it allows to treat different regimes in a unified formalism. One can simply add the desired interaction term, multiplied by its coupling constant, in the exponential of (1.143); then if one is studying a process in which this coupling constant is small ($\ll 1$) then one will need only to expand the exponential and (1.141) will give the usual Feynman rules for the process. To be honest, perturbation theory with lattice regularization [74] converges more slowly with respect to the dimensional regularization case, but the functional formalism allows one to obtain a non perturbative estimate of physical quantities associated to various operators using Monte Carlo techniques. This estimate is made possible by approximating the integrals in (1.141) and (1.143), defined in the formal theory on an infinite volume, on a discreet space-time of finite volume (the so called *lattice*). Hence, let us introduce an hypercubical lattice

$$\Lambda = aZ^4 = \{x | x_\mu/a \in Z\} \ , \tag{2.8}$$

where a represents the lattice spacing. Boundary conditions for such a lattice can be chosen in different ways: the most used one is employ periodic boundary conditions (PBC), and in the beginning we will suppose this is the case. In section 2.5 we will describe an alternative choice for boundary conditions, as they are going to be used in this work. On the lattice, the value of a generic field $\Phi(x)$ will be defined on each $x \in \Lambda$, and so operator mean values will become multiple integrals which can be numerically evaluated. At the same time, having introduced a lattice, allows one to non perturbatively regularize the integral (1.143) because of the inverse lattice spacing (a^{-1}) acts like an ultraviolet *cut-off* in momentum space. On a discrete lattice the only allowed momenta are

$$-\frac{\pi}{a} < p_\mu < \frac{\pi}{a} \ . \tag{2.9}$$

In what follows, we will indicate with x,y ... a set of integer numbers which identify a lattice site, with μ,ν ... the four hypercubic lattice directions and with $\hat{\mu}$,$\hat{\nu}$ ... the

corresponding unit vectors. We will also show how the integrands must be modified after undergoing the discretization they need to be put on the lattice; essentially the discretization procedure can be summarized by means of these three steps

- Integrands must be discretized;
- It must be checked that the discretization procedure of step 1 does not produce unwanted features (as the fermion doubling problem, which will be treated in section 2.2.2).
- It must be checked that in the continuum limit, $a \to 0$, the discretized integrands tend to their continuum expression and that *irrelevant* operators (which have dimension greater than 4) go to zero in that limit.

In the next sections, we will follow these three steps to get a discretized version of the fermionic as well as bosonic action and in the end we will present (2.5) in a suitable way for numerical lattice simulations.

2.2.1 Gauge bosons action

In the continuum the gauge fields G_μ are introduced, for instance, int the fermionic free field action in order to promote the global gauge invariance to a local one, which means invariance under the transformation

$$\psi(x) \longrightarrow \psi'(x) = \Lambda(x)^{-1}\psi(x) \,, \tag{2.10}$$

with the matrix Λ function of x. To obtain the invariance of the Dirac action under (2.10) the gauge field is introduced, and it is brought into the theory using the covariant derivative defined as (2.6). In this way the term $\bar{\psi}(x)\not{\partial}\psi(x)$ becomes the gauge invariant term $\bar{\psi}(x)\not{D}\psi(x)$; this substitution produce an invariant term because, in the continuum, the derivative operator depends only on infinitesimal increments. On a hypercubical lattice, however, the shortest distance different from zero is the lattice spacing a and so the (forward) derivative is defined as a ratio of finite increments

$$\partial_\mu\psi(x) \longrightarrow \nabla^f_\mu\psi(x) = \frac{\psi(x + a\hat{\mu}) - \psi(x)}{a} \tag{2.11}$$

and, as a consequence, if one consider a kinetic term either bilinear in $\nabla^f_\mu\psi(x)$ (scalar field action kinetic term) or linear in $\nabla^f_\mu\psi(x)$ (Dirac action kinetic term) non gauge invariant[1] terms of the kind $\bar{\psi}(x)\gamma_\mu\psi(x+a\hat{\mu})$ are generated. In order to restore gauge invariance, we must define a parallel transport operator which allows the field to be transported from one point of the lattice to its nearest neighbor and so it follows that a gauge field on the lattice will be associated to the b *links*, which connect nearest neighbor among them; if x is a lattice point and $x+a\hat{\mu}$ his nearest neighbor in the μ direction, the corresponding link b will be the path which goes straight from x to $x+a\hat{\mu}$. This b link will be identified with the ordered points couple as

$$b =< x+a\hat{\mu}, x >\equiv (x,\mu)\ . \tag{2.12}$$

The parallel transport operator, associated to the b link, will be the one which bring the field from x to $x+a\hat{\mu}$, and will be represented as

$$U(b)\equiv U(x+a\hat{\mu},x)\equiv U_{x\mu}\in G\ , \tag{2.13}$$

where G is the gauge symmetry group of the theory. $U(b)$ is called *link variable*. Considering an arbitrary path on the lattice,

$$\mathcal{C}=b_n\circ....\circ b_2\circ b_1\ , \tag{2.14}$$

the associated parallel transport operator will be

$$U(\mathcal{C})=U(b_n)....U(b_2)U(b_1)\equiv\prod_{b\in\mathcal{C}}U(b) \tag{2.15}$$

and is composed of link variables. We will consider as *lattice gauge field* the ensemble of all the gauge link variables $\{U(b)\}$.

Under a local gauge transformation the link variables transform as

[1]The reason why such terms are not gauge invariant is because the fields ψ are not in the same space-time point.

$$U(y,x) \longrightarrow U(y,x)' = \Lambda(y)^{-1} U(y,x) \Lambda(x) \ , \tag{2.16}$$

from which one can infer that coupling terms like

$$\bar{\psi}(x) U(x,y) \psi(y) \qquad \text{or} \qquad Tr\left(U(x,x)\right) \tag{2.17}$$

are gauge invariant terms. It is the second term in (2.17) which will be used in the lattice invariant gauge fields action.

The smallest closed path which can be taken on a lattice is called *plaquette* and is composed of four links

$$< x + a\hat{\mu}, x >, < x + a\hat{\mu} + a\hat{\nu}, x + a\hat{\mu} >, < x + a\hat{\nu}, x + a\hat{\mu} + a\hat{\nu} >, < x, x + a\hat{\nu} > \tag{2.18}$$

with the following orientation

$$\begin{array}{ccc} x + a\hat{\nu} & \longleftarrow & x + a\hat{\mu} + a\hat{\nu} \\ \downarrow & & \uparrow \\ x & \longrightarrow & x + a\hat{\mu} \end{array} \tag{2.19}$$

let us refer to this plaquette as

$$p = (x; \mu\nu) \ , \tag{2.20}$$

while the corresponding parallel transport operator will be

$$\begin{aligned} U_p \equiv U_{x;\mu\nu} \equiv U(x, x + a\hat{\nu}) U(x + a\hat{\nu}, x + a\hat{\mu} + a\hat{\nu}) \cdot \\ \cdot U(x + a\hat{\mu} + a\hat{\nu}, x + a\hat{\mu}) U(x + a\hat{\mu}, x) \ , \end{aligned} \tag{2.21}$$

and is called *plaquette variable*. The action, which was first proposed by Wilson, for a free lattice gauge field (with no matter field interaction term) can now be defined in term of the plaquette variable as

$$S(U) = \sum_p S_p(U_p) \tag{2.22}$$

where

$$\begin{aligned} S_p(U) &= -\beta \left\{ \frac{1}{2Tr\mathbb{I}} \left(TrU + TrU^{-1} \right) - 1 \right\} \\ &= \beta \left\{ 1 - \frac{1}{N} Re[Tr(U)] \right\} \end{aligned} \tag{2.23}$$

and the last step is true for the case of $SU(N)$ gauge symmetry group. The sum over plaquettes is to be understood as

$$\sum_p \equiv \sum_x \sum_{1 \leq \mu < \nu \leq 4} . \tag{2.24}$$

The constant term of the action, see (2.23), has no physical meaning and can be omitted; thus we arrive to the final expression for the hypercubical lattice $SU(N)$ lattice gauge fields action

$$\mathbb{S}_{\mathcal{G}}^{\mathcal{W}}(U) = \sum_p -\frac{\beta}{N} Re[Tr(U_p)] \, , \tag{2.25}$$

where $\sum_p$ is limited to the domain defined in (2.24). As $U \equiv U_p \equiv U(x,x)$ (the plaquette lives over a closed path) one can show, substituting (2.16) into (2.17), that (2.25) is gauge invariant, real and positive.

It can be shown that the $SU(N)$ Wilson action just defined has, as its own limit, the Yang-Mills action. To this end, one must think that as an $SU(N)$ object, it can always be written as[1]

$$U(x,\mu) \equiv e^{-iag_s A_\mu^a(x) T^a} \, , \tag{2.26}$$

[1] When it will not be necessary for a specific reason, we will adopt the convention of omitting sums over repeated indices.

so that, expanding in powers of the lattice spacing a and using the two following expression

$$A_\nu(x + a\hat{\mu}) = A_\nu(x) + a\nabla^f_\mu A_\nu(x) \ , \tag{2.27}$$

and the Campbell-Baker-Hausdorff formula

$$e^x e^y = e^{x+y+\frac{1}{2}[x,y]+\dots} \ , \tag{2.28}$$

one has

$$U_p = e^{-a^2 G_{\mu\nu}} + O(a^4) \tag{2.29}$$

with $G_{\mu\nu}(x) = \nabla^f_\mu A_\nu(x) - \nabla^f_\nu A_\mu(x) + [A_\mu(x), A_\nu(x)]$; it is enough to substitute (2.29) in (2.25) to obtain

$$\mathcal{S}^{\mathcal{W}}_{\mathcal{G}}(U) \quad \xrightarrow[a\longrightarrow 0]{} - \frac{\beta}{4N} \int d^4x G^a_{\mu\nu} G^{\mu\nu}_a + O(a^2) \tag{2.30}$$

which clearly shows that the leading term of $\mathcal{S}^{\mathcal{W}}_{\mathcal{G}}(U)$, for $a \to 0$, is equal to the Yang-Mills action, assuming $\beta = 2N_c/g_s^2$ and identifying g_s with the lattice bare coupling constant.

2.2.2 Fermionic Wilson action

It is more difficult to obtain a discrete fermionic action, with the right physical properties, in comparison to the bosonic case. In what follow, we will give a lagrangian formulation of the fermionic action and we will show the solution of the so called *fermion doubling* problem. The fermionic lagrangian density in euclidean space-time can be written as[1]

$$\mathscr{L}_F = \bar{\psi}(x) \left(\not{\partial} + M_0 \right) \psi(x) \ , \tag{2.31}$$

[1] In this section, flavour indices will be understood in each fermionic action and lagrangian formulas, for the sake of readability. This means that each expression must be thought as summed over the flavour of the quark involved.

from which it is straightforward to write the fermionic action

$$\mathcal{S}_{\mathcal{F}} = \int d^4x d^4y \bar{\psi}(x)_\alpha K(x,y)_{\alpha\beta} \psi_\beta(y) \; , \tag{2.32}$$

with $K(x,y)_{\alpha\beta} = (i\not{\partial} + M_0)_{\alpha\beta}\delta(x-y)$. Symmetrizing derivative operators and imposing that fermionic fields are zero at spatial infinity in (2.32), one gets

$$\mathcal{S}_{\mathcal{F}} = \int d^4x \bar{\psi}(x) \left(-\frac{1}{2}\gamma_\mu \overleftarrow{\partial^\mu} + \frac{1}{2}\gamma_\mu \overrightarrow{\partial^\mu} + M_0 \right) \psi(x) \; . \tag{2.33}$$

Equation(2.33) can be put on the lattice by means of the usual substitutions

$$\begin{cases} \psi_\alpha(x) \to \psi_\alpha(x) & \text{with x } \in \Lambda \\ \partial_\mu \psi(x) \to \nabla^f_\mu \psi(x) = \frac{\psi(x+a\hat{\mu}) - \psi(x)}{a} & \\ \int d^4x \to \sum_x a^4 & \end{cases} \tag{2.34}$$

where we have indicated with Λ the hypercubical lattice of spacing a and side L; Substituting (2.34) in (2.33) it can be obtained

$$\mathcal{S}^{\mathcal{N}}_{\mathcal{F}} = a^4 \sum_{x,y} \left\{ M_0 \; \bar{\psi}(x)\delta(x-y)\psi(y) + \; \bar{\psi}(x) \left[\frac{1}{2a} \sum_{\mu=1}^{4} \gamma_\mu \delta(y - (x+\hat{\mu})) + \right. \right.$$
$$\left. \left. - \frac{1}{2a} \sum_{\mu=1}^{4} \gamma_\mu \delta(y - (x-\hat{\mu})) \right] \psi(y) \right\} \; , \tag{2.35}$$

where the suffix $\mathcal{N}$ stands for *naïve*[1]; it has been given that name because action (2.35) introduces in the theory new and unwanted degrees of freedom. To show this problem we will analyze the propagator $S(x)$ which can be calculated starting from the naïve fermionic action. $S(x)$ satisfy

$$M_0 S(x) + \frac{1}{2a} \sum_\mu \gamma_\mu (S(x+\hat{\mu}) - S(x-\hat{\mu})) = \delta_{x0} \; , \tag{2.36}$$

[1] In this context naïve, stands for sloppy regularization.

which, solved in the Fourier space, gives

$$S(p) = \frac{a}{-i\sum_\mu \gamma_\mu \sin ap_\mu + aM_0} \tag{2.37}$$

$$\text{with } S(x) = \frac{1}{\Omega}\sum_p S(p)e^{-iapx} \tag{2.38}$$

where Ω is the lattice site number and p can take values among the first *Brillouin* zone ($-\pi/a \leq p \leq \pi/a$). Expanding in powers of a one gets

$$S(p) \to \frac{1}{-i\gamma_\mu p_\mu + M_0} + O(a^2) \tag{2.39}$$

That result seems to show that, in the $a \to 0$ limit, one obtains the usual fermionic propagator in continuum space. However, while taking the previous limit, one must be very careful near the Brillouin zone boundary. In particular, when a p component, say p_μ, takes the value π/a the function $\sin ap_\mu$ in (2.37) becomes null (as it happens for $p_\mu = 0$). This, in turn, imply that near the point $p_\mu = 0$ or $p_\mu = \pi/a$ (let us call this point $\bar{p}$) the propagator $S(p)$ defined in (2.37) will tend to an expression similar to (2.39)[1] in the continuum limit.

As a result, if one discretizes the theory in that way, one is considering *16* different fermionic species with degenerate mass. This is the so called *fermion doubling* problem. From [75] one can learn that this multiplicity in the mass spectrum has its origin in the implemented regularization scheme which, when $m = 0$, retain an exact axial symmetry whatever the value of the lattice spacing is. As a consequence this theory cannot have an axial anomaly, in contrast with the usual regularization schemes employed in the continuum space, and it has created further fermionic species which cancel that anomaly. The latter can be recovered only by introducing some explicit axial symmetry breaking term. From this one can infer that there is no chance of finding a discrete version of (2.33) which solve the doubling problem and keeps chiral symmetry unbroken

[1] For a point $\bar{p}$, the fermionic propagator can be obtained substituting in (2.39) p_μ with $k_\mu = p_\mu - \bar{p}_\mu$ and the γ matrices with $s(\bar{p})\gamma_\mu s(\bar{p})^{-1}$ where the matrices $s(\bar{p})$ are combination of γ matrices, as can be found in [75].

in the $m \to 0$ limit. This can be shown calculating the propagator of an hypothetical chiral invariant action

$$S(p) = \frac{a}{\sum_\mu \gamma_\mu F_\mu(ap)} \,. \tag{2.40}$$

For small a values, it must be $F_\mu(ap) \sim ap_\mu$ so that the correct continuum limit is preserved; this means that the F-function will go to zero with a definite slope in $p_\mu = 0$ as well as in $p_\mu = 2\pi/a$ for periodicity. Being F a continuous function it will at least exist another zero in the interval $0 < ap_\mu < 2\pi$ (where F_μ vanishes with the opposite slope) and the theory will necessarily produce undesired fermionic species.

There are different approaches to avoid the doubling problem and in this work we will follow the Wilson's one [7], which we are going to explain below. This method consist of adding to (2.35) an irrelevant term which explicitly brakes chiral symmetry even in the $m = 0$ limit. In order to leave the action as local as possible, this term is composed of nearest neighbor lattice point

$$a^4 \sum_x \frac{r}{2a} \sum_{\mu=1}^{4} \left[\bar\psi(x+\hat\mu) - \bar\psi(x)\right] \left[\psi(x+\hat\mu) - \psi(x)\right] \tag{2.41}$$

and r is a parameter which takes values between 0 and 1. If we consider the action (2.35) together with the Wilson term (2.41), we have

$$\mathbb{S}_{\mathcal{F}}^{\mathcal{W}} = a^4 \sum_x \left\{ \bar\psi(x)(M_0 + \frac{4r}{a})\psi(x) - \frac{1}{2a}\sum_{\mu=1}^{4} \left[\bar\psi(x+\hat\mu)(r+\gamma_\mu)\psi(x) + \right.\right. \\ \left.\left. - \frac{1}{2a}\sum_{\mu=1}^{4} \bar\psi(x)(r-\gamma_\mu)\psi(x+\hat\mu)\right] \right\} \,, \tag{2.42}$$

which is the fermionic Wilson action without the doubling problem; this action is invariant under rotations and translations on an hypercubic 4-dimensional lattice. What must be stressed is that, as already mentioned, if on one hand the Wilson term solves the doubling problem, on the other it breaks chiral symmetry for finite values of the lattice spacing. Chiral symmetry is restored in the continuum limit, but the fact that it

is broken on the lattice has important consequences. First of all it introduces $\mathcal{O}(a)$ errors, while the original naïve formulation (2.35) is affected only by $\mathcal{O}(a^2)$ errors. Then, the chiral symmetry breaking implies that the quark mass renormalize multiplicatively as well as additively; in fact, in the limit $m \to 0$, only if chiral symmetry is unbroken and no anomaly is present then the mass renormalization is multiplicative and one is guaranteed, to all orders, that quantum correction will not generate a mass different from zero. If chiral symmetry is no longer a symmetry of the theory, nothing forbids additive terms to appear which are no longer proportional to the *bare* mass. In this context it is useful to introduce a mass, called *critical* mass, which must be subtracted from the *bare* mass M_0

$$m_q = M_0 - M_{cr} \ . \tag{2.43}$$

The critical mass will be determined so as to properly define the chiral point, for instance by imposing that the lightest pseudoscalar meson (which is the pion in the two flavour case) is massless at that point.

In the Euclidean space discretization one is free to choose a normalization for the fields which greatly simplifies the lattice action. The first step is to make (2.42) gauge invariant

$$\mathbb{S}_{\mathcal{F}}^{\mathcal{W}} = a^4 \sum_x \Bigg\{ \bar{\psi}(x)(m_0 + \frac{4r}{a})\psi(x) - \frac{1}{2a}\sum_{\mu=1}^{4} \big[\bar{\psi}(x)U_\mu(x)(r-\gamma_\mu)\psi(x+\hat{\mu}) + \\ - \frac{1}{2a}\sum_{\mu=1}^{4} \bar{\psi}(x+\hat{\mu})U_\mu^\dagger(x)(r+\gamma_\mu)\psi(x)\big] \Bigg\} \ ; \tag{2.44}$$

then, introducing the *Hopping* parameter

$$k = \frac{1}{8r + 2am_0} \tag{2.45}$$

and defining new dimensionless quark fields

$$\psi(x) \longrightarrow \sqrt{\frac{2k}{a^3}}\psi(x) \tag{2.46}$$

one can obtain an equivalent version of the discrete Dirac action, in the Wilson's approach

$$\mathbb{S}_{\mathcal{F}}^{\mathcal{W}} = \sum_x \left\{ \bar{\psi}(x)\psi(x) - k\sum_{\mu=1}^{4} \left(\bar{\psi}(x)U_\mu(x)(r-\gamma_\mu)\psi(x+\hat{\mu}) + \right.\right. \\ \left.\left. -k\sum_{\mu=1}^{4} \bar{\psi}(x+\hat{\mu})U_\mu^\dagger(x)(r+\gamma_\mu)\psi(x) \right) \right\} . \tag{2.47}$$

The free quark propagator satisfies

$$S(x) - k_q \sum_\mu [(r-\gamma_\mu)S(x+\hat{\mu}) + (r+\gamma_\mu)S(x-\hat{\mu})] = a^{-4}\delta_{x0} \tag{2.48}$$

which is solved, in momentum space, by

$$S(p) = \frac{a}{1 - 2k_q \sum_\mu [i\gamma_\mu \sin(ap_\mu) + r\cos(ap_\mu)]} . \tag{2.49}$$

It can be verified that for $p \to 0$ the new propagator (2.49) will tend to (2.39) form as in the case of (2.35) action. On the other hand, when a p component approaches the value π/a, the effective quark mass is of order $\mathcal{O}(1/a)$ implying $S(p) \sim \mathcal{O}(a)$; this guarantees that, in the continuum limit, the extra fermions gain infinite mass and only one species with mass m survive.

Action (2.47) represents the starting point for writing the fermionic Dirac action on the lattice and it is important to underline that even if this formulation contains the r parameter, the physical quantities in the continuum limit must be independent from the value chosen for that parameter. The numerical results which we are going to show have been obtained using $r = 1$.

2.3 Improvement

In this section we will briefly present the procedure, commonly known as *improvement*, which allows one to reduce the *cut-off* dependence of the physical quantities calculated on the lattice. If $a \simeq 0$, the lattice theory can be described by means of a *local* effective theory, defined in the continuum, with action

$$\mathcal{S}_{\mathit{eff}} = \int d^4x \left\{ \mathscr{L}_0 + a\mathscr{L}_1 + a^2\mathscr{L}_2 + \dots \right\} , \tag{2.50}$$

where $\mathscr{L}_0$ is the continuum QCD lagrangian while the $\mathscr{L}_k$ terms represent linear combination of local operators with dimension $4+k$. Among all the possible operators, the allowed ones are the ones which share the same symmetry of the lattice action.

It is not only the lattice action which is responsible for the cut-off effects, but also the *composite* local operators which enter the green functions of interest. Let us consider a gauge invariant operator $\Phi(x)$, composed of a product of quark and gluon fields; for the sake of simplicity let us assume that the renormalization procedure does not mix $\Phi(x)$ with other operators. We will expect then that the renormalized *n-point* correlation function[1]

$$G_n(x_1, \dots, x_n) = (\mathcal{Z}_\Phi)^n \left\langle \Phi(x_1) \dots \Phi(x_n) \right\rangle_{cont} \tag{2.51}$$

will have a well defined continuum limit if the renormalization constant $\mathcal{Z}_\Phi$ is properly chosen and the points $x_1, \dots, x_n$ are kept well separated each other. Within the framework of the local effective theory, the renormalized field $\mathcal{Z}_\Phi \Phi(x)$ can be represented as the effective field

$$\Phi_{\mathit{eff}}(x) = \Phi_0(x) + a\Phi_1(x) + a^2\Phi_2(x) + \mathcal{O}(a^2) , \tag{2.52}$$

where again the fields $\Phi_k(x)$ are a linear combination of local fields with the proper dimension and symmetry properties. At order $\mathcal{O}(a)$, the connected correlation function on the lattice are given by

$$\begin{aligned} G_n(x_1, \dots, x_n) = & \left\langle \Phi_0(x_1), \dots, \Phi_0(x_n) \right\rangle_0 \\ & - a \int d^4y \left\langle \Phi_0(x_1), \dots, \Phi_0(x_n) \mathscr{L}_1(y) \right\rangle_0 \\ & + a \sum_{k=1}^{n} \left\langle \Phi_0(x_1), \dots, \Phi_1(x_k), \dots, \Phi_0(x_n) \right\rangle_0 + \mathcal{O}(a^2) , \end{aligned} \tag{2.53}$$

[1] Green functions calculated in euclidean space are usually called *correlation* function.

where the subscript 0 indicate that the expectation values on the right hand side must be taken in the continuum limit, *i.e.* using $\mathscr{L}_0$ as the lagrangian on the functional exponential. The second term is the $\mathcal{O}(a)$ effective action contribution to the correlation function which, being an integral over y, it is in principle divergent for $y = x_k$ and need a subtraction prescription. The exact subtraction procedure does not really matter as a different choice for the inserted local operator cause only a redefinition of the field $\Phi_1(x)$.

However it must be stressed that equation (2.53) does not take into account all the lattice spacing dependence of the correlation functions, as there are also implicit dependencies. These hidden dependence's have their root in the Φ_1 and $\mathscr{L}_1$ operators, which are a linear combination of a lattice fields basis. The basis elements are independent of a indeed, but the coefficients may be. These coefficient can be calculated within perturbation theory and they are a function of $g_s^2 \sim \log a$ and aM_0.

The *improvement* consists of adding both to the action and field operators a complete set of *irrelevant* operators. The coefficient will be determined, at a given order in perturbation theory, to cancel at that order (which is typically $\mathcal{O}(a)$ for the fermionic action and $\mathcal{O}(a^2)$ for the pure gauge action) the finite lattice spacing effects. The original idea, due to Symanzik [76; 77; 78], involved only the fermionic action but the procedure has been extended to the gauge sector too [79]. In this case the tree-level Symanzik improved gauge action [80] can be written as

$$\mathbb{S}_G^{TSI}[U] = \frac{\beta}{3}\sum_x \left(b_0 \sum_{1\le\mu\le\nu\le 4} [1 - ReTr(U_p(x;\mu,\nu))] + b_1 \sum_{\mu\neq\nu} [1 - ReTr(U_{1\times 2}(x;\mu,\nu))] \right) \tag{2.54}$$

where besides the plaquette term U_p there is also the rectangular (1×2) Wilson loop term, $U_{1\times 2}$, and $\beta = 6/g_s^2$ is again the bare inverse coupling and the coefficient are $b_1 = -1/12$ and $b_0 = 1 - 8b_1$.

It will be shown in section 2.4.1 that using a particular formulation for the fermionic lattice action, known as *twisted mass* lattice QCD (tm-LQCD) action, one is able to gain $\mathcal{O}(a)$ improvement in an automatic way only by tuning appropriately M_0 to its

critical value M_{cr}, instead of improving both the action and the operators involved in the simulation.

2.4 Twisted-mass Lattice QCD

In this section we will present the fermionic action employed in the simulations, known as *twisted mass* lattice QCD action [8; 81; 82; 83]; the choice for this particular kind of regularization is justified, as we have already said and as we will show in section (2.4.1), because it provides the $\mathcal{O}(a)$ improvement for the correlation functions in a automatic way.

Let us consider two flavors, $N_f = 2$, of degenerate quark and let us write down the action for the two flavors doublet χ

$$S_{tm}[\chi, \bar{\chi}, G] = a^4 \sum_x \bar{\chi}(x) \left[D_W + m_0 + i\mu\gamma_5\tau_3 \right] \chi(x) = a^4 \sum_x \bar{\chi}(x) D_{tm} \chi(x) \ , \quad (2.55)$$

where we have called with D_W the Wilson-Dirac operator of (2.44), written in the more convenient form as

$$D_W \equiv D_W[U] = \gamma_\mu(\nabla_\mu + \nabla^*_\mu) - ar\nabla_\mu\nabla^*_\mu \ , \quad (2.56)$$

with the covariant (forward and backward) lattice derivative defined as

$$\begin{aligned} \nabla_\mu\psi(x) &\equiv \tfrac{1}{a}[U_\mu(x)\psi(x + a\hat{\mu}) - \psi(x)], \\ \nabla^*_\mu\psi(x) &\equiv \tfrac{1}{a}[\psi(x) - U^\dagger_\mu(x - a\hat{\mu})\psi(x - a\hat{\mu})] \ . \end{aligned} \quad (2.57)$$

In (2.55) μ is the so called *twisted mass* and τ_3 is the third Pauli matrix of the flavour symmetry group $SU(2)_f$. We have used the term *regularization* because it is easy to show that this action differs from the original Wilson scheme only by cut off effects (which are irrelevant in the continuum limit)[1]. Let us start by taking the continuum limit of (2.55)

[1] Moreover, it is possible to prove that the twisted Dirac operator is bounded from below, and this was the first reason why this operator has been originally proposed [8].

$$S_{tm}[\chi,\bar{\chi},G] \quad \xrightarrow[a\longrightarrow 0]{} \int d^4x\bar{\chi}(x)\left[\gamma_\mu D_\mu + m_q + i\mu\gamma_5\tau_3\right]\chi. \tag{2.58}$$

We can write the mass term in the polar form as

$$m_q + i\mu\gamma_5\tau_3 = Me^{i\alpha\gamma_5\tau_3}\ , \tag{2.59}$$

where

$$M = \sqrt{m_q^2+\mu^2}, \quad \tan\alpha = \mu/m_q\ . \tag{2.60}$$

It is now easy to recognize that (2.58) is the standard Wilson action with a mass M, written in a different basis connected to the ψ one by

$$\chi \to e^{-i\omega\gamma_5\tau_3/2}\chi = \psi, \qquad \bar{\chi} \to \bar{\chi}e^{-i\omega\gamma_5\tau_3/2} = \bar{\psi}\ , \tag{2.61}$$

provided we have choose $\omega = \alpha$, *i.e.* $\tan\omega = \mu/m_q$. Indeed, under transformation (2.61)

$$Me^{i\alpha\gamma_5\tau_3} \to Me^{i(\alpha-\omega)\gamma_5\tau_3}\ , \tag{2.62}$$

and for that choose of ω one has

$$S_{tm}^{cont}[\chi,\bar{\chi},G]|_{M_0,\mu} \to S_W^{cont}[\chi,\bar{\chi},G]|_M = \int d^4x\bar{\psi}(x)\left(\gamma_\mu D_\mu + M\right)\psi(x)\ . \tag{2.63}$$

Once established this, we will call *twisted* the basis χ, $\bar{\chi}$ while *physical* the basis ψ, $\bar{\psi}$. The physical interpretation for quark and gluon correlation function is easier and more transparent in that basis, hence the name *physical* basis, but it can be proved that the *twisted* one makes easier to work out the renormalization of the gauge invariant correlators, including the ones with local operators insertion. It is of particular relevance the case $m_q = 0$, hence $M_0 = M_{cr}$ (see (2.43))

$$S^{cont}_{mtm}[\chi,\bar{\chi},G] = \int d^4x\bar{\chi}(x)\left[\gamma_\mu D_\mu + i\mu\gamma_5\tau_3\right] \ , \tag{2.64}$$

which is connected to the standard action by a rotation of $\omega = \pi/2$ and which is called *maximally twisted* action (or twisted mass action at *maximal twist*). On the lattice this is equivalent to the *mtm*-LQCD action

$$S_{mtm}[\chi,\bar{\chi},G] = a^4\sum_x \bar{\chi}(x)\left[D_W + m_{cr} + i\mu\gamma_5\tau_3\right]\chi \ . \tag{2.65}$$

Let us note that the term M_{cr} is again present because of the Wilson term, implicit in D_W, breaks chiral symmetry and so the additive quark mass renormalization is still needed.

Applying (2.61) to the Wilson action and using the definition (2.56) of D_W we can explicitly write the twisted mass action in the physical basis as

$$\begin{aligned} S_{tm}[\psi,\bar{\psi},G] = a^4\sum_x \bar{\psi}(x)\Bigg[\frac{1}{2}\sum_\mu \gamma_\mu(\nabla^*_\mu + \nabla_\mu) + \\ \left(-\frac{ar}{2}\sum_\mu \nabla^*_\mu\nabla_\mu + m_{cr}\right)e^{-i\omega\gamma_5\tau_3} + m_q\Bigg]\psi(x) \ . \end{aligned} \tag{2.66}$$

In this basis, the Wilson term is the *twisted* one, while the mass term is left real.

2.4.1 Automatic improvement

The idea is to show that, if quarks are arranged in $SU(2)_{\rm f}$ flavour doublets, O(a) discretization effects are absent from the average of correlators (Wilson average, WA) computed with lattice actions having Wilson terms of opposite sign and a common value of the subtracted (unrenormalized) lattice quark mass

$$m_q = M_0 - M_{\rm cr} \, , \tag{2.67}$$

where M_0 is the bare mass. For short, in the following, we will occasionally call m_q the "excess" quark mass.

Absence of $\mathcal{O}(a)$ discretization errors in WA's is proved by referring to the Symanzik expansion of (connected, on-shell) lattice correlators in terms of continuum Green functions and exploiting the relations derived by matching the "$\mathcal{R}_5$-parity" of lattice correlators under the transformation

$$\mathcal{R}_5 : \begin{cases} \psi & \to \psi' = \gamma_5 \psi \\ \bar{\psi} & \to \bar{\psi}' = -\bar{\psi}\gamma_5 \end{cases} \tag{2.68}$$

to the $\mathcal{R}_5$-parities of the related continuum Green functions. $\mathcal{R}_5$ is an element of the chiral $SU(2)_L \otimes SU(2)_R$ group, for it can be expressed as the product of the following three transformations $u_V^{(1)}(\pi) = \exp(i\pi\tau_1/2)$, $u_V^{(2)}(\pi) = \exp(i\pi\tau_2/2)$, $u_A^{(3)}(\pi) = \exp(i\pi\gamma_5\tau_3/2)$, with τ_1, τ_2, τ_3 the Pauli matrices. Obviously $[\mathcal{R}_5]^2 = \mathbb{1}$. The improvement of WA's is the result of the use of simple dimensional and symmetry considerations combined with certain algebraic identities holding between pairs of correlators computed with opposite signs of M_0 and r. These identities come from a generalized spurion analysis, which in turn follows from the fact that the lattice fermionic action is left invariant if the field transformation (2.68) is accompanied by a simultaneous change of sign of M_0 and the coefficient, r, sitting in front of the Wilson term. From these considerations one can prove that the Symanzik coefficients necessary to match lattice correlators to the continuum ones have such properties under $r \to -r$ that all $\mathrm{O}(a)$ corrections to the continuum result cancel in WA's. What we are going to show, following [82], is that fully $\mathrm{O}(a)$ improved lattice data for energy levels (hence hadronic masses), matrix elements and renormalization constants can be obtained, without the need of computing anyone of the usual lattice improvement coefficients, if one takes averages of correlators evaluated with tm-LQCD actions having twisted Wilson terms of opposite sign.

2.4.2 Wilson Average and $\mathcal{O}(a)$ improvement

Exploiting expression (2.56) for the Wilson Dirac operator, one can rewrite the usual Wilson action (2.44) as

$$\mathbb{S}_F^W(\psi, \bar{\psi}, U) = a^4 \sum_x \bar{\psi}(x) \left[\frac{1}{2} \sum_\mu \gamma_\mu (\nabla_\mu^\star + \nabla_\mu) - a\frac{r}{2} \sum_\mu \nabla_\mu^\star \nabla_\mu + M_0 \right] \psi(x) \ , \tag{2.69}$$

where again we have used the lattice forward and backward derivatives defined in (2.57). The key observation of the work [82] is that under the $\mathcal{R}_5$ transformation (2.68) the fermionic action (2.69) goes into itself, if at the same time we change sign to the Wilson term (*i.e.* to r) and M_0. In the spirit of the spurion analysis, a quick way of studying the situation is to consider r and M_0 momentarily as fictitious fields and consider the combined transformation

$$\mathcal{R}_5^{\rm sp} \equiv \mathcal{R}_5 \times [r \to -r] \times [M_0 \to -M_0] \tag{2.70}$$

as a symmetry of the lattice theory. In this situation it is easy to prove that any multiplicative renormalizable (m.r.) operator will be either even or odd under $\mathcal{R}_5^{\rm sp}$. This means that indicating with O that m.r. operator we can write

$$\langle O(x_1, x_2, \ldots, x_n)\rangle \Big|_{(r,M_0)} = (-1)^{P_{\mathcal{R}_5}[O]} \langle O(x_1, x_2, \ldots, x_n)\rangle \Big|_{(-r,-M_0)} \ , \tag{2.71}$$

where the sign inversion of r and M_0 has to be performed both in the action and in the mixing coefficients. This result can be proved by performing the change of fermionic integration variables induced by (2.68) in the functional integral defining the l.h.s. of (2.71).

The interest of (2.71) lies in the fact that from it one can prove that discretization effects associated to the presence of the Wilson term in the action, induce in correlators $\mathcal{O}(a)$ corrections having well defined properties under $r \to -r$ (r-parity for short). The latter are such that averages of Green functions computed in lattice theories with opposite values of r have a faster approach to the continuum limit and a better chiral behavior than the two correlators separately.

Before explaining how cut- off effects are eliminated, let us establish how the r-parity property of $M_{\rm cr}(r)$. Since Wilson's lattice theory is invariant under the spurionic transformation $\mathcal{R}_5^{\rm sp}$, the mass action counterterm $a^4 \sum_x \bar{\psi}(x) M_{\rm cr}(r) \psi(x)$ must be naturally chosen so as to maintain this spurionic invariance. From this simple but crucial remark, given the definition of $\mathcal{R}_5$, it is immediately concluded that the critical mass must be an odd function of r[1]

[1]The interested reader will find in [82] how this this key property is born out by the definitions of $M_{\rm cr}$ that are commonly employed either in PT or at the non-perturbative level on the lattice.

$$M_{\rm cr}(-r) = -M_{\rm cr}(r)\,. \tag{2.72}$$

Once established this, we start by noting that, since $M_{\rm cr}(r)$ is odd in r, the excess quark mass m_q (2.43), changes sign under $M_0 \to -M_0$ and $r \to -r$. The transformation $\mathcal{R}_5^{\rm sp}$ under which the Wilson action is invariant can then be also written as

$$\mathcal{R}_5^{\rm sp} = \mathcal{R}_5 \times [r \to -r] \times [m_q \to -m_q]\,. \tag{2.73}$$

Correspondingly, the relation (2.71), which expresses the implications of the spurionic symmetry $\mathcal{R}_5^{\rm sp}$ on lattice correlators, takes the form

$$\langle O\rangle \Big|_{(r,m_q)} = (-1)^{P_{\mathcal{R}_5}[O]} \langle O\rangle \Big|_{(-r,-m_q)}\,, \tag{2.74}$$

where, by slightly changing the notation employed up to here, we have indicated the parameters that specify the fermionic action by using, besides r, the excess quark mass, $m_q = M_0 - M_{\rm cr}$, instead of the bare mass M_0.

In order to discuss the issue of $\mathcal{O}(a)$ improvement we will follow the formalism of [82] and where it is made reference to the notion of effective theory introduced by Symanzik and use the related Symanzik expansion of lattice correlators in terms of correlators of the continuum theory [84]. Schematically up to $\mathcal{O}(a)$ terms, one can write for the lattice expectation value of a m.r. operator the expansion

$$\begin{aligned}\langle O\rangle|_{(r,m_q)} = [\zeta_O^O(r) + a m_q \xi_O^O(r)]\langle O\rangle\big|^{\rm cont}_{(m_q)} + \\ + a \sum_\ell (m_q)^{n_\ell} \eta^O_{O_\ell}(r) \langle O_\ell\rangle \Big|^{\rm cont}_{(m_q)} + {\rm O}(a^2)\,.\end{aligned} \tag{2.75}$$

The label $|^{\rm cont}_{(m_q)}$ in the correlators appearing on the r.h.s. of eq. (2.75) is meant to recall that they are continuum Green functions renormalized at the scale a^{-1}. They are computed employing the continuum QCD action, regularized by using, e.g., a second lattice regularization with lattice spacing much smaller than a. Consistently, the parameter m_q on the r.h.s. is to be interpreted as the continuum value of the quark mass at the

subtraction point a^{-1}. Even in the limit of vanishing lattice spacing, the previous equation has a logarithmically divergent a-dependence. This divergency can be disposed of by multiplying both sides of eq. (2.75) by the renormalization constant of the operator O. The coefficients ζ, ξ and η are finite functions of r and g_0^2. All these coefficients are necessary to match the lattice correlator on the l.h.s. to the continuum Green functions on the r.h.s. of (2.75).

The sum over ℓ is extended over all operators, $O_\ell \neq O$, with (mass) dimension ($d[O]$ is the dimension of O)

$$d[O_\ell] = d[O] - n_\ell + 1\,, \tag{2.76}$$

having the same unbroken quantum numbers of O. The obvious positivity of $d[O]$ and $d[O_\ell]$ puts an upper bound, $n_{\max}$, to the possible values of $n_\ell \geq 0$. The sum over ℓ is extended to all the operators O_ℓ which share the same symmetry of the operator O on the l.h.s of (2.75). Moreover we observe that the transformation (2.68) is part of the chiral group and, acting on the continuum action, is equivalent to changing the sign of m_q; since $[\mathcal{R}_5]^2 = \mathbb{1}$, the operators O_ℓ can always be taken to have well defined γ_5-chiralities, $P_{\mathcal{R}_5}[O_\ell]$; consequently their continuum expectation values will have a definite parity under $m_q \to -m_q$, namely

$$\langle O_\ell \rangle \Big|^{\rm cont}_{(m_q)} = (-1)^{P_{\mathcal{R}_5}[O_\ell]} \langle O_\ell \rangle \Big|^{\rm cont}_{(-m_q)}\,. \tag{2.77}$$

Now, using (2.77) and the Symanzik expansion (2.75) together with (2.74) and by making some algebraic manipulations, it is possible to show that the Symanzik coefficients ζ are even functions of r, while all the others (ξ and η) are odd, which in turn imply [82]

$$\langle O \rangle|^{WA}_{(m_q)} \equiv \frac{1}{2}\left[\langle O\rangle|_{(r,m_q)} + \langle O\rangle|_{(-r,m_q)}\right] = \zeta_O^O(r)\ \langle O\rangle|^{\rm cont}_{(m_q)} + {\rm O}(a^2)\,. \tag{2.78}$$

Making use of (2.74) in the second term of previous relation, we can rewrite the latter in the equivalent form (mass average - MA)

$$\langle O\rangle\Big|^{MA}_{(m_q)} \equiv \frac{1}{2}\Big[\langle O\rangle\Big|_{(r,m_q)} + (-1)^{P_{\mathcal{R}_5}[O]}\langle O\rangle\Big|_{(r,-m_q)}\Big] = \\ = \zeta^O_O(r)\langle O\rangle\Big|^{\rm cont}_{(m_q)} + \mathrm{O}(a^2)\,, \tag{2.79}$$

which says that an $\mathrm{O}(a)$ improved lattice correlator can be obtained by taking the sum with an appropriate relative sign of the two correlators computed within the same lattice regularization (same value of r) but with opposite sign of the excess quark mass, m_q.

Since, as we have seen, (2.78) and (2.79) are identical, in the following we will often refer to either one of them as Wilson average.

2.4.3 Improved physics from tm-LQCD

To make the discussion of the improvement technique more transparent it is convenient to use the form (2.66) of the tm-LQCD action. The proof of the improvement of WA's (or MA's) of correlators in tm-LQCD exactly parallels the argument presented in section 2.4.2, observing that tm-LQCD action (2.66) is invariant under the spurionic transformation (2.73). We only remark for future use that changing the sign of the Wilson term is equivalent to shifting the twisting angle by π. In other words the combined transformation $[r \to -r] \times [\omega \to \omega + \pi]$ leaves the action (2.66) invariant.

The proof proceeds by showing that all the steps considered in the untwisted, Wilson case remain valid also here. One starts with the Symanzik expansion

$$\langle O\rangle\Big|^{(\omega)}_{(r,m_q)} = [\zeta^O_O(\omega,r) + a m_q \xi^O_O(\omega,r)]\langle O\rangle\Big|^{\rm cont}_{(m_q)} + \\ + a\sum_\ell (m_q)^{n_\ell}\eta^O_{O_\ell}(\omega,r)\langle O_\ell\rangle\Big|^{\rm cont}_{(m_q)} + \mathrm{O}(a^2)\,, \tag{2.80}$$

where O is again a multi-local, m.r. operator. Lattice expectation values in (2.80) are characterized by r, m_q and ω. The parameter ω is kept fixed in all the arguments of this section and the dependence on g_0^2 is always understood. As in the standard Wilson case we are concerned with the r-dependence of the Symanzik coefficients ζ, ξ and η. It should be noted that for generic values of ω more operators, O_ℓ, contribute to the expansion (2.80), as compared to the standard Wilson case. The new operators arise due to the breaking of parity and isospin induced by the chiral twist of the Wilson term

in (2.66). This fact, however, does not harm the argument presented in section 2.4.2 as well as the presented formulas which remain valid in this context at any fixed value of ω; in particular formula (2.78) becomes

$$\langle \mathcal{O} \rangle|^{(\omega)WA}_{(m_q)} \equiv \frac{1}{2}[\langle \mathcal{O} \rangle|^{(\omega)}_{(r,m_q)} + \langle \mathcal{O} \rangle|^{(\omega)}_{(-r,m_q)}] = \zeta_O(\omega, r)\, \langle \mathcal{O} \rangle|^{cont}_{(m_q)} + O(a^2)\,, \tag{2.81}$$

and as in the case of standard Wilson fermions, O(a) improvement via WA's is equivalent to the observation that the Symanzik coefficients ζ, ξ and η appearing in the r.h.s. of eq. (2.80) have definite r-parity properties

$$\begin{aligned} \zeta^O_O(\omega, r) &= \zeta^O_O(\omega, -r) = \zeta^O_O(\omega + \pi, r) \\ \xi^O_O(\omega, r) &= -\xi^O_O(\omega, -r) = -\xi^O_O(\omega + \pi, r) \\ \eta^O_{O_\ell}(\omega, r) &= -\eta^O_{O_\ell}(\omega, -r) = -\eta^O_{O_\ell}(\omega + \pi, r)\,. \end{aligned} \tag{2.82}$$

In (2.82) the second equality of each line follows from the invariance of the action (2.66) under $[r \to -r] \times [\omega \to \omega + \pi]$.

Starting from (2.81) one can show some interesting relations which can be proved introducing a set of eigenstates of the transfer matrix $\hat{T}(\omega, r, m_q)$ represented as

$$|h, n, \mathbf{k}\rangle|^{(\omega)}_{(r,m_q)} \tag{2.83}$$

where h, $\mathbf{k}$ ed n stand for the quantum numbers, the spatial momentum and the excitation level, respectively, which characterize the (covariantly normalized) state under consideration; moreover at each eigenstate is associated an eigenvalue $E_{h,n}(\ \mathbf{k}\ ; \omega, r, m_q)$. It is possible to show that [82]

$$\frac{1}{2}\left[E_{h,n}(\mathbf{k}; \omega, r, m_q) + E_{h,n}(\ \mathbf{k}\ ; \omega, -r, m_q)\right] = E^{cont}_{h,n}(\ \mathbf{k}; m_q) + O(a^2)\,, \tag{2.84}$$

and

$$\frac{1}{2}\left[\langle h, n, \mathbf{k}|\, B\, |h', n', \mathbf{k}'\rangle|^{(\omega)}_{(r,m_q)} + (r \to -r)\right] = \zeta_B(\omega, r)\, \langle h, n, \mathbf{k}|\, B\, |h', n', \mathbf{k}'\rangle|^{cont}_{(m_q)} + O(a^2) \tag{2.85}$$

where B is a generic multi-local m.r. and gauge invariant operator. We want to stress the fact that in [82] all the steps which prove the WA's in (2.84) and (2.85) involve the ω angle merely as a parameter. A very special instance is represented by the case $\omega = \pi/2$ which is the already mentioned *full twist* case. In this situation all the ω *-even* quantities are automatically $\mathcal{O}(a)$ improved with no need to perform WA's at all. This result is a consequence of the invariance of (2.66) under the spurionic symmetry

$$\mathcal{P} \times (r \to -r) \tag{2.86}$$

where

$$\mathcal{P} : \begin{cases} U_0(x) \to U_0(x_P) \quad U_k(x) \to U_k^\dagger(x_P - a\hat{k}) \quad k = 1,2,3 \\ \psi(x) \to \gamma_0 \psi(x_P) \\ \bar{\psi}(x) \to \bar{\psi}(x_P)\gamma_0 \end{cases} \tag{2.87}$$

which imply the possibility of defining a kind of parity of the transfer matrix eigenstates, even if the *twisting* term in the action makes the theory non invariant under the physical parity $\mathcal{P}$. Hence, it can be introduced for each eigenstate $|h, n, \ \mathbf{k}\ \rangle^{(\omega)}_{(r,m_q)}$ the index $\eta_{h,n}$, ω- independent, which is equivalent to the physical parity of the continuum state to which $|h, n, \mathbf{k}\rangle|^{(\omega)}_{(r,m_q)}$ is associated. Similarly, it can be proved that any multi- local m.r. operator O can be chosen such as it always has a well defined parity p which can be inferred from

$$\langle O^{(p)}(\{x_i\})\rangle\Big|^{(\omega)}_{(r,m_q)} = (-1)^p \, \langle O^{(p)}(\{x_{iP}\})\rangle\Big|^{(-\omega)}_{(r,m_q)} .$$

In particular, choosing the value $\omega = \pi/2$, it can be proved [82] that the WA's (2.84) and (2.85) can be written as

$$\begin{aligned} &\langle h, n, \mathbf{k}|B|h', n', \mathbf{k}'\rangle\Big|_{(r,m_q)} + \eta^B_{hnh'n'}\langle h, n, -\mathbf{k}|B|h', n', -\mathbf{k}'\rangle\Big|_{(r,m_q)} = \\ &= 2\zeta^B_B(r)\langle h, n, \mathbf{k}|B|h', n', \mathbf{k}'\rangle\Big|^{\text{cont}}_{(m_q)} + \mathrm{O}(a^2) \, , \end{aligned} \tag{2.88}$$

with $\eta^B_{hn,h'n'} = \eta_{hn}(-1)^{p_B}\eta_{h'n'} = \pm 1$, and

$$E_{h,n}(\mathbf{k};r,m_q)+E_{h,n}(-\mathbf{k};r,m_q)=2\,E^{\rm cont}_{h,n}(\mathbf{k};m_q)+\mathrm{O}(a^2)\,, \tag{2.89}$$

relations which clearly show how it can be possible to obtain $\mathcal{O}(a)$ improved estimates having at one's disposal matrix elements and energetic levels obtained by means of only one simulation with only one value of r.

2.4.4 Local operator renormalization within *mtm*-LQCD

In this section we are going to write down explicitly the expression of the renormalized operators (currents and quark densities) entering the flavour non- singlet WTI of the theory described by the fermionic action (2.66), in the maximally twisted case ($\omega=\pi/2$). The formulae presented here can be derived starting from the much more general one presented in [82], where they have been calculated starting from a fermionic action with a generic twist angle ω.

Let us write our expression in terms of the (bare) local currents and quark density operators; moreover, the relevant renormalization coefficients are expressed in terms of the renormalization constants of the local operators of the standard Wilson theory. The renormalized vector and axial currents can be taken to be

$$\hat{V}^1_\mu = Z_A\bar{\psi}\gamma_\mu\frac{\tau_1}{2}\psi \tag{2.90}$$
$$\hat{V}^2_\mu = Z_A\bar{\psi}\gamma_\mu\frac{\tau_2}{2}\psi \tag{2.91}$$
$$\hat{V}^3_\mu = Z_V\bar{\psi}\gamma_\mu\frac{\tau_3}{2}\psi \tag{2.92}$$
$$\hat{A}^1_\mu = Z_V\bar{\psi}\gamma_\mu\gamma_5\frac{\tau_1}{2}\psi \tag{2.93}$$
$$\hat{A}^2_\mu = Z_V\bar{\psi}\gamma_\mu\gamma_5\frac{\tau_2}{2}\psi \tag{2.94}$$
$$\hat{A}^3_\mu = Z_A\bar{\psi}\gamma_\mu\gamma_5\frac{\tau_3}{2}\psi \tag{2.95}$$

where we have indicated with the symbol $\hat{}$ the renormalized continuum operators and with Z_A (Z_V) the renormalization constant of the lattice axial (vector) current. With reference to the currents (2.90) to (2.95), the WTI's with the insertion of the renormalized (multi- local) generic operator $\hat{O}(y)$ ($y\neq x$) take the expected form ($b=1,2,3$)

$$\langle \partial^\star_\mu \hat{V}^b_\mu(x)\hat{O}(y)\rangle|^{\omega=\pi/2}_{(r,m_q)} = \mathrm{O}(a) \tag{2.96}$$

$$\langle \partial^\star_\mu \hat{A}^b_\mu(x)\hat{O}(y)\rangle|^{\omega=\pi/2}_{(r,m_q)} = 2\hat{m}_q\langle \hat{P}^b(x)\hat{O}(y)\rangle|^{\omega=\pi/2}_{(r,m_q)} + \mathrm{O}(a) \tag{2.97}$$

with

$$\hat{m}_q = Z_P^{-1} m_q \,, \tag{2.98}$$

provided we define in terms of bare quantities the renormalized pseudo-scalar operators, $\hat{P}^b$, to be

$$\hat{P}^b = Z_P\, \bar{\psi}\frac{\tau_b}{2}\gamma_5\psi \qquad b = 1,2 \tag{2.99}$$

$$\hat{P}^3 = Z_{S^0}\bar{\psi}\frac{\tau_3}{2}\gamma_5\psi + Z_P\, \rho_P(am_q,\pi/2)\mathbb{1}\frac{i}{a^3} \tag{2.100}$$

were we have indicated with $\partial^\star_\mu$ the discretized backward derivative, with Z_P the renormalization constant of the lattice pseudo-scalar quark current and with Z_{S^0} the multiplicative renormalization constant of the (subtracted) isosinglet scalar quark density. Two special comments to (2.100) are in order: the first one for the function $\rho_P(am_q,\omega)$, which is a coefficient function, even in ω, and it admits a simple polynomial expansion in am_q, while the second one about the unusual mixing (at the maximal twist[1]) of $\bar{\psi}\frac{\tau_3}{2}\gamma_5\psi$ with the identity operator, which is due to the breaking of parity and isospin induced in the action (2.66) by the twisting of the Wilson term.

2.5 Twisted boundary conditions

2.5.1 Continuum definition

Simulating QCD dynamics on a finite volume lattice imposes severe restrictions on the allowed hadron momenta which, usually, depend on the boundary conditions chosen. It is known that, on a lattice with finite volume $V = L^3$, the allowed momenta in the i ($i = 1,2,3$) direction are

[1] For a generic value of ω, in the physical basis, the mixing which we are going to show must include also the scalar operator $\bar{\psi}\psi$, in addition to the identity one.

$$k_i = \pm\frac{2\pi}{L}n_i \qquad n_i = 0, \ldots, L/2a \;, \tag{2.101}$$

and so it is clear that the possible values are quantized and depend on the lattice extension (L).

In particular, let us underline that the smallest permitted momenta different from zero is $2\pi/L$ and for certain lattices it can be rather constrictive (*e.g.*, for $a^{-1} = 2.3\ GeV$ and $L/a = 24$ one has $2\pi/L = 0.6\ GeV$). Moreover, for simulations where high values of momenta are employed, the *noise* to *signal* ratio is usually high and, as a result, the kinematically accessible region is small. This has severe consequences because it makes difficult to study quantities, such as form factors for decay processes, which depend on momenta.

In [85] It has been proved that using non periodic boundary conditions for the spatial directions, called *twisted boundary condition*, or $\theta-$ BC in short, allows to simulate hadrons with arbitrary small values of the spatial momentum. As choosing boundary condition is an infrared feature, we will treat the subject in the continuum. Let us choose, following [86], a euclidean space time with an infinite temporal dimension and cubic spatial volume, of side aL.

It is useful to specify boundary condition in order to avoid contact terms in the Green functions. Periodic boundary conditions are equivalent, for the spatial part, to consider a theory defined on a tridimensional torus with single- valued fields ($\phi(x_i+L) = \phi(x)$). It is not a necessary choice: the quantities which need to be single- valued on the torus are the physical observables that can be obtained from correlators evaluated with the (less constraining) condition of a single- valued action. This request means a greater freedom for defining boundary conditions for the fields, which can be expressed for a generic ϕ field as

$$\phi(x_i + L) = \mathcal{U}_i\phi(x_i)\,, \qquad i = 1, 2, 3\,, \tag{2.102}$$

where $\mathcal{U}_i$ is a global symmetry of the action.

The fermionic action can be specified by means of a Dirac operator and a mass matrix. In the N_f flavour continuum QCD, the more general continuous symmetry allowed for the Dirac operator is the flavour symmetry $U(N_f)$. The mass matrix, assuming N_f non- degenerate flavors, will reduce this symmetry to a subgroup, generated

by the $\{T^a\}$ algebra of the operators which commute with M. Hence, it is natural to identify

$$\mathcal{U}_i = e^{i\alpha_i^a T^a} =: e^{2\pi i \Theta_i} \,. \tag{2.103}$$

The boundary condition, brought in Fourier space, shows that the momentum is still quantized, but it gains an additional contribution related to the θ–BC. Assuming that Θ_i is a generic diagonal matrix in flavour space

$$\Theta_i = \mathrm{diag}\left(\theta_i^1, \dots \theta_i^{N_f}\right) \,, \tag{2.104}$$

the boundary condition for a given flavour f, in coordinate space, is

$$\tilde{q}^f(x_i + L) = \exp\left(2\pi i \theta_i^f\right) \tilde{q}^f(x_i) \qquad i = 1, 2, 3 \,, \tag{2.105}$$

which in Fourier space is equivalent to impose

$$\exp\left[i\left(p_i - \frac{2\pi\theta_i^f}{L}\right)L\right] = 1 \iff p_i = \frac{2\pi}{L}\left(\theta_i^f + n_i\right) \,, \qquad i = 1, 2, 3 \,, n_i \in \mathbb{Z} \,. \tag{2.106}$$

Let us show that choosing θ–BC is equivalent to introducing in the theory an external $U(1)$ gauge field. Rescaling the fields as

$$\tilde{q}(x) := V(x) q_\theta(x) \,, \qquad V(x) := \exp\left(2\pi i \frac{\Theta_i}{L} x_i\right) \,, \tag{2.107}$$

we have that they satisfy (spatial) *periodic* boundary conditions and can be described by a lagrangian with a *modified* Dirac operator in which appear the mentioned gauge field. We have

$$\bar{\tilde{q}}(x)\gamma_\mu D_\mu \tilde{q}(x) = \bar{q}_\theta(x)\gamma_\mu [D_\mu + V^\dagger(x)\partial_\mu V(x)] q_\theta(x) \tag{2.108}$$

$$= \bar{q}_\theta(x)\gamma_\mu \left(D_\mu + iB_\mu\right) q_\theta(x) \tag{2.109}$$

$$= \bar{q}_\theta(x)\gamma_\mu \tilde{D}_\mu q_\theta(x) \tag{2.110}$$

with

$$B_\mu = \begin{cases} 2\pi\Theta_i/L & \mu = i = 1,2,3 \\ 0 & \mu = 0 \end{cases} \tag{2.111}$$

In this basis it is clear that the topological contribute to allowed momenta is a physical one: the propagator is

$$\tilde{S}(x) := \langle \tilde{q}(x)\bar{\tilde{q}}(0)\rangle = \int \frac{dp_4}{2\pi}\frac{1}{L^3}\sum_{\vec{k}} \frac{e^{i(k+B)\cdot x}}{i\gamma_\mu(k+B)_\mu + M} = e^{iB\cdot x}S^\theta(x)\,, \tag{2.112}$$

where the sum is over the allowed momenta $\vec{k} = 2\pi\vec{n}/L$ and $\tilde{S}(x)$ satisfy θ–BC, while the propagator in the q_θ basis is

$$S^\theta(x) := \langle q_\theta(x)\bar{q}_\theta(0)\rangle = \int \frac{dp_4}{2\pi}\frac{1}{L^3}\sum_{\vec{k}} \frac{e^{ik\cdot x}}{i\gamma_\mu(k+B)_\mu + M}\,, \tag{2.113}$$

from which it is clear that, in Fourier space, fermionic lines carry a momentum which is $k+B$. Let us underline that the q_θ fields, as well as $S^\theta(x)$, satisfy periodic boundary conditions.

2.5.2 Lattice implementation

In order to employ θ–BC in lattice QCD simulations, let us point out that imposing such a condition on all quark fields we will need to generate a gauge field configurations for each value of the twisting vector $\vec{\theta}^f$, which in turn imply a considerable demand of computation time. In practice, we can obtain arbitrary shift of the simulated hadron momenta even imposing twisted boundary condition only in the valence sector, using the same formalism of the partial *quenching* [87]. Let us consider the theory, which we will call *partially twisted* QCD (ptQCD), defined by the generating functional

$$Z = \int \mathcal{D}q_v\,\mathcal{D}\bar{q}_v\,\mathcal{D}q_s\,\mathcal{D}\bar{q}_s\,\mathcal{D}q_g\,\mathcal{D}\bar{q}_g\mathcal{D}U \\ e^{-\int d^4x\left[\frac{1}{4}G^2 + \bar{q}_s(\gamma_\mu D_\mu + M)q_s + \bar{q}_v(\gamma_\mu D_\mu + M)q_v + \bar{q}_g(\gamma_\mu D_\mu + M)q_g\right]}\,, \tag{2.114}$$

where the variable q_s are sea quark fields, which are the ones involved in the gauge field configurations generation process, while the q_v are the valence quark fields whose determinant, instead, is cancelled out by construction by the corresponding (bosonic)

ghost fields q_g; hence, it follows that the sea sector is exactly the same as the QCD one considered that the valence quark fields have no influence on the gauge fields. Let us remind, moreover, that the ghost fields do not satisfy the spin- statistics theorem and ptQCD is not a unitary theory, as they are related to an Hilbert space with negative metric.

In ptQCD the mentioned fields obey to the following (spatial partially twisted) boundary conditions

$$q_s(x_i + L) = q_s(x_i)\,, \qquad \widetilde{q}_{v,g}(x_i + L) = e^{i2\pi\Theta_i}\widetilde{q}_{v,g}(x_i)\,. \tag{2.115}$$

In this scheme, the gauge field configurations generation is independent from the θ–BC and can be performed only once. The breaking of the *valence-sea* symmetry induced by the partial twist is a finite volume effect, which is expected to go to zero in the infinite volume limit. It has been proved in [86; 88] that, for many physical quantities of interest, the corrections induced by this effect exponentially decrease with the lattice volume, so it is negligible, and ptQCD can be used in the simulations.

On the lattice, for a given flavor, the all-to-all quark propagator $S(x,y) \equiv \langle q(x)\ \overline{q}(y)\rangle_U$, where $\langle \ldots \rangle_U$ indicates the average over gauge field configurations weighted by the lattice QCD action, satisfies the following equation

$$\sum_z D(x,z)\ S(z,y) = \delta_{x,y} \tag{2.116}$$

where $D(x,z)$ is the Dirac operator of the fermionic tm-LQCD action, and we have omitted color and Dirac indices, for simplicity. We now consider the case in which the valence and the sea quarks satisfy anti–periodic BC in time while spatially they satisfy BC as in (2.115). In this situation the propagator $\widetilde{S}(x,y) \equiv \langle \widetilde{q}(x)\ \overline{\widetilde{q}}(y)\rangle$ still satisfies (2.116), with the same Dirac operator $D(x,z)$, but with quark field with different BC's

$$\sum_z D(x,z)\ \widetilde{S}(z,y) = \delta_{x,y}\,. \tag{2.117}$$

Technically in order to work always with fields satisfying periodic BC's in space and time we follow [85; 89] by introducing a new quark field as

$$q_{\widetilde{\theta}}(x) = e^{-2\pi i \widetilde{\theta}\cdot x/L} \widetilde{q}(x) \tag{2.118}$$

where the four-vector $\widetilde{\theta}$ is given by $(L/2T, \vec{\theta})$[1]. In such a way the new quark propagator $S^{\widetilde{\theta}}(x,y) \equiv \langle q_{\widetilde{\theta}}(x)\ \overline{q}_{\widetilde{\theta}}(y)\rangle$ satisfies the equation

$$\sum_z D^{\widetilde{\theta}}(x,z)\ S^{\widetilde{\theta}}(z,y) = \delta_{x,y} \tag{2.119}$$

with a modified Dirac operator $D^{\widetilde{\theta}}(x,z)$ but periodic BC's in both space and time. The $\widetilde{\theta}$–dependent Dirac operator can be obtained by means of a simple re-phasing of the gauge links

$$U_\mu(x) \to U^{\widetilde{\theta}}_\mu(x) \equiv e^{2\pi i a \widetilde{\theta}_\mu/L}\ U_\mu(x)\ . \tag{2.120}$$

In terms of $S^{\widetilde{\theta}}(x,y)$, related to the quark fields $q_{\widetilde{\theta}}(x)$ with periodic BC's, the all-to-all quark propagator $\widetilde{S}(x,y)$, corresponding to the quark fields $\widetilde{q}(x)$ with twisted BC's, is simply given by

$$\widetilde{S}(x,y) = e^{2\pi i \widetilde{\theta}\cdot(x-y)/L}\ S^{\widetilde{\theta}}(x,y)\ . \tag{2.121}$$

2.6 Numerical methods for Gauge theories

The formulation of a field theory on the lattice, besides providing an ultraviolet cut off, represents also an operative definition for calculating vacuum expectation values of multilocal operators. Using a finite volume lattice transforms the functional integral (1.143) in an ordinary multiple integral. Hence, in the framework of a lattice theory, numerical simulations are the basis for a non perturbative calculation of the mean values of a generic operator

$$\langle O(U,q,\bar{q})\rangle = \frac{1}{Z}\int \mathcal{D}U\mathcal{D}\bar{q}\mathcal{D}q\ O(U,q,\bar{q}) e^{-S(U,q,\bar{q})}\ . \tag{2.122}$$

[1]The difference between q_θ and $q_{\tilde{\theta}}$ is that the former satisfy periodic BC only in space while the latter both in space and time.

In this section we will describe some of the numerical simulation techniques employed in this work first for a pure gauge theory and then in the more general case in which one has also fermionic fields.

2.6.1 Pure gauge theories

In a theory where the gauge fields are the only degrees of freedom, the mean value (2.122) can be written as

$$\langle O(U)\rangle = \int \mathcal{D}U\ O(U)e^{-S(U)} \tag{2.123}$$

where $S(U)$ is the action (2.25). In a $SU(N)$ gauge theory, on a lattice volume Ω, the number of integration variable for the measure

$$\mathcal{D}U \equiv \prod_{link} dU_l \tag{2.124}$$

of (2.123) is equal to $4\Omega(N^2-1)$ angles, which for the typically employed lattice volumes Ω is of the order of 10^7-10^8 variables; for systems described in terms of so many degree of freedom, the only chance for estimating the mean value (2.123) is to use Monte Carlo methods.

In principle, a Monte Carlo integration of (2.123) can be obtained extracting the $\{U\}$ configuration randomly and then calculating the mean value associating with each configuration the statistical weight e^{-S}. This procedure, called *static* Monte Carlo, is highly inefficient for large lattice volumes Ω; the reason is that in (2.123) the configuration which contribute more to the integral are the ones which make minimum the thermodynamic free energy F, defined as the difference between the action $S(U)$ and the thermodynamic entropy. Hence, if one extracts a finite number of gauge configurations by means of the static method, the configurations which, among the randomly extracted ones, will nearly minimize this energy will be a negligible fraction and the mean value integral estimate will be very imprecise.

This is the reason why it is preferred to employ the so called *dynamic* Monte Carlo, or *importance sampling*, method. In this approach, the sample of gauge field configuration ($\{U\}_n$, $n = 1, N$) is not generated following a random distribution, instead it is

generated according to the e^{-S} probability density; then, the mean value (2.123) can be evaluated by means of the mean over the sample

$$\langle O \rangle \simeq \overline{O} = \frac{1}{N} \sum_{i=1}^{N} O(\{U\}_i) \; . \tag{2.125}$$

The deviation from the mean value $\overline{O}$ of the values $O(\{U\}_i)$ will give a measure of uncertainty of $\overline{O}$ (2.125), related to the employed sample; in section 4.2 we will be discuss two different methods for evaluating statistical errors. It is possible, in general, to extract gauge field configuration samples following a desired probability distribution, using different Monte Carlo algorithms. This work is based on gauge ensemble generated by employing a state-of-the-art *Generalized Hybrid Monte Carlo* (GHMC) algorithm.

2.6.2 Numerical methods for fermionic systems

In section 2.6.1 it has been briefly described Monte Carlo simulations for pure gauge theories on the lattice. The extension of the subject to theories which include fermionic fields is a delicate matter, because the fermionic integration in (2.122), taking into account the anticommutation properties of the fermionic fields, can not be defined as an ordinary sum, but it becomes a complex linear operator from the anticommuting variables space to the complex numbers one. At present the only possible solution to overcome the problem is to analytically perform the integration over the fermionic variables and then apply Monte Carlo methods to the remaining bosonic effective theory, as it will be shown in what follows.

Quark fields, because of the anticommutation properties, must be represented in (2.122) by means of anticommuting numbers, called *Grassmann* variables

$$\{q_i, q_j\} = \{\bar{q}_i, \bar{q}_j\} = 0 \quad \{q_i, \bar{q}_j\} = 0 \; ; \tag{2.126}$$

then, the Grassmann variable integration is defined as a linear operator such as

$$\begin{aligned} \int d\bar{q}_i \; &= \; \int dq_i \; = \; 0 \\ \int d\bar{q}_i \bar{q}_i \; &= \; \int dq_i q_i \; = \; 1 \; . \end{aligned} \tag{2.127}$$

In principle, these variables could be described also using suited anticommuting matrix, but this approach would require too much memory and computation time as well as rather complicated algorithms. Moreover, being the Wilson- Dirac action (as well as the twisted mass one) bilinear in the q and $\bar{q}$ fields, for each gauge field configuration one has to calculate a fermionic integral which is analytically solvable. To this end, let us write the LQCD action as

$$S = S(U) + S_F = S(U) + \sum_{q;i,j} \bar{q}_i \Delta_{ij}(U, k_q) q_j \ , \tag{2.128}$$

where i and j generically represent all the indexes (lattice variable sites, color and spin) which characterize a quark field of q flavour; then, using Grassmann integration rules (2.127) the functional integral on the lattice can be written as

$$Z(J, \bar{\eta}, \eta) = \int \prod_{link} dU_l \left\{ \prod_{q=1}^{N_f} \det \Delta(U, k_q) e^{-(S(U) + J_m U_m + \bar{\eta}_i \Delta^{-1}_{ij}(U, k_q) \eta_j)} \right\} \ , \tag{2.129}$$

where we have indicated with J, η and $\bar{\eta}$ external currents coupled, respectively, to gauge and matter fields. Let us note that the determinant in (2.129) is real (as $\Delta = \gamma_5 \Delta^\dagger \gamma_5$) and assuming that it is positive defined, we can write

$$\left\{ \prod_{q=1}^{N_f} \det \Delta(U, k_q) \right\} e^{-S(U)} = e^{-[S(U) - \sum_{q=1}^{N_f} Tr \ln \Delta(U, k_q)]} \ . \tag{2.130}$$

In this way, after the fermionic variables integration, the gauge fields dynamic will be ruled by the bosonic effective action

$$S_{eff}(U) \equiv S(U) - \sum_{q=1}^{N_f} Tr \ln \Delta(U, k_q), \tag{2.131}$$

which can also be written as

$$S_{eff}(U) \equiv S(U) - \sum_{q=1}^{N_f} \ln \det \Delta(U, k_q) \ . \tag{2.132}$$

In the last two expression, the second term can be interpreted as the virtual quark loop effect as, considered the identity

$$\int \prod_x dq_x \prod_x d\bar{q}_x \, e^{-S_F} = \prod_{q=1}^{N_f} \det \Delta(U, k_q) \; , \tag{2.133}$$

the fermionic matrix determinant can be regarded as the *vacuum-to-vacuum* transition amplitude for the quark theory on a classical (arbitrary) gauge background.

Exploiting what we have seen up to here, the functional integral can be expressed as

$$Z(J, \bar{\eta}, \eta) = \int \prod_{link} dU_l e^{(-S_{eff}(U) + J_m U_m + \bar{\eta}_i \Delta^{-1}_{ij}(U, k_q)\eta_j)} \; , \tag{2.134}$$

and, as it was already mentioned in section (1.4.2), from the functional derivatives with respect to the external sources J, η, $\bar{\eta}$, evaluated at $J = \eta = \bar{\eta} = 0$, one can calculate the correlation function for any operator of the theory. In particular, for composite operators which involve only gauge fields, one will have

$$\langle O(U) \rangle = \int \mathcal{D}U \; O(U) e^{-S(U)_{eff}} \; . \tag{2.135}$$

This formula can be easily generalized to the case of mean values of observables which involve fermionic variables too.

Let us conclude this section with some considerations about the fermionic determinant. In principle, it is possible to perform simulations of lattice gauge theories with fermionic fields by generating a gauge field sample, $U_\mu(x)$, distributed with the Boltzmann density factor defined by the effective action (2.131); however, at present, this operation is still highly expensive in terms of computational time. The reason lies in the fact that the second term in (2.131) is a non local one: because of the virtual fermionic loop, a given link variable can directly interact not only with the nearest neighbor, but with far gauge variables too. Hence, in the *updating* procedure of each link, the computation time is mainly spent calculating the factor $Tr \ln \Delta(U)$. This is the reason why past lattice fermion simulations usually employed the so called *quenched* approximation, which consist in setting the fermion matrix determinant equal to one. From

a physical point of view, the *quenching* operation can be interpreted as neglecting the contribute to the process under consideration of the Feynman diagrams which involve internal fermion loop. Within this approximation, the Zweig rule is exactly observed and hadrons are composed of valence quark and gluons with no quark- antiquark sea pairs. This approximation is not so far from what happens in the real world, but for some observables the physical predictions obtained within this approximation are in disagreement from what can be observed in nature. For instance, let us consider the $\rho \to 2\pi$ decay, which is forbidden by the Zweig rule, while using the *quenched* approximation, it becomes the main decay channel for ρ mesons. For this and other physical reasons, in this work we have employed only *unquenched* gauge field configurations for the calculation we are going to present in chapter 4.

3

What has to be computed

This chapter will be dedicated to explain in details the employed techniques for the lattice calculation of the semileptonic form factors and, as an introductory study for a future calculation of the neutron EDM, we will present a critical review of the present available techniques for calculating the disconnected diagrams.

The section 3.1 will show how we can extract quantities such as meson masses or hadronic matrix elements from the two–point and three–point correlation functions which we are going to calculate on the lattice.

In section 3.2.1 we will explain our technique of the so–called double ratios method for calculating the $K \to \pi$ matrix element and the related semileptonic form factors.

Section 3.2.2 will be dedicated to discuss the relevant Feynman diagrams for the semileptonic two– and three–point functions as well as to introduce the stochastic methods for calculating connected diagrams.

We will close the chapter with section 3.3 in which we will consider, and explain, all the available techniques ([13; 14; 15]) for calculating the disconnected insertions characteristic of the flavour singlet physics; we will also present our hybrid method which we think can be a good tool for evaluating these noisy diagrams.

3.1 Extracting information from LQCD

This section will explain how one can extract the physical information of interest from tm-LQCD. We will restrict our attention to a special class of the euclidean operator expectation values (2.122), called two– and three–point correlation functions; these

quantities allow one to determine the hadron mass spectrum and the one particle to vacuum as well as the one particle to one particle matrix element.

The first part of the section describes how one can extract, from two–point correlators, hadron masses and one particle to vacuum matrix elements.

The second part shows that the matrix elements of a given operator between hadron states can be calculated starting from suitable three–point functions.

3.1.1 Two–point correlation functions

Let us show what is the relation between the quantities extracted from the euclidean theory, which is the one employed in simulations, and the physical ones proper of the Minkowskian theory, introducing the standard procedure used for the calculation of the hadronic masses in a given regularization of the fermionic action. Let us assume that the fields ψ and $\bar{\psi}$ are expressed in the physical basis.

The euclidean two–point correlation function, for two generic operators $\mathcal{O}_A$ and $\mathcal{O}_B$, can be written as

$$G(x,0) = \langle 0 | \, \mathcal{O}_A(x)\mathcal{O}_B(0) \, | 0 \rangle \ , \tag{3.1}$$

with x which is a shorthand for the four-vector $(x^0 = t, \vec{x}\,)$, hence we are in the case $t > 0$. $G(x,0)$, once rotated back to Minkowsky space-time, gives $\langle 0 | \, T[\mathcal{O}_A(x)\mathcal{O}_B(0)] \, | 0 \rangle$ with T which is the time-ordered product. This quantity represents the probability amplitude for the creation of a state with the $\mathcal{O}_B$ quantum number in the space–time point $x = 0$, the propagation of that state up to the point $x = (x^0, \vec{x}\,)$ and its final annihilation from the $\mathcal{O}_A$ operator. By integrating over space one can obtain the zero momentum component of the Fourier representation of the correlation function

$$C^{AB}(t) \doteq \sum_{\vec{x}} \langle 0 | \, \mathcal{O}_A(x)\mathcal{O}_B(0) \, | 0 \rangle \ . \tag{3.2}$$

Let us take $t > 0$ and insert in (3.2) a complete set of covariantly normalized energy eigenstates with well definite momentum $|n, \vec{p}_n\rangle$

$$\langle n, \vec{p}_n | m, \vec{p}_m \rangle = (2\pi)^3 2E_n \delta_{n,m} \ , \tag{3.3}$$

$$\sum_{n,\vec{p}_n} |n, \vec{p}_n\rangle \frac{1}{(2\pi)^3 2E_n} \langle n, \vec{p}_n | = \mathbb{1} \ , \tag{3.4}$$

where the sum indicates that we are integrating over all possible momenta (anticipating its application on the lattice). Identifying $x_0 = t$ one has

$$\begin{aligned} C^{AB}(t) &= \sum_{\vec{x}} \sum_{n,\vec{p}_n} \frac{\langle 0|\, \mathcal{O}_A(x)\, |n,\vec{p}_n\rangle \, \langle n,\vec{p}_n|\, \mathcal{O}_B(0)\, |0\rangle}{2E_n} \\ &= \sum_{\vec{x}} \sum_{n,\vec{p}_n} \frac{\langle 0|\, e^{Ht+i\vec{P}\cdot\vec{x}}\, \mathcal{O}_A(0,\vec{0}\,)\, e^{-Ht-i\vec{P}\cdot\vec{x}}\, |n,\vec{p}_n\rangle \, \langle n,\vec{p}_n|\, \mathcal{O}_B(0)\, |0\rangle}{2E_n} \\ &= \sum_{\vec{x}} \sum_{n,\vec{p}_n} \frac{\langle 0|\, \mathcal{O}_A(0)\, |n,\vec{p}_n\rangle \, \langle n,\vec{p}_n|\, \mathcal{O}_B(0)\, |0\rangle}{2E_n}\, e^{-E_n t - i\vec{p}_n\cdot\vec{x}} \\ &= \sum_{n} \frac{\langle 0|\, \mathcal{O}_A(0)\, |n,\vec{p}_n = \vec{0}\,\rangle \, \langle n,\vec{p}_n = \vec{0}\,|\, \mathcal{O}_B(0)\, |0\rangle}{2M_n}\, e^{-M_n t} \end{aligned} \tag{3.5}$$

where we have exploit the use of the translation operator which shifts the field in the origin $\mathcal{O}(x) = e^{Ht+i\vec{P}\cdot\vec{x}}\mathcal{O}(0,\vec{0})e^{-Ht-i\vec{P}\cdot\vec{x}}$ and the Dirac delta involved in the spatial "integration" $\sum_{\vec{x}} e^{-i\vec{p}_n\cdot\vec{x}} = \delta(\vec{p}_n)$; moreover we have assumed that single particle states $|n,\vec{p}_n\rangle$ which has an overlap different from zero with the operator $\mathcal{O}_i$ exists and are stable, in order that, for zero momentum, one has $E_n(\vec{p}_n = \vec{0}; M_n) = M_n$, with M_n which is the mass of the n^{th} state.

Without making further assumptions, the sum in (3.5) will be over a lot of possible intermediate states n; however, for t large enough, there will be only one term which will survive because of the exponential suppression, and it will be the single particle state ϕ with the lower mass value. Defining

$$\sqrt{Z_\phi^O} \doteq \langle 0|\, \mathcal{O}(0,\vec{0}\,)\, |\phi\rangle \ , \tag{3.6}$$

one has

$$\sum_{\vec{x}} \langle 0|\, \mathcal{O}_A(x)\mathcal{O}_B(0)\, |0\rangle \xrightarrow[t\to\infty]{} \frac{\sqrt{Z_\phi^{O_A}}\sqrt{Z_\phi^{O_B}}}{2M_\phi}\, e^{-M_\phi t}\,. \tag{3.7}$$

It is now possible to extract the M_ϕ mass from the *euclidean* correlator by means of an exponential fit in a suitable temporal region $t \in [t_{min}, t_{max}]$ which ensures one to have isolated the ground state contribution to the correlator. Let us stress the fact that the peculiar feature of this procedure is that it does not require to rotate the result back to the Minkowsky space. This consideration about euclidean correlation functions and

physical observables is valid also in the case of the hadronic matrix elements; what is important to bear in mind is that (3.5), and in particular (3.7) which is the one directly involving the physical quantities of interest, are valid only if the states involved in the n–sum are stable.

This procedure can be extended to other Fourier components, obtaining

$$C^{AB}(t;\vec{p}) := \sum_{\vec{x}} \langle 0|\, \mathcal{O}_A(x)\mathcal{O}_B(0)\,|0\rangle\, e^{i\vec{p}\cdot\vec{x}} \xrightarrow[t\to\infty]{} \frac{\sqrt{Z^{O_A}_{\phi,\vec{p}}}\sqrt{Z^{O_B}_{\phi,\vec{p}}}}{2E_\phi}\, e^{-E_\phi t}\,, \tag{3.8}$$

where $E^2_\phi = m^2_\phi + |\vec{p}_\phi|^2$, and $Z^{O_{A(B)}}_{\phi,\vec{p}=0}(\vec{0}\,) \equiv Z^{O_{A(B)}}_\phi$.

For fields defined in a finite time interval ($t \in [0,T]$), with periodic boundary conditions, (3.7) and (3.8) are no longer valid and must be modified in order to include contributions from forward and backward propagation; hence, if we call η the (temporal) parity of the two–point correlator with respect to the transformation $t \to T-t$ (which will be given by the product of $\eta_{O_A} \times \eta_{O_B}$), in the case of zero momentum we will have

$$C^{AB}(t) \xrightarrow[t\to\infty]{} \frac{\sqrt{Z^{O_A}_\phi}\sqrt{Z^{O_B}_\phi}}{2M_\phi}\left(e^{-M_\phi t} + \eta e^{-M_\phi(T-t)}\right)\,. \tag{3.9}$$

In the $\eta = 1$ case, this expression reads

$$C^{AB}(t) \xrightarrow[t\to\infty]{} \frac{\sqrt{Z^{O_A}_\phi}\sqrt{Z^{O_B}_\phi}}{M_\phi} e^{-M_\phi \frac{T}{2}} \cosh\left[\left(t-\frac{T}{2}\right)M_\phi\right]\,. \tag{3.10}$$

In the rest of the chapter our formulae will be always presented (for simplicity) in the infinite (lattice) time extension limit.

In this work we will consider local operators which *interpolate* mesons, *i.e.* operators with quantum numbers appropriate to create the meson states of interest from the vacuum. In the flavour non-singlet case, such composite operators can be written as

$$\mathcal{O}_\Gamma(x) = \sum_a \bar{q}^a_1(x)\Gamma q^a_2(x)\,, \tag{3.11}$$

where q_1 and q_2 are two valence quarks of different flavour, a is a color index and the spinorial indices have been omitted for the sake of readability. Γ is one of the 16 combination (see tab. 3.1) of Dirac γ matrices which are responsible for the *spin* (J),

State	J^{PC}	Dirac Matrix
Scalar	0^{++}	I
	0^{++}	γ_0
Pseudo–scalar	0^{-+}	γ_5
	0^{-+}	$\gamma_5\gamma_0$
Vector	1^{--}	γ_i
	1^{--}	$\gamma_0\gamma_i$
Axial Vector	1^{++}	$\gamma_5\gamma_i$
Tensor	1^{+-}	$\gamma_i\gamma_k$

Table 3.1: It is shown the J^{PC} quantum numbers of the 16 Dirac covariants and the Lorentz group transformation properties.

parity (P) and *charge conjugation* (C) quantum numbers of the composite operator $\mathcal{O}_\Gamma(x)$.

The correlators

$$\langle 0|\, P_5(x) P_5^\dagger(0)\, |0\rangle \ , \qquad \langle 0|\, A_0(x) P_5^\dagger(0)\, |0\rangle \ , \tag{3.12}$$

where $P_5 = \bar{q}_1\gamma_5 q_2$ and $A_0 = \bar{q}_1\gamma_0\gamma_5 q_2$, are of particular interest because thanks to the quantum numbers of the operators therein and, by suitably choosing the *1* and *2* flavors, it is possible to exploit (3.10) for estimating in LQCD the corresponding meson masses and matrix elements.

Let us close this section clarifying that, beside the exponential fit to the large time behavior of the euclidean lattice correlator, there is another method for estimating meson masses, inspired again by (3.7). It is possible to calculate the so–called effective mass (in lattice units), defined by

$$aM_{eff}(t) = \ln\left[\frac{C^{AB}(t)}{C^{AB}(t+1)}\right] \ , \tag{3.13}$$

a quantity which, for large t, will tend to a constant value equal to the mass of the ground state (or to its energy if the correlation $C^{AB}(t)$ has not been taken at zero momentum).

3.1.2 Three–point correlation functions

We have already anticipated, at the beginning of this section that, from the large time behavior of the three–point correlation functions, it is possible to extract matrix elements of operators between one particle states; hence, let us consider a three–point function in the Fourier space

$$C_\Gamma^{BA}(t,t_s;\vec{p},\vec{q}) \doteq \sum_{\vec{x},\vec{x}_s} \langle 0|\,\mathcal{B}(t_s,\vec{x}_s)O_\Gamma(t,\vec{x}\,)\mathcal{A}(0,\vec{0}\,)\,|0\rangle\; e^{i\vec{p}\cdot\vec{x}_s+i\vec{q}\cdot\vec{x}}\,, \tag{3.14}$$

where $\mathcal{A},\mathcal{B}$ are operators which interpolate two A and B mesons, differing by the flavour of one single quark, and O_Γ is the operator (3.11). Following the manipulation steps used for the two–point function case, let us insert the identity (3.4) twice

$$C_\Gamma^{BA}(t,t_s;\vec{p},\vec{q}) = \sum_{\vec{x},\vec{x}_s}\sum_{n,\vec{p}_n}\sum_{n',\vec{p}_{n'}} \langle 0|\,\mathcal{B}(t_s,\vec{x}_s)\,|n',\vec{p}_{n'}\rangle\,\frac{1}{(2\pi)^3 2E_{n'}}\,\langle n',\vec{p}_{n'}|\,O_\Gamma(t,\vec{x}\,)\,|n,\vec{p}_n\rangle\,\cdot$$
$$\frac{1}{(2\pi)^3 2E_n}\,\langle n,\vec{p}_n|\,\mathcal{A}(0,\vec{0}\,)\,|0\rangle\; e^{i\vec{p}\cdot\vec{x}_s+i\vec{q}\cdot\vec{x}}\,. \tag{3.15}$$

Using again the translation law to shift the operators in the origin and the Dirac delta to eliminate the spatial volume integration, we have that

$$C_\Gamma^{BA}(t,t_s;\vec{p},\vec{q}) = \sum_{n,n'} \frac{\sqrt{Z^{\mathcal{A}}_{A_n,\vec{p}}}\sqrt{Z^{\mathcal{B}}_{B_{n'},\vec{p}+\vec{q}}}\;e^{-E_{n'}(t_s-t)}e^{-E_n t}}{4E_nE_{n'}}\;\langle B_{n'},\vec{p}\,|\,O_\Gamma(0,\vec{0}\,)\,|A_n,\vec{p}+\vec{q}\rangle\;, \tag{3.16}$$

where A_n ($B_{n'}$) states belong to the subset of the states n (n'), with momentum $\vec{p}$ ($\vec{p}+\vec{q}$), which have the right quantum numbers to interpolate the $\mathcal{A}$ ($\mathcal{B}$) operator and with and $Z^{\mathcal{A}}_{A_n,\vec{p}}$ $Z^{\mathcal{B}}_{B_{n'},\vec{p}}$ we have indicated, as in (3.6), the square modulus of the matrix elements

$$Z^{\mathcal{A}}_{A_n,\vec{p}} = |\,\langle 0|\,\mathcal{A}(0,\vec{0}\,)\,|A_n,\vec{p}_n\rangle\,|^2\,, \tag{3.17}$$
$$Z^{\mathcal{B}}_{B_{n'},\vec{p}} = |\,\langle 0|\,\mathcal{B}(0,\vec{0}\,)\,|B_{n'},\vec{p}_{n'}\rangle\,|^2\,. \tag{3.18}$$

Considering a temporal region for which both t and t_s-t are large enough, only the first two excited states $A_1=A$ and $B_1=B$ will contribute to the sum; hence, the correlation function limit is (with somewhat simplified notation)

$$C_\Gamma^{BA}(t,t_s;\vec{p},\vec{q}) \xrightarrow[\substack{t\to\infty\\(t_s-t)\to\infty}]{} \frac{\sqrt{Z_A}\sqrt{Z_B}\,e^{-E_B(t_s-t)}e^{-E_A t}}{4E_A E_B}\,\langle B,\vec{p}\,|\,O_\Gamma(0,\vec{0}\,)\,|A,\vec{p}+\vec{q}\rangle\ . \quad (3.19)$$

It is now clear that the general strategy is to extract, from the corresponding two–point functions fit, the energies and the constants Z_A and Z_B and then, analyzing the large time behavior of the three-point correlator it is possible to extract the relevant operator matrix element (r.h.s. of (3.19)).

3.2 Semileptonic Kaon decays

In this section we will show in details how to extract the semileptonic $K \to \pi$ decay form factors starting from the three and two point function of suitable local composite operators. We will recall the so called *standard* method, employed for the first time in the pioneering quenched calculation [17] and also in the more recent one [19], and then we will generalize it to the case in which one is interested in calculating the full q^2 dependence of the form factor. We will also discuss some systematic errors of the standard technique and present a ratio method which is able to achieve a high precision at any value of q^2.

3.2.1 The ratio and the double ratio method

We want to extract form factors from lattice correlation functions, employing suitable ratios of two and three point functions, following what has already been done in the works [17; 18; 19]. The gain, using this technique, is that statistical fluctuations mainly get canceled out between the numerator and the denominator. Another source of systematic error, in these kind of analysis, is the determination of the lattice renormalization constants so, as much as we can, we will always avoid their explicit calculation by means of a suitable trick which modifies the ratio in order to avoid the renormalization constant direct estimate.

We are interested in the calculation of the $K \to \pi$ matrix element of the weak vector current $V_\mu = \bar{s}\gamma_\mu u$, defined as (*cfr.* (1.94) with $M' = \pi$ and $M = K$)

$$\langle \pi^i(p')|\,V_\mu(0)\,|K^i(p)\rangle = C_i\left[f_+^i(q^2)(p+p')_\mu + f_-^i(q^2)(p-p')_\mu\right],\ \ q^2=(p-p')^2 \quad (3.20)$$

where C_i is a Clebsch-Gordan coefficient, equal to 1 ($2^{1/2}$) for neutral (charged) kaons, p (p') is the kaon (pion) four–momentum and q^2 is the squared four–momentum transfer. As usual, we express $f_-^i(q^2)$ in terms of the so-called scalar form factor

$$f_0^i(q^2) = f_+^i(q^2) + \frac{q^2}{M_K^2 - M_\pi^2} f_-^i(q^2) \; . \tag{3.21}$$

By construction $f_0^i(0) = f_+^i(0)$ and the differences between $K^0 \to \pi^-$ and $K^+ \to \pi^0$ channels are only due to isospin–breaking effects. In the following we shall concentrate on the $K^0 \to \pi^-$ case and work in the isospin–symmetric limit, dropping also the superscript i on the form factors.

From (3.20) it is clear that the form factors can be expressed as a linear combination of hadronic matrix elements, as will be shown in a while; to this end, let us recall the two– and three– point formula written in a suitable notation

$$C_\mu^{K\pi}(t,t',\vec{p},\vec{p}\,') = \frac{1}{L^3 T} \sum_{x,y,z} \langle \mathcal{O}_\pi(y) V_\mu(x) \mathcal{O}_K^\dagger(z) \rangle \, \delta_{t,t_x - t_z} \delta_{t',t_y - t_z} \, e^{-i\vec{p}\cdot(\vec{x}-\vec{z}) + i\vec{p}\,'\cdot(\vec{x}-\vec{y})} \; , \tag{3.22}$$

$$C^{K(\pi)}(t,\vec{p}) = \frac{1}{L^3 T} \sum_{x,z} \langle \mathcal{O}_{K(\pi)}(x) \mathcal{O}_{K(\pi)}^\dagger(z) \rangle \, \delta_{t,t_x - t_z} \, e^{-i\vec{p}\cdot(\vec{x}-\vec{z})} \tag{3.23}$$

where $V_\mu = \bar{u}\gamma_\mu s$ while $\mathcal{O}_\pi^\dagger = \bar{u}\gamma_5 d$ and $\mathcal{O}_K^\dagger = \bar{s}\gamma_5 d$ are the operators interpolating the π and K mesons. Let us underline that since we want to use *all-two-all* propagators, in (3.22) and (3.23) there is an additional sum over the space–time lattice volume, which helps improving the signal quality with respect to the case of a fixed–point source ($z = 0$). We will not enter here in details about the particular techniques employed for the calculation of this particular lattice fermion propagator, as they will be the subject of subsection 3.2.3; in this section we will limit our discussion to the method for calculating the form factors.

Taking in (3.22) and (3.23) values of t and $t' - t$ large enough, one gets

$$C_\mu^{K\pi}(t,t',\vec{p},\vec{p}\,') \xrightarrow[(t'-t)\to\infty]{t\to\infty} \frac{\sqrt{Z_K Z_\pi}}{4 E_K E_\pi} \frac{1}{Z_V} \langle \pi(p') | \hat{V}_\mu | K(p) \rangle \, e^{-E_K(\vec{p})t - E_\pi(\vec{p}\,')(t'-t)} \; , \tag{3.24}$$

$$C^{K(\pi)}(t,\vec{p}) \xrightarrow[t\to\infty]{} \frac{Z_{K(\pi)}}{2E_{K(\pi)}(\vec{p})} \, e^{-E_{K(\pi)}(\vec{p})t} \tag{3.25}$$

with $\hat{V}_\mu$ which is the renormalized lattice vector current and where, up to discretization effects, $E_\pi(\vec{p}) = \sqrt{M_\pi^2 + |\vec{p}|^2}$, $E_K(\vec{p}\,') = \sqrt{M_K^2 + |\vec{p}\,'|^2}$ and $\sqrt{Z_{K(\pi)}} = \langle 0|\, \mathcal{O}_{K(\pi)}(0)\, |K(\pi)\rangle$. The latter is independent on the meson momentum $\vec{p}$ [90]. Then it follows

$$\frac{C_\mu^{K\pi}(t, t', \vec{p}, \vec{p}\,')}{C^K(t, \vec{p}) C^\pi(t' - t, \vec{p}\,')} \xrightarrow[(t' - t) \to \infty]{t \to \infty} \frac{1}{Z_V} \frac{\langle \pi(p')|\, \hat{V}_\mu\, |K(p)\rangle}{\sqrt{Z_K Z_\pi}}\,. \tag{3.26}$$

Consequently, the hadronic matrix element $\langle \pi(p')|\, \hat{V}_\mu\, |K(p)\rangle$ can be obtained from the plateau of the l.h.s. of (3.26), once Z_K and Z_π are separately extracted from the large–time behavior of the two–point correlators in (3.25) and Z_V has been calculated in the standard way which we are going to show in a while; for now let us concentrate about the fact that the procedure outlined above is the standard one to calculate form factors on the lattice. In this way, however, it is very hard to reach the percent level precision required for the present calculation; the operation which makes this procedure highly inefficient is the multiplication of the l.h.s. of (3.26) for the matrix elements Z_K and Z_π. The adopted solution is to introduce another three–point function, which is the symmetrized version of (3.22) and which corresponds to the unphysical process $\pi \to K$; for t and $t' - t$ large enough it goes as

$$\begin{aligned} C_\mu^{\pi K}(t, t', \vec{p}, \vec{p}\,') \xrightarrow[(t' - t) \to \infty]{t \to \infty} & \frac{\sqrt{Z_K Z_\pi}}{4 E_K(\vec{p}\,') E_\pi(\vec{p})} \frac{1}{Z_V} \langle K(p')|\, \hat{V}_\mu^\dagger\, |\pi(p)\rangle \cdot \\ & \cdot e^{-E_\pi(\vec{p}) t - E_K(\vec{p}\,')(t' - t)}\,, \end{aligned} \tag{3.27}$$

and allows one to calculate, in the *Breit* frame where $\vec{p} = -\vec{p}\,' = \vec{\theta}$, the improved double ratio $R_\mu(t, \theta)$

$$R_\mu(t, t'; \theta) = \frac{C_\mu^{K\pi}(t, t', \vec{\theta}, -\vec{\theta}) C_\mu^{\pi K}(t, t', \vec{\theta}, -\vec{\theta})}{C^K(t, \vec{\theta}) C^\pi(t' - t, -\vec{\theta}) C^\pi(t, \vec{\theta}) C^K(t' - t, -\vec{\theta})}\,. \tag{3.28}$$

Let us verify that this expression indeed tend to the desired matrix element; to this end, using (3.24), (3.25) and (3.27) one gets in the usual way

$$R_\mu(t,t';\theta) = \frac{C_\mu^{K\pi}(t,t',\vec{\theta},-\vec{\theta})}{C^K(t,\vec{\theta})C^\pi(t'-t,-\vec{\theta})} \cdot \frac{C_\mu^{\pi K}(t,t',\vec{\theta},-\vec{\theta})}{C^\pi(t,\vec{\theta})C^K(t'-t,-\vec{\theta})} \xrightarrow[(t'-t)\to\infty]{t\to\infty} \frac{1}{Z_V^2}\frac{\langle\pi(-\vec{\theta})|\,\hat{V}_\mu\,|K(\vec{\theta})\rangle\,\langle K(-\vec{\theta})|\,\hat{V}_\mu^\dagger\,|\pi(\vec{\theta})\rangle}{Z_K Z_\pi}\,; \tag{3.29}$$

on the other hand, realizing that

$$C^K(t,\vec{\theta})C^K(t'-t,-\vec{\theta}) \xrightarrow[t\to\infty]{} \frac{Z_K}{2E_K}\frac{Z_K}{2E_K}\,e^{-E_K t}e^{-E_K(t'-t)} = \frac{Z_K}{2E_K}\cdot C^K(t',\vec{\theta}) \tag{3.30}$$

the l.h.s. of (3.29) can be written as

$$R_\mu(t,t';\theta) = \frac{2E_K}{Z_K}\frac{C_\mu^{K\pi}(t,t',\vec{\theta},-\vec{\theta})}{C^K(t',\vec{\theta})}\cdot\frac{2E_\pi}{Z_\pi}\frac{C_\mu^{\pi K}(t,t',\vec{\theta},-\vec{\theta})}{C^\pi(t',\vec{\theta})} \tag{3.31}$$

which, compared with the r.h.s of (3.29), makes clear that we have gained the desired kinematic factors in order that, setting $\mathcal{N} = Z_K Z_\pi/(4E_K E_\pi)$, we can arrive to the following expression

$$\mathcal{N}\cdot R_\mu(t,t';\theta) = \frac{C_\mu^{K\pi}(t,t',\vec{\theta},-\vec{\theta})}{C^K(t',\vec{\theta})}\cdot\frac{C_\mu^{\pi K}(t,t',\vec{\theta},-\vec{\theta})}{C^\pi(t',\vec{\theta})} \xrightarrow[(t'-t)\to\infty]{t\to\infty} \frac{1}{Z_V^2}\frac{\langle\pi(-\vec{\theta})|\,\hat{V}_\mu\,|K(\vec{\theta})\rangle\,\langle K(-\vec{\theta})|\,\hat{V}_\mu^\dagger\,|\pi(\vec{\theta})\rangle}{4E_K E_\pi}\,. \tag{3.32}$$

It is important to stress the fact that in the right hand side there is no sum over μ.

Let us now turn our attention to what we had postponed at the beginning of this section: the calculation of the vector current renormalization constant and its automatic inclusion in the ratio (3.32). Let us introduce the pion-to-pion three–point correlation function, analogue to (3.22)[1] but formally with $K = \pi$, which in the large t and $t'-t$ limit goes as

[1] For a definition of the pion-to-pion three–point correlation function for every value of t and $t'-t$ see [90].

$$C_\mu^{\pi\pi}(t,t',\vec{p},\vec{p}\,') \xrightarrow[(t'-t)\to\infty]{t\to\infty} \frac{Z_\pi}{4E_\pi(\vec{p})E_\pi(\vec{p}\,')}\frac{1}{Z_V}\langle\pi(p')|\,\hat{V}_\mu^\dagger\,|\pi(p)\rangle\cdot \cdot\; e^{-E_\pi(\vec{p})t-E_\pi(\vec{p}\,')(t'-t)}\,; \tag{3.33}$$

now, exploiting the fact that the matrix element of the time component of the vector current evaluated between degenerate states is the matrix element of the conserved electromagnetic current, the electric charge normalization imply that

$$\langle\pi(K)|\,\hat{V}_0(0)\,|\pi(K)\rangle = 2M_{\pi(K)}f^{\pi(K)\to\pi(K)}(q^2=0) = 2M_{\pi(K)}\,, \tag{3.34}$$

and this allows one to introduce two equivalent definition of Z_V

$$Z_V^{\pi\pi} \doteq \frac{C^\pi(t',\vec{0}\,)}{C_0^{\pi\pi}(t,t',\vec{0},\vec{0}\,)} \xrightarrow[(t'-t)\to\infty]{t\to\infty} Z_V\,, \quad \text{and} \tag{3.35}$$

$$Z_V^{KK} \doteq \frac{C^K(t',\vec{0}\,)}{C_0^{KK}(t,t',\vec{0},\vec{0}\,)} \xrightarrow[(t'-t)\to\infty]{t\to\infty} Z_V\,. \tag{3.36}$$

For reasons which will become clear later, let us define the vector renormalization constant as the geometric mean

$$Z_V = \sqrt{Z_V^{\pi\pi}Z_V^{KK}}\,, \tag{3.37}$$

where $Z^{\pi\pi}$ and Z^{KK} are the one defined in (3.35) and (3.36). Exploiting (3.37), together with (3.35) and (3.36), one is able to modify (3.32) obtaining

$$\mathcal{N}\cdot R_\mu(t,t';\theta) = \frac{C_\mu^{K\pi}(t,t',\vec{\theta},-\vec{\theta}\,)}{C^K(t',\vec{\theta}\,)}\cdot\frac{C_\mu^{\pi K}(t,t',\vec{\theta},-\vec{\theta}\,)}{C^\pi(t',\vec{\theta}\,)}\cdot\frac{C^\pi(t',\vec{0}\,)}{C_0^{\pi\pi}(t,t',\vec{0},\vec{0}\,)}\cdot\frac{C^K(t',\vec{0}\,)}{C_0^{KK}(t,t',\vec{0},\vec{0}\,)}$$
$$\xrightarrow[(t'-t)\to\infty]{t\to\infty} \frac{\langle\pi(-\vec{\theta}\,)|\,\hat{V}_\mu\,|K(\vec{\theta}\,)\rangle\,\langle K(-\vec{\theta}\,)|\,\hat{V}_\mu^\dagger\,|\pi(\vec{\theta}\,)\rangle}{4E_KE_\pi}\,. \tag{3.38}$$

Let us make some considerations about the matrix elements involved in (3.38). Exploiting the symmetry of the theory under time reversal ($\mathcal{T}$) and charge conjugation

($\mathcal{C}$) transformations and profiting of the Breit kinematic employed in the calculation ($\vec{p}' = -\vec{p}$), one can write the $K \to \pi$ form factors in (3.21) as

$$\langle \pi(\vec{p}\,')|\, \hat{V}_\mu(0)\, |K(\vec{p})\rangle = f_+^{K\to\pi}(q^2)(p+p')_\mu + f_-^{K\to\pi}(q^2)(p-p')_\mu\,. \tag{3.39}$$

The corresponding (unphysical) $\pi \to K$ matrix element is given by

$$\langle K(\vec{p}\,')|\, \hat{V}_\mu^\dagger(0)\, |\pi(\vec{p})\rangle = f_+^{\pi\to K}(q^2)(p+p')_\mu + f_-^{\pi\to K}(q^2)(p-p')_\mu\,. \tag{3.40}$$

Indeed, only two of these four form factors are really independent. These matrix elements are connected by a time reversal and charge conjugation transformation and one can find

$$\langle K(-\vec{\theta})|\, \hat{V}_\mu^\dagger(0)\, |\pi(\vec{\theta})\rangle = \begin{cases} +\langle \pi(-\vec{\theta})|\hat{V}_0(0)|K(\vec{\theta})\rangle & \mu = 0 \\ -\langle \pi(-\vec{\theta})|\hat{V}_i(0)|K(\vec{\theta})\rangle & \mu = i = 1,2,3 \end{cases} \tag{3.41}$$

Writing (3.39) and (3.40) in the Breit frame, one can find these interesting relations between form factors

$$f_+^{\pi\to K}(q^2) = f_+^{K\to\pi}(q^2) \doteq f_+(q^2)\,, \tag{3.42}$$

$$f_-^{\pi\to K}(q^2) = -f_-^{K\to\pi}(q^2) \doteq -f_-(q^2)\,. \tag{3.43}$$

and using (3.41) we can finally write ($i = 1,2,3$)

$$\langle \pi(-\vec{\theta})|\, \hat{V}_\mu(0)\, |K(\vec{\theta})\rangle \cdot \langle K(-\vec{\theta})|\, \hat{V}_\mu^\dagger(0)\, |\pi(\vec{\theta})\rangle = \begin{cases} +\left(\langle \pi(-\vec{\theta})|\, \hat{V}_0(0)\, |K(\vec{\theta})\rangle\right)^2 & \mu = 0 \\ -\left(\langle \pi(-\vec{\theta})|\, \hat{V}_i(0)\, |K(\vec{\theta})\rangle\right)^2 & \mu = i \end{cases} \tag{3.44}$$

Let us note that for the maximum transfer momentum q^2_{MAX} which, in our language, correspond to $\theta = 0$ we find that (3.38) becomes

$$\mathcal{N}\cdot R_0(t,t';\vec{0}) = \frac{C_0^{K\pi}(t,t',\vec{0},\vec{0})C_0^{\pi K}(t,t',\vec{0},\vec{0})}{C_0^{\pi\pi}(t,t',\vec{0},\vec{0})C_0^{KK}(t,t',\vec{0},\vec{0})} \xrightarrow[(t'-t)\to\infty]{t\to\infty} \frac{(M_K+M_\pi)^2}{4M_KM_\pi} f_0^2(q^2_{MAX}) \tag{3.45}$$

expression which gives access directly to the form factor calculated at q^2_{MAX} with a high statistical precision, as can be seen from the results quoted in [17; 18; 19]. The reason why, by means of (3.45), one is able to achieve a high statistical precision is connected with the high precision which one has both in the meson mass extraction and in the numerical calculation of zero momentum correlation function.

The form factors for any value of q^2, different from q^2_{MAX}, can instead be calculated studying the following linear system; with respect to (3.39), we call $\langle \hat{V}_0 \rangle$ the time component of the matrix element of $\hat{V}_\mu$ given by

$$\langle \hat{V}_0 \rangle = (E_K + E_\pi)\, f_+(q^2) + (E_K - E_\pi)\, f_-(q^2)\,. \tag{3.46}$$

The divergence of the matrix element of the spatial component of $\hat{V}_\mu$, in momentum space, is

$$\langle q_i \hat{V}_i \rangle \doteq \sum_{i=1}^{3} q_i \, \langle \pi(\vec{p}\,') | \, \hat{V}_i(0) \, | K(\vec{p}) \rangle \;, \tag{3.47}$$

which, in the Breit system $\vec{p} = -\vec{p}\,' = 2\pi\vec{\theta}/L$, imply

$$\langle q_i \hat{V}_i \rangle = \frac{48\pi^2\theta^2}{L} f_-(q^2)\,; \tag{3.48}$$

then, the form factors $f_\pm(q^2)$ can be calculated solving the linear system defined by (3.46) and (3.48). Using (3.21), which connect f_0 and $f_\pm$, one can finally determine the form factors of interest.

3.2.2 Semileptonic correlators & the *all-to-all* propagator

In order to introduce the so–called *all-to-all* quark propagator, let us note that for the two– and three–point functions it exists also another representation, beside the (asymptotic) quantum mechanical one presented in (3.8) and (3.19); if one starts from the usual definition for the correlators (3.22) and (3.23), which we remind here for the reader's convenience

$$C_{\mu}^{K\pi}(t,t',\vec{p},\vec{p}\,') = \frac{1}{L^3T}\sum_{x,y,z}\langle \mathcal{O}_{\pi}(y)V_{\mu}(x)\mathcal{O}_{K}^{\dagger}(z)\rangle\,\delta_{t,t_x-t_z}\delta_{t',t_y-t_z}\,e^{-i\vec{p}\cdot(\vec{x}-\vec{z})+i\vec{p}\,'\cdot(\vec{x}-\vec{y})}\,, \tag{3.49}$$

$$C^{K(\pi)}(t,\vec{p}) = \frac{1}{L^3T}\sum_{x,z}\langle \mathcal{O}_{K(\pi)}(x)\mathcal{O}_{K(\pi)}^{\dagger}(z)\rangle\,\delta_{t,t_x-t_z}\,e^{-i\vec{p}\cdot(\vec{x}-\vec{z})}\,, \tag{3.50}$$

from the explicit decomposition of the V_μ, $\mathcal{O}_\pi$ and $\mathcal{O}_K$ composite operators in terms of the quark constituent fields and by expressing the *T-product* by means of the Wick theorem (*i.e.* by performing all the possible Wick contractions between equal flavour quark operators), one can actually find an equivalent expression for (3.49) and (3.50) as a function of the *all-to-all* quark propagators $S^{u,d,s}(x,z)$. The two–point functions becomes

$$C^{K(\pi)}(t,\vec{p}) = \sum_{x,z}\langle Tr\left[S_{s(u)}(x,z)\gamma_5 S_d(z,x)\gamma_5\right]\rangle\,\delta_{t,t_x-t_z}e^{-i\vec{p}\cdot(\vec{x}-\vec{z})}\,; \tag{3.51}$$

this expression can be pictorially represented, in terms of Feynman diagrams, as in figure 3.1

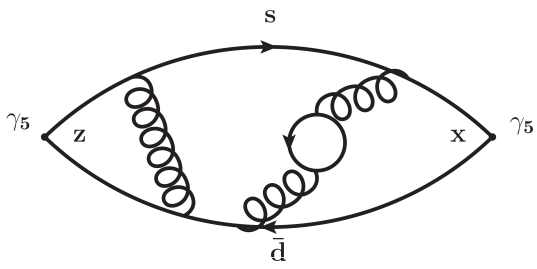

Figure 3.1: Kaon two–point function - It is shown the Feynman diagram corresponding to the (*connected*) two–point function of the Kaon, for the case $t_x > t_z$.

For the tm-LQCD action, the γ_5–hermiticity property

$$S_d(z,x) = \gamma_5 S_u^{\dagger}(x,z)\gamma_5 \tag{3.52}$$

holds with the dagger operation acting on the (suppressed) color and Dirac indices.

As for the three-point function (3.49) in the Breit frame, $C_{\mu}^{K\pi}(t,t',\vec{p},-\vec{p})$, one gets

$$C_\mu^{K\pi}(t,t',\vec{p},-\vec{p}) = \sum_{x,z} \langle Tr\left[S_s(x,z)\gamma_5 \bar{\Sigma}_{du}(z,x;t';-\vec{p})\gamma_\mu\right]\rangle \cdot \tag{3.53}$$

$$\cdot\, \delta_{t,t_x-t_z}\, e^{-2i\vec{p}\cdot(\vec{x}-\vec{z})}\,, \tag{3.54}$$

where $\overline{\Sigma}_{du}(z,x;t';-\vec{p}) = \gamma_5[\Sigma_{du}(x,z;t';-\vec{p})]^\dagger\gamma_5$ and

$$\Sigma_{du}(x,z;t';\vec{p}) = \sum_y S_d(x,y)\gamma_5 S_u(y,z)\; e^{-i\vec{p}\cdot(\vec{z}-\vec{y})}\; \delta_{t',t_y-t_z}\;. \tag{3.55}$$

The *sequential* propagator $\Sigma_{du}(x,z;t';\vec{p})$ satisfies the equation

$$\sum_y D_d(x,y)\; \Sigma_{du}(y,z;t';\vec{p}) = \gamma_5 S_u(x,z)\; \delta_{t',t_x-t_z}\; e^{i\vec{p}\cdot(\vec{x}-\vec{z})}\;. \tag{3.56}$$

The three–point function (3.53) can be represented as in figure 3.2.

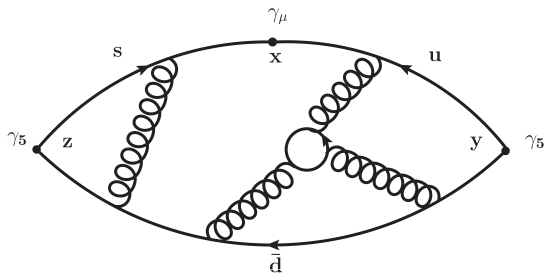

Figure 3.2: Kaon three–point function - It is shown the Feynman diagram corresponding to the (*connected*) three–point function describing the underlying quark process relative to the decay $K \to \pi$. It is the case $t_z < t_x < t_y$.

As we have anticipated in section 2.5, in this work we have employed θ–BC and so we must now rewrite the correlators in terms of quark fields which satisfy these constraints. For (3.51) to (3.56) we have only to replace the propagators S and Σ with the corresponding twisted ones, $\widetilde{S}$ and $\widetilde{\Sigma}$, and also take into account the change of the quantized momenta, namely $p_j \to \widetilde{p}_j = p_j + 2\pi\theta_j/L$ (see (2.106)). The two– and three–point correlators can be expressed in terms of quark propagators satisfying periodic BC's, e.g. in terms of the $S^{\widetilde{\theta}}$ in (2.121). We now write down the explicit formulae for sake of completeness.

In order to work in the Breit frame we consider three choices of the twisting four-vector $\widetilde{\theta}$, namely $\widetilde{\theta} = \widetilde{\theta}_{\pm} = (L/2T, \pm\vec{\theta}\,)$ and $\widetilde{\theta} = \widetilde{\theta}_0 = (L/2T, \vec{0}\,)$ for various values of $\vec{\theta}$. Writing $\vec{p}$ in the generic form $\vec{p} = 2\pi\vec{\theta}/L$, we get

$$C^{K(\pi)}(t, \frac{2\pi}{L}\vec{\theta}\,) = \frac{1}{L^3T}\sum_{x,z}\langle Tr[S^{\widetilde{\theta}_+}_{s(u)}(x,z)\gamma_5 S^{\widetilde{\theta}_0}_{d}(z,x)\gamma_5]\rangle\ \delta_{t,t_x-t_z}, \tag{3.57}$$

$$C^{K\pi}_{\mu}(t,t', \frac{2\pi}{L}\vec{\theta}, -\frac{2\pi}{L}\vec{\theta}\,) \quad = \quad \frac{1}{L^3T}\sum_{x,z}\langle Tr[S^{\widetilde{\theta}_+}_{s}(x,z)\gamma_5 \overline{\Sigma}^{\widetilde{\theta}_0,\widetilde{\theta}_-}_{du}(z,x;t')\gamma_\mu]\rangle\ \delta_{t,t_x-t_z} \tag{3.58}$$

where, thanks to the γ_5-hermiticity property, one has

$$\overline{\Sigma}^{\widetilde{\theta}_0,\widetilde{\theta}_-}_{du}(z,x;t') = \gamma_5[\Sigma^{\widetilde{\theta}_-,\widetilde{\theta}_0}_{du}]^{\dagger}(x,z;t')\gamma_5 \tag{3.59}$$

and the sequential propagator $\Sigma^{\widetilde{\theta}_-,\widetilde{\theta}_0}_{du}(x,z;t')$ satisfies the modified Dirac equation

$$\sum_y D^{\widetilde{\theta}_-}_{d}(x,y)\ \Sigma^{\widetilde{\theta}_-,\widetilde{\theta}_0}_{du}(y,z;t') = \gamma_5 S^{\widetilde{\theta}_0}_{u}(x,z)\ \delta_{t',t_x-t_z}\ . \tag{3.60}$$

Note that, because of (2.121), no exponential factors appear in the r.h.s. of (3.57)-(3.60) and the dependence on the vector $\vec{\theta}$ is totally embedded in the twisted quark propagators $S^{\widetilde{\theta_+}}$ and $\Sigma^{\widetilde{\theta}_-,\widetilde{\theta}_0}_{du}$.

3.2.3 Stochastic procedures for connected diagrams

The next point to be addressed is the evaluation of the all-to-all propagator $S^{\widetilde{\theta}}(x,z)$ which is the solution of the modified Dirac equation (2.119). Restoring color and spin indices, denoted by Latin and Greek letters respectively, one has

$$\sum_y [D^{\widetilde{\theta}}(x,y)]^{ab}_{\alpha\beta}\ [S^{\widetilde{\theta}}(y,z)]^{bc}_{\beta\gamma} = \delta_{x,z}\ \delta_{a,c}\ \delta_{\alpha,\gamma}\ . \tag{3.61}$$

The computation of exact all-to-all quark propagators is a formidable task well beyond present computational capabilities, because it involves a huge number of inversions of the Dirac equation for all possible locations of the source in space and time. Consequently most of the lattice computations of connected two– and three–point correlation

functions are till now carried out using the point-to-all propagator by fixing the source at some space-time point, referred to as the origin. To get the expressions of our two– and three–point correlators in terms of point-to-all propagators it is enough to limit the sum over the variable z to $z = 0$ everywhere in (3.57)–(3.60). The basic advantage of the all-to-all propagator with respect to the point-to-all one relies in the fact that the former contains all the information on the gauge configuration, which in turn means that the calculation of two– and three–point functions using all-to-all propagators is expected to have much less gauge noise.

An efficient way to estimate the all-to-all propagator is based on stochastic techniques with the help of variance reduction methods to better separate the signal from the noise (see [91] and references therein). In recent years new stochastic methods have been developed, like the dilution method [13] and the so-called "one-end-trick" [92; 93]. The former will be treated in section 3.3.1, where we will introduce the disconnected diagrams evaluation techniques, because this is one of the methods we have tested before choosing an optimal one; the latter, already applied by the ETM collaboration to the calculation of neutral meson masses (see [15] and [16]), allows to achieve a great reduction of the noise-to-signal ratio and it will be applied in this work to the calculation of the connected diagrams involved, for instance, in the semileptonic three–point correlation functions (see also [18] and [94]) and in general in all the connected diagram which we are going to calculate.

The starting point of all stochastic approaches is to consider random sources $\eta_r^a(x)$, which, for reasons that will become clear later on, we take independent of both the spin variable and the twisting vector $\widetilde{\theta}$ (i.e., of the quark momentum). The index r ($r = 1, ...N_r$) enumerates the generated random sources, which must satisfy the following constraint

$$\lim_{N_r\to\infty} \frac{1}{N_r} \sum_{r=1}^{N_r} \eta_r^a(x)[\eta_r^b(y)]^* = \delta_{a,b}\ \delta_{x,y}\ . \tag{3.62}$$

In this work we will always adopt for the sources a random choice of ± 1 values. Then one introduces the "ϕ-propagator"

$$[\phi_r^{\widetilde{\theta}}(x)]_{\alpha\beta}^a = \sum_y [S^{\widetilde{\theta}}(x,y)]_{\alpha\beta}^{ab}\ \eta_r^b(y)\ , \tag{3.63}$$

which is solution of the equation

$$\sum_y [D^{\widetilde{\theta}}(x,y)]^{ab}_{\alpha\beta}\ [\phi^{\widetilde{\theta}}_r(y)]^b_{\beta\gamma} = \eta^a_r(x)\ \delta_{\alpha,\gamma}\ . \tag{3.64}$$

where the sum over repeated color or spin indices is understood. As explained in details in [15], the quantity $(1/N_r)\sum_{r=1}^{N_r}[\phi^{\widetilde{\theta}}_r(x)]^a_{\alpha\beta}[\eta^b_r(y)]^*$ is an unbiased estimator of the all-to-all propagator $[S^{\widetilde{\theta}}(x,y)]^{ab}_{\alpha\beta}$. However, while the signal is of order $\mathcal{O}(\mathbb{1})$, the noise is of the order $\sqrt{V/N_r}$ (where V is the space-time volume) and therefore a huge number of random sources and inversions of (3.64) would be required.

The "one-end-trick" is based on the observation that the product of two "ϕ-propagators" is an unbiased estimator of the product of two all-to-all propagators summed over the intermediate space-time points. In this case, however, the signal is of order V, while the noise is of order $V/\sqrt{N_r}$, so that it is even sufficient to employ one random source ($N_r = 1$) per gauge configuration, as we do in this work.

Choosing the random source $\eta^r_a(x)$ to be non-vanishing only for a randomly-chosen time slice, located at t_r [1], the two–point correlation function (3.57) can be estimated as

$$C^{K(\pi)}(t, \frac{2\pi}{L}\vec{\theta}) = \sum_{\vec{x},t_x}\langle[\phi^{\widetilde{\theta}_+}_{s(u),r}(\vec{x},t_x)]^a_{\alpha\beta}\ \{[\phi^{\widetilde{\theta}_0}_{u,r}(\vec{x},t_x)]^a_{\beta\alpha}\}^*\ \delta_{t,t_x-t_r}\rangle \tag{3.65}$$

Looking at the above equation the ϕ-propagator $[\phi^{\widetilde{\theta}}_r(x)]^a_{\alpha\beta}$ plays a role quite similar to the one of the point-to-all propagator $[S^{\widetilde{\theta}}(x,0)]^{ab}_{\alpha\beta}$ with only one color index, being the other one carried by the random source. This means that the time needed for the calculation of the ϕ-propagator is 1/3 of the one required for the point-to-all propagator. Note also that both $\phi^{\widetilde{\theta}_+}_r(x)$ and $\phi^{\widetilde{\theta}_0}_r(x)$ are solutions of (3.64) with the same random source $\eta_r(x)$. This is essential to properly get the r.h.s. of (3.65). Moreover the independence of the random source from spin indices allows to evaluate two–point correlation functions with interpolating fields of the form $(\bar{q}\Gamma q')$ for any Dirac matrix Γ.

[1] The random choice of the time slice at t_r is mainly motivated by the reduction of autocorrelations observed for fermionic quantities using the ETM gauge ensembles (see [15]).

The stochastic estimate of the three–point correlation function (3.58) requires the introduction of the sequential "Φ-propagator"

$$[\Phi^{\widetilde{\theta}_-,\widetilde{\theta}_0}_{du,r}(x;t')]^a_{\alpha\beta} = \sum_y [\Sigma^{\widetilde{\theta}_-,\widetilde{\theta}_0}_{du,r}(x,y;t')]^{ab}_{\alpha\beta}\ \eta^b_r(y), \tag{3.66}$$

which is solution of the equation

$$\sum_y [D^{\widetilde{\theta}_-}_d(x,y)]^{ab}_{\alpha\beta}\ [\Phi^{\widetilde{\theta}_-,\widetilde{\theta}_0}_{du,r}(y;t')]^b_{\beta\rho} = [\gamma_5]_{\alpha\gamma}\ [\phi^{\widetilde{\theta}_0}_{u,r}(x)]^a_{\gamma\rho}\ \delta_{t',t_x-t_r}\ . \tag{3.67}$$

One gets

$$\begin{aligned} C^{K\pi}_\mu(t,t',\frac{2\pi}{L}\vec{\theta},-\frac{2\pi}{L}\vec{\theta}) \;=\; & \sum_{\vec{x},t_x} \langle\ [\phi^{\widetilde{\theta}_+}_{s,r}(\vec{x},t_x)]^a_{\alpha\beta}\ \{[\Phi^{\widetilde{\theta}_-,\widetilde{\theta}_0}_{du,r}(\vec{x},t_x;t')]^a_{\beta\gamma}\}^* \\ & \cdot\ [\gamma_5\gamma_\mu]_{\gamma\alpha}\ \delta_{t,t_x-t_r}\rangle\ . \end{aligned} \tag{3.68}$$

Let us note that for each value of the quark momentum $\vec{\theta}$ injected via the twisted BC an inversion of the θ-dependent Dirac operator is required.

3.3 The road to the neutron EDM calculation

We have already mentioned that the resolution of the $U(\mathbb{1})_A$ problem effectively adds the extra term (1.168) to the QCD lagrangian, and that this term is able to generate an EDM for the neutron. This quantity can be estimated using LQCD by means of several strategies. The first approach (*cfr.* [95] and the more recent one [96]) is to measure the energy difference between *spin-up* and *spin-down* neutrons, in presence of a uniform and static electric field. The second one [97; 98] is to parametrize the matrix element of the electromagnetic current between nucleons in terms of form factors and then measure the $\mathcal{CP}$–odd one ($F_3(q^2)$). The third [12] is based on the evaluation of the disconnected insertion of the singlet pseudo-scalar density, as we have outlined in section 1.4.2.

As we are planning a future calculation of the neutron EDM, it is of fundamental importance to carry out a feasibility study of the lattice techniques at our disposal for calculating these disconnected diagrams. To this end we have considered the methods

exposed in [13], [14] and [15] and applied them for calculating the disconnected part of the π^0 and (2–flavour) η' 2–point correlation functions.

The next section will be spent to explain in details these techniques, show their differences and then present an hybrid method which in our opinion can be a good tool for evaluating these noisy diagrams; in this framework we will also discuss how the all-to-all propagator fits within disconnected insertions.

The results and the comparisons among these techniques will be presented in chapter 4.

3.3.1 Quark-Disconnected diagrams & *all-to-all* propagators

Quark-Disconnected diagrams[1] are a particular class of Feynman diagrams in which fermionic lines are not explicitly connected, but they are linked only through the gluons of the underlying gauge bosons configuration. They are involved in the, so–called, flavour singlet physics observables which can be described by means of operators such as (1.172), which can be generically written as

$$\mathcal{O}_S^\Gamma = \bar{u}\Gamma u + \bar{d}\Gamma d + \bar{s}\Gamma s\,; \tag{3.69}$$

these operators contribute to many physically interesting observables in the low energy region of QCD. From a theoretical point of view, the correlation functions which involve flavour singlet operators differ from the non-singlet one because of the presence of this *disconnected* insertions which are correlations of hadronic propagators with a quark–antiquark loop or correlations between quark-antiquark loops. An example of the former has been seen in figure 1.6 which is the case where a composite particle, such as the neutron, because of the complex properties of the QCD vacuum ($G\widetilde{G}$), interacts with the pseudoscalar density (1.172) (for the sake of clearness, let us neglect its interaction with the other current J_0); then, quantum field theory tells us that beside the direct coupling between the current and the nucleon there is also another term coming from the interaction of the $P_S(x)$ current with a quark-antiquark loop within the neutron field.

[1] For the sake of shortness we will call this class of diagrams simply "disconnected diagrams" in what will follow.

The second kind of disconnected insertions are the correlations between quark-antiquark loops which, for instance, can be found in some mesonic two–point functions; let us use this second class of disconnected insertions and, in particular, the π^0 and the two–flavour[1] η' correlation functions, as a testing ground for the available methods which will result in a formulation of our hybrid technique that might give us a chance for a future evaluation of the much more complicated neutron EDM diagrams. To this end, let us consider the operators

$$\phi(x) = i\,\frac{\bar{u}(x)\gamma_5 u(x) - \bar{d}(x)\gamma_5 d(x)}{\sqrt{2}}\,, \qquad \text{with} \;\; \phi = \phi^\dagger\,, \tag{3.70}$$

$$\eta_2(x) = i\,\frac{\bar{u}(x)\gamma_5 u(x) + \bar{d}(x)\gamma_5 d(x)}{\sqrt{2}}\,, \qquad \text{with} \;\; \eta_2 = \eta_2^\dagger \tag{3.71}$$

which possess the same quantum numbers of the π^0 and the η', and let us define the related correlation functions

$$C^{\pi^0}(t,\vec{p}) = \frac{1}{L^3 T}\sum_{x,y}\langle\phi(\vec{y},t_y)\phi(\vec{x},t_x)^\dagger\rangle\,\delta_{t,t_y-t_x}\,e^{-i\vec{p}\cdot(\vec{x}-\vec{y})}\,, \tag{3.72}$$

$$C^{\eta'}(t,\vec{p}) = \frac{1}{L^3 T}\sum_{x,y}\langle\eta_2(\vec{y},t_y)\eta_2(\vec{x},t_x)^\dagger\rangle\,\delta_{t,t_y-t_x}\,e^{-i\vec{p}\cdot(\vec{x}-\vec{y})}\,. \tag{3.73}$$

By carrying out, as usual, all the Wick contractions between the quark fields composing the two operators ϕ and η_2, one arrive at the expression (for $t_y > t_x$)

$$C^{\pi^0}(t,\vec{p}) = \frac{1}{L^3 T}\sum_{x,y}\frac{1}{2}\left[A(x,y) + D_\pi(x,y)\right]\delta_{t,t_y-t_x}\,e^{-i\vec{p}\cdot(\vec{x}-\vec{y})} \tag{3.74}$$

$$C^{\eta'}(t,\vec{p}) = \frac{1}{L^3 T}\sum_{x,y}\frac{1}{2}\left[A(x,y) + D_\eta(x,y)\right]\delta_{t,t_y-t_x}\,e^{-i\vec{p}\cdot(\vec{x}-\vec{y})} \tag{3.75}$$

where, we have indicated with $A(x,y)$ and $D_{\pi,\eta}(x,y)$, respectively, the connected and the disconnected part of the two correlation functions. The connected part is the same for both the π^0 and the η' and can be explicitly written as

$$A(x,y) = Tr\left[S_u(x,y)\gamma_5 S_u(y,x)\gamma_5\right] + Tr\left[S_d(x,y)\gamma_5 S_d(y,x)\gamma_5\right]\,, \tag{3.76}$$

[1] From now on, for shortness, we will always refer to the 2–flavour η' considered in this work as simply η'.

indicating with $S_{u,d}(y,x)$ the all-to-all u,d quark propagator and with Tr the trace operator over all the propagator's degree of freedom (color, spin, space and time). The corresponding topology can be represented as in figure 3.3.

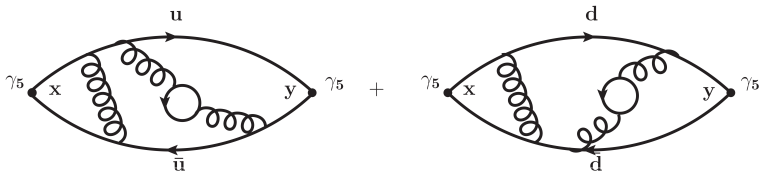

Figure 3.3: Connected topology - of the π^0 and η' 2–point correlation functions. Solid lines are quark propagators, while wavy lines are gluons. Extra (sea) quark loops are not shown.

The disconnected parts, instead, can be written as

$$\begin{aligned} D_\pi(x,y) = \quad & Tr\left[S_u(x,x)\gamma_5\right]\cdot Tr\left[S_d(y,y)\gamma_5\right] + Tr\left[S_d(x,x)\gamma_5\right]\cdot Tr\left[S_u(y,y)\gamma_5\right] \\ & - Tr\left[S_u(x,x)\gamma_5\right]\cdot Tr\left[S_u(y,y)\gamma_5\right] - Tr\left[S_d(x,x)\gamma_5\right]\cdot Tr\left[S_d(y,y)\gamma_5\right] \ ; \end{aligned} \tag{3.77}$$

$$\begin{aligned} D_\eta(x,y) = \quad & Tr\left[S_u(x,x)\gamma_5\right]\cdot Tr\left[S_d(y,y)\gamma_5\right] + Tr\left[S_d(x,x)\gamma_5\right]\cdot Tr\left[S_u(y,y)\gamma_5\right] \\ & + Tr\left[S_u(x,x)\gamma_5\right]\cdot Tr\left[S_u(y,y)\gamma_5\right] + Tr\left[S_d(x,x)\gamma_5\right]\cdot Tr\left[S_d(y,y)\gamma_5\right] \ . \end{aligned} \tag{3.78}$$

and the corresponding Feynman diagrams are represented in figure 3.4.

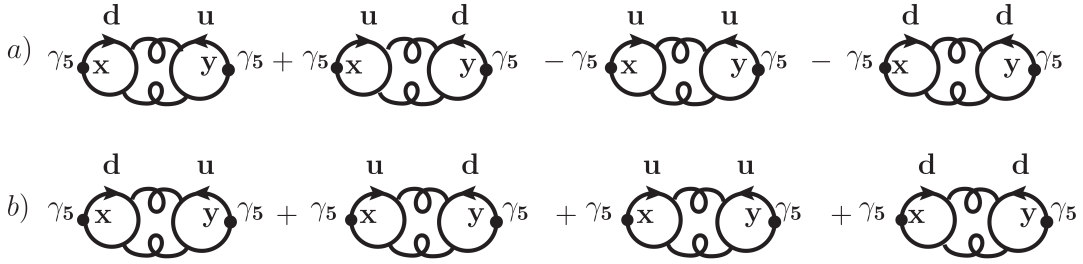

Figure 3.4: Disconnected topology - of the π^0 (a) and η' (b) 2–point correlation functions. Solid lines are quark propagators, while wavy lines are gluons. Extra (sea) quark loops are not shown.

It is now clear that the goal of the calculation is the estimate of the quantity, which we will call fermionic *bubble*, defined as

$$\mathcal{B}^{\Gamma}(t) = \sum_{\vec{x}} Tr\left[S_i(\vec{x},t;\vec{x},t)\Gamma\right] \quad \text{with } i = u,d \tag{3.79}$$

where Γ is any of the sixteen Dirac γ matrices combinations.

The are two main methods, conceived by the authors of [13] and of [14] which allows one to obtain the quantity in (3.79) and which we are going to explain in what follows; for reasons which will become clear later , after a detailed study of these techniques, we have worked out an hybrid method, which combine what we think are the best virtues of the two methods. We will also show a third method [15], which can be employed only with the twisted mass action and which is less general with respect to the one of [13] and [14] (and to our hybrid method too), but which is particularly effective in the case of η' correlation.

Let us start with the one exposed in [13], called "*dilution*" method. The method starts from equation (3.64) solved by the "ϕ-propagator", considered in this contest independent from the twisting vector $\widetilde{\theta}$, which can be rewritten and generalized as

$$\sum_{y} \left[D(x,y)\right]^{ab}_{\alpha\beta} \left[\phi_r(y)\right]^{b}_{\beta} = \left[\eta_r(x)\right]^{a}_{\alpha} \ . \tag{3.80}$$

We note that now the η_r sources are (color-spin) vectors, filled with (random) ± 1, and which must satisfy the orthogonality relation (3.62) as the only constraint; then, the dilution procedure uses one volume source η_r ($N_r = 1$), on the r.h.s. of (3.80) by breaking it up into pieces, which only have support on a single time–slice each,

$$\eta(\vec{x},t) = \sum_{j=0}^{N_t-1} \eta^{(j)}(\vec{x},t) \qquad \text{with} \quad \eta^{(j)}(\vec{x},t) = 0 \quad \text{if} \quad j \neq t \tag{3.81}$$

where j stands for the dilution index (in this example *time–dilution*) and N_t is the number of the lattice time–slices.

This dilution procedure can be carried out on any index of the employed source, up to the so called *homeopathic* limit in which one dilute every single degree of freedom of the η_r vector. Using a noise vector such as the one in (3.81) means that one will have to solve (3.80) for each $\eta^{(j)}$ obtaining, in the time–dilution case, N_t couples of vectors

$\{\phi^j, \eta^j\}$ while in the general case, defining $N_d = \prod_i N_i$ (with N_i which quantifies the dilution on the index i), one will have N_d vector couples $\{\phi^j, \eta^j\}$. These N_d couples of vectors can be used for estimating the fermionic bubble (3.79) by means of

$$\mathcal{B}^A(t) = \sum_{j=1}^{N_d} \mathcal{O}^{(j)A}(t) \qquad \text{with} \tag{3.82}$$

$$\mathcal{O}^{(j)A}(t) = \sum_{\vec{x}} \left[\eta_r^{(j)}(\vec{x},t)^\dagger\right]_\alpha^a \left[\Gamma^A \phi_r^{(j)}(\vec{x},t)\right]_\alpha^a . \tag{3.83}$$

We want to stress the fact that, in physical applications where N_f flavour are contemporary involved the computation cost is $N_d \times N_f$ inversions per configuration; moreover, we point out that for applications such as (3.77) and (3.78), in which one has to multiply propagators with the same flavour, the number of inversions get doubled ($2 \times N_d \times N_f$) because one has to give two *independent* estimates of the propagator for *each* flavour involved in the product in order to avoid undesired contractions between the η vectors. This is a general argument when dealing with amplitudes which involve products of fermionic bubbles of the same flavour, and from now on this multiplicity factor will be always omitted, unless otherwise specified.

Let us explain why one should use this method and spend N_d inversions per configuration, instead of only one for each flavour: the reason is that, diluting the source, one is able to exactly reconstruct the trace over the diluted degree of freedom, and this is of great importance when dealing with stochastic noise reduction[1].

Before moving to the second method, we summarize the dilution procedure, and its principal features, for calculating a single fermionic bubble

1. Generate a volume source $\eta(\vec{x},t)$ filled with random ± 1.

2. Dilute the volume source on the desired degree of freedom $\eta(\vec{x},t) \rightarrow \eta^{(j)}(\vec{x},t)$ (one must consider that the larger the variable is, the greater will be the number of inversion *per configuration*).

3. Calculate the solution vector solving $D\phi^{(j)} = \eta^{(j)}$, where D stands for any regularization of the Dirac operator.

[1] In principle, reaching the homeopathic limit, one is able to exactly calculate the all-to-all propagator and exactly reconstruct the trace over any degree of freedom of the source thus completely eliminating the stochastic noise. In practice this limit is not yet reachable.

4. Construct the quantity $\mathcal{O}^{(j)A}(t)$.

5. Repeat steps 1 to 4 N_d times.

6. Construct the fermionic bubble $\mathcal{B}^A(t)$.

7. Repeat preceding steps for each desired flavour and for each configuration.

It is of great importance to understand that, with this procedure (with N_r set to 1), the stochastic sample average, essential to get the orthogonality property (3.62), is carried out together with the gauge field configuration mean.

Let us now move to the method exposed in [14], which we will call the "*direct*" method; we will start with the procedure *recipe*, as the method is far easier that the dilution one, and then we will make some comments. The fermionic bubble calculation by means of the direct method proceeds as follows

1. Generate a volume source $\eta_r(\vec{x},t)$ filled with random ± 1, defined on the *whole* space–time.

2. Calculate the solution vector solving $D\phi_r = \eta_r$.

3. Construct the r^{th} fermionic bubble using

$$B_r^A(t) = \sum_{\vec{x}} \left[\eta_r(\vec{x},t)^\dagger\right]_\alpha^a \left[\Gamma^A \phi_r(\vec{x},t)\right]_\alpha^a \tag{3.84}$$

4. Repeat steps 1 to 3 for N_r stochastic sources ($r = 1, \ldots, N_r$).

5. Start the stochastic sample average by means of

$$\mathcal{B}^A(t) = \sum_{r=1}^{N_r} \frac{B_r^A}{N_r} \tag{3.85}$$

6. Repeat steps 1 to 5 for the number of desired flavors and for the number of gauge field configurations. Let us stress the fact that if one is dealing with expressions such as (3.77) and (3.78) one will have to calculate two *independent* determinations of the fermionic bubble (3.85) *i.e.* repeat steps 1 to 5 one time more for each flavour and gauge field configuration.

The differences with the dilution method are two: the first is about computation time while the second is about procedure. The direct method uses noise vector defined on the whole space–time and it means, translated at a computation time level, that the number of inversions employed by the method are $N_r \times N_f$, against the $N_d \times N_f$ of the dilution method which, depending on which index one is diluting, typically employs an N_d greater than the typical N_r used in the simulations. As a result the dilution method can have the drawback of being volume–dependent[1] and more time–consuming; moreover, looking, at the two procedures, it is easy to understand that the direct method, with the sample average at point 5, already starts, on each single configuration, the stochastic mean and this allows one to better suppress gauge-variant terms deriving from the non–exact closure of the fermionic trace (it becomes exact ony when relation (3.62) is exactly fulfilled).

From these simple features and from some numerical simulations, in the *quenched* approximation, which we are going to show it is easy to understand what will be the idea standing behind our hybrid method. We show in figure 3.5 and 3.6, respectively, the disconnected contributions (3.77) and (3.78) to the neutral pion and to the eta prime (zero momentum) correlators as a function of time, calculated using both the direct method and the dilution technique applied to the color and spin variables of the sources. The presented results has been obtained averaging data from 300 gauge field configurations, at $\beta = 6.0$, using a lattice volume of $V \times T = 16^3 \times 32$ and a bare quark mass which correspond to $300\, MeV$ pions[2]. In our opinion these tests show that the (spin) dilution technique is more effective in reproducing the euclidean Green function in the η' case (see figure 3.6) while start averaging over the stochastic sample on each gauge field configuration is more crucial for reproducing the π^0 Green function (see figure 3.5): so we have decided to combine these two main features in a method which we have called "*spin–direct*".

The *spin–direct* method uses sources which, like the one employed by the "one-end-trick", are spin independent and then are also diluted on the spin variable employing the usual technique as

[1] We are referring to the time–dilution case.

[2] For more detailed informations about the simulation set up, see [99]

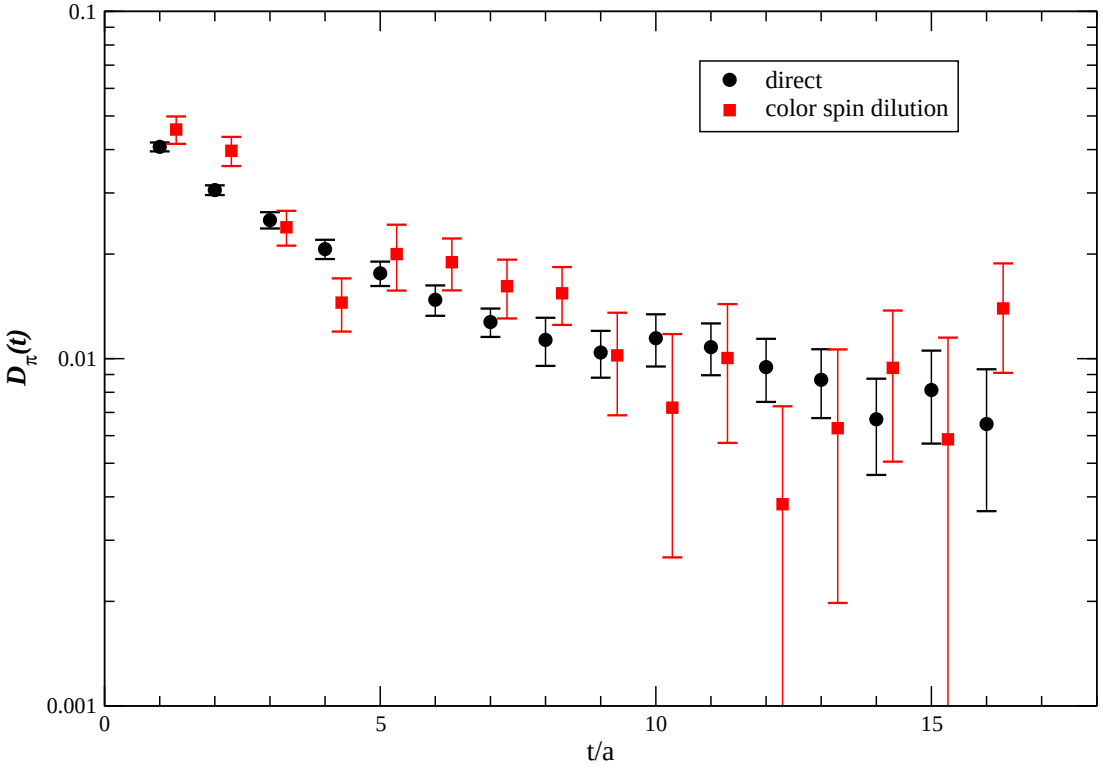

Figure 3.5: Direct V.S. color spin dilution method (π^0) - We show the disconnected part of the neutral pion correlator at zero momentum (disconnected part of (3.74), with $\vec{p} = 0$) as a function of time (in lattice units). The full dots represent the data obtained using the direct method, while the full squares are obtained using the color spin dilution technique. Data are obtained from 300 gauge field configuration at $\beta = 6.0$ for a volume of $V \times T = 16^3 \times 32$ and a bare quark mass which correspond to 300 MeV pions, generated in the quenched approximation. The number of inversions *per* configuration amounts to $N_f \times 2 \times 12$ for the color spin dilution method while for the direct one it is $N_f \times 24$. For the sake of readability, the color spin dilution correlator has been translated in t/a of 0.3.

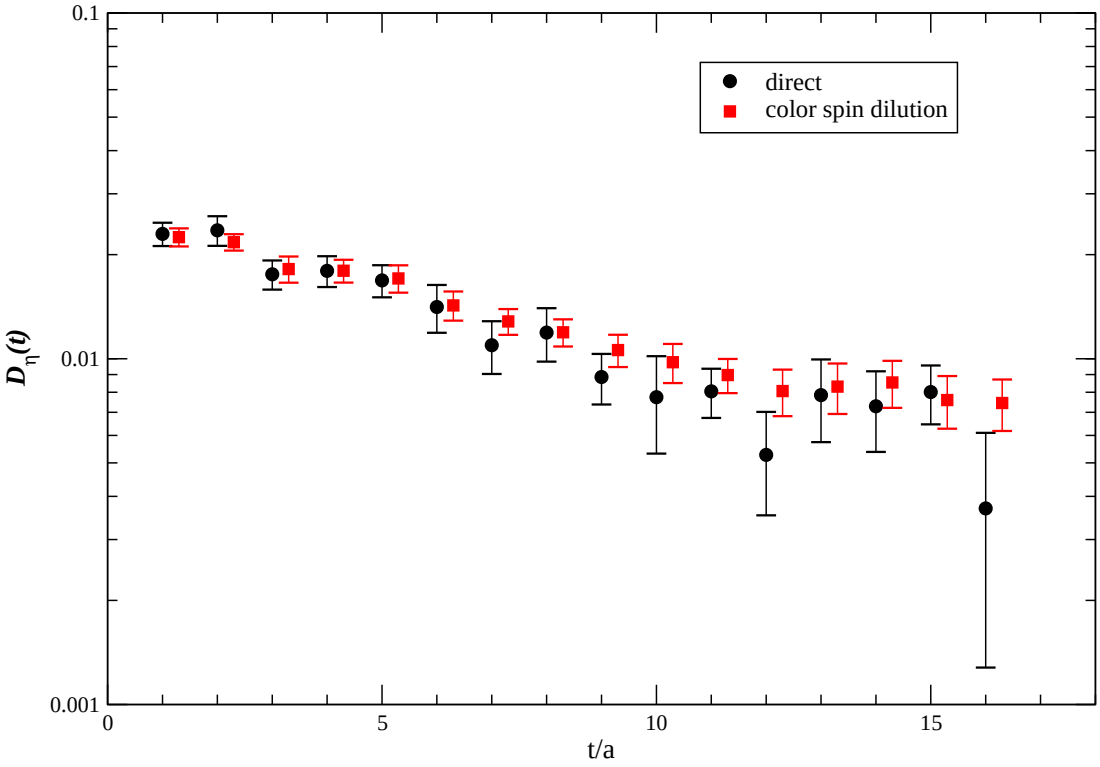

Figure 3.6: Direct V.S. color spin dilution method (η') - We show the disconnected part of the η' correlator at zero momentum (disconnected part of (3.75), with $\vec{p} = 0$) as a function of time (in lattice units). The full dots represent the data obtained using the direct method, while the full squares are obtained using the color spin dilution technique. Data are obtained from 300 gauge field configuration at $\beta = 6.0$ for a volume of $V \times T = 16^3 \times 32$ and a bare quark mass which correspond to $300\, MeV$ pions, generated in the quenched approximation. The number of inversions *per* configuration amounts to $N_f \times 2 \times 12$ for the color spin dilution method while for the direct one it is $N_f \times 24$. For the sake of readability, the color spin dilution correlator has been translated in t/a of 0.3.

$$\eta(\vec{x},t) = \sum_i \eta^{(i)}(\vec{x},t)\delta_{\alpha,\beta} \qquad \text{with } \eta^{(i)} = 0 \text{ if } i \neq \alpha\,, \tag{3.86}$$

then, the procedure for obtaining the fermionic bubble can be schematically presented as

1. Generate a volume source $\eta_r(\vec{x},t)$ filled with random ± 1, defined on the whole space–time.
2. Spin-dilute the noise vector $\eta_r(\vec{x},t) \rightarrow \eta_r^{(j)}(\vec{x},t)$.
3. Calculate the solution vector solving $D\phi_r^{(j)} = \eta_r^{(j)}$.
4. Construct the fermionic quantity
$$\mathcal{O}_r^{(j)A}(t) = \sum_{\vec{x}} \left[\eta_r^{(j)}(\vec{x},t)^\dagger\right]_\alpha^a \left[\Gamma^A \phi_r^{(j)}(\vec{x},t)\right]_\alpha^a . \tag{3.87}$$
5. Repeat steps 1 to 4 N_r times.
6. Start the stochastic sample average building
$$\mathcal{O}^{(j)A}(t) = \sum_{r=1}^{N_r} \frac{\mathcal{O}^{(j)A}(t)}{N_r}\,. \tag{3.88}$$
7. Repeat steps 1 to 6 N_d ($N_d = 4$) times and then construct the fermionic bubble as
$$\mathcal{B}^A(t) = \sum_{j=1}^{N_d} \mathcal{O}^{(j)A}(t)\,. \tag{3.89}$$

Let us stress the fact that with this method one is able to achieve an exact trace over the spin index while the mean operation of point 6 improves the trace over the other, non-diluted, degrees of freedom. The method's computation time is of $4 \times N_r$ and saves a factor of two with respect to the other methods because, as it uses spin-independent sources, inversions results are relevant both for the u flavour and the d one[1]. With this

[1] The reason for this extra gain with respect to the other methods must be traced back to the peculiar algorithm which we employ for the twisted-mass Dirac operator inversion which, in the physical basis, dut to the spin-independence of the sources, does not distinguish between the u–like and the d–like flavors.

technique one is able to well reproduce both the π^0 and the η' disconnected correlation functions, as can be seen in figure 3.7 and 3.8, where we show the comparison between this method and the *direct* one in the π^0 and η' case, respectively. These data have been calculated at the same beta, same number of gauge field configurations and volume of the previous comparisons, presented in figure 3.5 and 3.6.

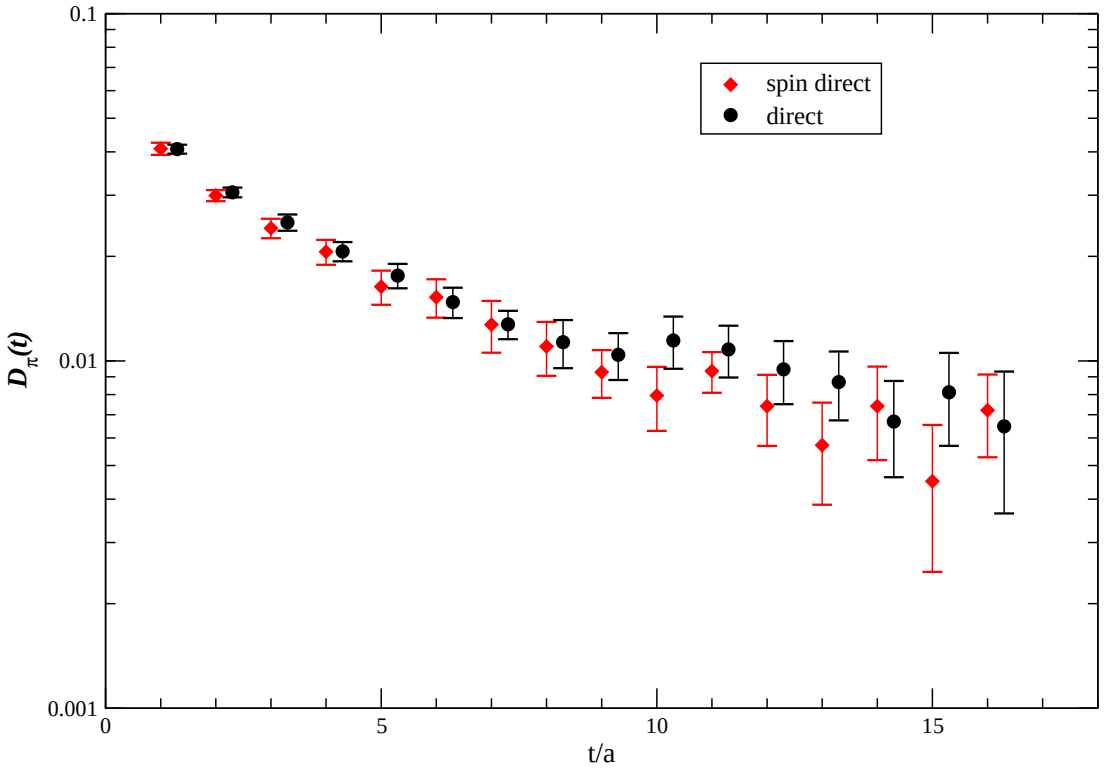

Figure 3.7: Spin–direct V.S. direct method (π^0) - We show the disconnected part of the neutral pion correlator at zero momentum (disconnected part of (3.74), with $\vec{p} = 0$) as a function of time (in lattice units). The full dots represent the data obtained using the direct method, while the full diamonds are obtained using the spin–direct technique. Data are obtained from 300 gauge field configuration at $\beta = 6.0$ for a volume of $V \times T = 16^3 \times 32$ and a bare quark mass which correspond to 300 MeV pions, generated in the quenched approximation. The number of inversions *per* configuration amount to 4×24 for the spin–direct method while for the direct one it is $N_f \times 24$. For the sake of readability, the direct correlator has been translated in t/a of 0.3.

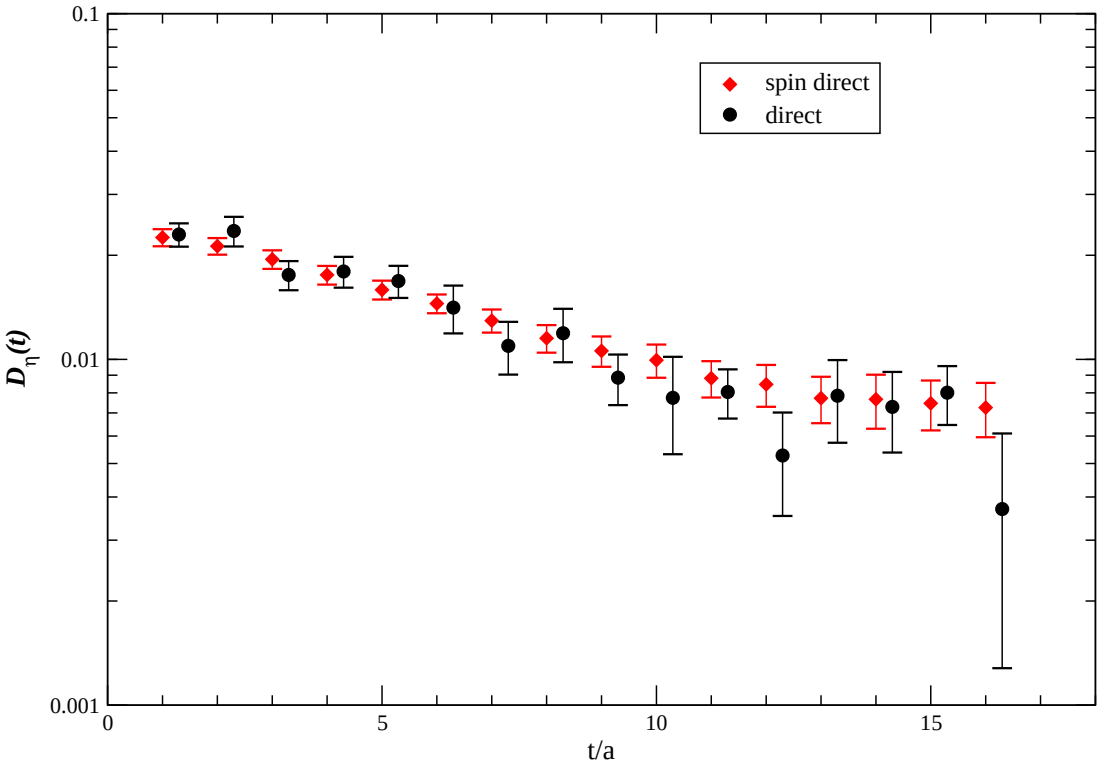

Figure 3.8: Spin–direct V.S. direct method (η') - We show the disconnected part of the η' correlator at zero momentum (disconnected part of (3.75), with $\vec{p} = 0$) as a function of time (in lattice units). The full dots represent the data obtained using the direct method, while the full diamonds are obtained using spin–direct technique. Data are obtained from 300 gauge field configuration at $\beta = 6.0$ for a volume of $V \times T = 16^3 \times 32$ and a bare quark mass which correspond to 300 MeV pions, generated in the quenched approximation. The number of inversions *per* configuration amount to 4×24 for the spin–direct method while for the direct one it is $N_f \times 24$. For the sake of readability, the direct correlator has been translated in t/a of 0.3.

The last method which we are going to present is the one used in [15], which we will call "*twisted*" method. The name of the method derive from the fact that it exploits a particular algebraic identity of the twisted mass operator in the twisted basis (2.55), for which one has that

$$D_{tw}|_u - D_{tw}|_d = -2i\mu\gamma_5 \,, \tag{3.90}$$

where we have omitted all the space, time, spin and color indices, as they are irrelevant

for what we are going to show and we have used the index *tw* to explicitly remind that we are considering the twisted mass Dirac operator in the twisted basis. Let us now consider a particular combination of the fermionic propagators

$$S_u^{tw} - S_d^{tw} \,, \tag{3.91}$$

and let us write it down as

$$S_u^{tw} \left[(S_d^{tw})^{-1} - (S_u^{tw})^{-1} \right] S_d^{tw} \,. \tag{3.92}$$

Using (3.90) one can find the relation

$$\left[S_u^{tw} - S_d^{tw} \right] = 2i\mu \; S_u^{tw} \gamma_5 S_d^{tw} \;; \tag{3.93}$$

multiplying by a generic Dirac Γ matrix and taking the trace of both the l.h.s and the r.h.s of (3.93), one is able to obtain the key identity

$$Tr\left[\Gamma \left(S_u^{tw} - S_d^{tw} \right)\right] = 2i\mu \; Tr\left[\Gamma S_u^{tw} \gamma_5 S_d^{tw}\right] \;. \tag{3.94}$$

Let us bring this expression to the physical basis, using the relations (at maximal twist)

$$S_u^{tw} = \; e^{i\gamma_5 \pi/4} \, S_u \, e^{i\gamma_5 \pi/4} \tag{3.95}$$

$$S_d^{tw} = \; e^{-i\gamma_5 \pi/4} \, S_d \, e^{-i\gamma_5 \pi/4} \tag{3.96}$$

which relate the twisted propagators S_i^{tw} to the physical ones S_i. Performing the transformations (3.95) and (3.96) in (3.94) one is able to obtain

$$Tr\left[\Gamma \left(S_u - S_d \right)\right] = \; 2\mu \; Tr\left[\Gamma S_u \gamma_5 S_d \gamma_5\right] \quad \text{if} \;\; \{\Gamma, \gamma_5\} = 0, \tag{3.97}$$

$$Tr\left[\Gamma \gamma_5 \left(S_u + S_d \right)\right] = \; 2\mu \; Tr\left[\Gamma S_u \gamma_5 S_d\right] \quad \text{if} \;\; [\Gamma, \gamma_5] = 0 \,; \tag{3.98}$$

these relations are very important because show that it is possible to express suited combination of fermionic bubbles as a *connected–like* diagrams, which we are able to determine with a high degree of precision exploiting the modified one-end-trick method.

A convenient extension of the one-end-trick, which allows (3.97) and (3.98) to be translated in terms of the usual ϕ–propagator, requires again the consideration of four ($\beta = 1, 2, 3, 4$) *linked* sources, as in (3.63), of the form

$$[\eta^a_\alpha(\vec{x}, t)]^\beta = \eta^a(\vec{x}, t)\delta_{\alpha\beta}\,, \tag{3.99}$$

which satisfy the usual orthogonality constraint (3.62) but that now, at variance with respect to the one-end-trick, are defined *not* only on a particular time slice[1] but are different from zero at all space-time lattice sites. This allows to rewrite (3.97) and (3.98) as

$$Tr\left[\Gamma\left(S_u - S_d\right)\right] = 2\mu \sum_{\vec{x}} Tr\left\{ \left[\phi^*_{u;r}(\vec{x}, t)\right]^a_{\gamma\alpha} \Gamma_{\alpha\beta} \left[\phi_{u;r}(\vec{x}, t)\right]^a_{\beta\gamma} \right\} \text{ if } \left\{ \Gamma, \gamma_5 \right\} = 0, \tag{3.100}$$

$$Tr\left[\Gamma\gamma_5\left(S_u + S_d\right)\right] = 2\mu \sum_{\vec{x}} Tr\left\{ \left[\phi^*_{u;r}(\vec{x}, t)\right]^a_{\gamma\alpha} (\Gamma\gamma_5)_{\alpha\beta} \left[\phi_{u;r}(\vec{x}, t)\right]^a_{\beta\gamma} \right\} \text{ if } \left[\Gamma, \gamma_5 \right] = 0\,. \tag{3.101}$$

Exploiting the γ_5-hermiticity property (3.52) of the tm-LQCD action, one can derive an analogue expression to (3.100) and (3.101) where, at the r.h.s. one has

$$Tr\left[\Gamma\left(S_u - S_d\right)\right] = -2\mu \sum_{\vec{x}} Tr\left\{ \left[\Gamma\phi^*_{d;r}(\vec{x}, t)\right]^a_{\gamma\alpha} \left[\phi_{d;r}(\vec{x}, t)\right]^a_{\beta\gamma} \right\} \text{ if } \left\{ \Gamma, \gamma_5 \right\} = 0, \tag{3.102}$$

$$Tr\left[\Gamma\gamma_5\left(S_u + S_d\right)\right] = 2\mu \sum_{\vec{x}} Tr\left\{ \left[\Gamma\gamma_5^*\phi^*_{d;r}(\vec{x}, t)\right]^a_{\gamma\alpha} \left[\phi_{d;r}(\vec{x}, t)\right]^a_{\alpha\gamma} \right\} \text{ if } \left[\Gamma, \gamma_5 \right] = 0\,, \tag{3.103}$$

which, together with (3.100) and (3.101), can help to improve the statistical precision for the fermionic bubble combination on the l.h.s.; let us stress the fact that with the twisted method, the procedure for evaluating these combination of fermionic bubbles is greatly simplified with respect to the other ones as it is enough to simply solve the ϕ–propagator equation, with $N_r = 1$, performing only $4 \times N_f$ inversions and then, with the need of diluting or averaging nothing, construct the connected operators on the

[1] This was the one called t_r in the one-end-trick method.

r.h.s. of (3.100), (3.101), (3.102), and (3.103). The drawback to that approach is that one is obliged to use the twisted mass Dirac action as fermionic regularization as well as that it allows to calculate only the disconnected diagrams combination obtainable from (3.100), (3.101), (3.102), and (3.103).

4

Results

In this chapter we will present the results obtained in this *PhD* thesis. As said before, the work is divided in two parts: the first consists of a LQCD study of the form factors for the semileptonic kaon decays $K \to \pi l \nu$ at different values of the momentum transfer. The second one consists of showing our preliminary results obtained for the disconnected fermionic bubble.

The first part start with section 4.1 giving some simulation details about the ETMC gauge field configurations with $N_f = 2$ dynamical flavour of quarks, paying special attention to the number and the values of valence light and strange quarks as well as the number and values of the momenta employed in the simulation.

In section 4.2 statistical errors will be treated, explaining in details the jackknife and bootstrap methods used in this work; with sections 4.3 and 4.4 the very form factor analysis begins: first we will show the time region in which we are able to isolate single ground state mesons and then we will show, for fixed kaon and pion masses, our results for the form factors at different values of the meson momenta. Section 4.5 will be dedicated to explain our procedure to interpolate the form factors at the physical kaon mass. Once fixed the kaon mass, in section 4.6 we will show how to keep under control the systematic errors which affect a typical lattice calculation: discretization effects and finite size effects. In Section 4.7 the chiral extrapolation will be treated and this first part will end with section 4.8 where we present our results, extrapolated at the physical point, for the vector form factor at zero momentum $f_+(0)$, the ratio f_K/f_π and for the CKM matrix element V_{us} calculated using both Kl_2 and Kl_3 decay amplitudes. A comparison with the *FLAVIANET* 2010 results [23] will also be given.

The chapter ends with section 4.9 in which we present some unquenched results obtained with our spin–direct and twisted stochastic techniques. We will compare the precision of the methods in obtaining the η' disconnected and complete correlators and make some considerations about the future applicability of the techniques.

4.1 Simulation details

ETM collaboration has recently completed an extensive program of lattice calculation of two– and three–point correlation functions, using the gauge field configurations generated with the tree-level Symanzik improved action (2.54) and the $N_f = 2$ twisted mass action, for two degenerate valence quarks, at maximal twist (2.66).

These simulations have been carried out for different values of the lattice spacing as well as for different sizes of the lattice space-time volume. It this work, taking [100] as a notation reference, we have used the gauge field configuration *ensemble* denoted as $A_2, \ldots, A_4$, $B_1, \ldots, B_7$, and $C_1, \ldots, C_3$ generated, respectively, at values of the inverse gauge coupling equal to $\beta = 3.8$ ($a = 0.10\ fm,\ a^{-1} = 1.94\ GeV$), $\beta = 3.9$ ($a = 0.079\ fm,\ a^{-1} = 2.30\ GeV$), and $\beta = 4.05$ ($a = 0.063\ fm,\ a^{-1} = 2.91\ GeV$).

We remark here that all the configurations produced by ETMC are now public and available on the international lattice data grid (ILDG[1]). Each ensemble corresponds to as many values of dynamical quark masses, they are

$$A_2 \ldots A_4 : \quad am_{sea} \in \left\{ 0.0080,\ 0.0110,\ 0.0165 \right\} , \tag{4.1}$$

$$B_1 \ldots B_7 : \quad am_{sea} \in \left\{ 0.0040,\ 0.0064,\ 0.0085,\ 0.0100,\ 0.0150,\ 0.0040,\ 0.0030 \right\} , \tag{4.2}$$

$$C_1 \ldots C_3 : \quad am_{sea} \in \left\{ 0.0030,\ 0.0060,\ 0.0080 \right\} ; \tag{4.3}$$

let us notice that for the ensembles $A_2, \ldots, A_4$ and $B_1 \ldots B_5$ the employed lattice volume was, in lattice units (l.u.), $L \times T = 24^3 \times 48$ while for the remaining ensembles $B_6, B_7, C_1, \ldots, C_3$ it was used $L \times T = 32^3 \times 64$; We have carried out several simulations at different lattice volumes keeping all the other parameters fixed in order to study finite size effects (FSE).

The simulation algorithm used to generate these ensembles is a Hybrid Monte Carlo algorithm with multiple time scales and mass preconditioning. It is described in [102]

[1] See [101], and references therein, for a further details about this network.

and one implementation described in [103] is freely available. With this procedure it has been generated a sample of 240 independent gauge field configurations for each of the ensembles $A_2, \ldots, A_4$, $B_1, \ldots, B_7$, and $C_1, \ldots, C_3$. For the sake of clarity, we have summarized all the gauge field configuration set up in table 4.1.

Ensemble	$(L/a)^3 \times T/a$	β	a (fm)	$a\mu_s$	k_{crit}	M_π	$M_\pi \cdot L$
A_2	$24^3 \times 48$	3.8	0.10	0.0080	0.164111	~ 400	4.9
A_3	$24^3 \times 48$			0.0110		~ 480	5.9
A_4	$24^3 \times 48$			0.0165		~ 580	7.1
B_1	$24^3 \times 48$	3.9	0.079	0.0040	0.160856	~ 300	3.3
B_2	$24^3 \times 48$			0.0064		~ 370	4.0
B_3	$24^3 \times 48$			0.0085		~ 435	4.7
B_4	$24^3 \times 48$			0.0100		~ 470	5.0
B_5	$24^3 \times 48$			0.0150		~ 575	6.2
B_6	$32^3 \times 64$			0.0040		~ 300	4.3
B_7	$32^3 \times 64$			0.0030		~ 260	3.7
C_1	$32^3 \times 64$	4.05	0.063	0.0030	0.157010	~ 300	3.3
C_2	$32^3 \times 64$			0.0060		~ 410	4.5
C_3	$32^3 \times 64$			0.0080		~ 470	5.3

Table 4.1: Gauge field configurations set up Summary of the ensembles generated by ETMC. We have given the lattice volume $L \times T$ (in lattice units), the value of the inverse coupling β, the lattice spacing a, the twisted mass parameter $a\mu$ for the sea quark masses, the critical hopping parameter k_{crit}, the approximate pion mass and the value of the product $M_\pi \cdot L$ which is an important quantity when considering FSE.

For each value of β, several values of the bare twisted mass parameter $a\mu_v$ have been employed in the simulation and they can be divided in two classes: *light* and *strange*. The light-one have the same mass of the sea quarks, and corresponds to the up and down quarks, which are degenerate in our simulation. We have always chose to work in the *unitary* limit, which means that we have employed equal masses for the light valence quarks and for the sea quarks, *i.e.*

$$m_l = m_{sea} \qquad \text{(for each ensemble)} \tag{4.4}$$

in order to avoid partial quenching effects for the two light quarks.

The latter have masses around the strange quark mass, and in particular

$$A_2 \dots A_4 : \quad am_s \in \Big\{ 0.016,\, 0.020,\, 0.030,\, 0.036 \Big\} \text{ around } m_s^{phys} \sim 0.020, \tag{4.5}$$

$$B_1 \dots B_7 : \quad am_s \in \Big\{ 0.015,\, 0.022,\, 0.027,\, 0.032 \Big\} \text{ around } m_s^{phys} \sim 0.018, \tag{4.6}$$

$$C_1 \dots C_3 : \quad am_s \in \Big\{ 0.015,\, 0.018,\, 0.022,\, 0.026 \Big\} \text{ around } m_s^{phys} \sim 0.015; \tag{4.7}$$

we have reported also the physical value of the strange quark mass (in l.u.) because, as we will explain in details in section 4.5, we will perform an interpolation in the strange quark mass, or equivalently in the K meson mass, in order to have our observables fixed at the physical point (for the Kaon mass variable); to carry out this operation as precisely as possible, we have chosen to employ a set of strange quark masses which encompasses the physical one.

It is important to underline that employing in a simulation light valence quark masses such as (4.1), (4.2), and (4.3) allows one to simulate pion as light as 280 MeV while using strange quark masses such as (4.5), (4.6), and (4.7) results in K meson masses between 530 and 650 MeV.

Let us close this section mentioning that for the valence light quarks we have used twisted boundary conditions, as already explained in section 2.5, which allows one to simulate smaller momenta on the lattice with respect to the discrete ones imposed by finite volume quantization. We remind that the chosen kinematic for the three–point functions is the *Breit* frame in which the two mesons carry the same momenta, but in opposite directions. At a quark level, referring to figure 3.2, this means that we have assigned a unique vector $\vec{\theta}$ in order that the decaying quark (s) carries $2\pi\vec{\theta}/L$ momentum while the produced quark (u) has $-2\pi\vec{\theta}/L$. The *spectator* quark (d), which is the same both for the two– and for the three–point functions, is always taken at rest. Hence, we are left to chose only one twisting vector, which we have taken as $\vec{\theta} = \theta(1,1,1)$ with a different θ for each set of gauge fields configuration in order that θ/L has the same value in physical units (and so the meson momentum) regardless of what simulation is considered. The values chosen are

$$A_2 \dots A_4 : \quad \theta \in \left\{ 0.00,\ 0.12,\ 0.22,\ 0.31,\ 0.40,\ 0.51 \right\} , \tag{4.8}$$

$$B_1 \dots B_5 : \quad \theta \in \left\{ 0.00,\ 0.11,\ 0.19,\ 0.27,\ 0.35,\ 0.44 \right\} , \tag{4.9}$$

$$B_6 \dots B_7 : \quad \theta \in \left\{ 0.00,\ 0.14,\ 0.25,\ 0.36,\ 0.46,\ 0.58,\ 0.70,\ 1.00 \right\} , \tag{4.10}$$

$$C_1 \dots C_3 : \quad \theta \in \left\{ 0.00,\ 0.11,\ 0.20,\ 0.28,\ 0.36,\ 0.46,\ 0.70,\ 1.00 \right\} . \tag{4.11}$$

4.2 Error analysis

In lattice simulations one has a certain number of uncertainty sources which enter the evaluation of the quantities of interest. Among them, there are the *statistical* errors which arise from the use of Monte Carlo methods for calculating hadronic quantities. As it is clearly not possible to calculate the expectation value mean over an infinite sample, the equality between the sample and the ensemble average will not be an exact one and will be affected by statistical errors. We will discuss in subsection 4.2.1 how to treat that kind of intrinsic error.

A second class of errors is represented by the so–called *discretization* errors, which arise from the finiteness of the lattice spacing a employed in the simulations. These effects can be systematically taken into account performing an à la Symanzik analysis of discretization effects and can be quantitavely estimated by means of a simple power law fit on data calculated using different values of the lattice spacing a (*i.e.* different values of the inverse gauge coupling β). Then one can take the continuum limit of the quantity of interest to keep under control discretization errors. These kind of systematics will be treated in subsection 4.6.1.

Another error source is the *finiteness* of the volume where one is going to simulate the quark dynamics. Finite size effects (FSE) can be estimated repeating the same analysis employing different volumes and will be treated in subsection 4.6.2.

In the end, we mention that using $N_f = 2$ gauge field configurations means that in our simulations we will systematically commit an error arising from the quenching of the strange quark. This kind of error will be treated in subsection 4.7.2.

4.2.1 Statistical errors

We will indicate with $\mathcal{O}_i$ the i-th measurement of the observable $\mathcal{O}$. In the ideal case in which the single measurements are not correlated and can be considered an infinite number of statistically independent estimates of the observable $\mathcal{O}$, the sample average will be equal to the ensemble average which by definition is the expectation value.

If, instead, we consider a finite sample of N independent measurements $\mathcal{O}_i$, the sample average will approximately be gaussianly distributed around the ensemble average with variance

$$\sigma_N^2(\mathcal{O}) = \frac{\langle \mathcal{O}^2 \rangle_N - \langle \mathcal{O} \rangle_N^2}{N-1}\,, \tag{4.12}$$

where $\langle \mathcal{O} \rangle_N$ is the sample average ($\sum_{i=1}^N \mathcal{O}_i/N$). We will then have that the expectation value $\bar{\mathcal{O}}$ in terms of $\langle \mathcal{O} \rangle_N$, and according to the central limit theorem, will be given by

$$\bar{\mathcal{O}} = \langle \mathcal{O} \rangle_N \pm \sigma_N(\mathcal{O})\,. \tag{4.13}$$

The error estimate (4.13) is not a realistic one, if employed in lattice QCD simulations. This is due to the fact that the updating procedure employed in Monte Carlo simulations, even if usually choosing not to consider as significant consecutive measurements and discard a certain number of them between one extraction and the next one can somewhat reduce the correlation, the sample will include partially correlated objects $\mathcal{O}_i$.

To properly take into account this correlation it is useful to introduce the integrated autocorrelation time τ_{int}

$$\tau_{int} \doteq \frac{1}{2} \sum_{t=-\infty}^{+\infty} \frac{\Gamma_{\mathcal{O}}(|t|)}{\Gamma_{\mathcal{O}}(0)}\,, \tag{4.14}$$

where with t we have indicated the "Monte Carlo time" and with $\Gamma_{\mathcal{O}}$ the autocorrelation function, defined as

$$\Gamma_{\mathcal{O}}(|t_i - t_j|) \doteq \langle \Big(\mathcal{O} - \langle \mathcal{O} \rangle \Big) \cdot \Big(\mathcal{O}_{|} - \langle \mathcal{O} \rangle \Big) \rangle\,. \tag{4.15}$$

This function exponentially decrease with a characteristic time scale of τ_c, called autocorrelation time, which usually is of the same order of magnitude of τ_{int}.

At this point, to incorporate the integrated autocorrelation time in the estimate of the statistical error, one can start from the naive error (4.13) and using the value of τ_{int} it is possible to estimate the statistical error of the correlated measurements by

$$\sigma_N^2(\mathcal{O}) \simeq \left(\langle \mathcal{O}^2 \rangle_N - \langle \mathcal{O} \rangle_N^2 \right) \frac{2\tau_{int}}{N} . \tag{4.16}$$

It is now clear that, because of the autocorrelation, the number of *really independent* measurement is $N/(2\tau_{int})$. If the numeric estimate of the quantity $\mathcal{O}$ requires a relevant computation time cost, it is convenient to ignore $2\tau_{int}$ measurements between one configuration and the next one.

In this work we have selected only one configuration on which performing the observable measurement among each sample of 20 generated.

4.2.2 Jackknife analysis

As discussed in the previous section, a reasonable estimate of the real statistical error of a numerical measure obtained using the Monte Carlo updating recipe requires a precise knowledge of the integrated autocorrelation time τ_{int}. This estimate can be obtained , in general, only thanks to accurate numerical procedure, as discussed in [104].

An alternative method is represented by the so–called *binning* procedure; it consist of calculating a certain number of consecutive gauge field configuration sub–samples, called *bins*, over which one calculates some preliminary means. These averages can be considered as the result of single (lattice) measures and exploited in the variance estimate procedure. If the bins are large enough these measure can be considered uncorrelated and the error estimator (4.12) can be considered appropriate.

If, as it usually happens, the bins are not a statistically significant sample, *i.e.* they are not large enough so that the bin averages can be considered as valid estimates of the expectation value, a good method is to perform a *jackknife* analysis. The idea is to use, as preliminary averages, the ones carried over the complement set with respect to each bin, in order that the sub–sample under exam is large enough.

In practice, starting from an N–objects sample, one must split the configurations in N_s bin and then consider N_s jackknife estimators, defined as the average over the complement set with respect to each bin

$$\mathcal{O}_s^J \doteq \frac{1}{N_s - 1} \sum_{r \neq s} \mathcal{O}_r \,. \tag{4.17}$$

The optimum estimate for the expectation value of the observable $\mathcal{O}$ is $\langle O \rangle_N \pm \sigma_{J,N_s}(\mathcal{O})$, where the jackknife variance estimator is given by

$$\sigma^2_{J,N_s} \doteq \frac{N_s - 1}{N_s} \sum_{s=1}^{N_s} \Big(\mathcal{O}_s^J - \langle O^J \rangle \Big)^2 \,. \tag{4.18}$$

4.2.3 Bootstrap analysis

The *bootstrap* procedure is a general purpose approach to statistical inference which falls within the broader class of *resampling* methods. Bootstrapping is the practice of estimating properties of an estimator (such as its variance) by measuring those properties when sampling from an approximating distribution. One standard choice for an approximating distribution is the empirical distribution of the observed data. In the case where a set of observations can be assumed to be from an independent and identically distributed population, this can be implemented by constructing a number of resamples of the observed dataset (and of equal size to the observed dataset), each of which is obtained by random sampling with replacement from the original dataset.

To be more clear let us consider an argument which is related to our specific case of the form factors analysis. We suppose we have to compare two, statistically independent, quantities $\mathcal{A}$ and $\mathcal{B}$, to obtain a third quantity, $\mathcal{C}$, which derive from the other two. We have at our disposal, for the input quantities, N_s jackknife averages $\mathcal{A}_s^J$ and $\mathcal{B}_s^J$, defined as in (4.17). By comparison of the mean values $\langle A \rangle$ and $\langle B \rangle$ one can obtain the ensemble average estimate of the dependent quantity $\mathcal{C}$.

A priori, one could calculate the statistical error by means of the jackknife procedure. However there is no particular reason for making a jackknife analysis on the N_s sub–samples defined by the couples $(\mathcal{A}_s^J, \mathcal{B}_s^J)$ with $s = 1, \ldots, N_s$. Actually, as there

is no correlation between the two samples $\mathcal{A}_s^J$ and $\mathcal{B}_s^J$, we can in principle chose as sub–samples whatever of the N_s^2 couples $(\mathcal{A}_s^J, \mathcal{B}_{s'}^J)$ with $s, s' = 1, \ldots, N_s$.

The bootstrap procedure consists of generating, following a random distribution, a N_{boot} number (high enough) of (i_b, j_b) couples; then, once defined the sub–samples $(\mathcal{A}_{i_b}^J, \mathcal{B}_{j_b}^J)$, one will proceed to evaluate for each b the dependent quantity $\mathcal{C}_b^B$. As already anticipated, the mean value $\mathcal{C}$ will be equal to the ensemble average. The *bootstrap* error for that quantity will be given by

$$\sigma^2_{B,N_{boot},N_s}(\mathcal{C}) \doteq \frac{N_s - 1}{N_{boot}} \sum_{b=1}^{N_{boot}} \left(\mathcal{C}_b^B - \langle \mathcal{C}_c^B \rangle\right)^2 . \tag{4.19}$$

4.3 Momentum dependence of the two–point correlation function

In section 3.1.1 we have shown that two–point correlation functions bear important information about the simulated lattice mesons. In particular, by means of a temporal dependence analysis, one can check if the lattice volume employed, as well as the lattice spacing used, allows to study single particle properties in order to isolate ground state within the correlators. Using this strategy it is possible to extract the mass and the probability amplitude $\sqrt{Z_P}$, related to the isolated single particle ground state. The knowledge of the masses and, more generally, of the energies of the simulated lattice mesons for different values of the quark masses is needed in the form factors analysis, as we have already explained in details in section 3.2.1.

The two–point correlation functions (3.65) have been calculated for various values of the twisting angle $\vec{\theta}$, listed in (4.8)-(4.11) depending on the simulation. From the time dependence of the effective mass, defined in (3.13), which we report here for the case under exam

$$aM_{eff}(t, \theta) = \log \left[\frac{C^{K(\pi)}(t, 2\pi\vec{\theta}/L)}{C^{K(\pi)}(t + a, 2\pi\vec{\theta}/L)} \right], \tag{4.20}$$

one is able to extract the time interval after which the ground state is reached. We show in figure 4.1 the time behavior of the effective mass of a light-light (π*–like*) meson

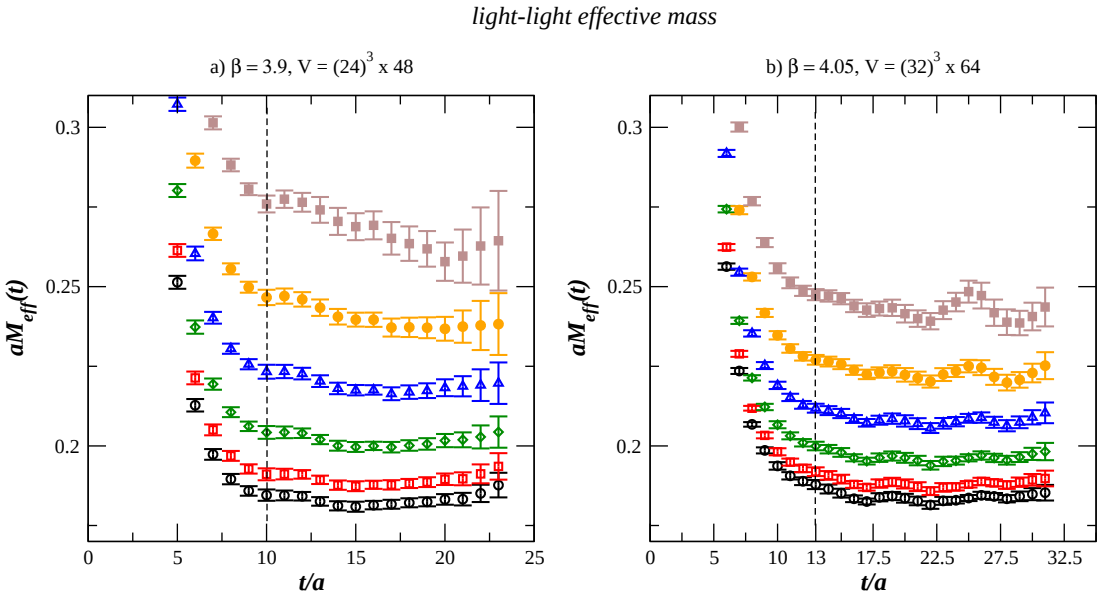

Figure 4.1: Light-light effective mass - versus the (Euclidean) time distance in lattice units. We have shown (4.20) calculated for $\beta = 3.9$ with $V \cdot T = 24^3 \cdot 48\, a^4$ (a) and for $\beta = 4.05$ with $V \cdot T = 32^3 \cdot 64\, a^4$ (b). The twisting angle $\vec{\theta}$ is chosen in the symmetric form $\vec{\theta} = \theta(1,1,1)$. The dots, squares,diamonds, triangles, full dots and full squares correspond to the first six θ values listed in (4.9) and (4.11), respectively. The dashed vertical line is drawn where the ground state starts to dominate.

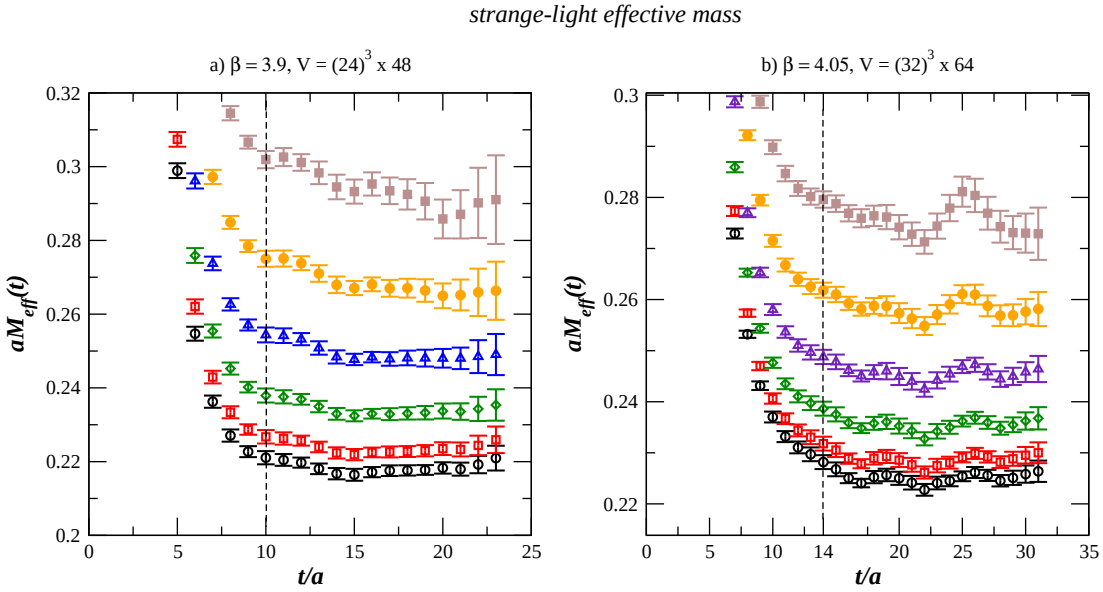

Figure 4.2: Strange-light effective mass - Same as figure 4.1, but in the case of a strange-light meson.

It can be seen that the statistical precision is remarkably high and it allows to extract quite precisely the energy $E_{\pi,K}(\vec{p})$ (see (3.25)), whose contribute to the correlator starts to dominate from $t/a = 10$ ($t/a = 13$) for a spatial volume of 24^3 (32^3).

The values obtained for the light-light (π–*like*) energy $E_\pi(\vec{\theta})$ are shown in figure 4.3 as a function of the pion momentum given by $\vec{p} \equiv 2\pi\theta/L$, again for ensemble B_2 (a) and C_3 (b); the same results are show in figure 4.4, but in the case of a strange-light meson (K–*like*).

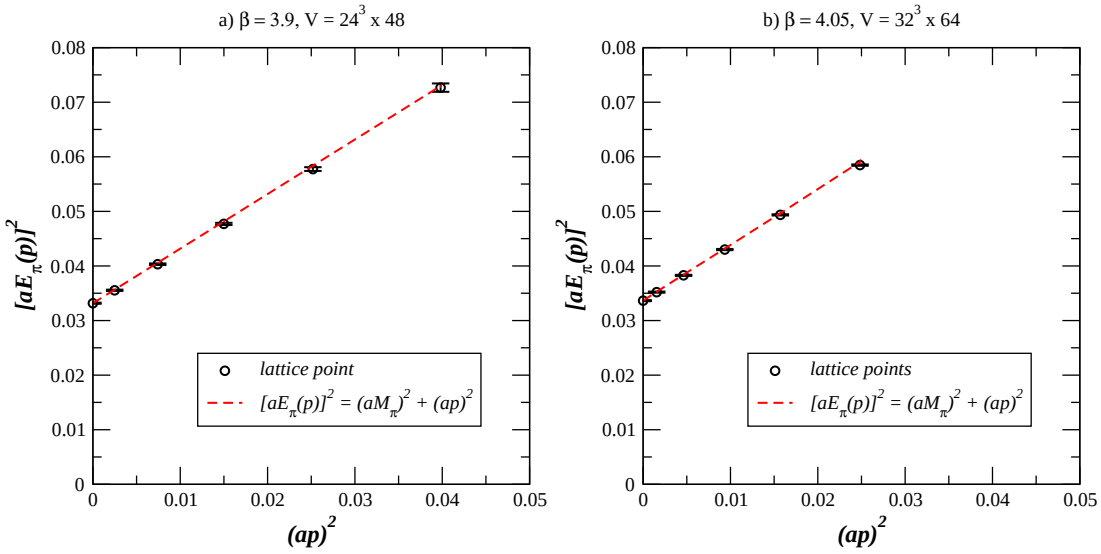

Figure 4.3: Light-light energy - $E(\vec{p})$ in lattice units obtained from the plateau of the effective mass shown in figure 4.1 (choosing the time interval $10 \leq t/a \leq 21$ and $13 \leq t/a \leq 30$ respectively) plotted against the squared pion momentum $p^2 \equiv 3(2\pi\theta/L)^2$ in lattice units, for $\beta = 3.9$ with $V \cdot T = 24^3 \cdot 48\, a^4$ (a) and for $\beta = 4.05$ with $V \cdot T = 32^3 \cdot 64\, a^4$ (b). The dashed line represents the continuum–like dispersion relation $E_\pi^2(\vec{p}) = (M_\pi^2(L) + |\vec{p}|^2)$.

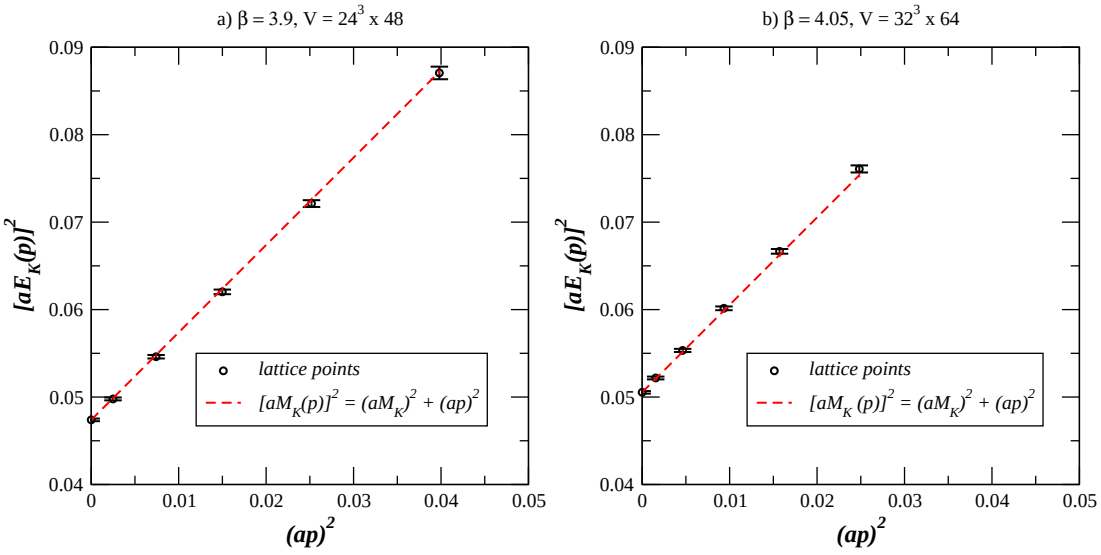

Figure 4.4: Strange-light energy - Same as figure 4.3, but in the case of a strange-light meson.

4.4 Momentum dependence of the semileptonic form factors

As discussed in section 3.2.1, considering the large time distances limit of the time and vector components of the ratio $R_\mu(t, t'; \theta)$ defined in (3.38), allows one to calculate the form factors $f_\pm(q^2)$, and then eventually determine the form factors of interest $f_{0,+}(q^2)$.

We show in figure 4.5 and 4.6, respectively, the scalar (f_0) and the vector (f_+) form factors as a function of time for different momenta, and for different values of M_π and M_K at $\beta = 3.9$ and $V \cdot T = 24^3 \cdot 48a^4$.

In figures 4.5 and 4.6 a plateau is identifiable for the time interval $t \in [10, 14]$ while for the other runs we give the plateau time intervals in table 4.2; in these regions both the initial kaon and the final pion ground states are isolated and within this time range one can extract the form factors by means of a weighted average. We have checked that different choices of the time interval for the plateau region lead to values of the vector and scalar form factors which are largely consistent within the statistical precision. It can be seen that a remarkable precision has been achieved in the plateau region: if we

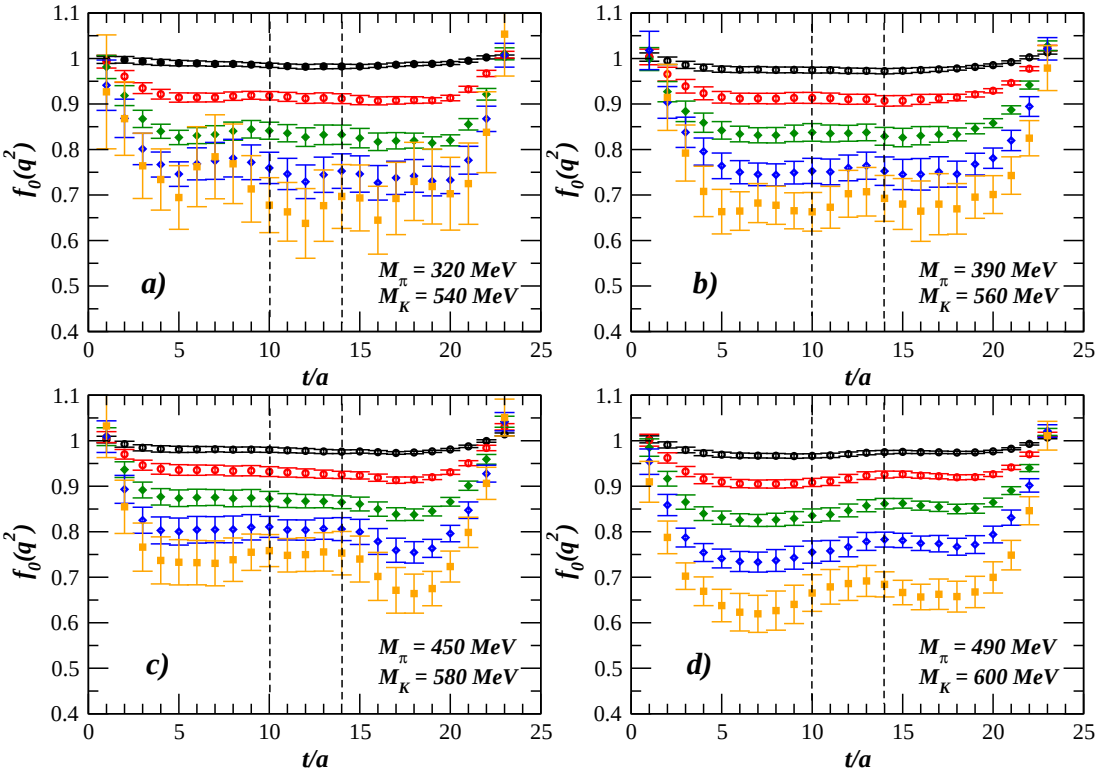

Figure 4.5: Scalar form factor (time) plateau - It is shown the scalar form factor $f_0(q^2)$ for different values of q^2 and for $M_\pi = 320\,MeV$ $M_K = 540\,MeV$ (a), $M_\pi = 390\,MeV$ $M_K = 560\,MeV$ (b), $M_\pi = 450\,MeV$ $M_K = 580\,MeV$ (c), $M_\pi = 490\,MeV$ $M_K = 600\,MeV$ (d) at $\beta = 3.9$ with $V \cdot T = 24^3 \cdot 48\,a^4$. The full dots, open dots, full diamonds, open diamonds and full squares correspond to $(aq)^2 = (-0.01, -0.03, -0.06, -0.10, -0.16)$, respectively. The dashed vertical lines identify the region $10 \leq t \leq 14$, where both the initial kaon and the final pion ground states are isolated, so that the scalar form factor can be calculated by means of a weighted average.

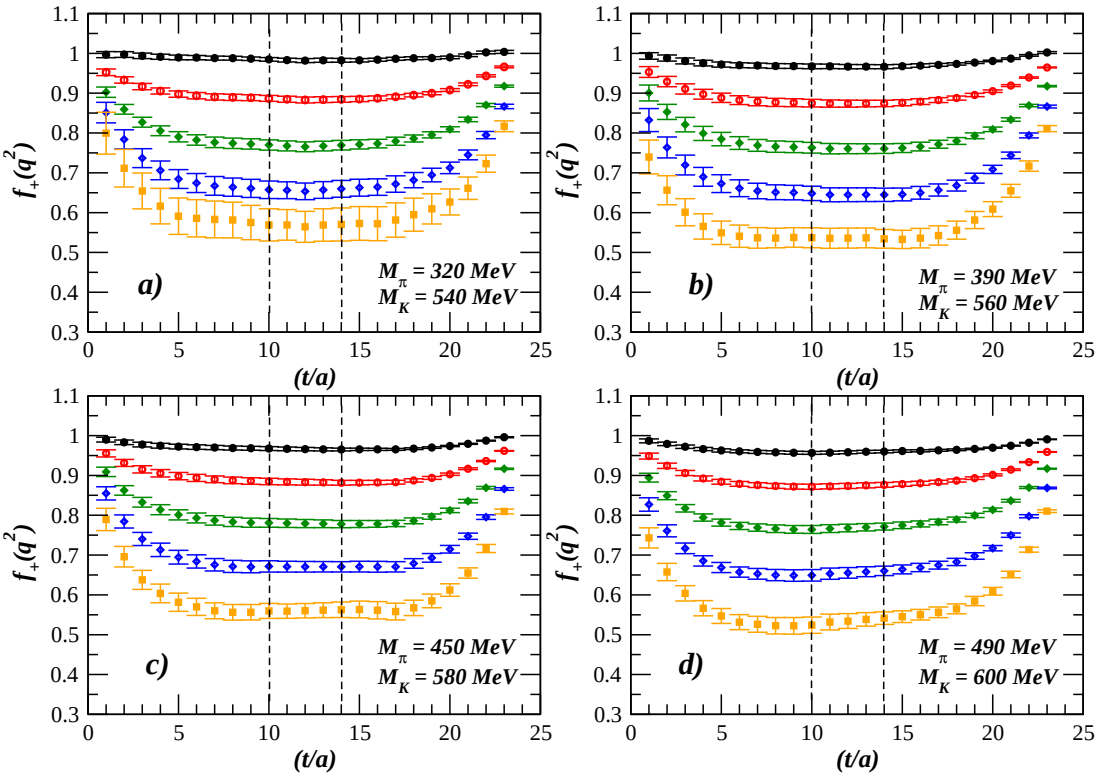

Figure 4.6: Vector form factor (time) plateau - It is shown the vector form factor $f_+(q^2)$ for different values of q^2 and for $M_\pi = 320\,MeV$ $M_K = 540\,MeV$ (a), $M_\pi = 390\,MeV$ $M_K = 560\,MeV$ (b), $M_\pi = 450\,MeV$ $M_K = 580\,MeV$ (c), $M_\pi = 490\,MeV$ $M_K = 600\,MeV$ (d) at $\beta = 3.9$ with $V \cdot T = 24^3 \cdot 48\,a^4$. The full dots, open dots, full diamonds, open diamonds and full squares correspond to $(aq)^2 = (-0.01, -0.03, -0.06, -0.10, -0.16)$, respectively. The dashed vertical lines identify the region $10 \leq t \leq 14$, where both the initial kaon and the final pion ground states are isolated, so that the vector form factor can be calculated by means of a weighted average.

Ensemble	$(L/a)^3 \times T/a$	*plateau*
A_2	$24^3 \times 48$	$t/a \in [10-14]$
A_3	$24^3 \times 48$	$t/a \in [10-14]$
A_4	$24^3 \times 48$	$t/a \in [10-14]$
B_1	$24^3 \times 48$	$t/a \in [10-14]$
B_2	$24^3 \times 48$	$t/a \in [10-14]$
B_3	$24^3 \times 48$	$t/a \in [10-14]$
B_4	$24^3 \times 48$	$t/a \in [10-14]$
B_5	$24^3 \times 48$	$t/a \in [10-14]$
B_6	$32^3 \times 64$	$t/a \in [10-22]$
B_7	$32^3 \times 64$	$t/a \in [10-22]$
C_1	$32^3 \times 64$	$t/a \in [12-20]$
C_2	$32^3 \times 64$	$t/a \in [12-20]$
C_3	$32^3 \times 64$	$t/a \in [12-20]$

Table 4.2: Time plateau We have reported the time interval (in lattice units), for each ensemble of gauge field configurations, in which it is possible to identify the plateau for the vector and scalar form factor, as in figure 4.5 and 4.6

consider the case presented in figures 4.5 we have reached a precision which is at best of (*full dots a,b,c,d*) 5‰ while at worst (*full squares a,b,c,d*) it is 5%; for the vector form factor case of figure 4.6 the situation is slightly better.

The scalar form factor $f_0(q^2_{MAX})$ deserves a special mention. We have said in section 3.2.1 that its determination, thanks to the special ratio (3.45), is a very accurate one because it is a ratio of *only* three–point functions at *zero momentum*: we show in figure 4.7 that it is indeed the case.

The precision level for the form factor at this special kinematic can be as good as 1 ‰, for each of the four M_π and M_K combinations presented.

Once extracted the form factors from the plateau presented in figure 4.5, 4.6 and 4.7, we are left only with the momentum dependence of the form factors $f_{+,0}(q^2)$, at each pion and kaon masses. The momentum dependencies of both the form factors are nicely fitted either by a pole behavior

$$f_{+,0}(q^2) = \frac{f_+(0)}{1 - s_{+,0} q^2} \tag{4.21}$$

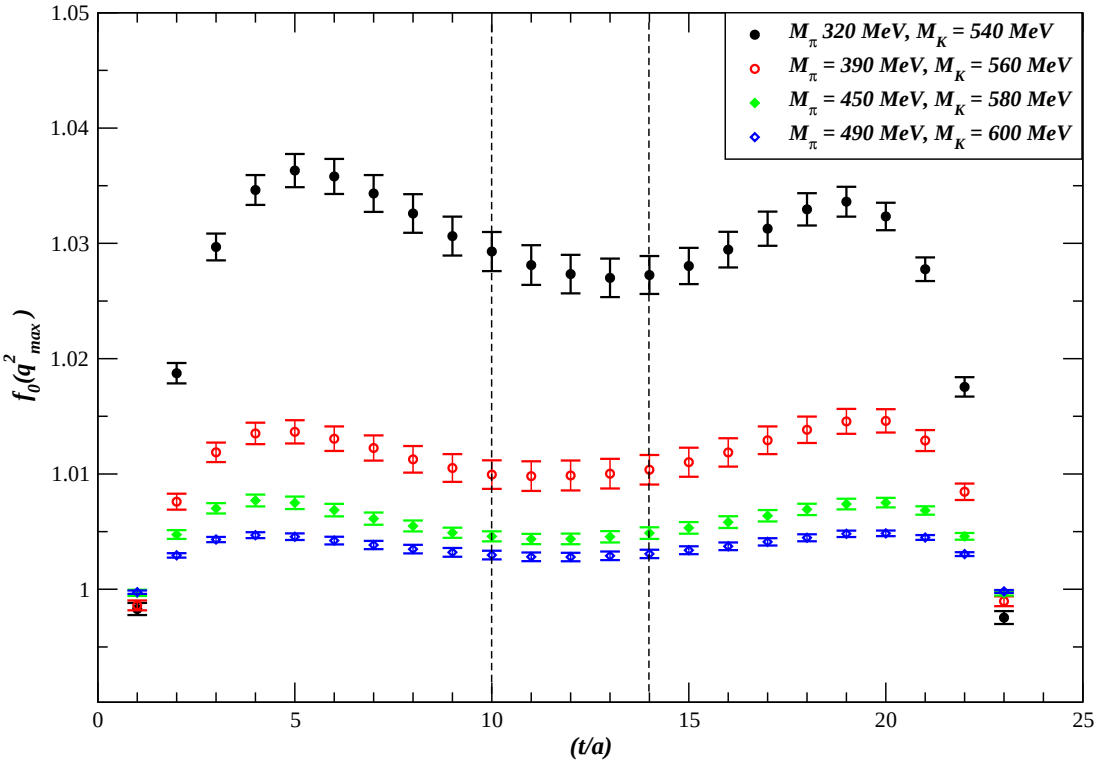

Figure 4.7: Scalar form factor at q^2_{MAX} (time) plateau - It is shown the scalar form factor f_0 for the special kinematic q^2_{MAX} and for $M_\pi = 320\,MeV$ $M_K = 540\,MeV$ (full dots), $M_\pi = 390\,MeV$ $M_K = 560\,MeV$ (*open dots*), $M_\pi = 450\,MeV$ $M_K = 580\,MeV$ (*full diamonds*), $M_\pi = 490\,MeV$ $M_K = 600\,MeV$ (*open diamonds*) at $\beta = 3.9$ with $V \cdot T = 24^3 \cdot 48\,a^4$. The dashed vertical lines identify the region $10 \leq t \leq 14$, where both the initial kaon and the final pion ground states are isolated, so that the scalar form factor can be calculated by means of a weighted average.

or by a quadratic dependence on q^2

$$f_{+,0}(q^2) = f_+(0) \cdot (1 + \bar{s}_{+,0} q^2 + \bar{c}_{+,0} q^4), \tag{4.22}$$

where the condition $f_0(0) = f_+(0)$ is understood. The quality of the two fits are illustrated in figure 4.8, for $M_\pi = 320\,MeV$ $M_K = 540\,MeV$ (a), $M_\pi = 390\,MeV$ $M_K = 560\,MeV$ (b), $M_\pi = 450\,MeV$ $M_K = 580\,MeV$ (c), $M_\pi = 490\,MeV$ $M_K = 600\,MeV$ (d) at $\beta = 3.9$ and $V \cdot T = 24^3 \cdot 48\,a^4$. We will come back later on to the details about the momentum parametrization of the form factors (section 4.7.1) when we will explain our analysis strategy.

4.5 Fixing the strange quark mass

The values obtained for the form factors $f_0(q^2)$ and $f_+(q^2)$, presented in figure 4.8, depend on both the pion and kaon masses. The dependence on the latter is shown in figure 4.9 at $\beta = 3.9$ and $M_\pi \sim 450\,MeV$; as already found in [19] it appears to be quite smooth so that an interpolation at the physical strange quark mass can be easily performed using quadratic splines. ChPT tells us that pseudoscalar masses can be written (at LO) in terms of quark masses,

$$M_K^2 = B(m_l + m_s) + \mathcal{O}(m^2) \tag{4.23}$$

$$M_{\pi\pm}^2 = B(2m_l) + \mathcal{O}(m^2) \tag{4.24}$$

where m_l stands for the mass of the light u,d quarks while B is a LEC entering the ChPT lagrangian at lowest order, which is related to the quark condensate. This allow us to trade the strange quark mass for the kaon mass and fix it to its physical value by fixing the combination $(2M_K^2 - M_\pi^2)$ at its physical value which, at each pion mass defines a *reference* kaon mass M_K^{ref}

$$2\left[M_K^{ref}\right]^2 - M_\pi^2 = 2\left[M_K^{phys}\right]^2 - \left[M_\pi^{phys}\right]^2 \tag{4.25}$$

using $M_\pi^{phys} = 135.0\,MeV$ and $M_K^{phys} = 494\,MeV$. Fixing the K mass instead of the s mass is very convenient as the first is known from experiments while the second is

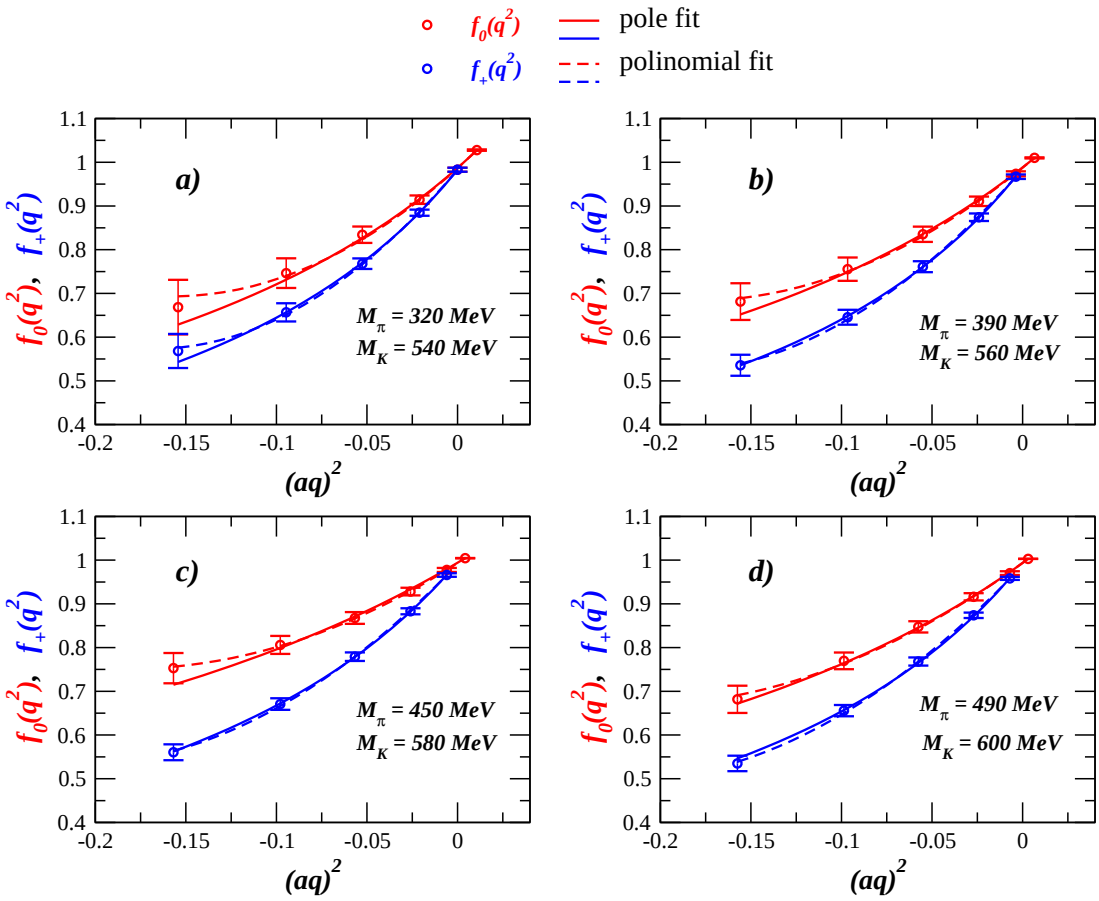

Figure 4.8: Form factors momentum dependence - It is shown the scalar $f_0(q^2)$ and vector $f_+(q^2)$ form factors versus q^2 (in lattice units) for $M_\pi = 320\,MeV$ $M_K = 540\,MeV$ (a), $M_\pi = 390\,MeV$ $M_K = 560\,MeV$ (b), $M_\pi = 450\,MeV$ $M_K = 580\,MeV$ (c), $M_\pi = 490\,MeV$ $M_K = 600\,MeV$ (d) at $\beta = 3.9$ with $V \cdot T = 24^3 \cdot 48\,a^4$. The solid and dashed lines are the results of the fits based on (4.21) and (4.22), respectively.

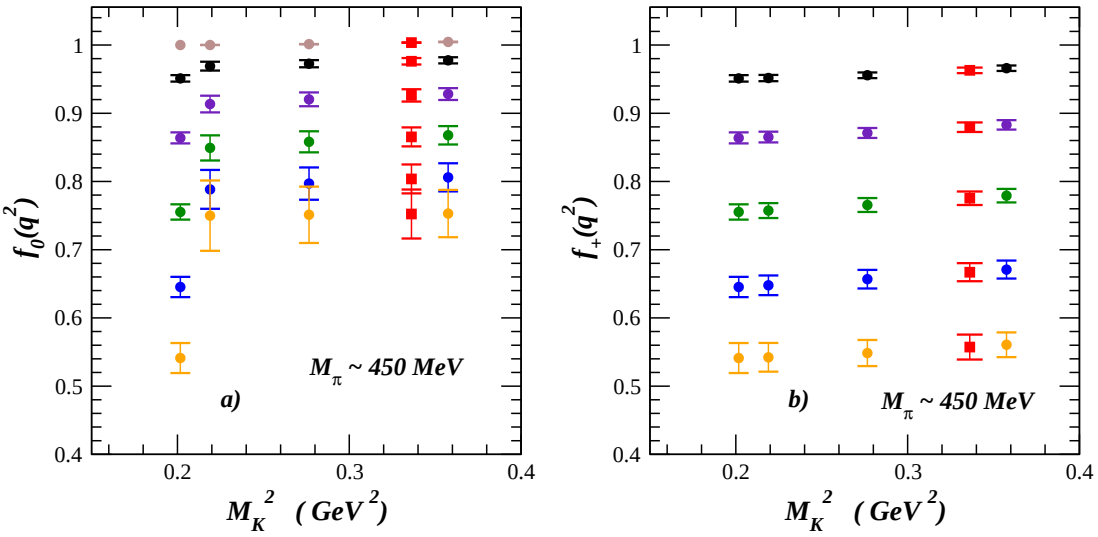

Figure 4.9: Form factors M_K^2 dependence - It is shown the scalar $f_0(q^2)$ (a) and the vector $f_+(q^2)$ (b) form factors, for different values of $\vec{\theta}$, versus M_K^2 for $M_\pi = 450\,MeV$ at $\beta = 3.9$ with $V \cdot T = 24^3 \cdot 48\,a^4$. The (full) red,violet, green, blue and orange circles corresponds to the θ listed in (4.9). The red full squares represent the value of the form factor at the reference Kaon mass $M_K^{ref} \sim 557\,MeV$ defined in (4.25).

not directly measurable, because of quark confinement, and it is know only from lattice calculation or other theoretical calculation which are affected by different systematic errors.

Once the form factors $f_{+,0}(q^2)$ has been interpolated to the reference kaon mass, they depend only on the pion mass, as can be seen in figure 4.10, and their dependence can be described using ChPT.

From now on we are getting to the second, and final, part of the analysis. As we have already said the first part consist of calculating the form factors at fixed values of the meson masses. The second one, by means of a study of the meson mass dependence of the form factors, consists of first interpolating the results at the physical kaon mass and then extrapolating them to the physical pion mass (we will also refer to this last step as *reaching the physical point*). The extrapolation to the physical pion is carried out using the $SU(2)$ limit of $SU(3)$ ChPT, as we will explain in section 4.7.

Before getting to the physical point let us discuss, in the next section, the issue of the systematic (non statistical) errors of this analysis.

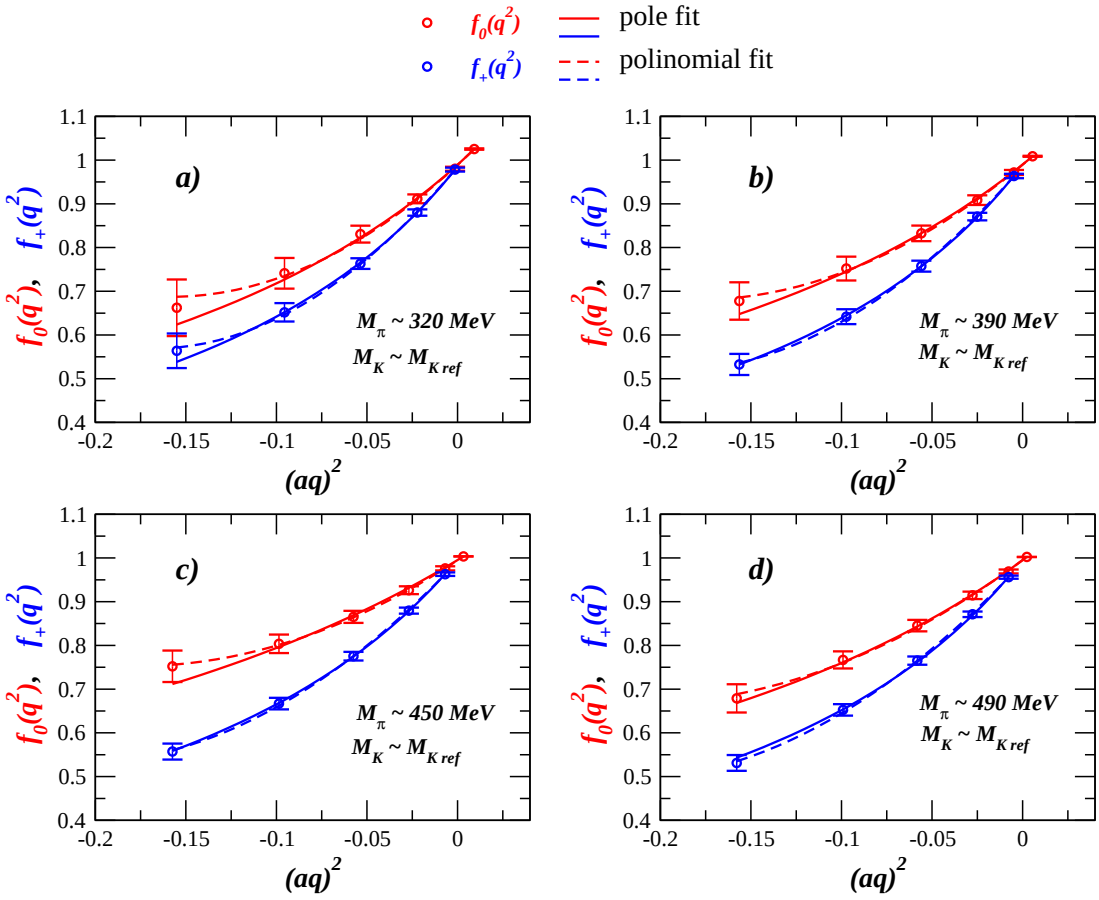

Figure 4.10: Form factors momentum dependence at M_K^{ref} - It is shown the scalar $f_0(q^2)$ and vector $f_+(q^2)$ form factors versus q^2 (in lattice units), interpolated at the reference kaon mass defined in (4.25), for $M_\pi = 320\,MeV$ (a), $M_\pi = 390\,MeV$ (b), $M_\pi = 450\,MeV$ (c), $M_\pi = 490\,MeV$ (d) at $\beta = 3.9$ with $V \cdot T = 24^3 \cdot 48\,a^4$. The solid and dashed lines are the results of the fits based on (4.21) and (4.22), respectively.

4.6 Systematic errors

We have already mentioned that, beside the statistical errors considered in section 4.2.1, there are also other sources of systematic errors on the lattice. The first is connected with the size of the lattice spacing a while the second is due to the size of the lattice volume.

Let us show, in the two next section, how these effects can be studied and how one can estimate them.

4.6.1 Discretization errors

In this section we will give a qualitative estimate of the discretization errors which affect our calculation of the quantities of interest, *i.e.* the semileptonic form factors.

We have investigated the impact of the lattice artifacts on the $K \to \pi$ form factors by considering together the results of the runs A_3, B_4 and C_3 (see table 4.1), extrapolated at the reference kaon mass (4.25). All these runs correspond to pion masses equal to $M_\pi \sim 480\, MeV$ and with a lattice size almost kept fixed but with a lattice spacing of $a \sim 0.10\, fm$, $a \sim\ 0.079\, fm$ and $a \sim 0.063\, fm$, respectively. This allows us to study the *a–scaling* of our form factors. In figure 4.11 and 4.12, we show our results versus the square transfer momentum (in GeV) for three values of the lattice spacings.

It can be clearly seen that the size of the discretization effects is comparable to the statistical error, as it has already been verified in [90].

4.6.2 Finite size effects

In this section we will give a qualitative estimate of the finite volume effects (FSE) affecting our lattice calculation of the semileptonic form factors.

We have investigated the effects of the FSE related to the finite L extension of our lattice boxes by comparing the results of the runs B_1 and B_6. In our simulation the former has the smallest value of the quantity $M_\pi L$, which governs finite size effects in the *p-regime*. The physical extension of the two boxes is $L \simeq 2.1\, fm$ and $L \simeq 2.8\, fm$, respectively. The values of the angle θ are chosen differently at the two volumes in order to keep the values of q^2 fixed (in physical units).

The comparison of semileptonic form factors calculated for different size of the boxes are shown in figures 4.13 and 4.14.

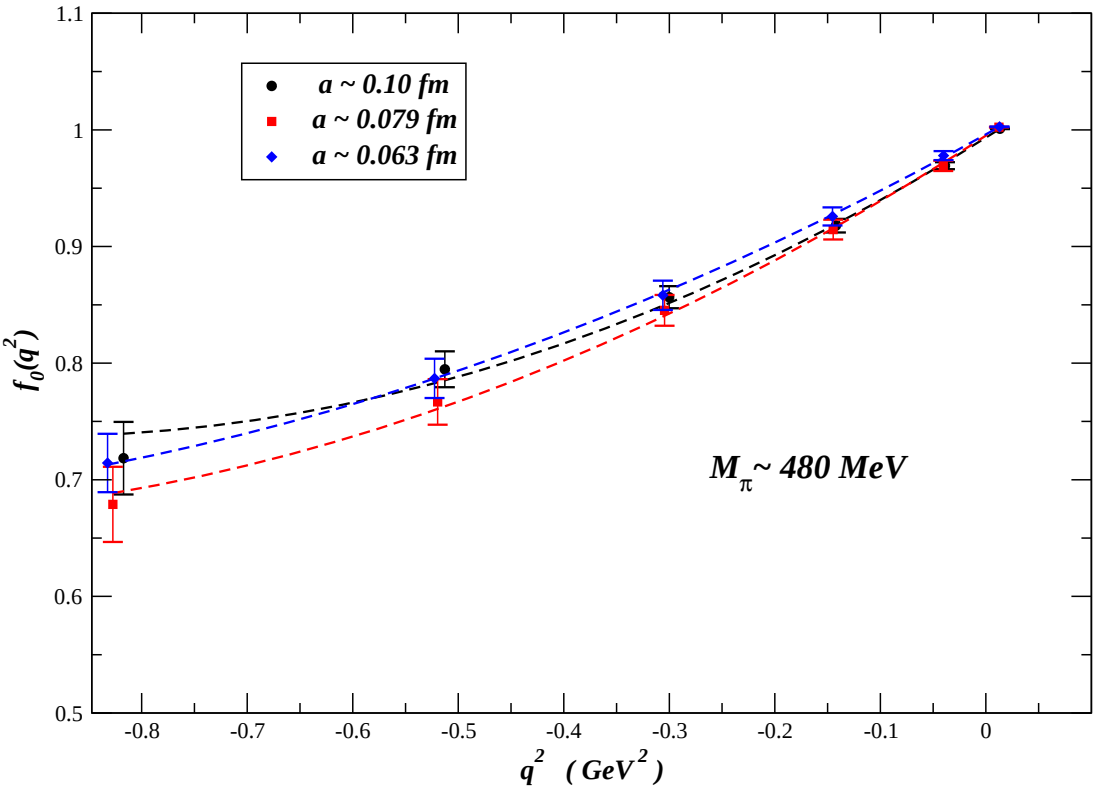

Figure 4.11: Discretization errors for $f_0(q^2)$ at M_K^{ref} - It is shown the scalar $f_0(q^2)$ form factor versus q^2, for $M_\pi \sim 480\, MeV$, interpolated at the reference kaon mass defined in (4.25), for the runs A_3, B_4 and C_3. The dashed lines are the results of the polynomial fit based on (4.22).

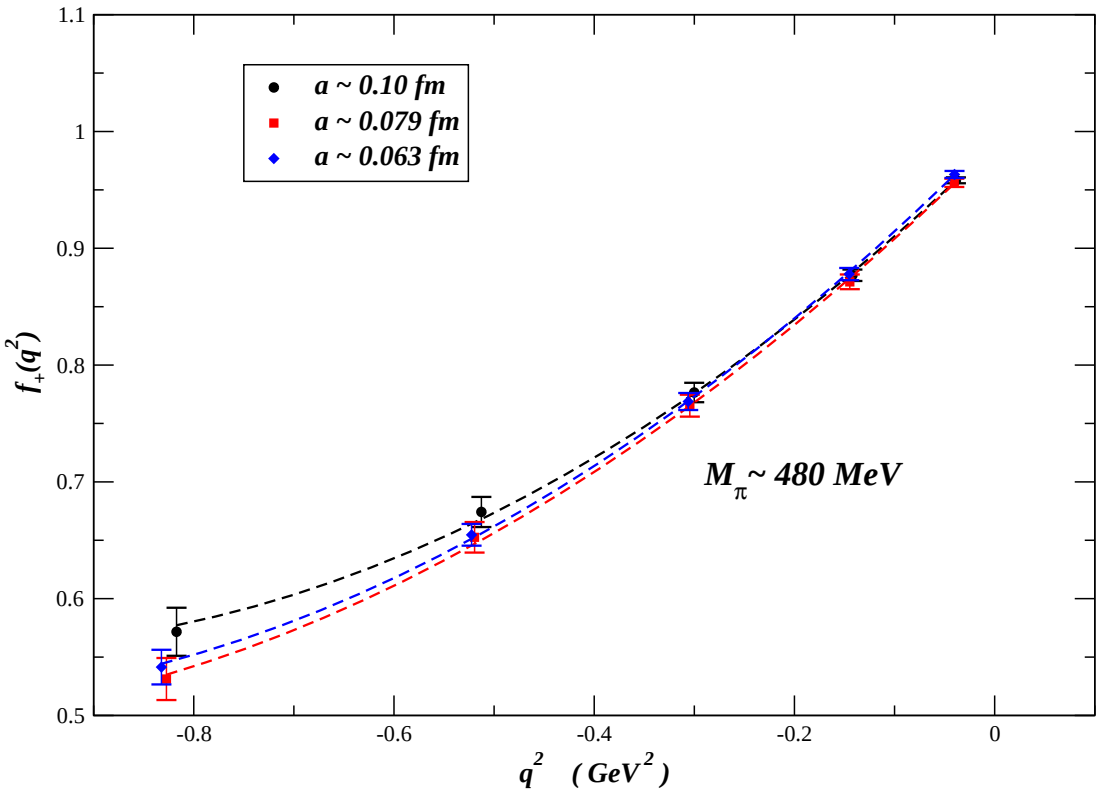

Figure 4.12: Discretization errors for $f_+(q^2)$ at M_K^{ref} - It is shown the vector $f_+(q^2)$ form factor versus q^2, for $M_\pi \sim 480\, MeV$, interpolated at the reference kaon mass defined in (4.25), for the runs A_3, B_4 and C_3. The dashed lines are the results of the polynomial fit based on (4.22).

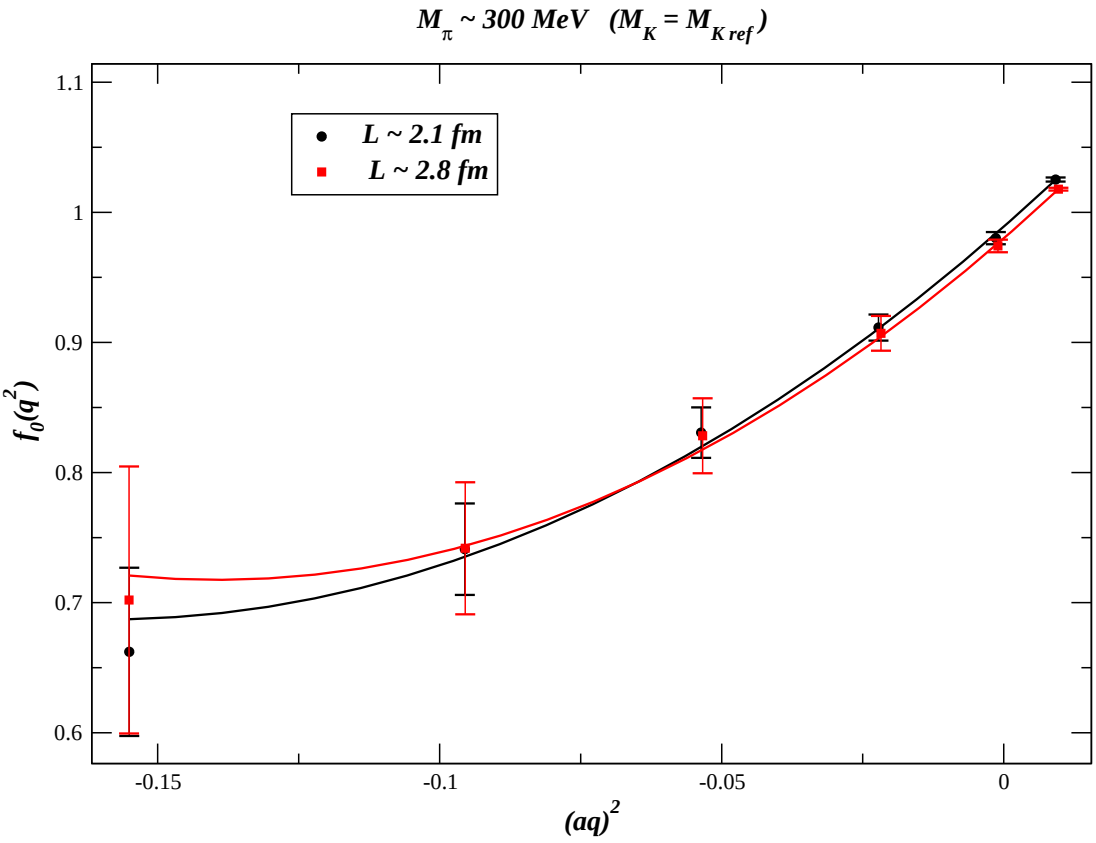

Figure 4.13: Finite size effects for $f_0(q^2)$ at M_K^{ref} - It is shown the scalar $f_0(q^2)$ form factor versus q^2 (lattice units), for $M_\pi \sim 300\,MeV$, interpolated at the reference kaon mass defined in (4.25), for the runs B_1 and B_6, which correspond to different lattice boxes of size $L \simeq 2.1\,fm$ and $L \simeq 2.8\,fm$, respectively. The lines are the results of the polynomial fit based on (4.22).

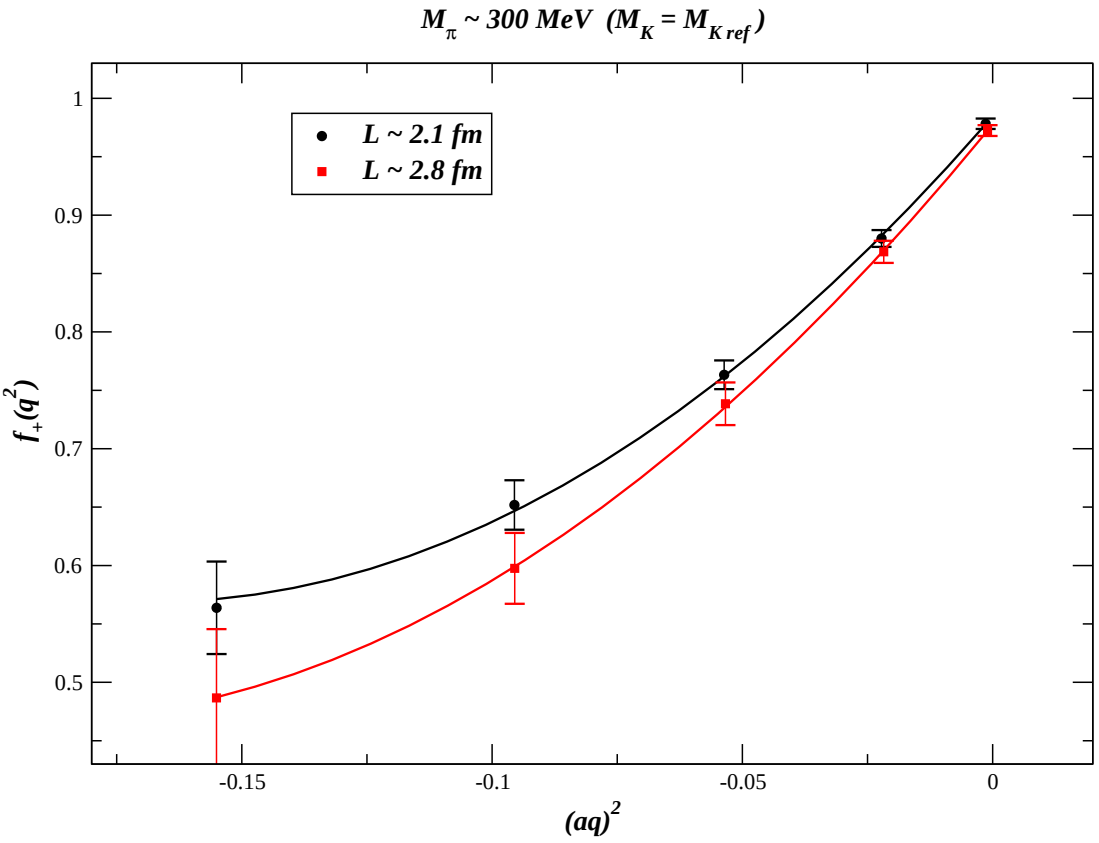

Figure 4.14: Finite size effects for $f_+(q^2)$ at M_K^{ref} - It is shown the vector $f_+(q^2)$ form factor versus q^2 (lattice units), for $M_\pi \sim 300\,MeV$, interpolated at the reference kaon mass defined in (4.25), for the runs B_1 and B_6 which correspond to different lattice boxes of size $L \simeq 2.1\,fm$ and $L \simeq 2.8\,fm$, respectively. The lines are the results of the polynomial fit based on (4.22).

It can be seen that in the case of the scalar form factor (figure 4.13) the size of the FSE is well comparable to the statistical error, while in the case of the vector form factor (figure 4.14) not all the kinematics are unaffected by FSE and a more quantitative analysis is required.

We show in table 4.3 a direct comparison of the form factor's key parameters $f_+(0)$, s_+ and $\bar{s}_+$ (see (4.21) and (4.22)) as obtained from a pole and polynomial fit to the data of runs B_1 and B_6.

(L/a)	$M_\pi \cdot L$	$f_+(0)$(pole)	$f_+(0)$(polynomial)	s_+(pole)	$\bar{s}_+$(polynomial)
24 (B_1)	3.3	0.9852(42)	0.9846(43)	0.290(21)	0.272(11)
32 (B_6)	4.3	0.9792(43)	0.9776(45)	0.330(29)	0.289(17)

Table 4.3: Form factor's parameters FSE We have reported the form factor's key parameters $f_+(0)$, s_+ and $\bar{s}_+$ as calculated from a pole (4.21) and a polynomial (4.22) fit to the data of runs B_1 and B_6, which correspond to $M_\pi \sim 300\, MeV$.

4.7 Reaching the physical point

Once obtained the scalar and the vector form factors, as a function of momentum, for each pion and kaon mass and once having interpolated them to the reference kaon mass, we can outline our final strategy which consist of performing a multi-combined fit of the form factor's q^2, M_π and a dependence in order to obtain an all-comprehensive parametrization. It will allow us to predict the vector form factor at zero momentum $f_+(0)$ as well as the q^2 shape, at the physical point, and to compare them with the experimental V_{us} and q^2 -shape results.

We will show in section 4.7.1 the main parametrization for the momentum dependence of the form factors, as well as the M_π dependence which will be described by means of $ChPT$. We will end next section introducing the polynomial parametrization chosen for taking into account lattice discretization artifacts.

4.7.1 Form factors structure

Following [23], among the different parametrization proposed in the literature, one can distinguish two classes [105]. Parametrization based on a systematic mathematical

expansion are the most widely used and in this class (called *Class II* in [105]) one finds the Taylor expansion

$$f_{+,0}^{Taylor}(q^2) = f_+(0)\left(1 + \lambda'_{+,0}\frac{q^2}{m_\pi^2} + \frac{1}{2}\lambda''_{+,0}\left(\frac{q^2}{m_\pi^2}\right)^2 + \frac{1}{6}\lambda'''_{+,0}\left(\frac{q^2}{m_\pi^2}\right)^3 + \dots\right) , \quad (4.26)$$

$\lambda'_{+,0}$ and $\lambda''_{+,0}$ are the slope and the curvature of the form factors, respectively. Another well known parametrization which belongs to Class II parametrization is the so called *z-parametrization* of [106]. In Class II parametrization the parameters describing higher order terms of the form factors expansion are free to be determined from data. It has been shown in [24] that in order to describe the form factor shapes accurately in the physical region ($0 < q^2 < q^2_{MAX}$, with $q^2_{MAX} = (M_K - M_\pi)^2$), one has to go at least up to the second order in the Taylor expansion. Moreover, as it will be discussed below, for tests of low - energy dynamics involving the Callan Treiman theorem, $f_0(q^2)$ must be extrapolated up to $q^2 = \Delta_{K\pi} \equiv M_K^2 - M_\pi^2$ which is well above the endpoint of the physical q^2 region of K_{l3} decays. A parametrization that accounts for even higher order terms is therefore desirable.

The parametrizations belonging to *Class I* circumvent this problem by incorporating additional physical constraints to reduce the number of independent parameters. A typical example is the pole parametrization

$$f_{+,0}^{pole}(0) = \frac{M_{V,S}^2}{M_{V,S}^2 - q^2} , \quad (4.27)$$

where the dominance of a single resonance is assumed, and the corresponding pole mass $M_{V,S}$ is the only free parameter. While for the vector form factor a pole parametrization with $M_V \sim 892\ MeV$ (*i.e.* K^* resonance mass) is enough to reproduce the observed shape, for the scalar form factor there is no such obvious dominance. The most well-motivated Class I parametrization are those based on *dispersion relations*. These are based on the observation that the vector and scalar form factors are analytic functions in the complex q^2 plane, except for a cut along the positive real axis for $q^2 > q^2_{lim} \equiv (M_K + M_\pi)^2$, where discontinuities are developed. One can therefore write

$$f_{0,+}(q^2) = \frac{1}{\pi}\int_{t_{lim}}^{\infty} dt\ \frac{Imf_{+,0}(t)}{(t-q^2-i\epsilon)} + sub\ terms\ . \tag{4.28}$$

The imaginary part, $Imf_{+,0}(t)$, can be determined from data on $K\pi$ scattering and contains all the intermediate state contributions with quantum numbers consistent with $f_{+,0}$ ones, *i.e.* $J^P = 1^-$ and $J^P = 0^+$, while the ultraviolet component of the integral is absorbed into the subtraction terms. In the vector case, the dispersive parametrization turns out to be very similar to the pole parametrization due to the dominant $K^*(892)$ contribution to $Imf_+(t)$. On the other hand the dispersive parametrization is particularly useful in the scalar case, where there is no such dominant one particle intermediate state.

There is also another form factors parametrization which is obtained within the framework of Chiral perturbation theory, the low energy theory of QCD. This theory has been developed after the observation that even if QCD is highly non perturbative at low energies, the spectrum of the theory at that energy is rather simple as it is composed of only the octet of the light pseudoscalar mesons π, K and η. Experimentally, we also know that, at very low energies, these pseudoscalar mesons interact weakly, both among themselves and with nucleons. It is then reasonable to expect that QCD can be treated pertubatively even at low energies, provided a suitable transformation of degree of freedom is performed. This is exactly the goal of ChPT, where the pseudoscalar mesons are assumed to be fundamental degree of freedom. Within this effective theory, it is "straightforward", using the technology developed in [21; 22], to calculate the vector and the scalar form factors of the $K \to \pi$ process to the first non leading order in the low energy expansion (NLO).

The vector form factor can be written as [21]

$$f_+(q^2) = 1 + \frac{3}{2}H_{K\pi}(q^2) + \frac{3}{2}H_{K\eta}(q^2)\,, \tag{4.29}$$

with the quantity $H(q^2)$ which is related to the invariant functions $M^r(q^2)$ and $L(q^2)$ by[1]

[1]The indices attached to $H(q^2)$ denote the masses of the mesons running around the loop; for instance, to obtain $H_{K\pi}(q^2)$ one has to substitute in $M^r(q^2)$, $L(q^2)$, and in all the sub-functions on which they depend on, $M_P = M_K$ and $M_Q = M_\pi$.

$$H(q^2) = \frac{1}{F_0^2}\left\{ q^2 M^r(q^2) - L(q^2)\right\} + \frac{2}{3F_0^2} L_9^r q^2. \tag{4.30}$$

In the previous expression, beside L_9^r which is one of the coupling constants in the effective lagrangian, renormalized at the running scale μ[1], the notation goes as follow

$$M^r = \frac{1}{12q^2}\left\{q^2 - 2\Sigma\right\}\bar{J} + \frac{\Delta^2}{2(q^2)^2}\bar{\bar{J}} - \frac{1}{6}k + \frac{1}{288\pi^2} \tag{4.31}$$

$$L = \frac{\Delta^2}{4q^2}\bar{J}\,, \tag{4.32}$$

$$K = \frac{\Delta}{2q^2}\bar{J}\,, \tag{4.33}$$

with

$$k = \frac{1}{32\pi^2}\frac{M_P^2 \log\left(M_P^2/\mu^2\right) - M_Q^2 \log M_Q^2/\mu^2}{M_P^2 - M_Q^2} \tag{4.34}$$

$$\bar{\bar{J}}(q^2) = \bar{J}(s) - q^2\bar{J}'(0)\,, \tag{4.35}$$

$$\bar{J}(q^2) = \frac{1}{32\pi^2}\left\{2 + \frac{\Delta}{q^2}\log\frac{M_Q^2}{M_P^2} - \frac{\Sigma}{\Delta}\log\frac{M_Q^2}{M_P^2} - \frac{\nu}{q^2}\log\frac{(s+\nu)^2 - \Delta^2}{(s-\nu)^2 - \Delta^2}\right\}, \tag{4.36}$$

and

$$\nu^2 \equiv \nu_{PQ}^2 = (q^2)^2 + M_P^4 + M_Q^4 - 2q^2(M_P^2 + M_Q^2) - 2M_P^2 M_Q^2\,, \tag{4.37}$$

$$\Sigma \equiv \Sigma_{PQ} = M_P^2 + M_Q^2, \quad \Delta \equiv \Delta_{PQ} = M_P^2 - M_Q^2\,, \tag{4.38}$$

the function $\bar{J}(q^2)$ represent the contribute of the scalar loop integrals, subtracted at $q^2 = 0$.

The analogous low-energy representation of the scalar form factor $f_0(q^2)$ is given by

[1]One can easily check that the scale dependence of the function $M^r(q^2)$ compensate the scale dependence of the constant L_9^r so that the function $H(q^2)$ is scale independent (as it should be being a physical observable).

$$f_0(q^2) = 1 + \frac{1}{8F_0^2}\left(5q^2 - 2\Sigma_{K\pi} - 3\frac{\Delta_{K\pi}^2}{q^2}\right)\bar{J}_{K\pi}(q^2) + \frac{1}{24F_0^2}\left(3q^2 - 2\Sigma_{K\pi} - \frac{\Delta_{K\pi}^2}{q^2}\right)\bar{J}_{K\eta} + \frac{q^2}{4\Delta_{K\pi}^2}(5\mu_\pi - 2\mu_K - 3\mu_\eta) + \frac{4L_5^r}{F_0^2}q^2\,; \tag{4.39}$$

where here we have

$$\mu_P = \frac{1}{32\pi^2}\frac{M_P^2}{F_0^2}\log\frac{M_P^2}{\mu^2}\,, \tag{4.40}$$

and the scale dependence of the low-energy constant L_5^r is compensated by the scale dependence of the chiral logarithms μ_π, μ_K and μ_η.

Even if conventionally it has been $SU(3)$ ChPT which has been applied to the study of K_{l3} decay amplitudes, we are going to take an $SU(2)$ limit of the NLO $SU(3)$ ChPT formulas (4.29) (4.39). The reason which motivates this procedure lays in the very difference between $SU(2)$ and $SU(3)$ expansions; in $SU(3)$ ChPT the strange quark satisfies chiral symmetry, and this means that we are in presence of a more general and predictive theory (respect to $SU(2)$) but which hides a subtlety: as we will see later on, starting from the chiral point ($m_u = m_d = m_s = 0$), around which an $SU(3)$ expansion is performed, we have to reach two physical points, the pion mass and the kaon mass. The pion mass is not too far from the chiral point but the kaon mass is heavy enough that the NLO expansion may not be sufficient to guarantee the convergence of our formulae. On the other hand, in $SU(2)$ ChPT the strange quark has been integrated out and as a result the LEC's will depend on m_s. This means that if we are able to fix somehow this dependence, as we have done interpolating our form factors at M_K^{ref}, we will be left with only one physical point to reach and it will be the pion mass for which a NLO order approximation will be enough to guarantee the expansion convergence.

Starting from the NLO $SU(3)$ ChPT formulas (4.29) (4.39) and rewriting them in terms of the two following variables

$$x = \frac{M_\pi^2}{M_K^2}\,, \tag{4.41}$$

$$s = \frac{q^2}{M_K^2}, \tag{4.42}$$

expanding in powers of x and keeping only $\mathcal{O}(x)$ and $\mathcal{O}(x\log x)$ terms, one is able to obtain this $SU(2)$ limit for the form factors

$$f_0(s) = F_0(s)\left\{1 + C_0(s)x + \frac{M_K^2}{(4\pi f)^2}\times\left[-\frac{3}{4}x\log x + T_1^0 - T_2^0\right]\right\}\,, \tag{4.43}$$

$$f_+(s) = F_+(s)\left\{1 + C_+(s)x + \frac{M_K^2}{(4\pi f)^2}\times\left[-\frac{3}{4}x\log x - T_1^+ - T_2^+\right]\right\} \tag{4.44}$$

where $F_{0,+}(s)$ and $C_{0,+}(s)$ are unknown LECs while $T_1^{0,+}(x,s)$ and $T_2^{0,+}(s)$ are known function of (s,x) and x, namely

$$T_1^0 = \; x(9+7s^2)\left[\frac{\log(1-s)+s(1+s/2)}{4s^2}\right]\,, \tag{4.45}$$

$$T_2^0 = \; (1-s)(3+5s)\left[\frac{(1-s)\log(1-s)+s(1-s/2)}{4s^2}\right]\,, \tag{4.46}$$

$$T_1^+ = \; 3x(1+s)\left[\frac{(1-s)\log(1-s)+s(1-s/2)}{4s^2}\right]\,, \tag{4.47}$$

$$T_2^+ = \; (1-s)^2\left[\frac{(1-s)\log(1-s)+s(1-s/2)}{4s^2}\right]\,. \tag{4.48}$$

As can be seen from their explicit expression, they are functions of both s and x, but the important terms are the ones involving

$$\log(1-s)\,. \tag{4.49}$$

These terms are zero at $q^2 = 0$ (*i.e.* $s = 0$), so that the chiral logarithm $(-3/4)x\log x$ receive no contribution and we are left with

$$f_0(0) = f_+(0) \propto -\frac{3}{4}M_\pi^2\log\left\{\frac{M_\pi^2}{\mu^2}\right\}\,; \tag{4.50}$$

however, when $q^2 \to q^2_{MAX}$ (*i.e.* $s \to (1-\sqrt{x})^2$) the chiral logarithm coefficient, as already calculated in [107] using $SU(2)$ ChPT, get a correction and we have

$$f_0(q^2_{MAX}) \propto -\frac{11}{4} M_\pi^2 \log\left\{\frac{M_\pi^2}{\mu^2}\right\} . \tag{4.51}$$

We have seen that these expressions involve a great number of LEC's so, in addition to these information about the form factors pion mass and q^2 dependence, it is a good thing to profit of another constraint coming from ChPT, which is the Callan-Treiman (CT) theorem [108]; it implies that the scalar form factor at the CT point, defined as $q^2 = \Delta_{K\pi} = M_K^2 - M_\pi^2$, is determined in terms of the ratio f_K/f_π, up to $\mathcal{O}(m_{u,d})$ corrections:

$$f_0(\Delta_{K\pi}) = \frac{f_K}{f_\pi} + \Delta_{CT} . \tag{4.52}$$

The quantity $\Delta_{CT} = \mathcal{O}(m_{u,d}/4\pi f_\pi)$ is vanishing in the $SU(2)$ chiral limit $m_{u,d} \to 0$; this means that using the chiral expansion for the decay constants

$$\frac{f_K}{f_\pi} = 1 + \frac{1}{4}(5\mu_\pi - 2\mu_K - 3\mu_\eta) + \frac{4}{F_0}\left(M_K^2 - M_\pi^2\right) L_5^r , \tag{4.53}$$

rewriting it in terms of the adimensional variables (s, x)

$$\frac{f_K}{f_\pi} = \left(\frac{f_K}{f_\pi}\right)_0 \left[1 + Bx + \frac{M_K^2}{(4\pi F_0)^2}\frac{5}{4} x \log x\right] , \tag{4.54}$$

and exploiting the Callan-Treiman theorem one is able to further constraint the scalar form factor as

$$F_0(s=1) = \left(\frac{f_K}{f_\pi}\right)_0 . \tag{4.55}$$

Let us conclude this section explaining explicitly our strategy for the form factors analysis: we are going to fit our ensemble of data using (4.43) and (4.44) formulas for the form factors, assuming for the momentum-depending LEC's $F_{0,+}(s)$ and $C_{0,+}(s)$ a functional form of the pole and polynomial kind, as follows

$$F_{0(+)}(s) = \frac{F}{1 - \lambda_{0(+)} s}\,, \tag{4.56}$$

$$C_{0(+)}(s) = C_0 + C_1^{0(+)} s + C_2^{0(+)} s^2\,, \tag{4.57}$$

where the constraint for the form factors at zero momentum ($f_+(0) = f_0(0)$) is implied. Moreover the CT theorem in the chiral limit ($M_\pi = 0$) imposes the constraint (4.55), which implies

$$\frac{F}{1 - \lambda_0} = \left(\frac{f_K}{f_\pi}\right)_0 . \tag{4.58}$$

To estimate lattice artifacts in the spirit of the Symanzik analysis of discretization effects, and taking into account $\mathcal{O}(a)$ improvement guaranteed by twisted mass fermions at maximal twist, we will also add to both our form factor formulas (4.43) and (4.44) the polynomial function

$$D = da^2 + d'a^2 s\,, \tag{4.59}$$

with d and d' two unknown coefficient.

In figure 4.15 and 4.16 we show, respectively, the fit quality for the scalar and the vector form factors, at fixed values of q^2, plotted against the squared pion mass, obtained from the data taken from ensembles $A_2, \ldots, A_4$, $B_2, \ldots, B_7$ and C_2, C_3; they are almost all the data at our disposal, except for ensemble B_1 and C_1 which have a value of the product $M_\pi \cdot L$ not high enough to be considered FSE-safe.

4.7.2 Quenching of the strange quark

The effect of our partially quenched (PQ) set up has already been estimated in [19] using $SU(3)$ ChPT.

Within $SU(3)$ ChPT one can perform a systematic expansion of the vector form factor at zero momentum, of the type

$$f_+(0) = 1 + f_2 + f_4 + \ldots\,, \tag{4.60}$$

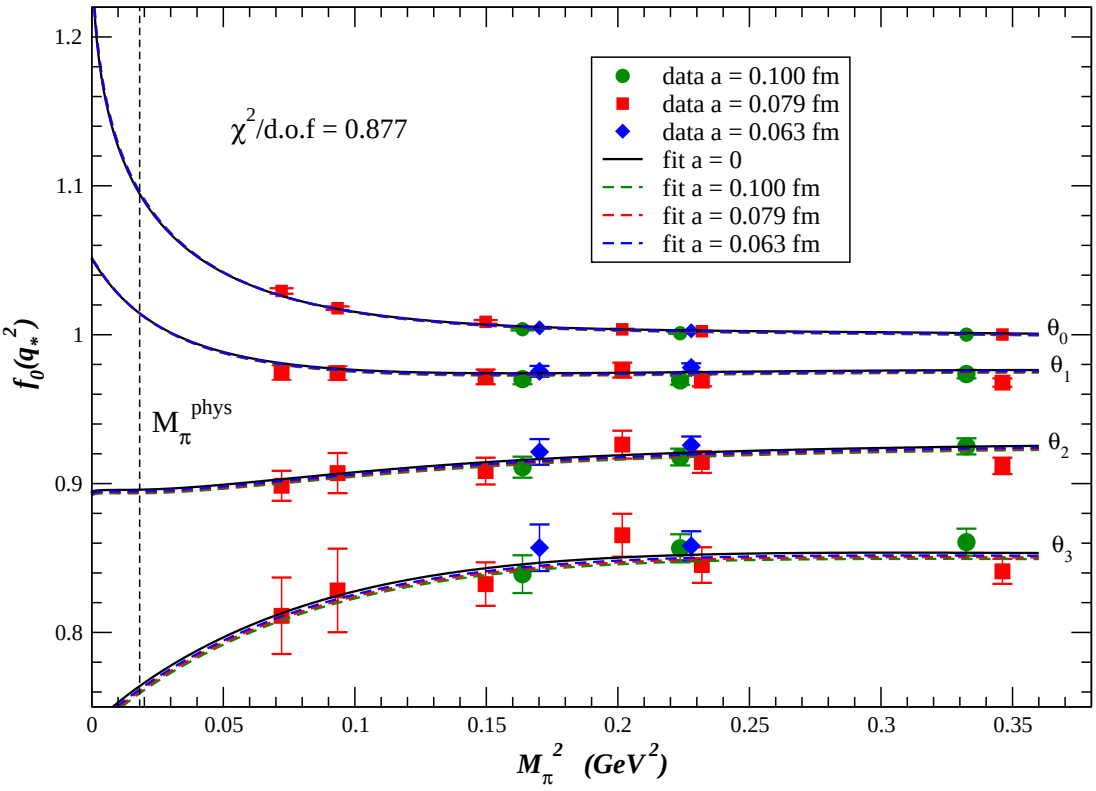

Figure 4.15: Scalar form factor fit quality - It is shown the scalar form factor $f_0(q^2)$, for the first four values of q^2 (*i.e.* θ) employed in our simulations, as a function of the squared pion mass M_π^2 in GeV^2; (full) circles, squares and diamonds are data taken, respectively, from the runs $A_2, \ldots, A_4$, $B_2, \ldots, B_7$ and C_2, C_3 in order to guarantee that $M_\pi \cdot L \geq 3.7$. The continuous black line is the result of an $a = 0$ fit while the dashed green, red and blue lines represent $a = 0.100\, fm$, $a = 0.079\, fm$ and $a = 0.063\, fm$ fits, respectively. The dashed vertical line represent the value of the physical pion mass.

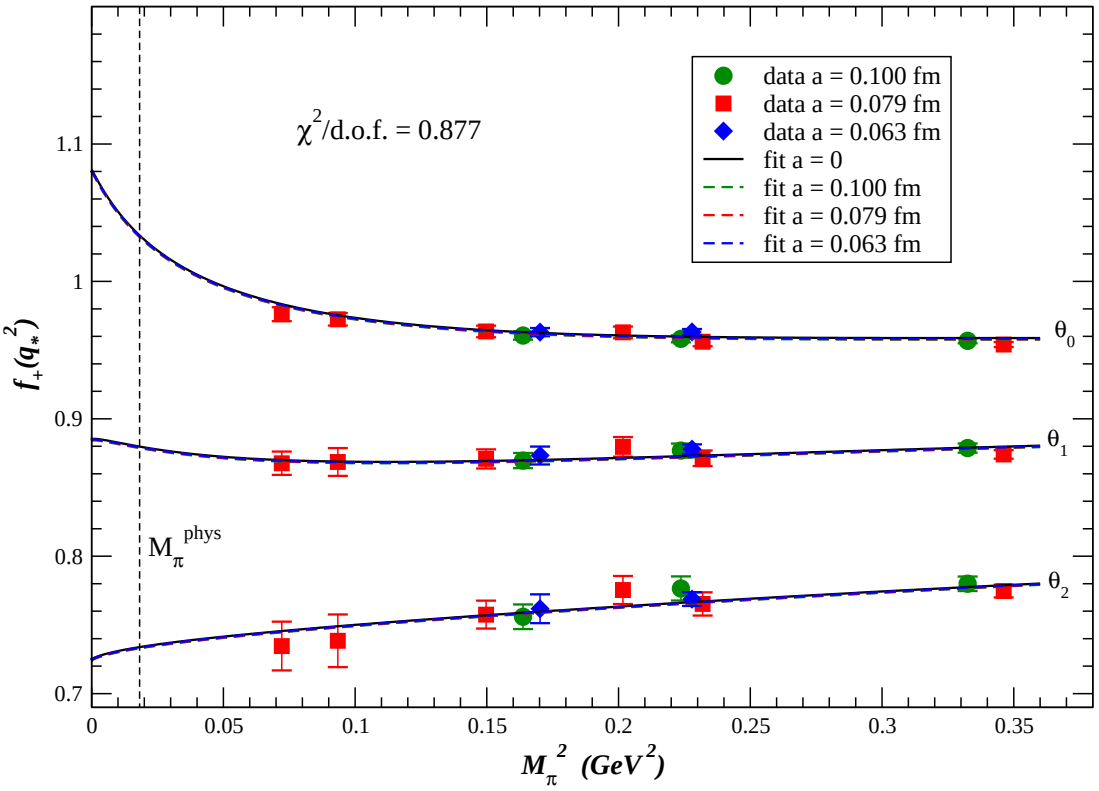

Figure 4.16: Vector form factor fit quality - It is shown the vector form factor $f_+(q^2)$, for the first three values of q^2 (*i.e.* θ) employed in our simulations, as a function of the squared (physical) pion mass M_π^2 in GeV^2; (full) circles, squares and diamonds are data taken, respectively, from the runs $A_2, \ldots, A_4$, $B_2, \ldots, B_7$ and C_2, C_3 in order to guarantee that $M_\pi \cdot L \geq 3.7$. The continuous black line is the result of an $a = 0$ fit while the dashed green, red and blue lines represent $a = 0.100\, fm$, $a = 0.079\, fm$ and $a = 0.063\, fm$ fits, respectively. The dashed vertical line represent the value of the physical pion.

where $f_n = \mathcal{O}[M_{K,\pi}^n/(4\pi f_\pi)^n]$, and the first term is equal to unity due to the current conservation in the $SU(3)$ limit; because of the the AG theorem [46], valid also in both quenched (Q) [17] and PQ [109] setups, the NLO terms f_2 can be unambiguously computed in terms of M_K, M_π and f_π. At the physical point it takes the values: $f_2^Q = +0.022$ in the quenched case $N_f = 0$ [17], $f_2^{PQ} = -0.0168$ for our PQ setup with $N_f = 2$ [109] and $f_2 = -0.0226$ for $N_f = 2 + 1$ [110]. Thus the effect of quenching the strange quark is exactly known at NLO: at the physical point $f_2 - f_2^{PQ} = 0.0058$ ($\simeq 26\%$ of f_2). This correction will be added to the central value of our estimate of $f_+(0)$ and it has no error.

Introducing the quantity

$$\Delta f \equiv f_4 + f_6 + \cdots = f_+(0) - (1 + f_2) \tag{4.61}$$

the task is reduced to the problem of estimating the quenching effect on this $\mathcal{O}(p^6)$ term. For this quantity, it has been found evidence [19] that the chiral logs, which are the most sensitive to quenching effects, are small compared to the contribution of the local terms. The authors of [19] have thus estimated that the relative quenching effect in Δf is at most 50% of the same relative effect on f_2, which amounts to 0.0028 (*i.e.* $\simeq 13\%$ of Δf). Note that this value is of the same size of the difference between the estimate of Δf at $N_f = 2$ and the quenched one of [17]. Thus this estimate of the quenching error is expected to be a conservative one. We will add (in quadrature) the value 0.0028 to the systematic error we will give for $f_+(0)$. Let us conclude this section showing in figure 4.17 our Δf ($N_f = 2$) as a function of the pion mass squared compared with the Δf ($N_f = 2+1$) calculated by the RBC collaboration in [111]; as can be seen in figure our values fit well with the one calculated by the RBC collaboration.

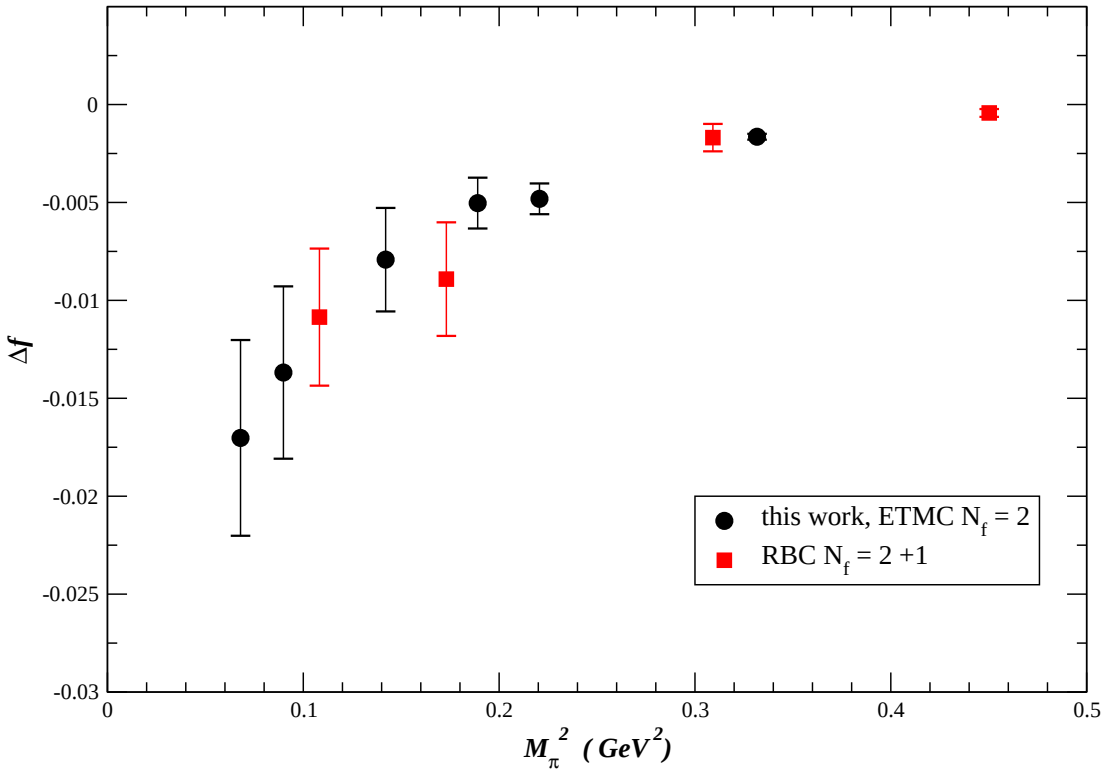

Figure 4.17: Δf comparison - It is shown our Δf ($N_f = 2$), defined in (4.61), as a function of the pion mass squared compared with the Δf ($N_f = 2 + 1$) calculated by the RBC collaboration [111]. It can be clearly seen that our data fit well with the RBC ones.

4.8 Physical results: semileptonic form factors & V_{us}

We present here our results for the semileptonic form factors at the physical point, obtained from simulations with two flavour of dynamical twisted-mass fermions, using pion masses in the range 260 to 575 MeV.

Our main results are listed in the first column of table 4.4 and are the vector form factor at zero momentum $f_+(0)$, the ratio of the Kaon decay constant over the pion one f_K/f_π and the related prediction for the CKM-matrix element V_{us}, as obtained from the analysis of the runs $A_2, \cdots, A_4$, $B_2, \cdots, B_7$ and $C_1, \ldots, C_3$ (all with $M_\pi \cdot L \geq 3.7$). For the vector form factors we have quoted two errors: the first one is the statistical one while the second is the systematic one and is due mainly to the quenching of the strange quark.

	this work	***FLAVIANET* 2010**
$f_+(0)$	$0.9610 \pm 0.0030 \pm 0.0028$	0.959(5) [112]
(f_K/f_π)	1.189 ± 0.008	1.193(6) [23]
V_{us}^{Kl3}	0.2250 ± 0.0014	0.2254 ± 0.0013 [23]
V_{us}^{Kl2}	0.2258 ± 0.0016	0.2252 ± 0.0013 [23]

Table 4.4: Physical results We show in the first column the physical results using ETMC configurations $A_2, \cdots, A_4$, $B_2, \cdots, B_7$ and $C_1, \ldots, C_3$ (all with $M_\pi \cdot L \geq 3.7$). The errors, where both available, are statistical and systematical. The second column shows the corresponding values as given in [23].

Our results for $f_+(0)$ and f_K/f_π in table 4.4 (first column) compares positively within errors with the ETMC results already published, namely $f_+(0) = 0.9560(84)$ of [19] and $(f_K/f_\pi) = 1.210(18)$ of [113].

As can be seen from the table, and as we have already explained in chapter 1, we have quoted two values for the V_{us} matrix element. The first one, which we have indicated with $V_{us}^{K_{l3}}$, is obtained using the experimental measure of the product $|V_{us}| \cdot f_+(0) = 0.2163(5)$, from K_{l3} semileptonic decays in [23], combined with our estimate of $f_+(0)$ given in the first row of table 4.4.

The second one, called $V_{us}^{K_{l2}}$, can be obtained from the ratio of K_{l2} to π_{l2} decay rates (1.83), using the experimental measure of the quantity $|V_{us}/V_{ud}| \cdot (f_K/f_\pi) =$

0.2758(5) given in [23] and exploiting our estimate for the f_K/f_π ratio combined with the knowledge of $V_{ud} = 0.97425(22)$ from nuclear beta decays.

We also quote, in the second column of table 4.4, the results given by the FLAVIANET collaboration [23] for the presented quantities. They were able to give predictions for V_{us} using the lattice input of $f_+(0)$ and f_K/f_π taken, respectively, from their symmetrization of the recent $RBC/UKQCD$ results [112] and from a weighted average (by means of the statistical errors) of the results of the analysis from BMW [114], $MILC$ '09 [115] and $HPQCD/UKQCD$[116].

As can be clearly seen our results turn out to be in good agreement with the ones quoted by the FLAVIANET collaboration.

In table 4.5 we present a comparison between our scalar and vector form factor's slopes and curvature (with respect to q^2) parameters (see (4.26)) with the ones evaluated in [23] by means of an average of the experimental results of $KLOE$, $KTeV$, $NA48$ (without muons branching ratios) and $ISTRA+$; we also show our form factors as a function of q^2, extrapolated to the physical point, togheter with the ones obtained from a *dispersive fit*, based on the form factor parametrization of [24], to the *experimental data* (from the already mentioned experiments) performed by the authors of [23]. This second comparison is shown in figure 4.18 and it can be clearly seen that there is a good agreement for the vector and the scalar form factor.

	this work	***FLAVIANET* 2010** [23]
λ'_0	$(16.01 \pm 0.80) \cdot 10^{-3}$	$(15.90 \pm 0.79) \cdot 10^{-3}$
λ'_+	$(23.78 \pm 1.10) \cdot 10^{-3}$	$(25.04 \pm 0.82) \cdot 10^{-3}$
λ''_+	$(1.15 \pm 0.09) \cdot 10^{-3}$	$(1.57 \pm 0.36) \cdot 10^{-3}$

Table 4.5: Form factor's parameters We show in the first column the form factor's slopes (λ') and curvature (λ'') as obtained using the ETMC configurations $A_2, \cdots, A_4$, $B_2, \cdots, B_7$ and $C_1, \ldots, C_3$ (all with $M_\pi \cdot L \geq 3.7$). The errors, where both available, are statistical and systematical. The second column shows the corresponding values as given in [23].

4.9 Present status of our stochastic technique

We show in this section our results obtained using the *spin–direct* and the *twisted* stochastic technique for calculating the disconnected fermionic bubble (3.79). We have

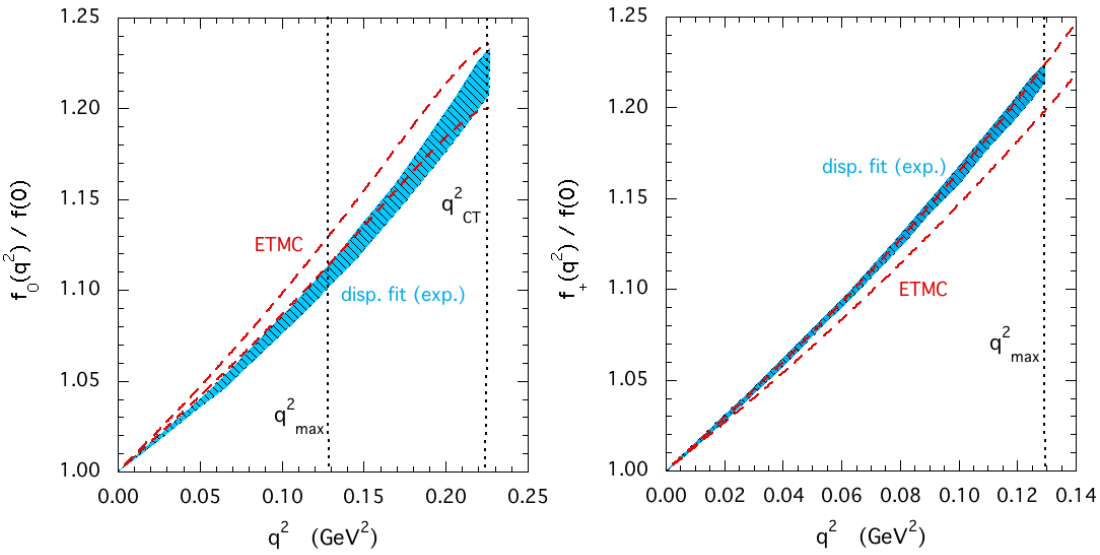

Figure 4.18: Scalar and vector form factors experimental comparison - It is shown the scalar (left) and vector (right) form factors 1σ allowed region, as a function of q^2 at the physical point. The form factors has been obtained from the runs $A_2, \ldots, A_4$, $B_2, \ldots, B_7$ and C_2, C_3 in order to guarantee that $M_\pi \cdot L \geq 3.7$. The shaded blue region is the 1σ allowed region for the form factors as obtained from the authors of [23] performing the dispersive fit of the form [24] on the *KLOE*, *KTeV*, *NA48* (without muons branching ratios) and *ISTRA+* experimental data.

used, as testing ground, the η' zero momentum two–point function (3.75), obviously paying a particular attention to the disconnected part of the correlator. The data at our disposal were calculated using the ETMC gauge field configurations generated with the tree-level Symanzik improved action (2.54) and the $N_f = 2$ twisted mass action, for two degenerate valence quarks, at maximal twist (2.66). As we were carrying out a feasibility study, we have tested our methods using a single $\beta = 3.9$ ($a = 0.0079\, fm$, $a^{-1} = 2.30\, GeV$) a single lattice volume of $V = 24^3 \times 48\, a^4$ and a single sea quark mass $a\mu_{sea} = 0.0040$. To work in the *unitary limit* we have employed a valence quark mass equal to our sea quark mass.

In figure 4.19 we show the comparison between the disconnected part (3.78) of the η' correlator as a function of time, evaluated both with the spin direct method (full dots) and with the twisted method (full squares) on 120 gauge field configurations. The twisted method appear to be superior with respect to the spin–direct one especially if one looks at figure 4.20 where we have shown the same quantities shown in figure 4.19 but with the spin–direct method calculated using 480 gauge field configuration while the twisted one is again a 120 configurations estimate, and it appears to be still better.

Even if the precision of the methods is an encouraging one, when one calculate the complete, zero momentum, η' correlator (3.75), encounter some difficulties.

We show in figure 4.21 the complete η' (zero momentum) two–point correlator as a function of time, calculated using both the methods at our disposal. It can be seen that we are able to extract no signal, because the stochastic fluctuations make our correlator still noisy. This means that there are two options once obtained such a result: the first one is turn our attention to a more powerful machine with which one can use more stochastic sources *per* gauge field configurations, thus easily reducing the stochastic noise. The second one is to employ further techniques or tricks to achieve the desired signal to noise ratio.

In the η' case, the authors of [16] have succeeded to extract a signal and were able to calculate the η' mass; although they employed some, so–called, *variance reduction* methods, these techniques are specific of the zero momentum two–points function characteristic of the η' case. For instance, one of these methods consists in the excited state removal for which one basically replace the connected neutral pseudoscalar correlator by just the ground state contribution. It is clear that such a trick can only be used

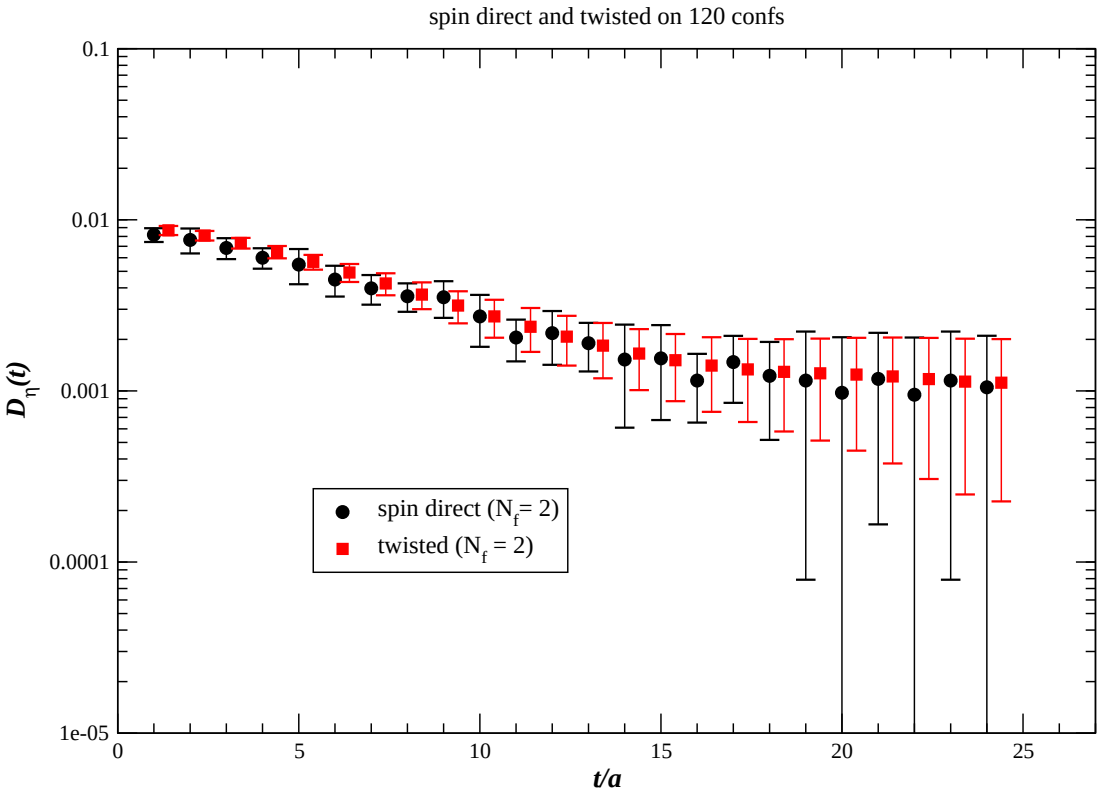

Figure 4.19: η' disconnected diagrams (I) - We show the disconnected part of the η' correlator at zero momentum (disconnected part of (3.75), with $\vec{p} = 0$) as a function of time (in lattice units). The full dots represent the data obtained using the spin–direct method, while the full squares are obtained using the twisted technique. Data are obtained from 120 gauge field configuration at $\beta = 3.9$ for a volume of $V = 24^3 \times T = 48$, in the $N_f = 2$ case. The number of inversions *per* configuration amount to 4×24 for the spin direct method while for the twisted one it is only $N_f \times 4$. For the sake of readability, the twisted correlator has been translated in t/a of 0.3.

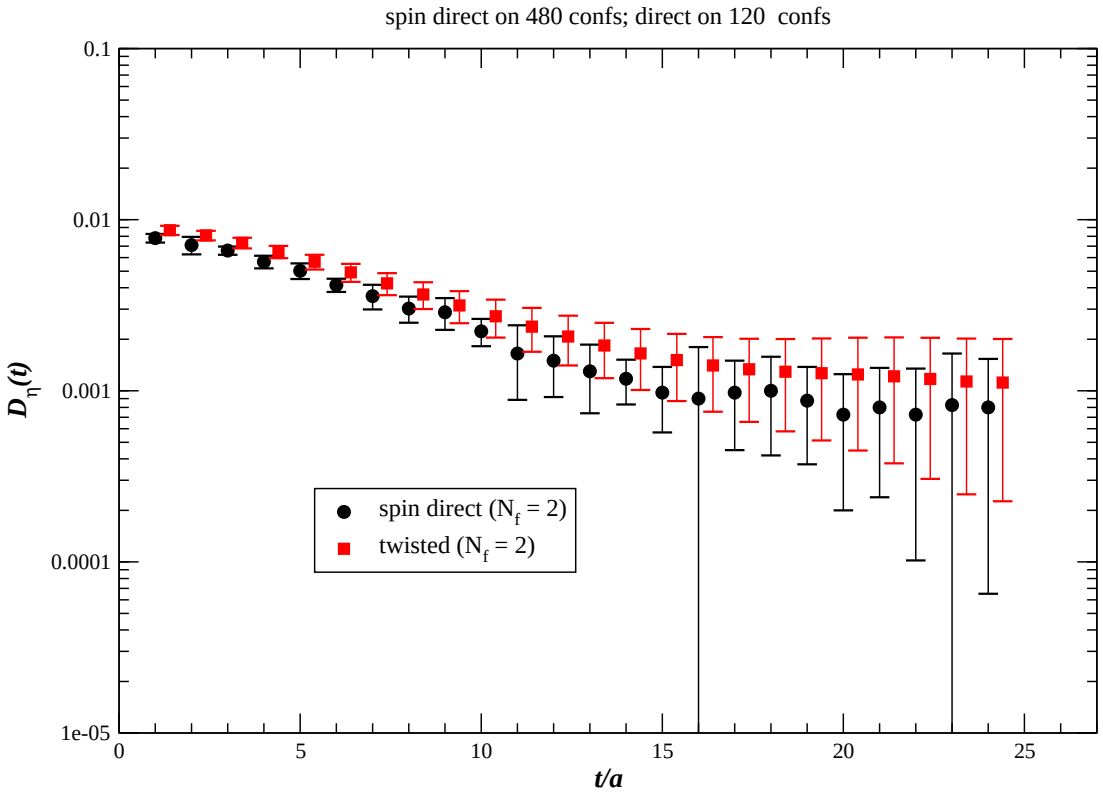

Figure 4.20: η' disconnected diagrams (II) - We show the disconnected part of the η' correlator at zero momentum (disconnected part of (3.75), with $\vec{p} = 0$) as a function of time (in lattice units). The full dots represent the data obtained using the spin–direct method, while the full diamonds are obtained using the twisted technique. Data are obtained in the $N_f = 2$ case, at $\beta = 3.9$, for a volume of $V = 16^3 \times T = 32$ from 480 gauge field configurations for the spin–direct method while for the twisted method only 120 have been used. The number of inversions *per* configuration amount to 4×24 for the spin direct method while for the twisted one it is only $N_f \times 4$. For the sake of readability, the twisted correlator has been translated in t/a of 0.3.

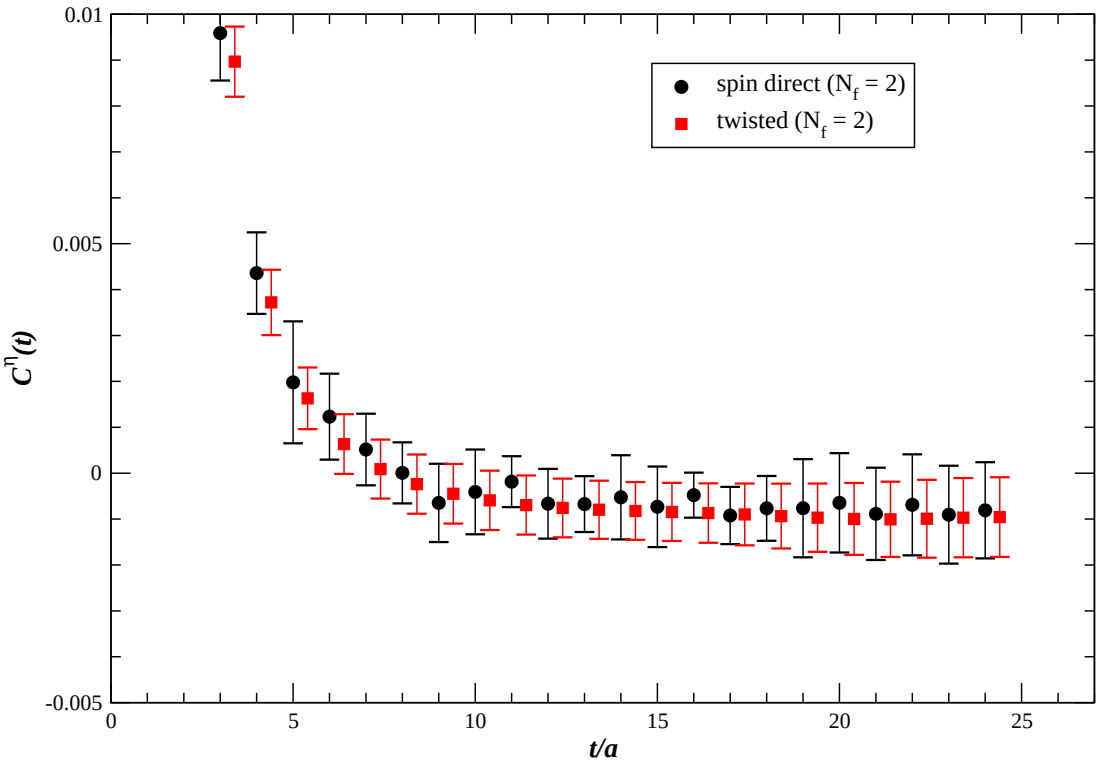

Figure 4.21: η' complete correlator - We show the η' complete correlator at zero momentum ((3.75), with $\vec{p} = 0$) as a function of time (in lattice units). The full dots represent the data obtained using the spin–direct method, while the full squares are obtained using the twisted technique. Data are obtained from 120 gauge field configuration at $\beta = 3.9$ for a volume of $V = 24^3 \times T = 48$, in the $N_f = 2$ case. For the sake of readability, the twisted correlator has been translated in t/a of 0.3.

when doing spectroscopy while, on the other hand, we want to apply our methods to the neutron EDM calculation and so we can not profit of their variance reduction tricks.

Our next step will be to use an increased number of stochastic sources, of the order of hundreds, with respect to the few dozen employed in our present calculation carried out on the TeraFlop ApeNext supercomputing center. It is clear that using such a number of stochastic sources is a target achievable only on super computers with a computing power at the PetaFlop scale which will be available in the next future.

Conclusions

In this work we have presented a lattice QCD determination of the form factors for the semileptonic decay $K \to \pi l \nu_l$ and a preliminary study of the stochastic techniques needed to reproduce the disconnected fermionic bubble in view of a future calculation of the neutron electric dipole moment.

We have used the correlation functions calculated by the European Twisted Mass collaboration using the tree–level Symanzik improved gauge action and the Twisted Mass $N_f = 2$ flavour of degenerate dynamical quarks, at maximal twist [9]. In particular we have considered three different lattice spacings $a = 0.10\ fm$ $(a^{-1} = 1.94\ GeV)$, $a = 0.079\ fm$ $(a^{-1} = 2.30\ GeV)$ and $a = 0.063\ fm$, $(a^{-1} = 2.91\ GeV)$ and two different volumes ($V \times T = 24^3 \times 48\, a^4$ and $V \times T = 32^3 \times 64\, a^4$). The method we have employed in calculating the form factors is the double ratios method, which uses three–point double ratios in order to minimize the statistical fluctuations which cancel out in this ratio.

Our analysis strategy was that of extracting the form factors for different M_K and M_π. Then, since the Kaon masses employed in the simulations cover a range which includes the physical Kaon mass, we have performed a smooth interpolation of our data to a reference Kaon mass, which corresponds to fix the strange quark mass at its physical value. Then we have performed a multi–combined fit of the q^2, M_π and a dependence of the form factors using, respectively, a pole parametrization, an $SU(2)$ chiral parametrization and a polynomial parametrization. The quality of the multi–combined fit is very high and , at the physical point, gives us the following values for the quantity of interest

$$f_+(0) = 0.9610(30)(28), \qquad \frac{f_K}{f_\pi} = 1.189(8).$$

where the first error is statistical while the second, where available, is systematic. Our results are in very good agreement with the ones obtained from the *FLAVIANET* collaboration [23] and from the $N_f = 2+1$ simulations of the *RBC/UKQCD* collaboration; also the compatibility of our form factor's q^2 shape with the one obtained by a dispersive fit, based on the form factor parametrization of [24], to the *experimental data* from *KLOE*, *KTeV*, *NA48* (without muons branching ratios) and *ISTRA+* performed by the authors of [23] is good as well. Using our zero momentum vector form factor and our ratio of the kaon to pion decay constants together with, respectively, the Kl_3 and Kl_2 decay width quoted in [23], we have calculated the values of the *CKM* matrix element V_{us} obtaining

$$V_{us}^{Kl_3} = 0.2250(14), \qquad V_{us}^{Kl_2} = 0.2258(16). \tag{4.62}$$

Also in this case our results are in good agreement with the ones quoted in [23] where the lattice input used were taken from their symmetrization of the recent *RBC/UKQCD* results [112] ($f_+(0)$) and from a weighted average (by means of the statistical errors) of the results of the analysis from *BMW* [114], *MILC '09* [115] and *HPQCD/UKQCD*[116] (f_K/f_π).

Our stochastic technique analysis has given us two powerful tools, the *spin–direct* and the *twisted* methods, for calculating the trace of the fermionic *all-to-all* propagator, even if they are not yet precise enough to be used in the neutron electric dipole moment calculation.

There are several future perspective for this work. For the semileptonic decay sector we are planning to employ a different q^2 form factor parametrization, the so–called *z–parametrization* of [106] and eventually to repeat this analysis on the future ensemble with $N_f = 2 + 1 + 1$ flavours of dynamical quarks.

For the neutron electric dipole moment calculation instead there is a lot of work to be done, as we have to improve our two methods developing some variance reduction tricks in analogy to the ones employed by the authors of [16]. An important enhancement, however, is expected to come when the access to supercomputers at the PetaFlop scale will be available.

References

[1] S. Weinberg, "A model of leptons," *Physical Review Letters* **19** no. 21, (Nov., 1967) 1264. http://link.aps.org/doi/10.1103/PhysRevLett.19.1264. xi, 1

[2] N. Cabibbo, "Unitary symmetry and leptonic decays," *Physical Review Letters* **10** no. 12, (June, 1963) 531. http://link.aps.org/doi/10.1103/PhysRevLett.10.531. xi, 10, 30

[3] M. Kobayashi and T. Maskawa, "CP-Violation in the renormalizable theory of weak interaction," *Progress of Theoretical Physics* **49** no. 2, (1973) 652–657. http://ptp.ipap.jp/link?PTP/49/652/. xi, 10, 30

[4] H. Fritzsch, M. Gell-Mann, and H. Leutwyler, "Advantages of the color octet gluon picture," *Physics Letters B* **47** no. 4, (Nov., 1973) 365–368. http://www.sciencedirect.com/science/article/B6TVN-46YSK10-29/2/83344826d0252e372def415f61afd67b. xi, 47

[5] D. J. Gross and F. Wilczek, "Ultraviolet behavior of Non-Abelian gauge theories," *Physical Review Letters* **30** no. 26, (June, 1973) 1343. http://link.aps.org/doi/10.1103/PhysRevLett.30.1343. xi, 47

[6] S. Weinberg, "Non-Abelian gauge theories of the strong interactions," *Physical Review Letters* **31** no. 7, (1973) 494. http://link.aps.org/doi/10.1103/PhysRevLett.31.494. xi, 47

[7] K. G. Wilson, "Confinement of quarks," *Physical Review D* **10** no. 8, (Oct., 1974) 2445. http://link.aps.org/doi/10.1103/PhysRevD.10.2445. xi, 49, 58

[8] R. Frezzotti, P. A. Grassi, S. Sint, and P. Weisz, "A local formulation of lattice QCD without unphysical fermion zero modes," *hep-lat/9909003* (Sept., 1999) . http://arxiv.org/abs/hep-lat/9909003. Nucl.Phys.Proc.Suppl. 83 (2000) 941-946. xiii, 63

[9] C. Urbach, "Lattice QCD with two light wilson quarks and maximally twisted mass," *0710.1517* (Oct., 2007) . http://arxiv.org/abs/0710.1517. PoSLAT2007:022,2007. xiii, 169

[10] R. Peccei, "The strong CP problem and axions," in *Axions*, pp. 3–17. 2008. http://dx.doi.org/10.1007/978-3-540-73518-2_1. xiv, 40

[11] M. Gckeler, A. S. Kronfeld, M. L. Laursen, G. Schierholz, and U. J. Wiese, "Can the topological susceptibility be calculated from SU(N) lattice gauge theories?," *Physics Letters B* **233** no. 1-2, (Dec., 1989) 192–196. http://www.sciencedirect.com/science/article/B6TVN-46YTOKY-3NM/2/3ccdba147799cbf3c37ca895bea274da. xiv, 43

[12] D. Guadagnoli, V. Lubicz, G. Martinelli, and S. Simula, "Neutron electric dipole moment on the lattice: a theoretical reappraisal," *Journal of High Energy Physics* **2003** no. 04, (2003) 019–019. http://iopscience.iop.org/1126-6708/2003/04/019/. xiv, 43, 44, 45, 103

[13] J. Foley, K. J. Juge, A. . Cais, M. Peardon, S. M. Ryan, and J. Skullerud, "Practical all-to-all propagators for lattice QCD," *Computer Physics Communications* **172** no. 3, (Nov., 2005) 145–162. http://www.sciencedirect.com/science/article/B6TJ5-4GV97XX-4/2/5bebd1933f387053181efba609d16430. xv, 85, 101, 104, 107

[14] K. Jansen, C. McNeile, C. Michael, K. Nagai, M. Papinutto, J. Pickavance, A. Shindler, C. Urbach, and I. Wetzorke, "Flavour breaking effects of wilson twisted mass fermions," *Physics Letters B* **624** no. 3-4, (Sept., 2005) 334–341. http://www.sciencedirect.com/science/article/B6TVN-4GX6G49-4/2/54e004b5b815274804dcf545dc65349b. xv, 85, 104, 107, 109

[15] P. Boucaud, P. Dimopoulos, F. Farchioni, R. Frezzotti, V. Gimenez, G. Herdoiza, K. Jansen, V. Lubicz, C. Michael, G. Mnster, D. Palao, G. Rossi, L. Scorzato, A. Shindler, S. Simula, T. Sudmann, C. Urbach, and U. Wenger, "Dynamical twisted mass fermions with light quarks: simulation and analysis details," *Computer Physics Communications* **179** no. 10, (Nov., 2008) 695–715. http://www.sciencedirect.com/science/article/B6TJ5-4SWWT6T-1/2/bd5003a420b7e53fdb9af3ed54680531. xv, 85, 101, 102, 104, 107, 116

References

[16] E. T. M. Collaboration, K. Jansen, C. Michael, and C. Urbach, "The eta' meson from lattice QCD," *0804.3871* (Apr., 2008) . http://arxiv.org/abs/0804.3871. xv, 101, 163, 170

[17] D. Becirevic, G. Isidori, V. Lubicz, G. Martinelli, F. Mescia, S. Simula, C. Tarantino, and G. Villadoro, "The k–>[pi] vector form factor at zero momentum transfer on the lattice," *Nuclear Physics B - Proceedings Supplements* **140** (Mar., 2005) 387–389. http://www.sciencedirect.com/science/article/B6TVD-4F7YGGS-2R/2/4dce55825f5f298c0fbeb76437b15918. xvi, 91, 97, 158

[18] E. T. M. Collaboration and S. Simula, "Pseudo-scalar meson form factors with maximally twisted wilson fermions at nf = 2," *0710.0097* (Oct., 2007) . http://arxiv.org/abs/0710.0097. PoSLAT2007:371,2007. xvi, 91, 97, 101

[19] E. T. M. Collaboration, V. Lubicz, F. Mescia, S. Simula, and C. Tarantino, "K–> pi l nu semileptonic form factors from two-flavor lattice QCD," *Physical Review D* **80** no. 11, (Dec., 2009) 111502. http://link.aps.org/doi/10.1103/PhysRevD.80.111502. xvi, 91, 97, 139, 155, 158, 160

[20] C. Allton, D. J. Antonio, Y. Aoki, T. Blum, P. A. Boyle, N. H. Christ, M. A. Clark, S. D. Cohen, C. Dawson, M. A. Donnellan, J. M. Flynn, A. Hart, T. Izubuchi, C. Jung, A. Jttner, A. D. Kennedy, R. D. Kenway, M. Li, S. Li, M. F. Lin, R. D. Mawhinney, C. M. Maynard, S. Ohta, B. J. Pendleton, C. T. Sachrajda, S. Sasaki, and E. E. Scholz, "Physical results from 2+1 flavor domain wall QCD and SU(2) chiral perturbation theory (RBC-UKQCD collaboration)," *Physical Review D* **78** no. 11, (Dec., 2008) 114509. http://link.aps.org/doi/10.1103/PhysRevD.78.114509. xvi

[21] J. Gasser and H. Leutwyler, "Low-energy expansion of meson form factors," *Nuclear Physics B* **250** no. 1-4, (1985) 517–538. http://www.sciencedirect.com/science/article/B6TVC-4DKD02X-R/2/ce7e618b0eeea33e10495747b04e50de. xvi, 150

[22] J. Gasser and H. Leutwyler, "Chiral perturbation theory: Expansions in the mass of the strange quark," *Nuclear Physics B* **250** no. 1-4, (1985) 465–516. http://www.sciencedirect.com/science/article/B6TVC-4DKD02X-P/2/af5be680316220a89a7de9a9dbb26152. xvi, 150

[23] M. Antonelli, V. Cirigliano, G. Isidori, F. Mescia, M. Moulson, H. Neufeld, E. Passemar, M. Palutan, B. Sciascia, M. Sozzi, R. Wanke, O. P. Yushchenko, and for the FlaviaNet Working Group on Kaon Decays, "An evaluation of |Vus| and precise tests of the standard model from world data on leptonic and semileptonic kaon decays," *1005.2323* (May, 2010) . http://arxiv.org/abs/1005.2323. xvi, 16, 28, 121, 148, 160, 161, 162, 170

[24] V. Bernard, M. Oertel, E. Passemar, and J. Stern, "KL3 decay: A stringent test of right-handed quark currents," *Physics Letters B* **638** no. 5-6, (July, 2006) 480–486. http://www.sciencedirect.com/science/article/B6TVN-4K4WG33-8/2/f299bb1f2c76e74ee0c4edccf9e7ae31. xvi, 149, 161, 162, 170

[25] P. W. Higgs, "Broken symmetries and the masses of gauge bosons," *Physical Review Letters* **13** no. 16, (Oct., 1964) 508. http://link.aps.org/doi/10.1103/PhysRevLett.13.508. 2

[26] F. Englert and R. Brout, "Broken symmetry and the mass of gauge vector mesons," *Physical Review Letters* **13** no. 9, (1964) 321. http://link.aps.org/doi/10.1103/PhysRevLett.13.321. 2

[27] G. S. Guralnik, C. R. Hagen, and T. W. B. Kibble, "Global conservation laws and massless particles," *Physical Review Letters* **13** no. 20, (Nov., 1964) 585. http://link.aps.org/doi/10.1103/PhysRevLett.13.585. 2

[28] P. W. Anderson, "Plasmons, gauge invariance, and mass," *Physical Review* **130** no. 1, (Apr., 1963) 439. http://link.aps.org/doi/10.1103/PhysRev.130.439. 2

[29] C. N. Yang and R. L. Mills, "Conservation of isotopic spin and isotopic gauge invariance," *Physical Review* **96** no. 1, (Oct., 1954) 191. http://link.aps.org/doi/10.1103/PhysRev.96.191. 3, 48

[30] C. Amsler, M. Doser, M. Antonelli, D. Asner, K. Babu, H. Baer, H. Band, R. Barnett, E. Bergren, J. Beringer, G. Bernardi, W. Bertl, H. Bichsel, O. Biebel, P. Bloch, E. Blucher, S. Blusk, R. Cahn, M. Carena, C. Caso, A. Ceccucci, D. Chakraborty, M. Chen, R. Chivukula, G. Cowan, O. Dahl, G. D'Ambrosio, T. Damour, A. de Gouva, T. DeGrand, B. Dobrescu, M. Drees, D. Edwards, S. Eidelman, V. Elvira, J. Erler, V. Ezhela, J. Feng, W. Fetscher, B. Fields, B. Foster, T. Gaisser, L. Garren, H. Gerber, G. Gerbier, T. Gherghetta, G. Giudice, M. Goodman, C. Grab, A. Gritsan, J. Grivaz, D. Groom, M. Grnewald, A. Gurtu, T. Gutsche, H. Haber, K. Hagiwara, C. Hagmann, K. Hayes, J. Hernndez-Rey, K. Hikasa, I. Hinchliffe, A. Hcker, J. Huston, P. Igo-Kemenes, J. Jackson, K. Johnson, T. Junk, D. Karlen, B. Kayser, D. Kirkby, S. Klein, I. Knowles, C. Kolda, R. Kowalewski, P. Kreitz, B. Krusche, Y. Kuyanov, Y. Kwon, O. Lahav, P. Langacker, A. Liddle, Z. Ligeti, C. Lin, T. Liss, L. Littenberg, J. Liu, K. Lugovsky, S. Lugovsky, H. Mahlke, M. Mangano, T. Mannel, A. Manohar, W. Marciano, A. Martin, A. Masoni, D. Milstead, R. Miquel, K. Mnig, H. Murayama, K. Nakamura, M. Narain, P. Nason, S. Navas, P. Nevski, Y. Nir, K. Olive, L. Pape, C. Patrignani, J. Peacock, A. Piepke, G. Punzi, A. Quadt, S. Raby, G. Raffelt, B. Ratcliff, B. Renk, P. Richardson, S. Roesler, S. Rolli, A. Romaniouk, L. Rosenberg, J. Rosner, C. Sachrajda, Y. Sakai, S. Sarkar, F. Sauli, O. Schneider, D. Scott, W. Seligman, M. Shaevitz, T. Sjstrand, J. Smith, G. Smoot, S. Spanier, H. Spieler, A. Stahl, T. Stanev, S. Stone, T. Sumiyoshi, M. Tanabashi, J. Terning, M. Titov, N. Tkachenko, N. Trnqvist, D. Tovey, G. Trilling, T. Trippe, G. Valencia, K. van Bibber, M. Vincter, P. Vogel, D. Ward, T. Watari, B. Webber, G. Weiglein, J. Wells, M. Whalley, A. Wheeler, C. Wohl, L. Wolfenstein, J. Womersley, C. Woody, R. Workman, A. Yamamoto, W. Yao, O. Zenin, J. Zhang, R. Zhu, P. Zyla, G. Harper, V. Lugovsky, and P. Schaffner, "Review of particle physics," *Physics Letters B* **667** no. 1-5, (Sept., 2008) 1–6. http://www.sciencedirect.com/science/article/B6TVN-4T4VKPY-2/2/2fe3ceb40a4d144f48321db99160ecb2. 8, 14, 15, 16, 19

[31] S. L. Glashow, J. Iliopoulos, and L. Maiani, "Weak interactions with Lepton-Hadron symmetry," *Physical Review D* **2** no. 7, (Oct., 1970) 1285. http://link.aps.org/doi/10.1103/PhysRevD.2.1285. 10

[32] L. Maiani, "Proceedings of the international symposium on lepton and photon interactions at high energies," *edited by F. Gutbrod (DESY, Hamburg, 1977)* (1977) . 11

[33] C. Jarlskog, "Commutator of the quark mass matrices in the standard electroweak model and a measure of maximal CP nonconservation," *Physical Review Letters* **55** no. 10, (1985) 1039. http://link.aps.org/doi/10.1103/PhysRevLett.55.1039. 11

[34] C. Jarlskog, "A basis independent formulation of the connection between quark mass matrices, CP violation and experiment," *Zeitschrift fr Physik C Particles and Fields* **29** no. 3, (1985) 491–497. http://dx.doi.org/10.1007/BF01565198. 11

[35] R. Fleischer, "Flavour physics and CP violation: Expecting the LHC," *0802.2882* (Feb., 2008) . http://arxiv.org/abs/0802.2882. 12

[36] L. Wolfenstein, "Parametrization of the Kobayashi-Maskawa matrix," *Physical Review Letters* **51** no. 21, (Nov., 1983) 1945. http://link.aps.org/doi/10.1103/PhysRevLett.51.1945. 12

[37] A. J. Buras, M. E. Lautenbacher, and G. Ostermaier, "Waiting for the top quark mass, k+–> pi + nu nu -bar, Bs-B-bars mixing, and CP asymmetries in b decays," *Physical Review D* **50** no. 5, (1994) 3433. http://link.aps.org/doi/10.1103/PhysRevD.50.3433. 14

[38] M. Bona, M. Ciuchini, E. Franco, V. Lubicz, G. Martinelli, F. Parodi, M. Pierini, P. Roudeau, C. Schiavi, L. Silvestrini, and A. Stocchi, "The 2004 UTfit collaboration report on the status of the unitarity triangle in the standard model," *hep-ph/0501199* (Jan., 2005) . http://arxiv.org/abs/hep-ph/0501199. JHEP0507:028,2005. 19

[39] J. Charles, A. Hcker, H. Lacker, S. Laplace, F. R. L. Diberder, J. Malcls, J. Ocariz, M. Pivk, and L. Roos, "CP violation and the CKM matrix: assessing the impact of the asymmetric b factories," *The European Physical Journal C - Particles and Fields* **41** no. 1, (May, 2005) 1–131. http://dx.doi.org/10.1140/epjc/s2005-02169-1. 19

[40] V. Cirigliano and I. Rosell, "pi/k–>enu branching ratios to o(e2p4) in chiral perturbation theory," *Journal of High Energy Physics* **2007** no. 10, (2007) 005–005. http://iopscience.iop.org/1126-6708/2007/10/005. 24

[41] W. J. Marciano and A. Sirlin, "Radiative corrections to pi l2 decays," *Physical Review Letters* **71** no. 22, (Nov., 1993) 3629. http://link.aps.org/doi/10.1103/PhysRevLett.71.3629. 24, 28

[42] R. Decker and M. Finkemeier, "Short and long distance effects in the decay [tau] –> [pi][nu][tau]([gamma])," *Nuclear Physics B* **438** no. 1-2, (Mar., 1995) 17–53. http://www.sciencedirect.com/science/article/B6TVC-417NK82-2/2/c821ff0af9c19eb2b45090ff234d6580. 24

[43] M. Finkemeier, "Radiative corrections to [pi]l2 and kl2 decays," *Physics Letters B* **387** no. 2, (Oct., 1996) 391–394. http://www.sciencedirect.com/science/article/B6TVN-3VSTGJ0-81/2/0c35dfcb247c9770eaebe41ba535acd7. 24

[44] W. J. Marciano, "Precise determination of |V_us| from lattice calculations of pseudoscalar decay constants," *Physical Review Letters* **93** no. 23, (Dec., 2004) 231803. http://link.aps.org/doi/10.1103/PhysRevLett.93.231803. 24

[45] M. Knecht, H. Neufeld, H. Rupertsberger, and P. Talavera, "Chiral perturbation theory with virtual photons and leptons," *The European Physical Journal C - Particles and Fields* **12** no. 3, (Feb., 2000) 469–478. http://dx.doi.org/10.1007/s100529900265. 24

[46] M. Ademollo and R. Gatto, "Nonrenormalization theorem for the Strangeness-Violating vector currents," *Physical Review Letters* **13** no. 7, (1964) 264. http://link.aps.org/doi/10.1103/PhysRevLett.13.264. 28, 158

[47] A. Sirlin, "Current algebra formulation of radiative corrections in gauge theories and the universality of the weak interactions," *Reviews of Modern Physics* **50** no. 3, (July, 1978) 573. http://link.aps.org/doi/10.1103/RevModPhys.50.573. 28

[48] J. F. Donoghue, E. Golowich, and B. R. Holstein, *Dynamics of the Standard Model*, vol. 1 of *Cambridge Monographs on Particle physics, Nuclear physics and Cosmology*. Cambridge University Press, 1992. 28

[49] A. J. Buras, "Flavour dynamics: CP violation and rare decays," *hep-ph/0101336* (Jan., 2001) . http://arxiv.org/abs/hep-ph/0101336. 31

[50] L. Chau *Phys. Rep.* **95** (1983) . 35

[51] R. P. Feynman, "Space-Time approach to Non-Relativistic quantum mechanics," *Reviews of Modern Physics* **20** no. 2, (Apr., 1948) 367. http://link.aps.org/doi/10.1103/RevModPhys.20.367. 36, 47

[52] K. Osterwalder and R. Schrader, "Axioms for euclidean green's functions," *Communications in Mathematical Physics* **31** no. 2, (June, 1973) 83–112. http://dx.doi.org/10.1007/BF01645738. 37

References

[53] K. Fujikawa, "Path-Integral measure for Gauge-Invariant fermion theories," *Physical Review Letters* **42** no. 18, (Apr., 1979) 1195. http://link.aps.org/doi/10.1103/PhysRevLett.42.1195. 39

[54] K. Fujikawa, "Path integral for gauge theories with fermions," *Physical Review D* **21** no. 10, (May, 1980) 2848. http://link.aps.org/doi/10.1103/PhysRevD.21.2848. 39

[55] S. L. Adler, "Axial-Vector vertex in spinor electrodynamics," *Physical Review* **177** no. 5, (Jan., 1969) 2426. http://link.aps.org/doi/10.1103/PhysRev.177.2426. 39

[56] J. Bell and R. Jackiw, "A PCAC puzzle: 0 in the -model," *Il Nuovo Cimento A (1965-1970)* **60** no. 1, (Mar., 1969) 47–61. http://dx.doi.org/10.1007/BF02823296. 39

[57] W. A. Bardeen, "Anomalous ward identities in spinor field theories," *Physical Review* **184** no. 5, (1969) 1848. http://link.aps.org/doi/10.1103/PhysRev.184.1848. 39

[58] W. A. Bardeen, "Anomalous currents in gauge field theories," *Nuclear Physics B* **75** no. 2, (June, 1974) 246–258. http://www.sciencedirect.com/science/article/B6TVC-472T0F6-K8/2/be7b98fb6c7716c243db2190b6ad50fb. 40

[59] G. 't Hooft, "Symmetry breaking through Bell-Jackiw anomalies," *Physical Review Letters* **37** no. 1, (July, 1976) 8. http://link.aps.org/doi/10.1103/PhysRevLett.37.8. 40

[60] G. 't Hooft, "Computation of the quantum effects due to a four-dimensional pseudoparticle," *Physical Review D* **14** no. 12, (Dec., 1976) 3432. http://link.aps.org/doi/10.1103/PhysRevD.14.3432. 40

[61] G. 't Hooft, "Erratum: Computation of the quantum effects due to a four-dimensional pseudoparticle," *Physical Review D* **18** no. 6, (1978) 2199. http://link.aps.org/doi/10.1103/PhysRevD.18.2199.3. 40

[62] C. G. Callan, R. F. Dashen, and D. J. Gross, "The structure of the gauge theory vacuum," *Physics Letters B* **63** no. 3, (Aug., 1976) 334–340. http://www.sciencedirect.com/science/article/B6TVN-472JPT2-14C/2/4c16f3b100a8fb2c1b4193f1faf665e7. 40

[63] R. Crewther, "Effects of topological charge in gauge theories.," *Acta Phys. Austriaca Suppl.* **19** (1978) p. 47. 41

[64] C. A. Baker, D. D. Doyle, P. Geltenbort, K. Green, M. G. D. van der Grinten, P. G. Harris, P. Iaydjiev, S. N. Ivanov, D. J. R. May, J. M. Pendlebury, J. D. Richardson, D. Shiers, and K. F. Smith, "Improved experimental limit on the electric dipole moment of the neutron," *Physical Review Letters* **97** no. 13, (2006) 131801. http://link.aps.org/doi/10.1103/PhysRevLett.97.131801. 42

[65] B. L. Ioffe, "Calculation of baryon masses in quantum chromodynamics," *Nuclear Physics B* **188** no. 2, (Sept., 1981) 317–341. http://www.sciencedirect.com/science/article/B6TVC-4719KH8-12G/2/c7e076ba3e472d9f11244c11b68bfa9c. 44

[66] S. Aoki, A. Gocksch, A. V. Manohar, and S. R. Sharpe, "Calculating the neutron electric dipole moment on the lattice," *Physical Review Letters* **65** no. 9, (1990) 1092. http://link.aps.org/doi/10.1103/PhysRevLett.65.1092. 44

[67] D. J. Gross and F. Wilczek, "Asymptotically free gauge theories. i," *Physical Review D* **8** no. 10, (Nov., 1973) 3633. http://link.aps.org/doi/10.1103/PhysRevD.8.3633. 47

[68] H. D. Politzer, "Asymptotic freedom: An approach to strong interactions," *Physics Reports* **14** no. 4, (Nov., 1974) 129–180. http://www.sciencedirect.com/science/article/B6TVP-46SWY7T-V/2/ab433983bfdcfa473c26cc003ed688cd. 47

[69] G. 't Hooft, "Unpublished remarks at the 1972 marseille conference on yangmills fields,". 47

[70] H. D. Politzer, "Reliable perturbative results for strong interactions?," *Physical Review Letters* **30** no. 26, (June, 1973) 1346. http://link.aps.org/doi/10.1103/PhysRevLett.30.1346. 47

[71] G. Altarelli, "A QCD primer," *hep-ph/0204179* (Apr., 2002) . http://arxiv.org/abs/hep-ph/0204179. 48

[72] G. Altarelli, "Concluding talk: QCD 2005," *hep-ph/0510095* (Oct., 2005) . http://arxiv.org/abs/hep-ph/0510095. Int.J.Mod.Phys. A21 (2006) 799-806. 48

[73] J. Greensite, "The confinement problem in lattice gauge theory," *Progress in Particle and Nuclear Physics* **51** no. 1, (2003) 1–83. http://www.sciencedirect.com/science/article/B6TJC-4995P64-2/2/4ecc745b329c344ce27c0fffab343f12. 48

[74] S. Capitani, "Lattice perturbation theory," *Physics Reports* **382** no. 3-5, (July, 2003) 113–302. http://www.sciencedirect.com/science/article/B6TVP-48V8516-2/2/8a1ae06258266b5377f8cf524bc0c44b. 50

[75] L. H. Karsten and J. Smith, "Lattice fermions: Species doubling, chiral invariance and the triangle anomaly," *Nuclear Physics B* **183** no. 1-2, (1981) 103–140. http://www.sciencedirect.com/science/article/B6TVC-47318FV-XS/2/665429bcf82a7b54cce83b8bb1fc48c9. 57

[76] R. e. a. Schrader, "Some topics in quantum field theory, presented at 6th int. conf. on mathematical physics.," *Mathematical problems in theoretical physics* **153** (1981) . 62

[77] K. Symanzik, "Continuum limit and improved action in lattice theories : (I). principles and [phi]4 theory," *Nuclear Physics B* **226** no. 1, (Sept., 1983) 187–204. http://www.sciencedirect.com/science/article/B6TVC-47187PB-8B/2/635b43b752bf383a49380d8ce67cac25. 62

[78] K. Symanzik, "Continuum limit and improved action in lattice theories : (II). O(N) non-linear sigma model in perturbation theory," *Nuclear Physics B* **226** no. 1, (Sept., 1983) 205–227. http://www.sciencedirect.com/science/article/B6TVC-47187PB-8C/2/f5d2e3c34932058bc55fb58cebf972cb. 62

[79] M. L\"uscher and P. Weisz, "Efficient numerical techniques for perturbative lattice gauge theory computations," *Nuclear Physics B* **266** no. 2, (Mar., 1986) 309–356. http://www.sciencedirect.com/science/article/B6TVC-47199FV-8F/2/54191702d8a3cc5957bc0e0f7d81adec. 62

[80] P. Weisz, "Continuum limit improved lattice action for pure Yang-Mills theory (I)," *Nuclear Physics B* **212** no. 1, (Feb., 1983) 1–17. http://www.sciencedirect.com/science/article/B6TVC-472SXWY-2Y/2/fcf272f19f501348df265a63e97d3ca8. 62

[81] R. Frezzotti, P. A. Grassi, S. Sint, and P. Weisz, "Lattice QCD with a chirally twisted mass term," *hep-lat/0101001* (Dec., 2000) . http://arxiv.org/abs/hep-lat/0101001. JHEP 0108:058,2001. 63

[82] R. Frezzotti and G. Rossi, "Chirally improving wilson fermions i. o(a) improvement," *Journal of High Energy Physics* **2004** no. 08, (2004) 007–007. http://iopscience.iop.org/1126-6708/2004/08/007/. 63, 66, 67, 68, 69, 71, 72, 73

[83] A. Shindler, "Twisted mass lattice QCD," *Physics Reports* **461** no. 2-3, (May, 2008) 37–110. http://www.sciencedirect.com/science/article/B6TVP-4S2MHV7-1/2/36a8446b1fac3c366215e81d96eedc6f. 63

[84] K. Symanzik *Nucl. Phys. B* **226** (1983) 187 and 205. 68

[85] P. F. Bedaque, "Aharonov-Bohm effect and nucleon-nucleon phase shifts on the lattice," *Physics Letters B* **593** no. 1-4, (July, 2004) 82–88. http://www.sciencedirect.com/science/article/B6TVN-4CGNBDM-3/2/e4a4a0bb48e026d0638be43f49cec13d. 75, 78

[86] C. Sachrajda and G. Villadoro, "Twisted boundary conditions in lattice simulations," *Physics Letters B* **609** no. 1-2, (Mar., 2005) 73–85. http://www.sciencedirect.com/science/article/B6TVN-4F9N5S2-2/2/98a6c411969865ab64aa66627d9fd282. 75, 78

[87] A. Morel, "Chiral logarithms in quenched QCD," *J. Phys.* **48** (1987) 1111–1119. 77

[88] P. F. Bedaque and J. Chen, "Twisted valence quarks and hadron interactions on the lattice," *Physics Letters B* **616** no. 3-4, (June, 2005) 208–214. http://www.sciencedirect.com/science/article/B6TVN-4G35XP2-6/2/e28d7bcf89c3824b4af9ec72341502ad. 78

[89] G. M. de Divitiis, R. Petronzio, and N. Tantalo, "On the discretization of physical momenta in lattice QCD," *Physics Letters B* **595** no. 1-4, (Aug., 2004) 408–413. http://www.sciencedirect.com/science/article/B6TVN-4CVWW9B-3/2/6fd7c01b1b2ae19b6941eb50ba403753. 78

[90] R. Frezzotti, V. Lubicz, and S. Simula, "Electromagnetic form factor of the pion from twisted-mass lattice QCD at n_f=2," *Physical Review D* **79** no. 7, (Apr., 2009) 074506. http://link.aps.org/doi/10.1103/PhysRevD.79.074506. 93, 94, 143

[91] W. Wilcox, "Noise methods for flavor singlet quantities," *hep-lat/9911013* (Nov., 1999) . http://arxiv.org/abs/hep-lat/9911013. 101

[92] M. Foster and C. Michael, "Hadrons with a heavy color-adjoint particle (UKQCD collaboration)," *Physical Review D* **59** no. 9, (Apr., 1999) 094509. http://link.aps.org/doi/10.1103/PhysRevD.59.094509. 101

[93] C. McNeile and C. Michael, "Decay width of light quark hybrid meson from the lattice," *Physical Review D* **73** no. 7, (Apr., 2006) 074506. http://link.aps.org/doi/10.1103/PhysRevD.73.074506. 101

[94] P. Boyle, C. Kelly, R. Kenway, and A. Jttner, "Use of stochastic sources for the lattice determination of light quark physics (RBC-UKQCD collaboration)," *Journal of High Energy Physics* **2008** no. 08, (2008) 086–086. http://iopscience.iop.org/1126-6708/2008/08/086/. 101

[95] S. Aoki and A. Gocksch, "Neutron electric dipole moment in lattice QCD," *Physical Review Letters* **63** no. 11, (1989) 1125. http://link.aps.org/doi/10.1103/PhysRevLett.63.1125. 103

[96] E. Shintani, S. Aoki, N. Ishizuka, K. Kanaya, Y. Kikukawa, Y. Kuramashi, M. Okawa, A. Ukawa, and T. Yoshi, "Neutron electric dipole moment with external electric field method in lattice QCD," *Physical Review D* **75** no. 3, (Feb., 2007) 034507. http://link.aps.org/doi/10.1103/PhysRevD.75.034507. 103

References

[97] E. Shintani, S. Aoki, N. Ishizuka, K. Kanaya, Y. Kikukawa, Y. Kuramashi, M. Okawa, Y. Taniguchi, A. Ukawa, and T. Yoshi, "Neutron electric dipole moment from lattice QCD (CP-PACS collaboration)," *Physical Review D* **72** no. 1, (July, 2005) 014504. http://link.aps.org/doi/10.1103/PhysRevD.72.014504. 103

[98] F. Berruto, T. Blum, K. Orginos, and A. Soni, "Calculation of the neutron electric dipole moment with two dynamical flavors of domain wall fermions," *Physical Review D* **73** no. 5, (Mar., 2006) 054509. http://link.aps.org/doi/10.1103/PhysRevD.73.054509. 103

[99] D. Becirevic, P. Boucaud, V. Lubicz, G. Martinelli, F. Mescia, S. Simula, and C. Tarantino, "Exploring twisted mass lattice QCD with the clover term," *Physical Review D* **74** no. 3, (2006) 034501. http://link.aps.org/doi/10.1103/PhysRevD.74.034501. 110

[100] R. Baron, P. Boucaud, P. Dimopoulos, F. Farchioni, R. Frezzotti, V. Gimenez, G. Herdoiza, K. Jansen, V. Lubicz, C. Michael, G. Muenster, D. Palao, G. C. Rossi, L. Scorzato, A. Shindler, S. Simula, T. Sudmann, C. Urbach, and U. Wenger, "Light meson physics from maximally twisted mass lattice QCD," *0911.5061* (Nov., 2009) . http://arxiv.org/abs/0911.5061. 122

[101] T. Yoshie, "Making use of the international lattice data grid," *0812.0849* (Dec., 2008) . http://arxiv.org/abs/0812.0849. PoS LATTICE2008:019,2008. 122

[102] C. Urbach, K. Jansen, A. Shindler, and U. Wenger, "HMC algorithm with multiple time scale integration and mass preconditioning," *Computer Physics Communications* **174** no. 2, (2006) 87–98. http://www.sciencedirect.com/science?_ob=ArticleURL&_udi=B6TJ5-4H6XM51-3&_user=2920338&_coverDate=01in=search&_sort=d&_docanchor=&view=c&_acct=C000059161&_version= 122

[103] K. Jansen and C. Urbach, "tmLQCD: a program suite to simulate wilson twisted mass lattice QCD," *0905.3331* (May, 2009) . http://arxiv.org/abs/0905.3331. 123

[104] U. Wolff, "Monte carlo errors with less errors," *Computer Physics Communications* **156** no. 2, (2004) 143–153. http://www.sciencedirect.com/science/article/B6TJ5-4B3NPMC-3/2/94bd1b60aba9b7a9ea69ac39d7372fc5. 127

[105] E. Abouzaid, M. Arenton, A. R. Barker, L. Bellantoni, E. Blucher, G. J. Bock, E. Cheu, R. Coleman, M. D. Corcoran, B. Cox, A. R. Erwin, C. O. Escobar, A. Glazov, R. A. Gomes, P. Gouffon, Y. B. Hsiung, D. A. Jensen, R. Kessler, K. Kotera, A. Ledovskoy, P. L. McBride, E. Monnier, H. Nguyen, R. Niclasen, D. G. Phillips, E. J. Ramberg, and R. E. Ray, "Dispersive analysis of KLmu3 and KLe3 scalar and vector form factors using KTeV data (KTeV collaboration)," *Physical Review D* **81** no. 5, (Mar., 2010) 052001. http://link.aps.org/doi/10.1103/PhysRevD.81.052001. 148, 149

[106] R. J. Hill, "Constraints on the form factors for k–> pi l nu and implications for |Vus|," *Physical Review D* **74** no. 9, (Nov., 2006) 096006. http://link.aps.org/doi/10.1103/PhysRevD.74.096006. 149, 170

[107] J. Flynn and C. Sachrajda, "SU(2) chiral perturbation theory for kl3 decay amplitudes," *Nuclear Physics B* **812** no. 1-2, (May, 2009) 64–80. http://www.sciencedirect.com/science/article/B6TVC-4V34D6P-4/2/a421d85b7de48c2357dbc180d53d978c. 154

[108] C. G. Callan and S. B. Treiman, "Equal-Time commutators and K-Meson decays," *Physical Review Letters* **16** no. 4, (Jan., 1966) 153. http://link.aps.org/doi/10.1103/PhysRevLett.16.153. 154

[109] D. Becirevic, G. Martinelli, and G. Villadoro, "The Ademollo-Gatto theorem for lattice semileptonic decays," *Physics Letters B* **633** no. 1, (Feb., 2006) 84–88. http://www.sciencedirect.com/science/article/B6TVN-4HKCSWJ-8/2/9d8fffe7fda64d48b90dff53fd27a670. 158

[110] H. Leutwyler and M. Roos, "Determination of the elementsV us andV ud of the Kobayashi-Maskawa matrix," *Zeitschrift fr Physik C Particles and Fields* **25** no. 1, (1984) 91–101. http://www.springerlink.com/content/u24ggm3228223289/. 158

[111] P. A. Boyle, A. Jttner, R. D. Kenway, C. T. Sachrajda, S. Sasaki, A. Soni, R. J. Tweedie, and J. M. Zanotti, "K_l3 semileptonic form factor from (2+1)-Flavor lattice QCD (RBC-UKQCD collaboration)," *Physical Review Letters* **100** no. 14, (Apr., 2008) 141601. http://link.aps.org/doi/10.1103/PhysRevLett.100.141601. 158, 159

[112] P. A. Boyle, J. M. Flynn, A. Juttner, C. Kelly, C. Maynard, H. P. de Lima, C. T. Sachrajda, J. M. Zanotti, and R. Collaboration, "K->pi form factors with reduced model dependence," *1004.0886* (Apr., 2010) . http://arxiv.org/abs/1004.0886. 160, 161, 170

[113] B. Blossier, P. Dimopoulos, R. Frezzotti, B. Haas, G. Herdoiza, K. Jansen, V. Lubicz, F. Mescia, D. Palao, A. Shindler, S. Simula, C. Tarantino, C. Urbach, U. Wenger, and E. T. M. Collaboration, "Pseudoscalar decay constants of kaon and d-mesons from nf=2 twisted mass lattice QCD," *0904.0954* (Apr., 2009) . http://arxiv.org/abs/0904.0954. 160

[114] S. Durr, Z. Fodor, C. Hoelbling, S. D. Katz, S. Krieg, T. Kurth, L. Lellouch, T. Lippert, A. Ramos, and K. K. Szabo, "The ratio FK/Fpi in QCD," *1001.4692* (Jan., 2010) . http://arxiv.org/abs/1001.4692. 161, 170

[115] A. Bazavov, C. Bernard, C. DeTar, X. Du, W. Freeman, S. Gottlieb, U. M. Heller, J. E. Hetrick, J. Laiho, L. Levkova, M. B. Oktay, J. Osborn, R. Sugar, D. Toussaint, and R. S. V. de Water, "MILC results for light pseudoscalars," *0910.2966* (Oct., 2009) . http://arxiv.org/abs/0910.2966. 161, 170

[116] E. Follana, C. T. H. Davies, G. P. Lepage, and J. Shigemitsu, "High-Precision determination of the pi , k, d, and d_s decay constants from lattice QCD (HPQCD and UKQCD collaboration)," *Physical Review Letters* **100** no. 6, (Feb., 2008) 062002. http://link.aps.org/doi/10.1103/PhysRevLett.100.062002. 161, 170